

# QUANTUM MECHANICAL ASSESSMENT OF SUBSTITUENT EFFECT OF DOUBLY BONDED SILICON COMPOUNDS

Thesis Submitted to the **University of Calicut** for the award of

DOCTOR OF PHILOSOPHY

IN CHEMISTRY

By

**AMRUTHA K**

Under the Supervision of

**Dr. Jose John Mallikasseri** (Guide)

**Dr. Jomon Mathew** (Co-Guide)



DEPARTMENT OF CHEMISTRY

ST. JOSEPH'S COLLEGE (AUTONOMOUS), DEVAGIRI, CALICUT,  
KERALA – 673008

*(Affiliated to the University of Calicut)*

May 2024



# ST. JOSEPH'S COLLEGE

AUTONOMOUS

DBT STAR COLLEGE  
(Under Strengthening Component)

Re-accredited with A<sup>+</sup> + Grade

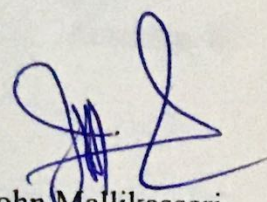
DEVAGIRI, CALICUT-673008, KERALA

Affiliated to the University of Calicut

## CERTIFICATE

This is to certify that the thesis entitled "QUANTUM MECHANICAL ASSESSMENT OF SUBSTITUENT EFFECT OF DOUBLY BONDED SILICON COMPOUNDS" is an authentic record of the research work carried out by Ms. Amrutha. K, under my supervision and guidance in partial fulfillment of the requirements for the award of the degree of **Doctor of Philosophy in Chemistry** under the **Faculty of Science**, University of Calicut, Kerala. The work presented in this thesis has not been submitted for any other degree or diploma earlier. It is also certified that Ms. Amrutha. K has fulfilled the course requirements and qualified the course work examination for the Ph. D. degree of the University.

Kozhikode

  
Dr. Jose John Mallikasseri  
Principal (Retired)  
Research Guide  
St. Joseph's College (Autonomous)  
Devagiri, Kozhikode 673008

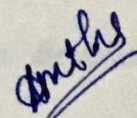


ACKNOWLEDGEMENT

**DECLARATION**

I hereby declare that the thesis entitled "QUANTUM MECHANICAL ASSESSMENT OF SUBSTITUENT EFFECT OF DOUBLY BONDED SILICON COMPOUNDS" is an authentic research work carried out by me under the guidance of Dr. Jose John Mallikasseri, Assistant Professor (Retd.), Department of Chemistry, St. Joseph's College (Autonomous), Devagiri, Calicut, and with the co-supervision of Dr. Jomon Mathew, Assistant Professor, Department of Chemistry, St. Joseph's College (Autonomous), Devagiri, Calicut. This Work is entirely original in its contents and has not been submitted before either in part or in full to any University or Institute for the award of any degree or diploma.

Kozhikode



Amrutha. K



## ACKNOWLEDGEMENT

*I am profoundly moved by the serendipity of circumstances and the unwavering support that has illuminated the path to the realization of my academic dreams. The profound impact of extraordinary individuals surrounding me has been akin to a guiding light, and their influence on this transformative journey is immeasurable.*

*At the forefront of my gratitude stands Dr. Jose John Mallikasseri; formerly Head of the Department of Chemistry and Principal of St. Joseph's College (Autonomous), Devagiri, Calicut. His mentorship has not only served as a guiding light but also as a source of profound wisdom and support throughout the intricate process of shaping this thesis. Dr. Jose John Mallikasseri's extraordinary patience, coupled with his adept problem-solving abilities, has not merely navigated challenges but has sculpted a profound academic mentorship. Beyond the confines of academia, he has stood as an unwavering pillar, offering motivational encouragement at pivotal junctures. My educational journey, enriched by his wealth of knowledge and experience, has been transformed into a deeply rewarding experience. I am genuinely thankful for the grace, guidance, and kindness he has generously shared.*

*In tandem, my heartfelt appreciation extends to my Co-guide, Dr. Jomon Mathew, Assistant Professor, Department of Chemistry, St. Joseph's College (Autonomous), Devagiri, Calicut. Dr. Jomon Mathew's steadfast guidance and invaluable support have laid the foundation upon which this thesis stands. His multifaceted role, extending beyond academia to unwavering support during crucial moments, has left an indelible mark on this academic*



*endeavor. My gratitude is sincere for the wisdom, mentorship, and consideration he has bestowed, rendering this journey profoundly enriching.*

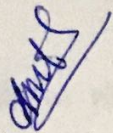
*To Dr. Tania Francis, Head of the Department, and all the esteemed teachers and non-teaching staff of the Department of Chemistry, St. Joseph's College (Autonomous), Devagiri, my heartfelt thanks for your unwavering support, benevolent wishes, and generous spirit.*

*I extend my deepest appreciation to the Management, Principal Dr. Bobby Jose, former Principal Dr. Sibichen M Thomas, Dr. Sabu K Thomas, and former head of the department Dr. Joy Joseph for their gracious permission, invaluable assistance, and encouraging presence during my research tenure.*

*I would like to extend my heartfelt gratitude to all my friends and colleagues at St. Joseph's College (Autonomous), Devagiri, Calicut, for their invaluable support and assistance throughout every phase of my research. Your contributions have been indispensable to my journey.*

*Lastly, I would like to extend my heartfelt gratitude to my family members, specially my mother and husband.*

Kozhikode

  
Amrutha K



# TABLE OF CONTENT

LIST OF FIGURES	i
LIST OF TABLES	vii
LIST OF SCHEMES	ix
LIST OF ABBREVIATIONS	xi
LIST OF SYMBOLS	xiii
ABSTRACT	xv
PREFACE	xix

## Chapter 1: Introduction

Part A: Computational Chemistry	1
1.1. Introduction	1
1.1.1 Computational Chemistry	1
1.1.1.1 Quantum Chemical Methods	3
1.1.1.1.1 Ab initio Molecular Orbital Theory	3
1.1.1.1.2 Hartree-Fock Theory	5
1.1.1.1.3 Basis Sets	10
1.1.1.2 Post HF Methods	11
1.1.1.2.1 Configuration Interaction	12
1.1.1.2.2 Coupled Cluster Methods	13
1.1.1.2.3 Perturbation Theory	14
1.1.1.3 Density Functional Theory (DFT)	16
1.1.1.4 Potential Energy Surface	21
Part B: Doubly Bonded Silicon Compounds	23
1.2. Introduction	23
1.2.1 Silenes $R_2C=SiR_2$	24
1.2.1.1 Discovery and synthesis	24
1.2.1.2 Stability of silences	27
1.2.2 Disilenes	32
1.2.2.1 The discovery and synthesis of disilene	32
1.2.2.2 Structure of Disilenes	33
1.2.3 Silylene	34
1.2.4 Cyclotrisilene	34
1.2.4.1 Synthesis	34
1.2.4.2 Structure	36
1.3 Conclusion	38
Reference	39

## Chapter 2: Substituent effects on the dimerization reaction of silenes: the di-radical and the zwitter-ion reaction pathways

2.1 Introduction	47
2.2 Objectives	50
2.3 Computational Methods	50
2.4 Results and Discussion	51
2.4.1 Molecular electrostatic potential and polarity of the C=Si in silences	53
2.4.2 Dimerization - The zwitter-ion pathway	55



2.4.3	The diradical pathway	62
2.5	Conclusion	66
	Reference	67

**Chapter 3:** Substituent effects on the addition of small molecules (NH<sub>3</sub>, NO, CO) to silene and silene-silylene isomerization

3.1	Introduction	71
3.2	Objectives	78
3.3	Computational methods	78
3.4	Results and discussion	78
3.4.1	NH <sub>3</sub> : The N-H bond activation	78
3.4.2	NO: N-O bond activation	82
3.4.3	CO: C-O bond activation	86
3.4.4	The silene-silylene rearrangement	90
3.5	Conclusion	94
	Reference	95

**Chapter 4:** Reactions of 1,2,3,3-tetramethyl cyclotrisilene with propylene, phenylacetylene, trimethylsilylacetylene, formaldehyde and benzaldehyde

4.1	Introduction	99
4.2	Objectives	103
4.3	Computational Methods	103
4.4	Results and Discussion	103
4.4.1	Reaction pathways of c-Si <sub>3</sub> Me <sub>4</sub> (I) with C <sub>6</sub> H <sub>5</sub> -C≡CH (R1)	105
4.4.1.1	π-addition	105
4.4.1.2	σ-insertion	106
4.4.1.3	Ring opening	108
4.4.1.4	Exocyclic sigma insertion	109
4.4.2	Reaction pathways of c-Si <sub>3</sub> Me <sub>4</sub> (I) and CH <sub>3</sub> -C≡CH (R2)	111
4.4.2.1	π-addition	111
4.4.2.2	σ-insertion	112
4.4.2.3	Ring opening	113
4.4.2.4	Exocyclic σ-insertion	115
4.4.3	Reaction pathways of c-Si <sub>3</sub> Me <sub>4</sub> (I) with (CH <sub>3</sub> ) <sub>3</sub> Si-C≡CH(R3)	116
4.4.3.1	π-addition	116
4.4.3.2	σ-insertion	117
4.4.3.3	Ring opening	118
4.4.3.4	Exocyclic σ-insertion	120
4.4.4	Reaction pathways between c-Si <sub>3</sub> Me <sub>4</sub> (I) + C <sub>6</sub> H <sub>5</sub> -CHO (R'1)	122
4.4.4.1	π-addition	122
4.4.4.2	σ-insertion	123
4.4.4.3	Ring opening	126
4.4.4.4	Exocyclic sigma insertion	127
4.4.5	Reaction pathways between c-Si <sub>3</sub> Me <sub>4</sub> (I) and formaldehyde (R'2)	129
4.4.5.1	π-addition	129
4.4.5.2	σ-insertion	130
4.4.5.3	Ring opening	131
4.4.5.4	Exocyclic σ-insertion	132



4.5	Conclusion	134
	Reference	135

**Chapter 5:** Reactions of 1,2-bis(trimethylsilyl)-3,3-dimethyl cyclotrisilene with propylene, phenyl acetylene, trimethylsilylacetylene, formaldehyde and benzaldehyde

5.1	Introduction	139
5.2	Objectives	140
5.3	Computational Methods	141
5.4	Results and discussion	141
5.4.1	Reaction pathways of c-Si <sub>3</sub> Me <sub>2</sub> (SiMe <sub>3</sub> ) <sub>2</sub> (II) with C <sub>6</sub> H <sub>5</sub> -C≡CH (R1)	142
5.4.1.1	π-addition	142
5.4.1.2	σ-insertion.	143
5.4.1.3	Ring opening	144
5.4.1.4	Exocyclic sigma insertion	145
5.4.2	Reaction pathways of c-Si <sub>3</sub> Me <sub>2</sub> (SiMe <sub>3</sub> ) <sub>2</sub> (II) and CH <sub>3</sub> -C≡CH (R2)	147
5.4.2.1	π-addition	147
5.4.2.2	σ-insertion	149
5.4.2.3	Ring opening	150
5.4.2.4	Exocyclic σ-insertion	151
5.4.3	Reaction pathways of c-Si <sub>3</sub> Me <sub>2</sub> (SiMe <sub>3</sub> ) <sub>2</sub> (II) with (CH <sub>3</sub> ) <sub>3</sub> Si-C≡CH (R3)	153
5.4.3.1	π-addition	153
5.4.3.2	σ-insertion	154
5.4.3.3	Ring opening	156
5.4.3.4	Exocyclic σ-insertion	157
5.4.4	Reaction pathways of c-Si <sub>3</sub> Me <sub>2</sub> (SiMe <sub>3</sub> ) <sub>2</sub> (II) with C <sub>6</sub> H <sub>5</sub> -CHO (R'1)	159
5.4.4.1	π-addition.	159
5.4.4.2	σ-insertion.	161
5.4.4.3	Ring opening	162
5.4.4.4	Exocyclic σ-insertion reaction	163
5.4.5	Reaction pathways of c-Si <sub>3</sub> Me <sub>2</sub> (SiMe <sub>3</sub> ) <sub>2</sub> (II) with H-CHO (R'2)	165
5.4.5.1	π-addition	165
5.4.5.2	σ-insertion reaction	166
5.4.5.3	Ring opening	167
5.4.5.4	Exocyclic σ-insertion	168
5.5	Conclusion	171
	Reference	172

**Chapter 6:** Recommendations for Future Works 175

Lists of Publications and Conferences Presentations xxv



## LIST OF FIGURES

Figure No.	Title of Figures	Page No.
<b>Chapter 1: Introduction</b>		
<b>1.1</b>	A model potential energy surface	<b>22</b>
<b>1.2</b>	Structure of disilene	<b>34</b>
<b>1.3</b>	Structure cyclotrisilene synthesised by Ichinohe et al. 1999	<b>36</b>
<b>Chapter 2: Substituent effects on the dimerization reaction of silenes: the di-radical and the zwitter-ion reaction pathways</b>		
<b>2.1</b>	Intermediates and transition states located for the dimerization of H-CSi-H via zwitter-ion pathway. Relative free energies are given in kcal/mol and bond lengths in Å. Natural charges are also shown.	<b>55</b>
<b>2.2</b>	Intermediates and transition states located for the dimerization of HO-CSi-H via Zwitter- ion pathway. Relative free energies are given in kcal/mol and bond lengths in Å. A reactant complex with totally separated silenes could not be optimized.	<b>58</b>
<b>2.3</b>	Intermediates and transition states located for the dimerization of NC-CSi-H via Zwitter- ion pathway. Relative free energies are given in kcal/mol and bond lengths in Å. A reactant complex with totally separated silenes could not be optimized.	<b>58</b>
<b>2.4</b>	Comparative free energy profile diagram for the dimerization of R-CSi-H, H-CSi-R and R-CSi-R via zwitter-ionic pathway.	<b>59</b>
<b>2.5</b>	Z-TS2 of (a) H-CSi-CH <sub>3</sub> , (b) H-CSi-SiH <sub>3</sub> (c) H-CSi-OH and (d) H-CSi-CN	<b>60</b>
<b>2.6</b>	Intermediates and transition states located for the trimerization of H-CSi-H via diradical pathway. Relative free energies are given in kcal/mol and bond lengths in Å	<b>63</b>
<b>2.7</b>	Comparative free energy profile diagram for the dimerization of R-CSi-H, H-CSi-R and R-CSi-R via diradical formation.	<b>65</b>
<b>Chapter 3: Substituent effects on the addition of small molecules (NH<sub>3</sub>, NO, CO) to silene and silene-silylene isomerization</b>		
<b>3.1</b>	Reaction scheme for N-H activation by H-CSi-H. Relative free energies are given in kcal/mol and bond lengths in Å.	<b>79</b>
<b>3.2</b>	Comparative free energy profiles for N-H activation by R-CSi-H, H-CSi-R and R-CSi-R	<b>81</b>
<b>3.3</b>	Calculated reaction scheme for the NO addition to H-CSi-H. Relative free energy values in kcal/mol, bond lengths in Å and Mulliken spin density in a.u	<b>83</b>
<b>3.4</b>	Comparative free energy profile for NO activation by R-CSi-H, H-CSi-R and R-CSi-R	<b>85</b>
<b>3.5</b>	Calculated reaction scheme for the CO addition to H <sub>2</sub> C= SiH <sub>2</sub> . Relative	<b>86</b>



	free energy values in kcal/mol and bond lengths in Å.	
<b>3.6</b>	Comparative free energy profile for CO activation by R-CSi-H, H-CSi-R and R-CSi-R	<b>89</b>
<b>3.7</b>	Reaction scheme for silene-silylene rearrangement. Relative free energy values in kcal/mol and bond lengths in Å.	<b>90</b>
<b>3.8</b>	Comparative free energy profile for the silene-silylene rearrangement in R-CSi-H, H-CSi-R and R-CSi-R.	<b>93</b>
<b>Chapter 4: Reactions of 1,2,3,3-tetramethyl cyclotrisilene with propylene, phenylacetylene, trimethylsilylacetylene, formaldehyde and benzaldehyde</b>		
<b>4.1</b>	First stable cyclotrisilene synthesised by Iwamoto et.al. (1999)	<b>99</b>
<b>4.2</b>	1,2,3,3-tetramethyl cyclotrisilene (c-Si <sub>3</sub> Me <sub>4</sub> ; <b>I</b> )	<b>104</b>
<b>4.3</b>	Intermediates and transitions states involved in the $\pi$ -addition pathwa of <b>I</b> and <b>R1</b> . Relative free energies are given in kcal/mol and bond lengths in Å	<b>105</b>
<b>4.4</b>	Intermediates and transitions states involved in the $\sigma$ -insertion pathway of <b>I</b> + <b>R1</b> . Relative free energies are given in kcal/mol and bond lengths in Å	<b>107</b>
<b>4.5</b>	Intermediates and transitions states involved in the ring opening reaction pathway of <b>I</b> + <b>R1</b> . Relative free energies are given in kcal/mol and bond lengths in Å	<b>108</b>
<b>4.6</b>	Intermediates and transitions states involved in the exocyclic $\sigma$ -insertion reaction pathway of <b>I</b> + <b>R1</b> . Relative free energies are given in kcal/mol and bond lengths in Å	<b>109</b>
<b>4.7</b>	Comparative free energy profile diagram for the different reaction pathways between <b>I</b> + <b>R1</b>	<b>110</b>
<b>4.8</b>	Intermediates and transitions states involved in the $\pi$ -addition pathway of <b>I</b> + <b>R2</b> . Relative free energies are given in kcal/mol and bond lengths in Å.	<b>111</b>
<b>4.9</b>	Intermediates and transitions states involved in the $\sigma$ -insertion pathway of <b>I</b> + <b>R2</b> . Relative free energies are given in kcal/mol and bond lengths in Å	<b>112</b>
<b>4.10</b>	Intermediates and transitions states involved in the ring opening pathway of <b>I</b> + <b>R2</b> . Relative free energies are given in kcal/mol and bond lengths in Å.	<b>114</b>
<b>4.11</b>	Intermediates and transitions states involved in the exocyclic $\sigma$ -insertion pathway of <b>I</b> + <b>R2</b> . Relative free energies are given in kcal/mol and bond lengths in Å.	<b>115</b>
<b>4.12</b>	Comparative free energy profile diagram for the different reaction pathways between <b>I</b> + <b>R2</b>	<b>116</b>
<b>4.13</b>	Intermediates and transitions states involved in the $\pi$ -addition pathway of <b>I</b> + <b>R3</b> . Relative free energies are given in kcal/mol and bond lengths in Å.	<b>117</b>
<b>4.14</b>	Intermediates and transitions states involved in the $\sigma$ -insertion pathway	<b>118</b>

	of <b>I</b> and <b>R3</b> . Relative free energies are given in kcal/mol and bond lengths in Å	
<b>4.15</b>	Intermediates and transitions states involved in the ring opening reaction pathway of <b>I</b> + <b>R3</b> . Relative free energies are given in kcal/mol and bond lengths in Å	<b>119</b>
<b>4.16</b>	Intermediates and transitions states involved in the exocyclic $\sigma$ -insertion reaction pathway of <b>I</b> and <b>R3</b> . Relative free energies are given in kcal/mol and bond lengths in Å	<b>121</b>
<b>4.17</b>	Comparative free energy profile diagram for the different reaction pathways between <b>I</b> and <b>R3</b>	<b>122</b>
<b>4.18</b>	Intermediates and transitions states involved in the $\pi$ -addition reaction pathway of <b>I</b> + <b>R'1</b> . Relative free energies are given in kcal/mol and bond lengths in Å	<b>123</b>
<b>4.19</b>	Intermediates and transitions states involved in the $\sigma$ -insertion reaction pathway of <b>I</b> + <b>R'1</b> . Relative free energies are given in kcal/mol and bond lengths in Å.	<b>125</b>
<b>4.20</b>	Intermediates and transitions states involved in the ring opening reaction pathway of <b>I</b> + <b>R'1</b> . Relative free energies are given in kcal/mol and bond lengths in Å.	<b>126</b>
<b>4.21</b>	Intermediates and transitions states involved in the exocyclic $\sigma$ -insertion reaction pathway of <b>I</b> + <b>R'1</b> . Relative free energies are given in kcal/mol and bond lengths in Å.	<b>127</b>
<b>4.22</b>	Comparative free energy profile diagram for the different reaction pathways between <b>I</b> + <b>R'1</b>	<b>128</b>
<b>4.23</b>	Intermediates and transitions states involved in the $\pi$ -addition reaction pathway of <b>I</b> and <b>R'2</b> . Relative free energies are given in kcal/mol and bond lengths in Å	<b>129</b>
<b>4.24</b>	Intermediates and transitions states involved in the $\sigma$ -insertion reaction pathway of <b>I</b> and <b>R'2</b> . Relative free energies are given in kcal/mol and bond lengths in Å.	<b>130</b>
<b>4.25</b>	Intermediates and transitions states involved in the ring opening reaction pathway of <b>I</b> and <b>R'2</b> . Relative free energies are given in kcal/mol and bond lengths in Å.	<b>131</b>
<b>4.26</b>	Intermediates and transitions states involved in the exocyclic $\sigma$ -insertion reaction pathway of <b>I</b> and <b>R'2</b> . Relative free energies are given in kcal/mol and bond lengths in Å.	<b>132</b>
<b>4.27</b>	Comparative free energy profile diagram for the different reaction pathways between <b>I</b> and <b>R'2</b>	<b>133</b>
<b>Chapter 5: Reactions of 1,2-bis(trimethylsilyl)-3,3-dimethyl cyclotrisilene with propylene, phenyl acetylene, trimethylsilylacetylene, formaldehyde and benzaldehyde</b>		
<b>5.1</b>	1,2-bis(trimethylsilyl)-3,3-dimethylcyclotrisilene; <b>II</b>	<b>141</b>
<b>5.2</b>	Intermediates and transitions states involved in the $\pi$ -addition pathway <b>II</b> and <b>R1</b> . Relative free energies are given in kcal/mol and bond lengths in Å	<b>142</b>



<b>5.3</b>	Intermediates and transitions states involved in the $\sigma$ -insertion pathway of <b>II</b> and <b>R1</b> . Relative free energies are given in kcal/mol and bond lengths in Å	<b>143</b>
<b>5.4</b>	Intermediates and transitions states involved in the ring opening pathway of <b>II</b> and <b>R1</b> . Relative free energies are given in kcal/mol and bond lengths in Å	<b>144</b>
<b>5.5</b>	Intermediates and transitions states involved in the exocyclic $\sigma$ -insertion pathway of 1,2-bis(trimethylsilyl)-3,3-dimethyl cyclotrisilene ( <b>II</b> ) and Phenyl acetylene ( <b>R1</b> ). Relative free energies are given in kcal/mol and bond lengths in Å	<b>146</b>
<b>5.6</b>	Comparative free energy profile diagram for the different reaction pathways between <b>II</b> and <b>R1</b> .	<b>147</b>
<b>5.7</b>	Intermediates and transitions states involved in the $\pi$ -addition pathway of <b>II</b> and <b>R2</b> . Relative free energies are given in kcal/mol and bond lengths in Å.	<b>148</b>
<b>5.8</b>	Intermediates and transitions states involved in the $\sigma$ -insertion pathway <b>II</b> and <b>R2</b> . Relative free energies are given in kcal/mol and bond lengths in Å.	<b>149</b>
<b>5.9</b>	Intermediates and transitions states involved in the ring opening pathway of <b>II</b> and <b>R2</b> . Relative free energies are given in kcal/mol and bond lengths in Å.	<b>150</b>
<b>5.10</b>	Intermediates and transitions states involved in the exocyclic $\sigma$ -insertion pathway of <b>II</b> and <b>R2</b> . Relative free energies are given in kcal/mol and bond lengths in Å.	<b>151</b>
<b>5.11</b>	Comparative free energy profile diagram for the different reaction pathways between <b>II</b> and <b>R2</b>	<b>152</b>
<b>5.12</b>	Intermediates and transitions states involved in the $\pi$ -addition pathway of <b>II</b> and <b>R3</b> . Relative free energies are given in kcal/mol and bond lengths in Å.	<b>153</b>
<b>5.13</b>	Intermediates and transitions states involved in the $\sigma$ -insertion pathway of <b>II</b> and <b>R3</b> . Relative free energies are given in kcal/mol and bond lengths in Å.	<b>155</b>
<b>5.14</b>	Intermediates and transitions states involved in the ring opening reaction pathway of <b>II</b> and <b>R3</b> . Relative free energies are given in kcal/mol and bond lengths in Å.	<b>156</b>
<b>5.15</b>	Intermediates and transitions states involved in the exocyclic $\sigma$ -insertion reaction pathway of <b>II</b> and <b>R3</b> . Relative free energies are given in kcal/mol and bond lengths in Å.	<b>157</b>
<b>5.16</b>	Comparative free energy profile diagram for the different reaction pathways between <b>II</b> and <b>R3</b>	<b>158</b>
<b>5.17</b>	Intermediates and transitions states involved in the $\pi$ -addition pathway of <b>II</b> and <b>R'1</b> . Relative free energies are given in kcal/mol and bond lengths in Å	<b>160</b>
<b>5.18</b>	Intermediates and transitions states involved in the $\sigma$ -insertion pathway of <b>II</b> and <b>R'1</b> . Relative free energies are given in kcal/mol and bond	<b>161</b>

	lengths in Å	
<b>5.19</b>	Intermediates and transitions states involved in the ring opening pathway of <b>II</b> and <b>R'1</b> . Relative free energies are given in kcal/mol and bond lengths in Å	<b>162</b>
<b>5.20</b>	Intermediates and transitions states involved in the exocyclic $\sigma$ -insertion pathway of <b>II</b> and <b>R'1</b> . Relative free energies are given in kcal/mol and bond lengths in Å	<b>163</b>
<b>5.21</b>	Comparative free energy profile diagram for the different reaction pathways between <b>II</b> and <b>R'1</b>	<b>164</b>
<b>5.22</b>	Intermediates and transitions states involved in the $\pi$ -addition reaction pathway of <b>II</b> and <b>R'2</b> . Relative free energies are given in kcal/mol and bond lengths in Å	<b>165</b>
<b>5.23</b>	Intermediates and transitions states involved in the $\sigma$ -insertion reaction pathway of <b>II</b> and <b>R'2</b> . Relative free energies are given in kcal/mol and bond lengths in Å	<b>166</b>
<b>5.24</b>	Intermediates and transitions states involved in the ring opening reaction pathway of <b>II</b> and <b>R'2</b> . Relative free energies are given in kcal/mol and bond lengths in Å	<b>167</b>
<b>5.25</b>	Intermediates and transitions states involved in the exocyclic $\sigma$ -insertion reaction pathway of <b>II</b> and <b>R'2</b> . Relative free energies are given in kcal/mol and bond lengths in Å	<b>168</b>
<b>5.26</b>	Comparative free energy profile diagram for the different reaction pathways between <b>II</b> and <b>R'2</b>	<b>169</b>





## LIST OF TABLES

Table No.	Title of Table	Page No.
<b>Chapter 1: Introduction</b>		
<b>Chapter 2: Substituent effects on the dimerization reaction of silenes: the di-radical and the zwitter-ion reaction pathways</b>		
<b>2.1</b>	Isodesmic reaction energy values	<b>52</b>
<b>2.2</b>	H-CSi-R: Mono substituent on Si, R-CSi-H: Mono substituent on C, R-CSi-R: One substituent each on C and Si. $V_C$ : MSEP at C, $V_{Si}$ : MSEP at Si.	<b>53</b>
<b>2.3</b>	Relative free energy values (in kcal/mol) of intermediates and transition states involved in the dimerization of R-CSi-H, H-CSi-R and R-CSi-R via zwitter-ion pathway	<b>56</b>
<b>2.4</b>	Relative free energy values (in kcal/mol) of intermediates and transition states involved in the dimerization of R-CSi-H, H-CSi-R and R-CSi-R via zwitter-ion pathway calculated at PW6B95D3/6-311++G(d,p)	<b>61</b>
<b>2.5</b>	Relative free energy values (in kcal/mol) of intermediates and transition states involved in the dimerization of R-CSi-H, H-CSi-R and R-CSi-R via diradical pathway	<b>63</b>
<b>Chapter 3: Substituent effects on the addition of small molecules (NH<sub>3</sub>, NO, CO) to silene and silene-silylene isomerization</b>		
<b>3.1</b>	Relative free energy values of intermediates and transition states involved in the N-H activation by R-CSi-H, H-CSi-R and R-CSi-R	<b>80</b>
<b>3.2</b>	Relative energy values of intermediates and transition states involved in the N-H activation by R-CSi-H, H-CSi-R and R-CSi-R calculated at PW6B95D3/6-311++G(d,p)	<b>82</b>
<b>3.3</b>	Relative free energy values of intermediates and transition states involved in the addition of NO to R-CSi-H, H-CSi-R and R-CSi-R	<b>83</b>
<b>3.4</b>	Relative energy values of intermediates and transition states involved in the addition of NO to R-CSi-H, H-CSi-R and R-CSi-R calculated at PW6B95D3/6-311++G(d,p)	<b>86</b>
<b>3.5</b>	Relative free energy values of intermediates and transition states involved in the addition of CO to R-CSi-H, H-CSi-R and R-CSi-R	<b>87</b>
<b>3.6</b>	Relative energy values of intermediates and transition states involved in the addition of CO to R-CSi-H, H-CSi-R and R-CSi-R calculated at PW6B95D3/6-311++G(d,p)	<b>89</b>
<b>3.7</b>	Relative free energy values of intermediates and transition states involved in the silene-silylene rearrangement of R-CSi-H, H-CSi-R and R-CSi-R	<b>91</b>
<b>3.8</b>	Relative energy values of intermediates and transition states involved in the silene-silylene rearrangement of R-CSi-H, H-CSi-R and R-CSi-R calculated at PW6B95D3/6-311++G(d,p)	<b>93</b>





## LIST OF SCHEMES

Scheme No.	Title of Schemes	Page No.
<b>Chapter 1: Introduction</b>		
<b>1.1</b>	Flash pyrolysis of 1,1-dimethyl-1-silacyclobutane indicating the intermediate formation of a compound with C=Si	<b>25</b>
<b>1.2</b>	Photochemical decomposition of trimethylsilyldiazomethane resulted in the first generation of a silene	<b>26</b>
<b>1.3</b>	Photochemical rearrangement of acyl silane to generate the first stable silene (Brook silene)	<b>26</b>
<b>1.4</b>	Addition of an alcohol to silene	<b>28</b>
<b>1.5</b>	Reverse polarisation in silenes	<b>29</b>
<b>1.6</b>	Substituent effect leading to reverse polarisation in silene	<b>29</b>
<b>1.7</b>	Reaction of 1-substituted 1-methylsilacyclobutanes with alcohols generating silene intermediate, detectible by flash photolysis	<b>31</b>
<b>1.8</b>	Photolysis of 2,2- bis(mesityl)hexamethyltrisilane led to the discovery of a stable disilene	<b>33</b>
<b>1.9</b>	Reaction between 2,2,2-tribromo-1,1-di(tert-butyl)-1-methyldisilane and 2,2-dibromo-1,1,3,3- tetra(tert-butyl)-1,3-dimethyltrisilane: formation of the first stable cyclotrisilene.	<b>35</b>
<b>1.10</b>	Reaction of ( <sup>t</sup> Bu <sub>2</sub> MeSi) <sub>2</sub> SiLi <sub>2</sub> with <sup>t</sup> Bu <sub>3</sub> SiBr <sub>2</sub> SiBr <sub>2</sub> Si <sup>t</sup> Bu <sub>3</sub> led to the generation of a highly crowded stable cyclotrisilene	<b>35</b>
<b>1.11</b>	Slow isomerisation of the disilyne <b>5</b> in solution at room temperature generated cyclotrisilene <b>6</b> as the only product.	<b>36</b>
<b>1.12</b>	Step-wise synthesis of cyclotrisilene ( <b>6</b> ) from Dsi <sub>2</sub> NpSiSiH <sub>2</sub> Cl ( <b>1</b> )	<b>36</b>
<b>Chapter 2: Substituent effects on the dimerization reaction of silenes: the di-radical and the zwitter-ion reaction pathways</b>		
<b>2.1</b>	Addition of alkynes to silene; the diradical pathway	<b>48</b>
<b>2.2</b>	The [4+2] cyclo-addition and ene-addition of silenes to dienes	<b>49</b>
<b>2.3</b>	The head-to-tail and head-to-head modes of dimerization of silenes	<b>49</b>
<b>2.4</b>	The zwitter-ion intermediate pathway (Z) and the diradical intermediate pathway (DR) for the head-to-tail dimerization of the parent silene.	<b>52</b>
<b>2.5</b>	Isodesmic reaction scheme used for the analysis	<b>52</b>

<b>Chapter 3: Substituent effects on the addition of small molecules (NH<sub>3</sub>, NO, CO) to silene and silene-silylene isomerization</b>		
<b>3.1</b>	CO <sub>2</sub> activation by the chiral silene <b>I</b>	<b>72</b>
<b>3.2</b>	Addition of alcohols to silene	<b>73</b>
<b>3.3</b>	The silene-silylene isomerisation	<b>74</b>
<b>3.4</b>	The silene-silylene isomerisation (reported by S. Ishida et al)	<b>74</b>
<b>3.5</b>	Preparation of the precursor 1,3-Diaza-2,2-dichloro-2-sila-4-cyclopentene for silylene synthesis	<b>75</b>
<b>3.6</b>	Preparation of the first (cyclic) silylene from 1,3-Diaza-2,2-dichloro-2-sila-4-cyclopentene	<b>75</b>
<b>3.7</b>	Synthesis of the stable acyclic (aryl-thio) substituted silylene	<b>76</b>
<b>3.8</b>	Hydrogen activation by silylene	<b>77</b>
<b>3.9</b>	O-H bond activation by silylene	<b>77</b>
<b>Chapter 4: Reactions of 1,2,3,3-tetramethyl cyclotrisilene with propylene, phenylacetylene, trimethylsilylacetylene, formaldehyde and benzaldehyde</b>		
<b>4.1</b>	Formation of a $\pi$ -addition product between a cyclotrisilene molecule and an unsaturated reactant	<b>100</b>
<b>4.2</b>	Formation of an $\sigma$ -insertion product between a cyclotrisilene molecule and an isocyanide.	<b>101</b>
<b>4.3</b>	Formation of an exocyclic $\sigma$ -insertion product between a cyclotrisilene molecule and an unsaturated reactant.	<b>101</b>
<b>4.4</b>	Formation of disilylenyl silylene(intermediate) between a cyclotrisilene molecule and an unsaturated reactant	<b>102</b>
<b>4.5</b>	Four possible reaction pathways of cyclotrisilene	<b>104</b>
<b>Chapter 5: Reactions of 1,2-bis(trimethylsilyl)-3,3-dimethyl cyclotrisilene with propylene, phenyl acetylene, trimethylsilylacetylene, formaldehyde and benzaldehyde</b>		
<b>5.1</b>	Four distinct reaction pathways that can be expected between cyclotrisilene and an unsaturated substrate on their encounter	<b>140</b>



## LIST OF ABBREVIATIONS

ADF	Amsterdam Density Functional
AO	Atomic Orbital
BO	Born-Oppenheimer
CC	Coupled Cluster
CGTO	Contracted Gaussian Type Orbital
CI	Configuration Interaction
CIS	Configuration Interaction Single-excitation
CISD	Configuration Interaction Double-excitation
CISDT	Configuration Interaction Triple-excitation
CISDTQ	Configuration Interaction Quadruple-excitation
D-	Diradical pathway
DFT	Density Functional Theory
DR	Diradical
D-TS	Diradical pathway Transition State
DZ	Double Zeta
GGA	Generalized Gradient Approximation
GS	Ground State
GTO	Gaussian Type Orbital
HF	Hartree-Fock
HK	Hohenberg-Kohn
INT	Intermediate
LCAO	Linear Combination of Atomic Orbital
LDA	Local Density Approximation
MBPT	Many Body Perturbation Theory
MD	Molecular Dynamics

MEP	Minimum Energy Path
MESP	Molecular Electrostatic Potential
MM	Molecular Mechanics
MO	Molecular Orbital
MP	Møller–Plesset
NMR	Nuclear Magnetic Resonance
PDT	Product
PES	Potential Energy Surface
PGTO	Primitive Gaussian Type Orbital
PHF	Post Hartree-Fock
QM	Quantum Mechanics
RHF	Roothaan-Hartree-Fock
RNT	Reactant
ro	Ring Opening
RSPT	Rayleigh-Schrodinger Perturbation Theory
SCF	Self Consistent Filed
STO	Slater Type Orbital
STQN	Synchronous Transit-Guided Quasi-Newton
TMS	Trimethylsilane
TS	Transition State
TST	Transition State Theory
X $\sigma$	Exocyclic $\sigma$ -insertion
Z-	Zwitter-ionic pathway
Z-TS	Zwitter-ionic pathway Transition State
ZW	Zwitter-ion

## LIST OF SYMBOLS

$\alpha$	Alpha
$\beta$	Beta
$\Delta$	Delta
$\varepsilon$	Epsilon
H	Eta
$\theta$	Theta
$\lambda$	Lambda
$\mu$	Mu
N	Nu
O	Omicron
$\pi$	Pi
$\rho$	Rho
$\Sigma, \sigma$	Sigma
$\Phi, \varphi$	Phi
X	Chi
$\Psi$	Psi
$\omega$	Omega





## ABSTRACT

As a landmark discovery in organosilicon chemistry, in 1981, Brook et al synthesised a compound containing C=Si double bond and West et al another one, containing Si=Si double bond. The present research titled 'Quantum Mechanical Assessment of Substituent Effect of Doubly Bonded Silicon Compounds' encompasses the computational analysis of some typical reactions of the substituted silenes (compounds with C=Si) and cyclotrisilene (compounds with Si=Si) with special emphasis on the substituent effects. The effect of substituents including R = CH<sub>3</sub>, SiH<sub>3</sub>, OH, CN and F on the dimerization of H<sub>2</sub>C=SiH<sub>2</sub> is deeply explored and discussed. The study revealed that the dimerization process preferentially adopted a free radical reaction pathway and the substituents affecting the natural polarity of the C=Si bond of the silene have a remarkable control over the energetics of the dimerization. Being a highly reactive species, silenes can be made use of for the small molecule activation process. The activity of silenes on NH<sub>3</sub>, CO and NO is systematically examined and the effect of substituents on the reactive potential of silenes is scrutinised. Our analysis endorsed the competence of silenes in activating the polar bonds in small molecules and identified that the  $\sigma$ -withdrawing and  $\pi$ -donating substituents improve their potential significantly. Silylene is the silicon alternative of carbene. It is an extremely reactive species and can activate even the most stable chemical bonds. We have studied the silene-silylene rearrangement in detail and the effect of the substituents on the energetics and mechanism of the process. Our study revealed that the  $\pi$ -donating substituents that are successful in inducing a polarity reversal of the C=Si bond of silene can bring down the barrier height of the silene-silylene rearrangement to great extends. Cyclotrisilene is the simplest cyclic compound containing a Si=Si double bond. We have conducted a detailed exploration of the reaction pathways and energetics of 1,2,3,3-tetramethyl cyclotrisilene with a few alkynes and aldehydes. Our investigation ascertained that the  $\sigma$ -insertion and  $\pi$ -addition are the spontaneous reaction pathways of the silenes with substrates carrying multiple bonds. Ring opening reactions yielding disilylenyl silylene and is also feasible under normal conditions. However, exocyclic  $\sigma$ -insertion reaction involves huge activation energy and is not practicable. The energetics of the reaction significantly depends on the characteristics of the substrate involved. An exactly similar study is carried out with 1,2-bis(trimethylsilyl)-3, 3-dimethylcyclotrisilene instead of 1,2,3,3-tetramethyl cyclotrisilene. This corroborative study manifested the effect of substituents on the cyclotrisilene ring on the four reaction pathways subjected to analysis.



# സംഗ്രഹം

1981 ൽ ബ്രൂക്ക് എന്ന ശാസ്ത്രജ്ഞനും സംഘവും C=Si ഉൾച്ചേർന്ന സംയുക്തങ്ങൾ വികസിപ്പിച്ചെടുത്തതും, വെസ്റ്റ് എന്ന ശാസ്ത്രജ്ഞനും സംഘവും Si=Si ഉൾച്ചേർന്ന സംയുക്തങ്ങൾ വികസിപ്പിച്ചെടുത്തതും ഓർഗാനോ സിലിക്കൺ കെമിസ്ട്രി എന്ന ശാസ്ത്ര ശാഖക്ക് വലിയ കുതിച്ചു ചട്ടം സമ്മാനിച്ചു. 'ഇരുട്ട ബോണ്ടുകൾ ഉൾച്ചേർന്ന സിലിക്കോൺ സംയുക്തങ്ങളിലെ സബ്സ്റ്റിറ്റ്യൂവ്നുകളുടെ പ്രഭാവത്തിന്റെ ക്യാണ്ടം മെക്കാനിക്കൽ വിലയിരുത്തൽ' എന്ന ഈ ഗവേഷണ പ്രബന്ധത്തിൽ സബ്സ്റ്റിറ്റ്യൂട്ടഡ് സിലീൻ ( C=Si ബോണ്ടുകളുള്ള സംയുക്തം ) സൈക്ലോ ട്രൈ സിലീൻ (Si=Si ബോണ്ടുകളുള്ള സംയുക്തം ) എന്നിവയുടെ മേലുള്ള സബ്സ്റ്റിറ്റ്യൂവ്നുകളുടെ പ്രഭാവത്തെ കുറിച്ചാണ് പ്രധാനമായി ചർച്ച ചെയ്യുന്നത്. ഇതൊരു സൈദ്ധാന്തിക തലത്തിലുള്ള കമ്പ്യൂട്ടേഷനൽ പഠനമാണ് . സിലീൻ എന്ന സംയുക്തത്തിന്റെ ഡൈമെറൈസേഷൻ റീയാക്ഷന്റെ മേൽ സബ്സ്റ്റിറ്റ്യൂവ്നുകളായ R = CH<sub>3</sub>, SiH<sub>3</sub>, OH, F, CN എന്നിവയ്ക്കുള്ള സ്വാധീനം വിശദമായി പഠിച്ചിട്ടുണ്ട്. ഈ ഡൈമെറൈസേഷൻ റീയാക്ഷൻ ഒരു ഫ്രീ റാഡിക്കൽ പഥത്തിലൂടെയാണ് കടന്നുപോകുന്നതെന്നും, C=Si യുടെ സ്വാഭാവിക ചാർജ്ജ് വിതരണത്തെ സ്വാധീനിക്കാൻ കഴിയുന്ന സബ്സ്റ്റിറ്റ്യൂവ്നുകൾക്ക് റീയാക്ഷന്റെ മേൽ നിർണായകമായ സ്വാധീനം ഉണ്ടെന്നും കണ്ടെത്താനായി . ഗംഭീരമായ റീയാക്ടിവിറ്റിയുള്ള സംയുക്തം എന്നനിലക്ക്, സിലീൻ തന്മാത്രക്ക് ചെറു തന്മാത്രകളെ കഠിനമായ രീതിയിൽ ഉത്തേജിപ്പിക്കാനാവും. NH<sub>3</sub>, CO, NO എന്നീ ചെറു തന്മാത്രകളെ ഉത്തേജിപ്പിക്കാനുള്ള സിലീന്റെ കഴിവും സബ്സ്റ്റിറ്റ്യൂവ്നുകളുടെ ഈ റീയാക്ഷന്റെ മേലുള്ള സ്വാധീനവും ആഴത്തിൽ പഠിച്ചു. പോളാർ ബോണ്ടുള്ള ചെറു തന്മാത്രകളിലെ ബോണ്ടിനെ നിർണായകമായി സ്വാധീനിക്കാൻ സിലീനുകൾക്ക് സാധിക്കുമെന്നും, പൈ-ഇലക്ട്രോണുകളെ നൽകാനും സിഗ്മ - ഇലക്ട്രോണുകളെ വലിച്ചെടുക്കാനും കഴിയുന്ന സബ്സ്റ്റിറ്റ്യൂവ്നുകൾ ഇക്കാര്യത്തിൽ വളരെ പ്രയോജനകരമാണെന്നും കണ്ടെത്തി. കാർബീനെന്ത കാർബൺ സംയുക്തത്തിന്റെ സിലിക്കൺ പതിപ്പാണ് സിലൈലീൻ. ഈ വസ്തു അങ്ങേയറ്റം റീയാക്ടിവിറ്റിയുള്ളതും ഏറ്റവും ഉറച്ച ബോണ്ടുകളെ പോലും വിഘടിപ്പിക്കാൻ കഴിവുള്ളതും ആണ്. സിലീൻ-സിലൈലീൻ റീഅറേഞ്ച്മെന്റ് പഠന വിധേയമാക്കുകയും അതിന്റെമേൽ സബ്സ്റ്റിറ്റ്യൂവ്നുകൾക്കുള്ള സ്വാധീനം ആഴത്തിൽ പരിശോധിക്കുകയും ചെയ്തു. പൈ-ഇലക്ട്രോണുകളെ നൽകാനും സിഗ്മ - ഇലക്ട്രോണുകളെ വലിച്ചെടുക്കാനും കഴിയുന്ന സബ്സ്റ്റിറ്റ്യൂവ്നുകൾ ഈ റീഅറേഞ്ച്മെന്റിന്റെ ആക്ടിവേഷൻ ഊർജ്ജത്തെ വളരെയേറെ താഴ്ത്തിക്കൊണ്ടുവരുവാൻ സഹായിക്കും എന്ന നിർണായകമായ കണ്ടെത്തൽ നടത്താൻ കഴിഞ്ഞു. Si=Si ഡബിൾ ബോണ്ടുള്ള ഏറ്റവും ലളിതമായ സൈക്ലിക് സംയുക്തമാണ് സൈക്ലോട്രൈസിലീൻ. 1,2,3,3-ടെട്രാ മീതൈൽ സൈക്ലോട്രൈസിലീൻ എന്ന സംയുക്തവും ഏതാനും ആൽകൈനുകളും ആൽഡിഹൈഡുകളും തമ്മിലുള്ള റീയാക്ഷനുകളും വളരെ വിശദമായ പഠനത്തിന് വിധേയമാക്കി. മൾട്ടിപ്പിൾ ബോണ്ട് അടങ്ങിയ സംയുക്തങ്ങളുമായി 1,2,3,3-ടെട്രാ മീതൈൽ സൈക്ലോട്രൈസിലീൻ പൈ-അഡീഷൻ സിഗ്മ-ഇൻസെർഷൻ എന്നീ റീയാക്ഷനുകളാണ് സ്വാഭാവികമായി ഏർപ്പെടുക എന്ന് കണ്ടെത്തി. ഡൈ സിലീനെൻ സിലൈലീൻ എന്ന



സംയുക്തം ഉല്പാദിപ്പിക്കപ്പെടുന്ന റിങ് ഓപ്പണിങ് റീയാക്ഷനും സാധാരണ പരീക്ഷണ സാഹചര്യങ്ങളിൽ നടത്താനാവും എന്നും തെളിഞ്ഞു . എന്നിരുന്നാലും, എക്സ്ട്രാ സൈക്ലിക് സിഗ്മ ഇൻസെർഷൻ റീയാക്ഷൻ, അതുൾപ്പെടുന്ന എത്തിപ്പെടാനാവാത്ത ആക്ടിവേഷൻ ഊർജ്ജം മൂലം നടത്താൻ സാധിക്കുകയില്ല എന്ന നിഗമനത്തിൽ എത്തി. റീയാക്ഷനുകളുടെ സ്വഭാവവും, അതിൽ കടന്നുവരുന്ന ഊർജ്ജ മാറ്റങ്ങളും, ഉപയോഗിക്കുന്ന സബ്സ്ട്രേറ്റിന്റെ പ്രത്യേകതകളുമായി അങ്ങേയറ്റം ബന്ധപ്പെട്ടിരിക്കുന്നതായി കണ്ടെത്തി. 1,2,3,3-ടെട്രാ മീതൈൽ സൈക്ലോടെസീലിനുമായിനുമായി നടത്തിയ എല്ലാ പരീക്ഷണങ്ങളും 1,2-ബിസ് (ട്രിമീതൈൽസിലൈൽ) - 3,3 - ഡിമീതൈൽ സൈക്ലോടെസീലിൻ എന്ന സംയുക്തവും ആയി പുനഃ പരിശോധന ചെയ്തു. സൈക്ലോടെസീലിൻതന്മാത്രയിൽ ഘടിപ്പിച്ചിരിക്കുന്ന സബ്സ്ട്രിക്ട്യൂവന്റുകൾക്ക് മേൽപ്പറഞ്ഞ റീയാക്ഷനുകൾക്ക് മേൽ വലിയ സ്വാധീനം ഉള്ളതായി കണ്ടെത്തി .

## PREFACE

Schrödinger equation is the principal equation of quantum mechanics. An exact solution of the Schrödinger equation is unachievable for systems having more than one electron. Therefore, modified versions of the fundamental Schrödinger equation, collectively known as approximation methods are designed systems containing more than one interaction. One of the rapidly developing subfields of quantum mechanics is computational chemistry, where the chemical problems are solved in extreme precision using automated calculations. Most popular methods in computational chemistry include (a) Molecular mechanics (MM) (b) ab-initio methods (c) semiempirical treatments (d) the DFT methods (e) Monte Carlo and molecular dynamics simulations and (f) molecular mechanics (QM/MM) and hybrid quantum mechanics methods. Ab initio treatments, which provide the most accurate results, are employable with relatively small systems only. The Hartree-Fock theory which provides an approximation to the Schrodinger equation forms the fundamental Ab initio treatment. The methods which attempt further refinement of the HF method are collectively named as Post Hartree-Fock (PHF) methods. The most popular among them are the configuration interaction treatment (CI) coupled cluster method (CC) and many body perturbation theory (MBPT). The DFT method which expresses the many electrons system as a function of the total electron density is another widely accepted approach in computational chemistry.

Chemistry before 1980s believed that the multiple bonds to silicon is so unstable that it is impossible generate such compounds. As a landmark discovery in organosilicon chemistry, in 1981, Brook et al synthesised a compound containing C=Si double bond and West et al another one, containing Si=Si double bond. This brings to light enormous scope in multiple bond chemistry of silicon compounds. The present research titled 'quantum mechanical assessment of substituent effect of doubly bonded silicon compounds' encompasses the computational analysis of some typical reactions of the substituted silenes (compounds with C=Si) with special emphasis on the substituent effects. The parent compounds included are silene ( $\text{H}_2\text{C}=\text{SiH}_2$ ) and cyclotrisilene ( $\text{Si}_3\text{H}_4$ ). Chapter one dealing with these introductory sessions.

Chapter 2 describes the substituent effects on the dimerization reaction of silenes: the di-radical and the zwitter-ion reaction pathways. Due to the inherently polar nature of the silene bond ( $\delta^+\text{Si}=\text{C}\delta^-$ ), they freely react with nucleophilic substrates including amines, carboxylic acids, alcohols, dienes, alkenes, carbonyl compounds, water and alkoxysilanes

etc. In the absence of such reagents, they easily undergo dimerization, usually by head-to-tail [2 + 2]-cycloaddition fashion and the reaction is highly regioselective. We have made a detailed computational investigation of the possible reaction pathways and the energetics of the head-to-tail coupling reactions of silenes, resulting in the formation of 1,3-disilacyclobutanes. The analysis included the effect of substituents on the mechanism and free energy profile for the dimerization of monosubstituted ( $\text{RHSi}=\text{CH}_2$ ,  $\text{H}_2\text{Si}=\text{CHR}$ ) and disubstituted ( $\text{RHSi}=\text{CHR}$ ) silenes. The substituents used in the study are  $\text{R} = -\text{CH}_3$ ,  $-\text{SiH}_3$ ,  $-\text{OH}$ ,  $-\text{CN}$  and  $-\text{F}$ ; spanning a wide range of electronic properties. The molecular electrostatic potential (MSEP) values on C and Si are determined in each case to assess the nature of polarity of the bond. B3LYP/6-31G(d,p) level of density functional theory using Gaussian 16 suite of programs is employed in the study to perform the computations. Minimas were ascertained by the method of IR frequency analysis, and the saddle points were located by a single imaginary frequency.

The dimerization reaction of silenes is an exothermic process with low activation energy ( $< 20$  kcal/mol) and is therefore, feasible under ambient condition. Our investigation corroborated the finding that the course of dimerization of silenes is more stabilised in the diradical pathway than the zwitter-ionic pathway. Therefore, it can safely comprehend that the dimerization reaction of silenes prefers a diradical pathway over the zwitter-ionic pathway. Our analysis came up with the conclusion that certain substituents have decisive control over the dimerization reaction pathway of silenes. As far as mono substituted silenes  $\text{R-CSi-H}$  and  $\text{H-CSi-R}$  are concerned, the substituents are more effective in promoting the dimerization when the substituent is attached to Si than to C of the  $\text{C}=\text{Si}$  bond. Electron donating substituents,  $-\text{CH}_3$  and  $-\text{SiH}_3$  destabilise the dimerization reaction in both the mono substituted and disubstituted systems in comparison with the dimerization process of the unsubstituted silene. Electron withdrawing substituents stabilize the dimerization of silenes; specially when they are attached to the Si atom. The electron withdrawing and  $\pi$  donating substituent  $-\text{OH}$  is found to be the most effective among the five substituents attempted. The H-bond formation at the intermediate stages of the reaction by the  $-\text{OH}$  substituent has an active role in stabilising the reaction.

In Chapter 3 we discussing about, the substituent effects on the addition of small molecules ( $\text{NH}_3$ ,  $\text{NO}$ ,  $\text{CO}$ ) to silene and silene-silylene isomerization. Silenes are proposed to be a possible option for the small molecule activation, due their high reactivity and possibility of modulation of the polarity of the  $\text{C}=\text{Si}$  double bond by the proper selection of substituents.

Their vigorous reactions with nucleophiles including simple alcohols and amines invite special attention so that these are the most used trapping reaction for transient silences. The reaction with alcohols and water proceeds through a stepwise mechanism involving initial nucleophilic attack at positively polarised silicon by the substrate to form a  $\sigma$ -bonded complex. We have made a detailed computational exploration of the energetics and reaction pathways of the addition of  $\text{NH}_3$ ,  $\text{NO}$  and  $\text{CO}$  to silenes. The effect of substituents on the silene on the reaction parameters also investigated. As part of the present investigation, the effect of substituents on the energetics of the silene-silylene rearrangement is also studied systematically. Silylene ( $\text{R}_2\text{Si}:$ ) is the silicon alternative of carbene ( $\text{R}_2\text{C}:$ ). It is an extremely reactive species and can activate even the most stable chemical bonds. Unlike carbenes, they can be obtained in the stable form.

Silene is found to be extremely effective in N-H and N-O activation process. The reaction is taking place with low activation energy and is highly exothermic for the parent silene.  $\sigma$ - withdrawing and  $\pi$ - donating substituents -OH and -F are found to be ardently effective in promoting the activation process by largely stabilizing the reaction pathway and increasing the exothermicity of the reaction. The substituents are found to be more effective in H-CSi-R and R-CSi-R substituted forms. The CO addition reaction of the parent silene requires relatively high activation energy and is endothermic in nature. The OH and F substituents are found to be profoundly effective in stabilizing the energy profile of the CO addition reaction and reducing the endothermicity, especially in H-CSi-R and R-CSi-R. As far silene-silylene rearrangement is concerned, the introduction of substituents on carbon did not make any change on the endothermicity of the reaction but showed a significant effect on the magnitude of the energy barrier. Electron donating  $-\text{SiH}_3$  and electron withdrawing  $-\text{CN}$  increased the activation barrier while  $-\text{CH}_3$ , -OH and  $-\text{F}$  groups lowered the barrier height. A notable decrease in the barrier height is seen with the presence of  $\pi$ -donating substituents -OH and  $-\text{F}$  which can be attributed to the polarity reversal in HO-CSi-H and F-CSi-H. When -OH or -F substituents present on both C and Si (R-CSi-R), the rearrangement proceeds with low activation energy and becomes even exothermic.

Chapter 4 discussing about the reactions of 1,2,3,3-tetramethyl cyclotrisilene with propylene, phenylacetylene, trimethylsilylacetylene, formaldehyde and benzaldehyde. The simplest cyclic compound with a Si=Si bond cyclotrisilene which is the silicon analogue of cyclopropene. The first stable derivative of cyclotrisilene is synthesized by Iwamoto et.al. in 1999. Whatever may be the substituents attached, all the cyclotrisilenes are highly reactive;



which may be a blessing in disguise, qualifying their use as a synthetic rudiment for wide variety of products. The interaction of cyclotrisilenes with unsaturated molecules can advance through four reaction pathways. i) The  $\pi$ -addition reaction to the silicon - silicon double bond of the cyclotrisilene in [2+2] fashion, generating a pentagonal product bearing no Si - Si double bond. ii) The  $\sigma$ -insertion of the substrate into one of the endocyclic silicon-silicon single bonds, resulting in the ring expansion with the formation of a product with a Si - Si double bond. iii) The reaction in which the unsaturated reactant find place between a ring Si atom of the cyclotrisilene and its substituent (exocyclic -  $\sigma$  insertion). iv) Ring opening reaction which results in the formation of a disilyl silylene. We have studied comprehensively the reactions of cyclotrisilene with a few alkynes and aldehydes. The cyclotrisilene derivative used in our study is 1,2,3,3-tetramethyl cyclotrisilene (**I**). The alkynes employed were phenylacetylene (**R1**) propylene (**R2**) and trimethylsilylacetylene (**R3**) and the aldehydes were benzaldehyde (**R'1**) and formaldehyde (**R'2**). All calculations were carried out at the M06-2X/6-311G(d,p) level of density functional theory using the Gaussian 16 suite of programs. Transition states were optimized by using the Synchronous Transit-Guided Quasi-Newton (STQN) method implemented in Gaussian 16. Minima were ascertained by the IR frequency analysis, and the saddle points were characterized by a single imaginary frequency. The solvent effects (benzene) were accounted by single point calculation at SMD-M06-2X/6-311+G(d,p) level and the single point energy was corrected by adding the thermal correction to Gibbs free energy obtained from the gas phase calculation (at 298.15 K)

Regarding all the five substrates (3 alkynes and 2 aldehydes) investigated, the  $\pi$ -addition the  $\sigma$ -insertion reactions are found to follow a relatively better stabilized reaction path. Even though the activation energy required for both these classes of reactions are almost same with the three alkynes **R1**, **R2** and **R3**, the exoergicity is found to be slightly greater for the  $\sigma$ -insertion reactions. This can be attributed to the well-defined pentagonal structure of the product generated. Even though less exothermic, the ring opening reactions of the alkynes are feasible under ambient conditions due to the low activation energy barrier. The ring opening reaction is found to follow the most stabilized course with **R3** among the three acetylenes. Regarding the aldehydes, all the four categories of reactions of **R'2** with **I** are direct single-step processes; probably due to the smaller size of the substrate. The ring opening reactions of **I** with the carbonyl compounds are endothermic. The activation barrier is also relatively higher in comparison with the ring opening reactions of the alkynes.

Generally, reactions of **I** with alkynes follow a more stabilized path than that with carbonyl compounds. The exocyclic  $\sigma$ -insertion reaction pathway is found to be associated with formidable energy barrier in all the five cases investigated. Our study arrived at the conclusion that by the proper selection of the substituents on the substrates based on their electronic and steric capabilities, the reaction with the cyclotrisilene **I** can be driven through the desired pathway.

Similarly, Chapter 5 describing the reactions of 1,2-bis(trimethylsilyl)-3,3-dimethyl cyclotrisilene with propylene, phenyl acetylene, trimethylsilylacetylene, formaldehyde and benzaldehyde. As the conclusive part of the present investigation, we have repeated the studies performed on 1,2,3,3-tetramethyl cyclotrisilene (**I**) (ref. Chapter 4) with 1,2-bis(trimethylsilyl)-3,3-dimethyl cyclotrisilene (**II**) to elucidate the effect of substituents attached to the cyclotrisilene ring on the reaction with the five unsaturated substrates (**R1**, **R2**, **R3**, **R'1** and **R'2**). A comparison of the relative reactivity of 1,2,3,3-tetramethyl cyclotrisilene (**I**) and 1,2-bis(trimethylsilyl)-3,3-dimethyl cyclotrisilene (**II**) should centre on the difference in the electronic and steric influence of the substituents; Me ( $-\text{CH}_3$ ) and TMS ( $-\text{Si}(\text{CH}_3)_3$ ) attached to the Si atoms forming the disilenepart of the cyclotrisilene ring. TMS has a significantly greater steric bulk. The steric influence is evident in the energy involved in the of shaping of the reactant complex itself: in the reactions of **I** it is 3-5 kcal/mol where as in the reactions involving **II**; it is 6-7 kcal/mol. This increase in the energy requirement with **II** is applicable to all the four categories ( $\pi$ -addition,  $\sigma$ -insertion, exocyclic  $\sigma$ -insertion and ring opening) of the reactions. In general, the reaction pathways are found to be better stabilised in the reactions of **I** than the sterically more crowded **II**. Thus, the change of substituents on the cyclotrisilene ring also has an influence on the energetics of the reaction pathways.



# Chapter 1: Introduction

---

## Part A: Computational Chemistry

### 1.1 Introduction

#### 1.1.1 Computational Chemistry

One of the most advanced branches of science that dealing with the constitution, construction, transformation and properties of matter at molecular level is chemistry. Molecules are units of matter made of atoms or, more precisely, a cluster of particles carrying charges, negatively charged electrons and positively charged nuclei. The Coulomb interaction between these charged particles is the sole factor exclusively responsible for the chemical phenomena. The subfield of chemistry where advanced mathematical methods are clubbed with laws of physical science to explore the processes involving chemical relevance is termed as theoretical chemistry. One of the rapidly developing subfields of theoretical chemistry is computational chemistry, where the chemical problems are solved with extreme precision using automated calculations.

The amalgamation of wave mechanics and particle mechanics by Max Planck in 1900 to explain the full spectrum of thermal radiation using the harmonic oscillator model pioneered the formulation of quantum mechanics. Various discoveries by Albert Einstein, J. J Thomson, Ruther Ford, Neils Bohr, Louis de Broglie, Werner Heisenberg, Erwin Schrödinger and others contributed to the maturing of quantum mechanics in to the mathematical modelling of atoms and molecules. Erwin Schrödinger successfully incorporated the de Broglie ‘matter wave’ formulation in to the classical Maxwell wave equation, to develop the illustrious Schrödinger equation which is the sole elemental equation of quantum mechanics. The Schrödinger equation generates wave functions that describe the motion of micro-objects which relate the external electromagnetic influences by the alteration of these wave functions. However, for systems having more than one electron an exact solution of the Schrödinger equation is impossible.

Great efforts extending through decades were expended to develop mathematical methods to solve the time-independent Schrödinger equation concerning the multi-particle systems. However, precise solutions possessing chemical accuracy have been remained elusive. This necessitated the designing of approximate methods for the electron systems

containing more than one interaction. Mathematical tools developed in the recent past for multi-dimensional calculations have revealed new alternatives toward such solutions. This enabled precise calculation of physical and chemical properties of molecules of varying measures. These developments enable the solution of many problems in Physics, chemistry, material sciences and biology. Refinement of the computational techniques for complex chemical systems in the recent past based on multi-scale models (2013 Nobel Prize) and formulation of a great variety of software have enabled the scientists to deal with complicated molecular problems. Now a day's quantum chemical computations are extensively used in several fields including thermo-chemistry, enzymology, catalysis, material science, cluster science, reaction mechanisms and so on.

A variety of software are developed possessing divergent range of capabilities and ease of use with excellent performance. Gaussian, MOPAC, GAMESS, Sybyl, Spartan, Hyperchem, CASTEP, Amsterdam Density Functional (ADF), etc are a few among them. Molecular visualization programs enabling the direct picturisation of the molecular structures are also available. They include Gauss View, MolDen, PCMODEL, Molekel, Chemcraft, RasMol and Moplot. Methods in computational chemistry are range from most precise to rather approximate. The highly accurate methods are employable for small systems only. Most popular quantum chemical computational methods include (a) Molecular mechanics (MM) (b) ab-initio methods (c) semi empirical treatments (d) the DFT methods (e) Monte Carlo and molecular dynamics simulations and (f) hybrid quantum mechanics/molecular mechanics (QM/MM) methods. The MM methods (Bowen and Allinger 1991; Boyd and Lipkowitz 1982; Dinur and Hagler 1991; Weiner and Kollman 1981) apply the laws of classical mechanics to molecular nuclei without explicit consideration of the electrons. MM calculations are computationally quite inexpensive. It is suitable for molecules containing thousands of atoms which include enzymes, proteins, polymers and macromolecules. Semi-empirical quantum methods (James J. P. Stewart 1990; Pople and Beveridge 1970) represents a midway between the qualitative results available from molecular mechanics and explicit quantitative results from the ab initio methods. Semi-empirical techniques which use approximations from empirical data to provide the input into the mathematical models are significantly faster, and are suitable for large polymeric molecular systems.

Ab initio (Latin for 'from first principle') methods provide a mathematical description of the chemical systems by solving the Schrödinger equation, using rigorous arithmetical extremities, without employing any empirical data except the universal constants. Hence, the



results obtained from these methods are known to be accurate and are generally in good agreement with the experimental results (Szabo and Ostlund 1996). Of course, ab initio treatments are employable with small systems only. Molecular dynamics (MD) uses Newton's laws of motion to analyse the time-dependent behaviour of systems, including vibrations and Brownian motion, using a classical mechanical description (Rapaport 2004). The molecular dynamics and Monte Carlo based methods can be used to investigate the macroscopic properties of a system (Doll and Freeman 1994). Density function treatment-based calculations provide dependable results about the properties and structure of chemical systems with relatively lesser computational expense. To compute the electronic structure of various systems, DFT methods are considered to be the most convenient and appropriate approach now a day's. The DFT method was formalised by Walter Kohn and Lu Jeu Sham (Kohn and Sham 1965). They were successfully proved that the functions based on the electron density (ED) of a system represent the physical observables of its ground state in the best way. The strength of QM (accurate) and MM (fast) calculations are brilliantly combined in the hybrid QM/MM approach. The hybrid QM/MM approach is highly useful in the computation of energies and structures of the ground and excited state properties of molecules, intermediates and transition states, atomic charges, reaction pathways etc.

### **1.1.1.1 Quantum Chemical Methods**

#### **1.1.1.1.1 Ab initio Molecular Orbital Theory**

The electronic structure any system is described by the Schrödinger equation, irrespective of the quantum chemical method adopted. In the ab-initio methods, the fundamental physical constants such as Planck's constant, velocity of light, mass of electrons and nuclei etc are used to express the chemical phenomena. Also, the ab-initio methods are independent of empirical data obtained from the experiments. Most of the chemical phenomena are originated from various time-independent interactions. Such conservative systems are better represented by the time-independent Schrödinger equation:

$$H\Psi = E\Psi \dots (\text{Eq. 1.1})$$

H is the total energy operator or the Hamiltonian operator of the system. It represents the sum of the kinetic energy operators of the nuclei and electrons and the potential energy operators of, nuclear-electron, nuclear-nuclear and electron-electron interactions.  $\Psi$  is the wave function that describes the particles of the system in the form of a mathematical equation. The

total energy of the system is represented by E and it is derived in the form of eigen values. For an N electron and M nucleus system, the Hamiltonian operator can be expressed as;

$$H = - \sum_{i=1}^N \frac{1}{2} \nabla_i^2 - \sum_{A=1}^M \frac{1}{2M_A} \nabla_A^2 - \sum_{i=1}^N \sum_{A=1}^M \frac{Z_A}{r_{iA}} + \sum_{i=1}^N \sum_{j>i}^N \frac{1}{r_{ij}} + \sum_{A=1}^N \sum_{B>1}^M \frac{Z_A Z_B}{R_{AB}} \dots \dots \text{(Eq. 1.2)}$$

$r_i$  and  $R_A$  represent the position vectors of electron and nuclei respectively.  $r_{ij}$  and  $r_{iA}$  represent the distance between the  $i^{\text{th}}$  and  $j^{\text{th}}$  electrons and that between the  $i^{\text{th}}$  electron  $A^{\text{th}}$  nucleus respectively. The inter-nuclear distance between the nuclei A and B is represented by  $R_{AB}$ . The atomic mass of the atom A is symbolised by  $M_A$  and  $Z_A$  its' atomic number.

Born and Oppenheimer proposed an approximation (BO approximation) (Born and Oppenheimer 1927) to solve the Schrödinger equation of based on the fact that, the nuclear and electronic motions in a system take place at different velocities; the former being extremely slower than the latter. Practically, an oscillating nucleus feels an averaged electronic motion, whereas, an electron in executing very fast motion sees relatively static nuclei. This assumption brings in the convenience of separating the nuclear and electronic Hamiltonians and the generation of the separate wave functions for the two. This enables the expression of the total wave function  $\Psi$  of any system as a product of the nuclear and electronic wave functions.

$$\Psi(\{r_i\}; \{R_A\}) = \Phi_{\text{elec}}(\{r_i\}; \{R_A\}) \Phi_{\text{nuc}}(\{R_A\}) \dots \dots \text{(Eq. 1.3)}$$

$\{R_A\}$  and  $\{r_i\}$  represent the positions of nuclei and electrons of the system respectively. The electronic part of the Schrodinger wave equation for a system can be written as:

$$H_{\text{elec}} \Phi_{\text{elec}}(\{r_i\}; \{R_A\}) = E_{\text{elec}} \Phi_{\text{elec}}(\{r_i\}; \{R_A\}) \dots \dots \text{(Eq. 1.4)}$$

Even though the electronic Hamiltonian parametrically depends on nuclear coordinates, it explicitly relies on the electronic coordinates. The processes of chemical nature take place primarily because of the interactions among the electrons of the systems concerned. Therefore, to investigate the chemical properties and reactions a system, the explicit treatment of the electronic Hamiltonian is quite adequate. The convention of dimensions used in quantum mechanics (QM) is the system of atomic units (a.u.), which is commonly referred as Hartree units. According to this system of dimension, the Planck's constant, the mass of an electron, the length equal to the radius of first Bohr orbit of the hydrogen atom, charge of a proton and permittivity of the free space multiplied by  $4\pi(4\pi\epsilon_0)$

are all fixed as unity in the corresponding measures. Half the energy of a hydrogen atom in the ground state (GS) is numerically equal to one a.u. of energy. The handling of electronic Hamiltonian (excluding the inter nuclear repulsion) is rendered much simplified and become convenient using atomic units as shown Eq. 1.5.

$$H_{\text{elec}} = \sum_{i=1}^N \frac{1}{2} \nabla_i^2 - \sum_{i=1}^N \sum_{A=1}^M \frac{Z_A}{r_{iA}} + \sum_{i=1}^N \sum_{j>i}^N \frac{1}{r_{ij}} \quad \dots\dots \text{(Eq. 1.5)}$$

The operator corresponding to the kinetic energy of the electrons, summed over for total N electrons of the system is the first term in the equation. The nucleus-electron Coulombic attraction summed over for N electrons and M nuclei is represented by the second term. The nuclear charges are symbolised by  $Z_A$ . The inter-electronic repulsions existing in system are represented in the last term. The wavefunction  $\Psi$  of the system can be obtained by the solution of the properly constructed the Schrödinger equation. Once  $\Psi$  is obtained, the observables (experimentally determinable parameters) of the system under consideration can be obtained as the expectation value of corresponding operator ( $O$ ), as  $\langle \Psi | O | \Psi \rangle$ . To determine the total electronic energy of a molecule, the operator employed should be the electronic Hamiltonian ( $O = H_{\text{elec}}$ ).

### 1.1.1.1.2 Hartree-Fock Theory

A solution of the Eq. (1.1) is acceptable only if the function generated ( $\Psi$ ) is well-behaved. Any wavefunction that is finite, continuous, single valued, obeying the appropriate boundary conditions and quadratically integrable is classified as a well-behaved one. Thus,

$$\int (\Psi^*(r_1, r_2, \dots, r_N) \Psi(r_1, r_2, \dots, r_N) d^3r_1 d^3r_2 \dots d^3r_N) = 1 \quad \dots\dots\dots \text{(Eq. 1.6)}$$

For many-electron systems Hartree developed a genius technique to generate an approximate wavefunction. It is expressed as a product of wave functions and is known as Hartree product (HP) function. The HP function is more generally referred to as basis function or orbital. In the HP function, each basis function is a spatial orbital ( $\psi(r)$ ). Spatial orbitals are functions of only the three position vectors ( $r$ ) and does not specify the spin of the constituent electrons. Thus, a spatial orbital can accommodate two electrons. To define an electron completely, the spin also should be specified. The electron spin is represented by either of the two spin functions:  $\alpha(\omega)$  (for up-spin) and  $\beta(\omega)$  (for down-spin). The complete label of an electron in a system is a multiple of the spatial orbital functions ( $\psi(r)$ ). The spin function of a spatial orbital is ( $\alpha(\omega)$  or  $\beta(\omega)$ ). The product is known as spin orbital and that depend on four

coordinates (x); three spaces coordinates (r) and one spin coordinate (ω). A spin-orbital can accommodate only one electron and is represented as χ<sub>j</sub>. For an N electron system, there will be 2N spin-orbitals. The spin orbital of the i<sup>th</sup> spatial orbital can be numbered as (2i-1)<sup>th</sup> and (2i)<sup>th</sup>

$$\begin{aligned}\chi_{2i-1}(\mathbf{x}) &= \psi_i(\mathbf{r})\alpha(\omega) \\ \chi_{2i}(\mathbf{x}) &= \psi_i(\mathbf{r})\beta(\omega) \dots\dots\dots (\text{Eq. 1.7})\end{aligned}$$

Now, for an N-electron system, the HP function is written as a product of single-electron spin functions:

$$\Psi^{\text{HP}}(\mathbf{x}_1, \mathbf{x}_2, \dots, \mathbf{x}_N) = \chi_1(\mathbf{x}_1)\chi_2(\mathbf{x}_2) \dots \chi_N(\mathbf{x}_N) \dots\dots\dots (\text{Eq. 1.8})$$

Being an independent-electron wavefunction, the HP function does not satisfy the Pauli's anti-symmetry principle. According to the Pauli's exclusion principle (Pauli 1925), the value of the four quantum numbers (viz. principal (n), azimuthal (l), magnetic (m) and spin (s)) of two electrons of a system cannot be same. Slater (Slater 1930) and Fock (Fock 1930) independently proved that an anti-symmetrized sum of all the permutations of HP functions would solve this problem for many-electron systems.

$$\Psi(\mathbf{x}_1, \mathbf{x}_2, \dots, \mathbf{x}_i, \dots, \mathbf{x}_j, \dots, \mathbf{x}_N) = -\Psi(\mathbf{x}_1, \mathbf{x}_2, \dots, \mathbf{x}_j, \dots, \mathbf{x}_i, \dots, \mathbf{x}_N) \dots\dots\dots (\text{Eq. 1.9})$$

The anti-symmetry condition can be achieved by conveying the function in the determinant form, which is popularly termed as the Slater determinant. In the Slater determinant form, the wavefunction within the HF formulation for an N-electron system is expressed as:

$$\Psi(\mathbf{x}_1, \mathbf{x}_2, \dots, \mathbf{x}_N) = \frac{1}{\sqrt{N!}} \begin{vmatrix} \chi_1(\mathbf{x}_1) & \chi_2(\mathbf{x}_1) & \dots & \chi_N(\mathbf{x}_1) \\ \chi_1(\mathbf{x}_2) & \chi_2(\mathbf{x}_2) & \dots & \chi_N(\mathbf{x}_2) \\ \dots & \dots & \dots & \dots \\ \chi_1(\mathbf{x}_N) & \chi_2(\mathbf{x}_N) & \dots & \chi_N(\mathbf{x}_N) \end{vmatrix} \dots\dots\dots (\text{Eq. 1.10})$$

The term  $\frac{1}{\sqrt{N!}}$  in the equation 1.10 is the normalization factor that helps to maintain the condition laid by equation 1.6. The elements of the Slater determinant are all spin orbitals. As noted above, each spin orbital is designated by four coordinates (x): three space coordinates

and one spin coordinate. Usually, the normalized Slater determinant is represented by a convenient notation as,

$$\Psi(x_1, x_2, \dots, x_N) = |\chi_i \chi_j \dots \chi_N\rangle \dots\dots\dots \text{(Eq. 1.11)}$$

In the above determinant, the electrons 1,2... etc. are supposed to sequentially occupy the spin orbital. The simplest anti-symmetric wave function to represent the ground state of an N-electron system, can be written as:

$$|\Psi_0\rangle = |\chi_i \chi_j \dots \chi_N\rangle \dots\dots\dots \text{(Eq. 1.12)}$$

According to the variation principle, the most appropriate wave function of this functional form is the one that gives the lowest values for the energy of the system in the form of eigen values.

$$E_0 = \langle \Psi_0 | H | \Psi_0 \rangle \dots\dots\dots \text{(Eq. 1.13)}$$

H symbolises the electronic part of the Hamiltonian operator of the system representing all electrons. The variation method offers a mathematical procedure to obtain the proper set of spin-orbitals that yields the lowest possible value of  $E_0$ , which cannot be further reduced. The set of equations that generate the optimal spin orbital, yielding the lowest possible energy value is called the Hartree-Fock (HF) equations. The orbitals are known as self-consistent field orbitals. The general eigen value equation form of the Hartree-Fock equation is:

$$f(i)\chi(x_i) = \mathcal{E}_i\chi(x_i) \dots\dots\dots \text{(Eq. 1.14)}$$

The single-electron operator is generally known as the Fock operator and is represented as  $f(i)$ . The corresponding single-electron energy is  $\mathcal{E}_i$ . The Fock operator is defined as

$$f(i) = -\frac{1}{2}\nabla_i^2 - \sum_{A=1}^M \frac{Z_A}{r_{iA}} + V^{HF}(i) \dots\dots\dots \text{(Eq. 1.15)}$$

Where,  $V^{HF}(i)$  is called the Hartree-Fock potential. It is the average repulsion potential experienced by the  $i^{\text{th}}$  electron due to the interaction with all the other (N-1) electrons of the system. Thus, the HF method enables the handling of the many-electron problem of an N electron system in a systematic way, by splitting it in to N one-electron problems. Here, the repulsion between electrons is treated in an average way. The mathematical procedure adopted for the solution of the Hartree-Fock equation is known as the self-consistent-field (SCF) method. It is briefly explained below.



To calculate the average field ( $V^{\text{HF}}(i)$ ) experienced by each electron of the system, an initial guess at the spin orbital is made. This ‘guess-set’ is applied to the eigen value equation (Eq. 1.14) which is solved to generate a new set of spin orbitals. These new spin orbitals, which are commonly known as the first ‘improved set’ are used to obtain still newer set of spin orbitals and the procedure is repeated for better functions until no further improvement in the spin orbitals and consequent eigen values are possible. The situation is mathematically termed as the self-consistency. The solution of this spin orbital yield a set ( $\chi_k$ ) of orthonormal HF spin functions called the self-consistent field orbitals that are guaranteed with the lowest orbital energies ( $\mathcal{E}_k$ ). In the orthonormal set generated, the  $N$  spin orbitals possessing the lowest energies are occupied in the sequential order of energy. In the set of self-consistent field orbitals  $\{\chi_k\}$ , orbitals other than the occupied ones are called virtual orbitals or unoccupied orbitals.

For each electron, the one-electron Fock operator defined by eq. 1.15. The first two terms of Fock operator represent one-electron operators which are together called the core-Hamiltonian. The core-Hamiltonian of a given electron is the sum of the kinetic energy operator of it and the nucleus-electron attraction operators.

The HF operator of electron-1 can be defined as:

$$V^{\text{HF}}(i) = \sum_j^N J_j(1) - K_j(1) \quad \dots \dots \dots (\text{Eq. 1.16})$$

The electron–electron repulsion due to each of the two electrons in the  $j^{\text{th}}$  spin-orbital is represented as  $J_j(1)$  and is called the Coulomb operator.

$$J_j(1) = \int \chi_j(2) \frac{1}{r_{12}} \chi_j(2) dx_2 \quad \dots \dots \dots (\text{Eq. 1.17})$$

The exchange operator  $K_j(1)$ , defining the electron exchange energy due to the antisymmetry of the total  $N$ -electron wave functions, can only be written through its effect when operating on a spin orbital as

$$K_j(1)\chi_i(1) = \left[ \int \chi_j(2) \frac{1}{r_{12}} \chi_i(2) dx_2 \right] \chi_i(1) \quad \dots \dots \dots (\text{Eq. 1.18})$$

For closed shell molecules or atoms, where all orbitals are doubly occupied, Roothaan and Hall (Hall 1951; Roothaan 1951) are developed a special set of HF equations. The method is often known as Restricted Hartree Fock theory.

$$\Psi_i = \sum_{\mu=1}^K C_{\mu i} \phi_{\mu} \quad i = 1, 2 \dots K \quad \dots \dots \dots \text{(Eq. 1.19)}$$

In the wavefunction  $\Psi_i$ , the functions represented as  $\phi_{\mu}$  are either Slater type orbitals or Gaussian type orbitals. They are used as basis functions representing the atomic orbitals. The  $C_{\mu i}$  terms are the coefficients of the respective  $\phi_{\mu}$ .  $K$  represent the total number of basis functions, better known as primitive gaussians used in contracted gaussian forming the guess set. By substituting Eq. 1.19, the HF equation given in Eq. 1.14 may be rewritten as:

$$f(i) \sum_{\mu=1}^K C_{\mu i} \phi_{\mu} = \mathcal{E} \sum_{\mu=1}^K C_{\mu i} \phi_{\mu} \quad \dots \dots \dots \text{(Eq. 1.20)}$$

Multiplication of RHS and LHS of Eq.1.20 by the complex conjugate of  $\phi_{\mu}$ ;  $(\phi_{\mu})^*$

and integrating the product equation generates the Roothaan Hall equation which is given as Eq.1.21

$$FC = SC\mathcal{E} \quad \dots \dots \dots \text{(Eq. 1.21)}$$

$S$  represents the overlap matrix.  $F$  stands for the Fock matrix and the  $\mathcal{E}$  values symbolise the orbital energies. The Fock matrix need to be diagonalized prior to the calculation of the eigen values of the orbital functions, to arrive at the unknown molecular orbital coefficients using the Roothaan Hall equation (Eq. 1.21) of the corresponding basis functions. The MO coefficients associated with the Fock matrix are also evaluated by the SCF procedure. It worth mentioning that, the single-electron nature of the Fock operator brings in certain constraints to the Hartree-Fock theory moulded using the Roothaan method (RHF). This is due to the fact that all the electron correlations other than that resulted from the exchange phenomenon are ignored in the RHF procedure. Still, the selection and construction of basis set (guess set) was a challenging task for the early computational chemists. The LCAO approach using the hydrogenic orbitals remained elusive, since such basis sets demands unavoidable numerical solution of the four index integrals appearing as the Fock matrix elements; which is a nearly unattainable process. There are  $4N$  integrals to be evaluated as each index extends to all the individual basis functions. The quartic scaling behaviour the

basis set of spin orbitals, increasing with respect to the size of the system became a bottleneck in the application of the HF theory to atomic and molecular problems.

### 1.1.1.1.3 Basis Sets

The term ‘basis set’ in computational chemistry designates a set of non-orthogonal, one-particle wavefunctions that are used in the construction of a molecular orbital. A linear combination of the basis functions used to generate the MO. The weights or coefficients of each function are to be evaluated by the variation method. Since the use of AOs as basis functions in many-electron systems bring in tedious mathematical complexities, Slater type orbitals (STOs) (Allen and Karo 1960) which mimic AOs were used in the early days (Clementi and McLean 1964). Francis S. Boys suggested the use of standard Gaussian functions, centred on atoms (Gaussian type orbitals, GTO) to reduce the difficulty in computing two- and other multi-centre integrals (Boys and A 1950; Feller and Davidson 1990).

A Cartesian Gaussian function conventionally used in the electronic structure calculations of atoms and molecules has the general form:

$$g(\alpha, l, m, n; x, y, z) = N_{lmn}(x - x_A)^l(y - y_A)^m(z - z_A)^n e^{-\alpha|r-r_A|^2} \quad \dots \dots \dots (\text{Eq. 1.22})$$

$l, m, n$  are the powers of the Cartesian components  $x, y$  and  $z$  respectively and  $\alpha$  stands for the orbital exponent. The centre of a symmetric bell-shaped Gaussian function is symbolised by  $r_A = (x_A, y_A, z_A)$ . The product of two GTOs is always a Gaussian function centred at the weighted midpoint of the two functions and is known as Gaussian product theorem. This is the primary computational advantage of GTOs over STOs. The resulting integrals can be conveniently evaluated analytically which reduces the mathematical complexity considerably. However, for attaining more computational convenience and improving the efficiency of the function in representing the system, it is a common practice (Stewart 1970) to combine a set of GTOs, the contribution of each of which is limited with fixed coefficients (Eq. 1.23) to prepare each basis function. Contracted Gaussian (CGTO) is the designation of such a linear combination.

$$g^{\text{CGTO}}(l, m, n, x, y, z) = \sum_i d_i g(\alpha_i, l, m, n, x, y, z) \quad \dots \dots \dots (\text{Eq. 1.23})$$

The contraction coefficients and orbital exponents are evaluated using the suitable methods in the atomic computation. Different types of Gaussian basis sets developed, which have been continuously improved in quality over the years. The minimal basis set which is also known

as single-zeta Gaussian basis sets, are the simplest among the GTOs. In the STO-3G, which is the most common single-zeta basis set; each Slater type orbital is formed by the linear combination of 3 Gaussian type orbitals (Primitive Gaussian) (PGTO). In a double zeta (DZ) basis set, the number of functions in the minimal basis set is doubled. When the doubling or tripling of the functions in the linear combination is restricted to valence orbitals alone, the basis set is termed as split valence basis sets. Pople and co-workers designed the split valence basis sets of type ‘k-nlmG’ where ‘k’ stands for the number of PGTOs used for preparing the core orbital and ‘nlm’ indicates both the number of functions forming the valence orbitals and the number of PGTOs used for their representation (Ditchfield, Hehre, and Pople 1971). 3-21G and 6-31G basis sets are examples of split valence basis sets (Ditchfield, Hehre, and Pople 1971; Krishnan et al. 1980). The polarisation basis sets are constructed by developing the CGTO using functions of higher angular momentum than the occupied atomic orbitals. In polarisation basis sets, the number of polarization functions used in the CGTO is noted after the G in the designation of the basis sets. There will be separate labelling for the heavy atoms and hydrogen. To effectively spread the electron density over the entire molecule, diffuse functions are added to the basis set. This is denoted in the representation of the basis set using the + or ++ signs. The Pople’s split valence basis set (multiple CGTOs are used for the valence shells only) are the most commonly used combinations, with different number of polarization functions as 6-31G(d,p), 6-311++G(2d,2p) etc. Dunning (Dunning 1970; Woon and Dunning 1993) basis sets and the correlation consistent (Dunning 1989) valence double and triple zeta basis functions (cc-pvdz, cc-pvtz) are also frequently used.

### 1.1.1.2 Post HF Methods

Post Hartree-Fock (PHF) methods is the collective name given to the approximation methods crafted by refining the Hartree-Fock method. The electron correlation is incorporated in to the original HF model to improve the accuracy of the function. The post-HF methods can be used obtain the correlation energy,  $E_{\text{corr}}$  (Boys and A 1950) which is the difference between the ab initio energy and HF energy calculated based on the Aufbau arrangement of electrons in the system.

$$E_{\text{corr}} = \mathcal{E}_0 - E_0 \quad \dots \dots \dots (\text{Eq. 1.24})$$

where,  $\mathcal{E}_0$  is the exact eigenvalue of electronic Hamiltonian of the system;  $H_{\text{elec}}$ .  $E_0$  represent the ‘best’ possible HF energy obtained using a basis set which is extrapolated to completeness. The most popular approaches that attempt to compute the correlation energy,

$E_{\text{corr}}$  are the configuration interaction (CI) (Foresman et al. 1992; John A. Pople, Binkley, and Seeger 1976), coupled cluster (CC) (Cramer et al. 1994) and many body perturbation theory (MBPT) (Bouckaert, Smoluchowski, and Wigner 1936; Miller and Kelly 1971) methods.

### 1.1.1.2.1 Configuration Interaction

Configuration interaction (CI) is a brilliant approach to incorporate the correlation effects into an ab initio molecular orbital calculation. Here, along with the Aufbau arrangement of electrons of the system, the excited states of the system are also included in the description of the electronic arrangement. The CI provides an exact solution for the many-electron system; at least in principle. In the CI treatments also the HF determinant is taken as the reference function. The energy minimisation of the HF determinant is achieved variationally by modifying the expansion coefficients of the determinant. A linear combination of Slater determinants with all the permutations of electron occupancies expanded is required to generate a complete CI wavefunction, which is shown below.

$$|\Phi_0\rangle = c_0|\Psi_a^r\rangle + \sum_{ar} c_a^r|\Psi_a^r\rangle + \sum_{\substack{a<b \\ r<s}} c_{ab}^{rs}|\Psi_{ab}^{rs}\rangle + \sum_{\substack{a<b \\ r<s}} c_{abc}^{rst}|\Psi_{abc}^{rst}\rangle \dots \dots \dots \text{(Eq. 1.25)}$$

The Slater determinant representing the HF wavefunction is symbolised by the first term at the RHS in the Eq. (1.25). The second, third etc terms are determinants representing singly, doubly, triply... etc. excited states along with the corresponding expansion coefficients. The expansion coefficients are evaluated variously. The subscripts and super scripts such as a, b, r, s, etc. appear in the equation, denote the occupied and virtual orbitals of the system, as the electron excitations occur. The letters a, b, c... symbolise the occupied orbital and r, s, t... represent the virtual ones. The level of configuration interaction calculations is assessed by the number of excited state configurations considered to construct each determinant. In the configuration interaction single-excitation (CIS) calculation, the configuration interaction is confined to the movement of a single electron and is evident in each determinant. The CIS calculations made approximations to the excited states of the molecule only, leaving the ground state energy untouched. Single as well as double excitation (CISD) calculations generate a ground state energy which is corrected for the correlation. Even though very high-accuracy results are generated by the computationally laborious triple-excitation (CISDT) and quadruple-excitation (CISDTQ) calculations, they are employed for special situations only. A full CI is the configuration interaction calculation with all possible excitations. In practice, the full CI calculation necessitate an infinitely large basis set and it is expected to generate a

perfect quantum mechanical result with full accuracy. Evidently, the full CI calculations require immense computer power and therefore cannot be accomplished.

### 1.1.1.2.2 Coupled Cluster Methods

The coupled cluster method marks a critical advancement over the practical CI method (Čížek 1966). This method provides a more refined mathematical technique for estimating the electron correlation energy with improved accuracy. The coupled cluster method assumes a full CI wavefunction which is explained above

$$\Psi_{CC} = e^T \Psi_{HF} \dots\dots\dots \text{(Eq. 1.26)}$$

$\Psi_{HF}$  in the equation symbolises a Slater determinant that is created using the Hartree-Fock molecular orbitals and

$$e^T = 1 + T + \frac{1}{2}T^2 + \frac{1}{6}T^3 + \dots = \sum_{k=0}^{\infty} \frac{1}{k!} T^k \dots\dots\dots \text{(Eq. 1.27)}$$

T is known as cluster operator. This operator on acting over  $\Psi_{HF}$  produces a linear combination of excited state Slater determinants which can be represented as

$$T = T_1 + T_2 + T_3 + \dots + T_n \dots\dots\dots \text{(Eq. 1.28)}$$

Here, ‘n’ stands for the total number of electrons in the system. The various  $T_i$  operators represent all the possible determinants subjected to  $i$  excitations from the reference determinant.

$$T_2 = \sum_{i < j}^{\text{occ.}} \sum_{a < b}^{\text{vir.}} t_{ij}^{ab} \Psi_{ij}^{ab} \dots\dots\dots \text{(Eq. 1.29)}$$

The magnitudes of the amplitude ‘t’ are assessed according to the constraints laid by Eq. 1.26. Regarding the double excitation; i.e.,  $T=T_2$ , the Taylor expansion of the exponential function in (Eq. 1.26) generate the coupled cluster wave function as

$$\Psi_{CCD} = \left( 1 + T_2 + \frac{1}{2!}T^2 + \frac{1}{3!}T^3 + \dots \right) \Psi_{HF} \dots\dots\dots \text{(Eq. 1.30)}$$

The CCD subscript attached to the wavefunction implies that the coupled cluster is limited to the double excitation operator. The configuration double excitation method is defined by the first two terms in parenthesis,  $(1+T_2)$ , and the proceeding terms symbolise the product of excitation operators. Evaluation the unknown coefficients  $t_{ij}^{ab}$  by solving the equation is necessary for finding an approximate solution of the  $|\Psi_{CC}\rangle$ . Singles and doubles coefficients



and the two electron MO integrals are used to evaluate the coupled cluster correlation energy. Even though the computational cost due to the inclusion of single excitations ( $T_1$ ) in addition to doubles is tiring, the significant improvement in accuracy produced justifies its use. This is the marked advantage of the CCSD models. In CCSDT methods, incorporation of the connected triple excitations originating with their amplitudes from  $T_3$  is done. However, if the singles/triples coupling term are also included, it is labelled in the designation as CCSD (T).

### 1.1.1.2.3 Perturbation Theory

Møller–Plesset perturbation theory (MP) belongs to the family of many-body perturbation theories (MBPTs) which, starting from an HF reference function, perturb atively introduce multiple excitations from unperturbed occupied orbitals to unoccupied (empty) orbitals (Attila Szabo and Neil S. Ostlund 1989). The method involves, estimation of energy corrections that take into account part of the electron correlation directly. More over, the MP theory enhances qualitatively the Hartree-Fock method by incorporating electron correlation impacts by using the Rayleigh-Schrodinger perturbation theory (RSPT) (Bartlett and Silver 1975; Pople et al. 1978), to the second (MP2), third (MP3) and fourth (MP4) orders. The true Hamiltonian operator  $H$  is modified to a sum of the perturbation  $U$  and a ‘zero<sup>th</sup> order’ Hamiltonian  $H_0$  in RS-PT.

$$H = H_0 + \lambda U \dots\dots\dots (\text{Eq. 1.31})$$

$\psi_i^{(0)}$  is the symbol used for the eigen functions of  $H_0$  and the corresponding energy values are labelled as  $E_i^{(0)}$ . Thus,  $\psi_0^{(0)}$  stands for the ground state wavefunction whereas the ground state energy  $E_0^{(0)}$ . The parameter  $\lambda$  defines the extent of perturbation and varies between 0 and 1. Evidently, a null valued  $\lambda$  indicate the zero<sup>th</sup>-order Hamiltonian and  $\lambda$  become unity as perturbation is fully turned on and  $H$  acquired its true value. The eigen functions and eigen values of the Hamiltonian  $H$ ;  $\psi_i$  and  $E_i$  respectively, are expressed in terms of powers of  $\lambda$

$$\Psi_i = \Psi_i^0 + \lambda\Psi_i^1 + \lambda^2\Psi_i^2 + \dots = \sum_{n=0} \lambda^n \Psi_i^n \dots\dots\dots (\text{Eq. 1.32})$$

$$E_i = E_i^0 + \lambda E_i^1 + \lambda^2 E_i^2 + \dots = \sum_{n=0} \lambda^n E_i^n \dots\dots\dots (\text{Eq. 1.33})$$

First order correction to the energy is represented as  $E_i^1$ , the second order correction term as  $E_i^2$  and so on. The values of these energy terms can be estimated from the eigen functions as given in the following equations.

$$E_i^{(0)} = \int \Psi_i^{(0)} H_0 \Psi_i^{(0)} \delta\tau \dots\dots\dots (\text{Eq. 1.34})$$

$$E_i^{(1)} = \int \Psi_i^{(0)} U \Psi_i^{(0)} \delta\tau \dots\dots (Eq. 1.35)$$

$$E_i^{(2)} = \int \Psi_i^{(0)} U \Psi_i^{(1)} \delta\tau \dots\dots (Eq. 1.36)$$

$$E_i^{(3)} = \int \Psi_i^{(0)} U \Psi_i^{(2)} \delta\tau \dots\dots (Eq. 1.37)$$

The method involves the generation of the wavefunctions of the necessary order prior to the evaluation of the corrections to the energy. According to the Möller-Plesset perturbation (Møller and Plesset 1934) theory, the unperturbed Hamiltonian ( $H_0$ ) is assumed as the sum of the single-electron Fock operators, for the N electrons of the system. The formulation of the higher order wavefunctions require the knowledge of the nature of perturbation (U) encountered by the system. The sum of the nucleus-electron attraction terms and inter-electron repulsion terms form the electronic Hamiltonian of a system.

$$H = \sum_{i=1}^N (H^{core}) + \sum_{i=1}^N \sum_{j=i+1}^N \frac{1}{r_{ij}} \dots\dots (Eq. 1.38)$$

The perturbation U can be evaluated as

$$U = \sum_{i=1}^N \sum_{j=i+1}^N \frac{1}{r_{ij}} - \sum_{j=1}^N (J_i + K_i) \dots\dots (Eq. 1.39)$$

The first order energy  $E_0^{(1)}$  can be calculated as

$$E_0^{(1)} = -\frac{1}{2} \sum_{i=1}^N \sum_{j=i+1}^N [(ii|jj) - (ij|ij)] \dots\dots (Eq. 1.40)$$

The added value of the zeroth and first order energy turns out to be the Hartree-Fock energy of the system.

$$E_0^{(0)} + E_0^{(1)} = \sum_{i=1}^N \epsilon_i - \frac{1}{2} \sum_{i=1}^N \sum_{j=i+1}^N [(ii|jj) - (ij|ij)] \dots\dots (Eq. 1.41)$$

The application of Moller-Plesset perturbation theory to at least the second order only can create a perceptible improvement over the Hartree-Fock energy. This level of Moller-Plesset perturbation theory is labelled as MP2. The integral representing MP2 is  $\int \Psi_0^{(0)} U \Psi_0^{(1)} \delta\tau$  a linear combination of the solutions of the zeroth –order Hamiltonian can be used to express the first order perturbation wavefunction  $\Psi_0^{(1)}$  as:

$$\Psi_0^{(1)} = \sum_j C_j^1 \Psi_j^{(0)} \quad \dots \dots \dots \text{(Eq. 1.42)}$$

In Eq. 1.42, the wave function in the summation,  $\Psi_j^{(0)}$  includes excitations of the order single, double etc. resulting from the excitation of the electrons into the virtual orbitals generated from the Hartree-Fock calculations. The evaluation of the second order energy can be done as:

$$E_0^{(2)} = \sum_i^{occupied} \sum_{j>i}^{virtual} \sum_a \sum_{b>a} \frac{\int \int [\delta\tau_1 \delta\tau_2 \chi_i(1) \chi_j(2)] \left(\frac{1}{r_{12}}\right) [\chi_a(1) \chi_b(2) - \chi_b(1) \chi_a(2)]}{\epsilon_a + \epsilon_b - \epsilon_i - \epsilon_j} \dots \dots \dots \text{(Eq. 1.43)}$$

The Brillouin theorem specifies that only double excitations can generate a non-zero output for the integral. The Möller-Plesset methods are computationally expensive. This made their application limited to single point calculations at geometry generated using a lower level of theory. Currently, the MP calculations are the most commonly used method to include the electron correlation effects in the quantum chemical calculations; particularly, the computation at the MP2 level.

### 1.1.1.3 Density Functional Theory (DFT)

The density functional theory (DFT) encompass a set of strategies for the quantum chemical electronic structure calculations with wide applications to main group and organic molecules as well as complex systems such as condensed matter. These strategies are specially applicable to transition metal complexes for which the electron correlation effects are large. It is equally applicable to systems bearing similar complexity including surfaces, metals and solid-state compounds. Effective investigations on the reaction pathway energetics, electronic structure of systems, charge and spin distributions and molecular geometries can be made using the DFT methods. The DFT calculations had been largely employed in the solid-state investigations even before 1970s. Still, DFT was not generally accepted as accurate enough for the conventional application in quantum chemical calculations. Lately, the approximations employed in the theory underwent great upgradations by the repeated mathematical refinements. Currently, DFT is one of the leading computational techniques adopted for the electronic structure calculations in all the conventional quantum mechanical problems.

The expression of a system of electrons as a function of the electron density ( $\rho(\mathbf{r})$ ) is the central idea of the DFT method. The wave-function of the system is an expression of the electron density. The wavefunction of an N-electron system depends on  $3N$  spatial coordinates. However, the electron density  $\rho(\mathbf{r})$  is defined by just three spatial coordinates (plus the spin coordinate when necessary). This greatly reduce computational task. Moreover, the electron density  $\rho(\mathbf{r})$  at a point in the system is measurable quantity, whereas the wavefunction is an intangible mathematical entity. Above all, the electron density is a conventional parameter covering the whole system where single particle co-ordinates lose their identity. It is ideal for a collective description of many-electron system. The preliminary version of the density functional theory was developed by Thomas and Fermi (TF model) in 1920s based on the hypothetical uniform electron gas (Thomas 1927). Based on this model, they arrived at a kinetic energy functional  $T_{TF}[\rho]$  of the system as:

$$T_{TF}(\rho) = \frac{3}{10} (3\pi^2)^{2/3} \int d^3 r \rho^{5/3}(\mathbf{r}) \quad \dots \dots \dots (\text{Eq. 1.44})$$

The Thomas-Fermi kinetic energy functional is not accurate enough for the application to chemical systems, even though it involved elaborate mathematical description. Being the first DFT functional that used the expression of non-electrostatic energy terms in terms of the electron density, the Thomas-Fermi kinetic energy functional is important.  $\rho(\mathbf{r})$ , the prime variable of the DFT method, can be expressed as:

$$\rho(\vec{r}) = N \int d^3 r_2 \int d^3 r_3 \dots \int d^3 r_2 \Psi^*(\vec{r}_1, \vec{r}_2, \dots, \vec{r}_3) \Psi(\vec{r}_1, \vec{r}_2, \dots, \vec{r}_3) \dots \dots \dots (\text{Eq. 1.45})$$

The TF model remained a qualitative model even after insightful modifications are incorporated in to it in later years. The Hohenberg-Kohn (HK) theorems formulated in 1964 formed the real foundation of the current DFT model. In the Hohenberg-Kohn (HK) theorems also, the electron density is the principal variable. Initially, it was presumed that the local electron density decides the electron density functionals. Lately, the functionals were found to depend on various additional parameters such as the gradient of the electron densities (in the generalized gradient approximation, GGA), the kinetic energy density, the occupied orbitals and unoccupied orbitals. The statements of the HK theorems include (i) the external potential of the system and the total energy is a specific functional of electron density (ii) the ground state energy of the system can be determined variationally: the electron density distribution corresponding to the minimum the total energy is the ground state density. A

direct impact of the first HK theorem is that, the ground state energy E can be evaluated from the ground-state charge density of the system.

For a given value of the ground state electron density, the corresponding wave function  $\Psi_0(\vec{r}_1 \dots \vec{r}_N)$  can be obtained using the HK theorem,  $\rho_0(\vec{r})$ . Evidently, the ground state wavefunction of the system  $\Psi_0$  is a function of the respective electron density  $\rho_0$ . i.e.,

$$\Psi_0 = \Psi_0[\rho_0] \dots\dots\dots (\text{Eq. 1.46})$$

It turns out to be that all the ground state observables (O) of the system are functionals of  $\rho_0$ .

$$\langle \mathbf{O} \rangle[\rho_0] = \langle \Psi_0[\rho_0] | \mathbf{O} | \Psi_0[\rho_0] \rangle \dots\dots\dots (\text{Eq. 1.47})$$

The ground state energy can be expressed as a function of  $\rho_0$ .

$$E_0 = E[\rho_0] = \langle \Psi_0[\rho_0] | T + U + V | \Psi_0[\rho_0] \rangle \dots\dots\dots (\text{Eq. 1.48})$$

The contribution of the external potential to the ground state energy of the system which is represented as  $\langle \Psi_0[\rho_0] | V | \Psi_0[\rho_0] \rangle$  can be expressed in terms of electron density as:

$$V[\rho] = \int V(\vec{r}) \rho(\vec{r}) d^3 r \dots\dots\dots (\text{Eq. 1.49})$$

For a system with known external potential V, minimisation of the functional can be done as,

$$E[\rho] = T[\rho] + U[\rho] + \int V(\vec{r}) \rho(\vec{r}) d^3 r \dots\dots\dots (\text{Eq. 1.50})$$

Clearly, reliable expressions of T[ρ] and U[ρ] are necessary for the evaluation of Eq.1.50. To get the ground state electron density  $\rho_0$  and all related ground state observables, a successful minimization of the energy functional is essential. The variational treatment in which the Lagrangian methods of undetermined multipliers are used can be effectively applied for the energy minimisation. Successful implementation of this on the energy functional E[ρ] was done by Kohn and Sham in 1965. Alternately, the energy functional in Eq.1.50 can be expressed as a fictitious density functional of a non-interacting system.

$$E[\rho] = \langle \Psi_s[\rho] | T_s + V_s | \Psi_s[\rho] \rangle \dots\dots\dots (\text{Eq. 1.51})$$

$V_s$  Symbolise an external effective potential where the particles are executing motion and  $T_s$  represents the non-interacting kinetic energy.

If the external effective potential  $V_s$  taken as

$$V_s = V + U + (T_s - T) \dots\dots\dots (\text{Eq. 1.52})$$

Then,  $\rho_s(\vec{r}) = \rho(\vec{r})$

Now, the Kohn-Sham equation for the non-interacting system can be solved as

$$\left( -\frac{\hbar^2}{2m} \nabla^2 + V_s(\vec{r}) \right) \phi_i(\vec{r}) = \epsilon_i \phi_i(\vec{r}) \quad \dots \dots \dots \text{(Eq. 1.53)}$$

Eq.1.53 can produce orbitals  $\phi_i$  which can regenerate the electron density  $\rho(\vec{r})$  of the original many-body system.

$$\rho(\vec{r}) = \rho_s(\vec{r}) = \sum_i^N |\phi_i(\vec{r})|^2 \quad \dots \dots \dots \text{(Eq. 1.54)}$$

A detailed expression of the effective single- particle potential  $V_s$  is as follows

$$V_s = V + \int \frac{e^2 \rho_s(\vec{r}')}{|\vec{r} - \vec{r}'|} d^3 r' + V_{XC}[\rho_s \vec{r}] \quad \dots \dots \dots \text{(Eq. 1.55)}$$

The middle term at the RHS of Eq.1.55 represent the Hartree term expressing the inter-electron repulsion whereas the last term stands for the exchange correlation potential.  $V_{XC}$  in the last term constitute all the inter-particle interactions operative in the system. The mutual dependence among the Hartree term,  $\rho(\vec{r})$ ,  $V_{XC}$ ,  $V_s$ , and  $\phi_i$  necessitates the solution of Kohn-Sham equations in the specified self-consistent method. Which means; from initial set of Kohn-Sham equations a new electron density is obtained and the procedure is repeated for better values. This repeated calculation is continued till the convergence of self-consistency is attained.

Even the KS and HK schemes cannot generate a perfect mode of the exchange-correlation functional  $V_{XC}$ . Still, much of it is left to guesswork and systematic trial. Naturally, this requires some approximations for arriving at the observables of the system. Local Density Approximation (LDA) is the commonly employed approximation in this regard. In LDA, the functional rely only on the density at the coordinate, about which the functional is estimated.

$$E_{XC}[\rho] = \int \mathcal{E}_{XC}(\rho) d^3 r \quad \dots \dots \dots \text{(Eq. 1.56)}$$

The Local Spin Density Approximation (LSDA) is arrived at by adding spin to the Local Density Approximation (LDA).

$$E_{XC}(\rho_\uparrow, \rho_\downarrow) = \int \mathcal{E}_{XC}(\rho_\uparrow, \rho_\downarrow) d^3 r \quad \dots \dots \dots \text{(Eq. 1.57)}$$



To generate relations giving extremely accurate values of the exchange-correlation energy density  $E_{XC}(\rho_{\uparrow}, \rho_{\downarrow})$ , simulations of a free electron gas are used. Till invention of functionals within KS formalism, this was considered as the best method for the evaluation of exchange-correlation energy density. The dependence of functionals on the gradient of densities in addition to the density values is the primary difference incorporated in the Generalized Gradient Approximation (GGA). The over counted binding energy calculated using LDA in solids and molecules can be rectified by the GGA and extend the processing system to the structure and energy of the hydrogen bond system. The gradient of the density at the same coordinate is the factor considered by GGA.

$$E_{XC}(\rho_{\uparrow}, \rho_{\downarrow}) = \int \mathcal{E}_{XC}(\rho_{\uparrow}, \rho_{\downarrow}, \vec{\nabla}_{\rho_{\uparrow}}, \vec{\nabla}_{\rho_{\downarrow}}) d^3r \dots\dots (Eq. 1.58)$$

Extensively used exchange functionals include Slater's  $X\alpha$  (Slater 1951), B88 (A. D. Becke 1988) (Becke's 1988 functional that includes Slater's exchange with gradient corrections), having the form as

$$E_{XC}^{Becke88} = E_{XC}^{LDA} - \gamma \int \frac{\rho^{4/3} x^2}{(1+6\gamma \sinh^{-1} x)} d^3r \dots\dots (Eq. 1.59)$$

$x = \rho^{4/3} |\nabla \rho|$  and  $\gamma$  is a parameter chosen to fit the exchange energy of inert gas particles ( $\gamma = 0.0042$  a.u. as defined by Becke). Similarly, local and gradient corrected correlations functional also exist. Popularly used functionals include P86 and PW91 by developed by Perdew and Wang (Perdew et al. 1992) etc. Functionals of the type that offers definite improvement over the corresponding original DFT functional are also being widely used. The betterment is achieved by using a combination of HF and DFT exchange integrals along with the DFT correlation. The widely used functional BLYP is developed by the coupling of the Becke's generalized gradient corrected exchange functional with the gradient corrected correlation functional of Lee, Yang and Parr (Lee, Yang, and Parr 1988). A popular hybrid functional is B3LYP; generated by the coupling of Becke-3 parameters non-local exchange functional with the non-local correlation functional of Lee et al. The functional has the form (Axel D. Becke 1993):

$$E_{XC}^{B3LYP} = (1 - a)E_X^{LSDA} + aE_X^{HF} + b\Delta E_X^{B88} + E_C^{VWN3} + (1 - c)E_C^{LSDA} + cE_C^{LYP} \dots (Eq. 1.60)$$

Truhlar et al. developed a M05 and M06 class hybrid meta functionals which are acclaimed brilliant for accurate prediction about various properties of transition metal-based systems as well as main group elements (Zhao and Truhlar 2008).

The impossibility of derivation of the exchange-correlation functional from the first principles stands as the major disadvantage of DFT. Fortreating molecules at the correlated level of theory, DFT is continue to be the best alternative.

### 1.1.1.4 Potential Energy Surface

The ever first attempt of splitting the nuclear and electronic motions of a system according to time scales and the introduction of an appropriate potential energy surface (PES) for the nuclear motion during the changes in the systemic interactions was done by Born and Oppenheimer. Even though their original method remains outdated, the current equivalents regarding these phenomena are still named as Born–Oppenheimer approximations and Born–Oppenheimer PE surfaces. The Potential energy surfaces form one of the central concepts in the theoretical description of molecular reactivities, properties, and structures. The application of the BO approximation to the solution of the Schrodinger equation of the system concerned generates the PES. The general form of the Hamiltonian is

$$H = T_r + T_R + V(r, R) \dots\dots\dots (\text{Eq. 1.61})$$

$T_R$  represents the kinetic energy operator of the nuclear motion,  $T_r$  is the operator for the kinetic energy of the electronic motion and  $V(r,R)$  is the total potential energy operating in the system due to repulsive and attractive electrostatic interactions between all the particles bearing charges. The omission of the nuclear kinetic energy term ( $T_R$ ) in the molecular Hamiltonian is permitted by the BO approximation. This provides the convenience of the separation of the nuclear and electronic degrees of freedom. The time-independent Schrödinger equation for the electronic degrees of freedom of system can be formulated by taking the advantage of non-nuclear movement BO approximation.

$$[T_r + V(r, R)]\Psi(r; R) = E(R)\Psi(r; R) \dots\dots\dots (\text{Eq. 1.62})$$

$\psi(r;R)$  symbolise the electronic wavefunction that depends parametrically on the nuclear position  $R$  and therefore on  $3N$  nuclear coordinates.  $r$  is the  $3n$ - Cartesian coordinates representing the electronic positions.  $E(R)$  stands for the energy of the system which depends on the positioning of the nuclei. A plot of energy of the system  $E$  versus the nuclear coordinate  $R$  shapes the PES. The analysis of chemical properties and processes in computational chemistry begins with the optimization of one or more structures of the system to arrive at the minima on PESs. The minima on PESs correspond to the equilibrium geometries. A simplified PES with a topographic surface, valleys and saddle points is shown

in Figure 1.1. A mountainous landscape is usually exemplified as an analogy of the topology of PESs. The positions of minima in the valleys represent stable structures of molecules. From the height and profile of the pathway connecting reactant and product valleys, the rates and activation energies of the reaction can be assessed. The shape of a valley allows the computation of the vibrational spectrum of a molecule, determination of molecular properties such as dipole moment, polarizability, NMR shielding, etc (Dykstra 1988; Frank Jensen 1999; Rauhut and Pulay 1995).

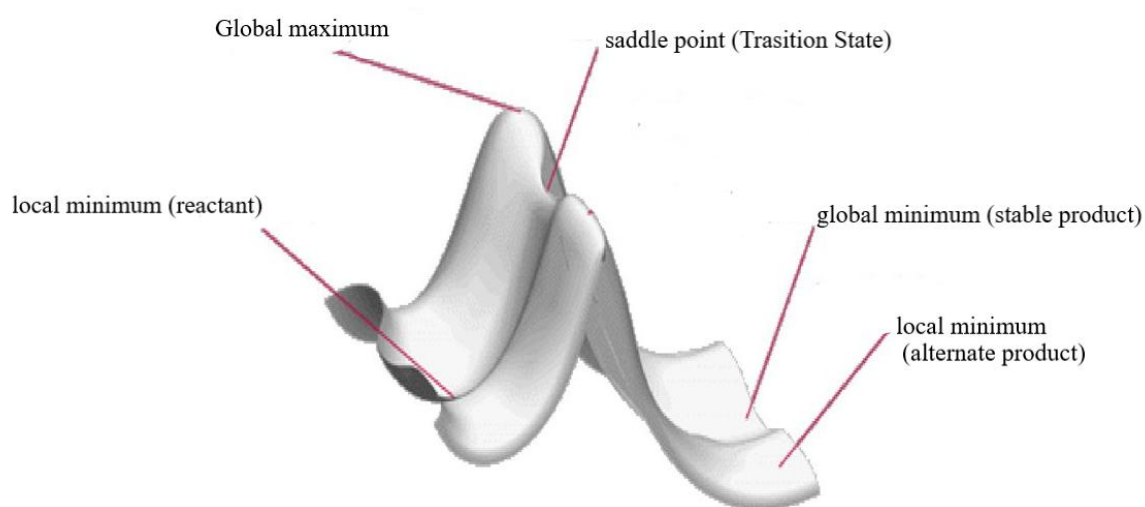


**Figure 1.1** A model potential energy surface.

The first-order saddle point on the PES represents the transition states (TS) of the reaction pathway. Locating these points in the PES is essential for the calculation of energy barriers of the reaction and to obtain reaction rates using the transition state theory (TST). A transition state structure on the PES is the topmost point on the minimum energy path (MEP) from the reactant to the product in the potential energy surface. It is popularly known as the saddle point on the PES. Saddle point is an energy point in the PES diagram which is a maximum in one direction (MEP) and a minimum in all other directions. In mathematical terms, a transition state is a point on PES for which the first derivatives should be necessarily zero and second derivative should be negative.

## Part B. Doubly Bonded Silicon Compounds

### 1.2 Introduction

Silicon is the 14<sup>th</sup> element of the periodic table, the second member of the 14<sup>th</sup> group in which carbon is the epitome element. In character, it is a semiconductor and a metalloid; in terms of abundance in the earth's crust, only second to oxygen. Due to its extreme affinity for oxygen, silicon seldom exists in the pure form; but always as a wide variety of oxides. In 1823, the Swedish chemist Jons Jakob Berzelius prepared it in the pure form which appears as a bluish crystalline solid with melting point 1687K. In all naturally occurring silicon compounds it maintains tetra valency and the compounds are generally polymeric.

Electronically, silicon is a semiconductor, the atom of which contains free electrons less than that present in an atom of a conductor but more than that of an insulator. Explaining in terms of conductance, the assumed energy bands in an atom are categorised as conduction and valence bands. The valence band in a solid constitutes a series of energy levels occupied by the valence electrons. The energy levels of valence band are filled at 0°K with allowed number of electrons according to the Pauli's principle. The band of higher energy levels, partially filled with electrons is called the conduction band. These electrons are known as the free electrons in solid state science, as they can move anywhere within the boundaries of the given solid. These free electrons are responsible for conduction and the flowing of current. The separation in energy among the valence band and the conduction band is known as the band gap. Being good conductors of electricity, in metals, the band gap is zero and generally the bands are overlapping. In insulators, the band gap is too wide that the electron exchange is forbidden. For semiconductors such as silicon, even though the bands are not overlapped the band gap is not large.

The semiconductor property of silicon earned it pivotal position in the electronic industry in modern times. It is the key ingredient of p-n junction in transistors which are the cardinal unit of computer chip. Silicon forms the fundamental element used in the 'hardware' of all electronic goods including the computers. Organo-silicon compounds, in which the carbon - silicon bond forms the principal structural characteristic, is widely implemented in pharmaceutical applications (Christopher J. Cramer 2002; Frank Jensen 1999; Tim Clark 1985) Silicon is rudimentary in solar cells, electronic gadgets, aerospace articles, thin film coatings etc.

Chemistry before 1980s believed that the multiple bonds to silicon is so unstable that it is impossible (Atkins and Paula 2006). The theoretical studies also reinforced the conclusion that  $p\pi-p\pi$  bond is unachievable between elements having a principal quantum number greater than two. The eye-opening breakthrough, which is a critical milestone in the organometallic chemistry, unfolded in 1981. At the 15<sup>th</sup> Organosilicon Symposium in Durham, North Carolina, US, companion papers announcing stable compounds containing double bond between carbon and silicon atoms, Si=C (Adrian G. Brook et al. 1981) and double bond between two silicon atoms, Si=Si (West, Fink, and Michl 1981) were presented by A.G. Brook et al and R. West et al respectively. The paradigm shifts in organometallic chemistry resulted from this revolutionary finding opened great channels led to the emphatic development of the chemistry of unsaturated compounds of the heavier elements of the group 14.

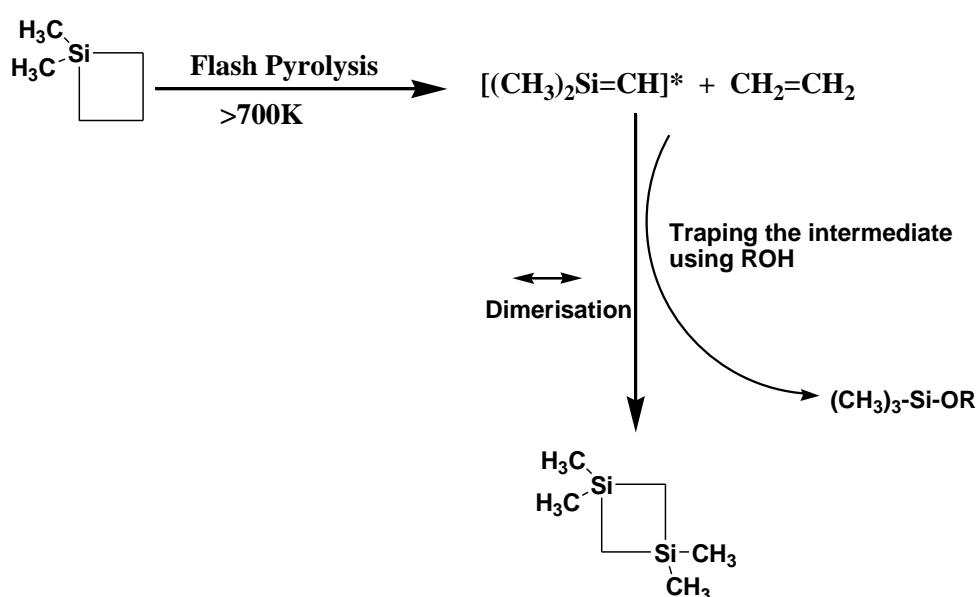
## 1.2.1 Silenes $R_2C=SiR_2$

### 1.2.1.1 Discovery and synthesis

In the history of synthetic chemistry, generation of molecules possessing chemical bonding of uncustomary nature often follows a common course of evolution. Primarily, someone announces the evidences of transient existence of the species during some chemical reactions. This may be followed by the isolation of it at very low temperatures; usually in a matrix, as is happened in the case of highly unstable species like the multiple bonded metalloids under the present discussion. The causes of instability of the species are subjected to thorough debate of theoreticians which will be reflected in the synthetic field as variety of adaptations and modifications. Finally, a molecule stable at room temperature, supported by brilliantly chosen steric and electronic stabilization, may be synthesized in a refined experimental condition. Such a sequence of events was exactly followed in the evolution of experiments led to the discovery of stable silenes also.

Convincing evidence of silene,  $R_2Si=CR_2$  as reaction intermediates came in 1966 during the studies of the high temperature gas phase thermal decomposition of 1,1-dimethyl-1-silacyclobutane by Gusel'nikov and co-workers (Gusel'Nikov and Flowers 1967). In the temperature range of 700–1000 K and at very low pressures, 1,1-dimethyl-1-silacyclobutane undergoes fragmentation and re-cyclisation. Ethylene and 1,1,3,3-tetramethyl-1,3-disilacyclobutane are the products generated in the reaction. 1,1,3,3-tetramethyl-1,3-disilacyclobutane is proposed to be formed because of the dimerization of the intermediate

silene generated. The proposed scheme is shown below (Scheme 1.1). The kinetics of this reaction has found to be very similar to the gas-phase thermolytic conversion of dialkylcyclobutanes into alkenes. Continued research revealed that the intermediate silene could be intercepted by various trapping agents like H<sub>2</sub>O, NH<sub>3</sub>, alcohols and carbonyl compounds; which confirmed its formation during the thermolytic decomposition of 1,1-dimethyl-1-silacyclobutane (Boudjouk and Sommer 1973; Butler 1962; Flowers and Gusel'nikov 1968; Gerberich and Walters 1961). When the pyrolysis stream is added with alcohol the corresponding alkoxy silanes is resulted, the formation of which cannot be explained without the presence of the proposed silene intermediate.

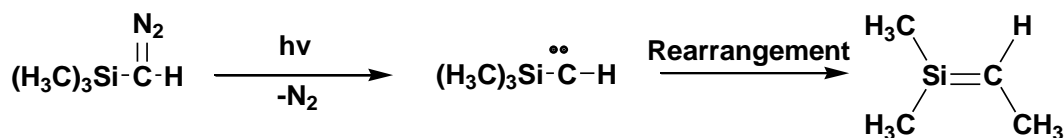


**Scheme 1.1**

Flash pyrolysis of 1,1-dimethyl-1-silacyclobutane indicating the intermediate formation of a compound with C=Si

By 1976, three different research groups including that of Chedekel et al were successful in synthesising silene in argon matrix at temperature below 12K. The photochemical decomposition of trimethylsilyldiazomethane was the technique mainly used. IR analysis revealed that the reaction proceeded through an unstable silyl carbene intermediate (Brook, Kallury, and Poon 1982; Chedekel et al. 1976; Mal'tsev, Khabashesku, and Nefedov 1976). Even though, the generated silene can survive only in deep low temperature reaction matrix, the Si=C stretching band of it near 1000 cm<sup>-1</sup> was identified for the first time by way of infrared spectroscopy. Still, most of the synthetic chemists believed that the synthesis of a stable silene is impossible as the 'double bond rule' denies the

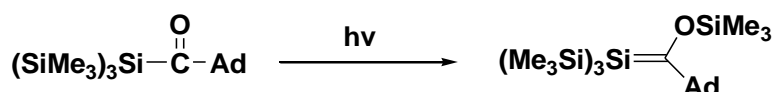
formation of such a compound. According to the ‘double bond rule,’ multiple bond formation is impossible for elements belonging to periods higher than two.



**Scheme 1.2**

Photochemical decomposition of trimethylsilyldiazomethane resulted in the first generation of a silene.

A.G. Brook and co-workers of the University of Toronto, working continuously for decades on silicon chemistry, explored the effect of the functional groups attached to the carbon and silicon atoms in the photochemical rearrangement of acyl silanes ( $\text{R}_3\text{Si}-\text{CO}-\text{R}'$ ) to silene. They recognised that a change of functional groups R and R' from lighter to heavier, enhanced the stability of the silene generated considerably. Their perpetual effort by using different groups in the place of R and R' of the acyl silane finally emerged triumphant in 1981. The successful substituents that generated a stable silene from the acyl silane by the photochemical rearrangement were  $(\text{Me}_3\text{Si}) = \text{R}$  and adamantyl group  $= \text{R}'$  (Adrian G. Brook et al. 1981). The discovery of a stable silene, which contradicted the ‘double bond rule’ was milestone in the development of chemistry in general and launched a paradigm shift in the synthetic organometallic chemistry.



**Scheme 1.3**

Photochemical rearrangement of acyl silane to generate the first stable silene (Brook silene) The silene materialised was a crystalline solid, stable at room temperature in anaerobic conditions.

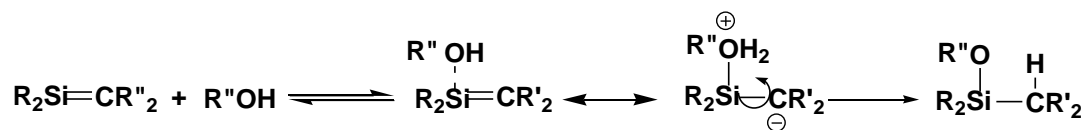
### 1.2.1.2 Stability of silenes

While studying the newly discovered Brook silenes, Y. Apeloig and M. Karni realized that, even though steric effects of the substituents definitively played an important role in stabilizing them, the contribution of electronic effects of the substituents is even more significant; but went unnoticed (Apeloig and Karni 1984). They have conducted a comprehensive study of a series of substituted silenes theoretically to elucidate the substituent



effect. Both mono- and di-substituted silenes were included in the study. The substituents they have chosen were -OH, -OSiH<sub>3</sub>, -SiH<sub>3</sub>, -CN, -NO<sub>2</sub>, -CH<sub>3</sub> and -F, evidently, these groups represent electronic properties spanning to a wide range. Because of the presence of lone-pair of electrons on the oxygen atom, the silyloxy and hydroxy and are strong  $\pi$ -donors. But, they weak as  $\sigma$ -acceptors, irrespective of the electro negative nature of oxygen atom. The nitrile and nitro groups are strong  $\pi$ -acceptors. They are powerful  $\sigma$ -acceptors also. The silyl group exertsonly milder electronic effects; it is a weak  $\sigma$ -donor and weak  $\pi$ -acceptor. The methyl group is a weak  $\sigma$ - as well as  $\pi$ -donor. Fluorine is a weak  $\pi$ -donor whereas it is strong  $\sigma$ -acceptor. Their studies proved that substituents have a strong influence on the C=Si double bond length. Changes in the bond length  $r_{C=Si}$  parallel the changes in the total bond polarity of the C=Si bond. Substitution at silicon is found to be significantly more stabilizing than substitution at carbon. Substituent influence on the stability of the C=Si double bond is calculated to be fairly low. The dimerization reactions of silenes to disilacyclobutanes also not much controlled by the substituents. Most importantly, the distribution of charge within the C=Si bond is strongly influenced by the substituents. A comparison of the total electron density over the double bond and the  $\pi$ -electron distribution alone showed that polarization occurs mainly in the  $\sigma$ -framework. The polarization experienced by the  $\pi$ -electrons is more relevant in the discussion of the reactivity of the C=Si double bond, even though it lesser in magnitude than the  $\sigma$ -polarization. As the extent of polarization of the C-Si  $\pi$ -bond increases, the reactivity of a particular silene increases is expected to increase. The natural  $C^{\delta-}=Si^{\delta+}$  bond polarity is reversed to  $C^{\delta+}=Si^{\delta-}$  in silenes in which strong  $\pi$ -donors such as -OH is attached to carbon atom. Reversed polarity of the C=Si bond plays a very important role in modifying and controlling the reactivity of silences (Apeloig and Karni 1984; Breidung and Thiel 1998; A. G. Brook et al. 1982; A. G. Brook, Kallury, and Poon 1982). Later, Bendikov and coworkers (Bendikov et al. 2002) carried out a systematic theoretical analysis of the effect of substituents on the kinetic stability of silenes for nucleophilic addition reactions with water and alcohol. The kinetic stability of silenes can be arrived at from the activation energy barriers for the addition reaction with suitable reagents which strongly influenced by the substituents. The addition of alcohols or water molecule is initiated through a nucleophilic attack by the oxygen atom of the reactant at the silicon atom of the silene. This result in the formation of a silene-alcohol complex which is reversible in nature. Further progress of the reaction resulted in the addition product: a silanol. This reaction pathway is notably different

from the typical mechanism of addition to C=C double bonds, which always involves a rate-determining step that is electrophilic.



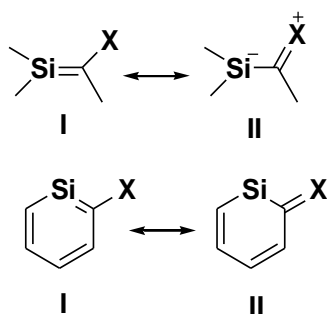
#### Scheme 1.4

Addition of an alcohol to silene

The activation energy of the addition reaction to silene is found to decrease as  $\text{H}_2\text{O} > \text{MeOH} > \text{EtOH} > \text{t-BuOH}$ . As is evident, this order shows a relation to the gas-phase acidity of the nucleophilic reactant molecule. The higher the alcohol acidity of the nucleophile, the lower is the activation energy of the addition to silene bond. One of the interesting findings of their study on the substituent effect is that the activation energy barriers for the nucleophilic addition of alcohol or water to silenes correlate linearly with the silene polarity. This was confirmed by measuring the difference in the total charge at the Si and at the C atoms of the Si=C bond of the investigated silenes. The substituents influence on the activation energies is found to be significantly large, spanning a range of 20 kcal/mol. Their calculations convincingly proved that for silenes with lesser polarity, the activation energy is greater for the addition reaction. Therefore, the kinetic stability of a silene towards nucleophilic addition can be predicted from the polarity of the C=Si double bond. In short, polarity of the C=Si double bond in silene is a reliable indicator of its stability. This observation led to the formulation and designing of novel strategy for the synthesis of kinetically stable silenes added with the well-established kinetic stabilization by bulky substituents.

Ottosson and co-workers explored the polarity reversal of the C-Si bond by  $\pi$ -electron donation from ortho/para substituents as a stabilizing factor for silabenzenes and also for the synthesis of transient silenes (El-Sayed et al. 2002). Reversed polarity of the  $\pi$ -bond, i.e.,  $\text{Si}^{\delta-}=\text{C}^{\delta+}$ , is the most important single electronic factor that reduces the reactivity of silenes (Apeloig and Karni 1984). The first solid silene, stable at ambient temperature made by Brook and coworkers and several other silenes and 2-silenolates that take advantage of this effect have been reported (Miracle et al. 1993; Sakamoto et al. 1997; Veszprémi et al. 1998). Because of the significant electronegativity difference between C and Si, the Si=C double bond in silenes is polar with the Si atom bearing the positive polarity and electrophilic nature. However, the direction and magnitude of polarity of this bond can be greatly modified and by

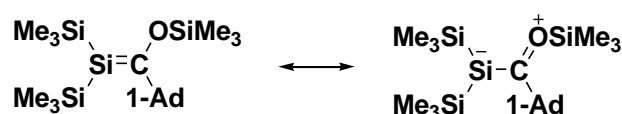
introducing  $\pi$ -electron-donating groups at the C end of the silenebond (Scheme 1.5). Such a substitution lowers the dimerization energy significantly and raises the barrier for addition of water to a considerable extent.



**Scheme 1.5**

Reverse polarisation in silenes

Similar to silenes, the reduction in the positive charge at Si atom of a silabenzene is achieved through the resonance structure II which is zwitter-ionic. For achieving these  $\pi$ -electron-donating groups are substituted in para and/or ortho positions. The partial positive charge at Si in silabenzene is found to be significantly reduced by ortho and/or para amino substitution. Substitution with halogen atoms has only mild effects on the structures and charge distributions and of silabenzenes. In the capability to supply electron density to Si atom of silabenzene, the alkoxy substituents remain intermediate between amino and halo substituents. Silyl substituents exert considerable impact on the depletion of positive charge on the Si atom but do not affect the geometries of silabenzenes. In the classical Brook's silene ( $\text{Me}_3\text{Si}$ )<sub>2</sub>Si=C(Ad)(OSiMe<sub>3</sub>), the  $\pi$ -electron donor/ $\sigma$ -electron acceptor nature of the trimethylsiloxy group at the carbon atom and  $\pi$ -electron acceptor/ $\sigma$ -electron donor nature of the trimethylsilane (TMS) at the silicon atom, reinforced with the steric protection of the substituent bulk, made it stable enough to remain at ambient conditions (Eklöf, Guliashvili, and Ottosson 2008). The  $\pi$ -electron donor capability of oxygen atom enhanced by the SiMe<sub>3</sub> group attached to it bring in the mesomeric effect culminating in contributing structures manifesting the reverse polarisation (Apeloig and Karni 1984; Bendikov et al. 2002; Leigh, Boukherroub, and Kerst 1998).



**Scheme 1.6**

Substituent effect leading to reverse polarisation in silene

The  $\pi$ -bond between silicon and carbon atoms in the silene molecule is less effective than the  $\pi$ -bond in alkenes. This is primarily due to the non-compatibility of the size of the  $3p_x$  and  $2p_x$  orbitals of the Si and C atoms respectively. The  $3p$  atomic orbital is significantly more diffused than the  $2p$  orbital (Apeloig and Karni 1984; Eklöf, Guliashvili, and Ottosson 2008). Electron withdrawing (electro-negative) substituents attached to any atom pulls out electron density from it, making it electron deficient. The loss of electron density intensifies the electron affinity of the nucleus led to a shrinking of its atomic orbitals. Electron donating substituents have an opposite effect. To make the silicon–carbon  $\pi$  bond more effective, the  $3p_x$  orbital of silicon atom should be less diffused than the original and the  $2p_x$  orbital of the carbon atom should be more diffused. For achieving congenial structural similarity of  $p$ -orbitals of different quantum numbers, Si atom of silene should be attached to electron withdrawing substituents and carbon atom should be attached with electron donating substituents (Apeloig and Karni 1984; Avakyan, Guselnikov, and Gusel'nikov 2003; Gusel'nikov, Avakyan, and Gusel'nikov 2001).

Leigh and co-workers studied the substituent effect on the reactivity of a number of silenes using the laser flash photolysis technique. They recognised that the nature of substituents profoundly influences the rate of addition of alcohols to silences which is nucleophilic. Substituents on either carbon or silicon that can reduce the natural polarity of C=Si bond give considerable kinetic stabilization to silences (Bradaric and Leigh 1997; Leigh et al. 2008; Leigh, Boukherroub, and Kerst 1998; Morkin and Leigh 2001). With the intention of obtaining experimental data directly relevant to the theoretical work, they have studied the effects on silene reactivity of several substituents attached to silicon, using a series of 1-substituted 1-methylsilacyclobutanes (a-k; scheme 7) as silene precursors (Leigh, Boukherroub, and Kerst 1998). The rate constants of their reactions with alcohols can be taken as a parameter of the kinetic stabilities of silences. To cover a wide a range of resonance and inductive electronic effects, many substituents were chosen spanning different electronic properties.

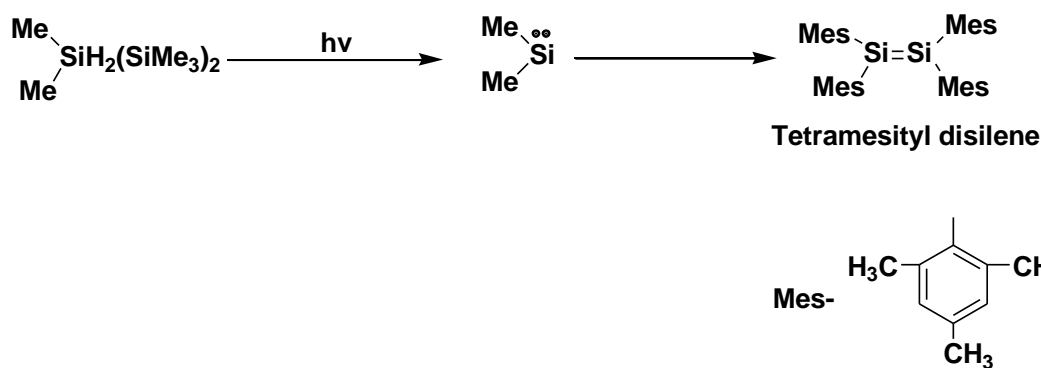


the Si atom. The analysis proved that the Si=C bond extended with reversed polarisation which causes a pyramidalization of the Si atom. Silenes substituted with two strong  $\pi$  electron-donors at the C atom involve resonance structures which are zwitterionic carrying negative charge of almost full magnitude on the Si atom. Nearly single bond nature of the Si-C bond and large pyramidalization of Si atoms are the characteristics of such 32ilences. There are instances where the reversed carbon – silicon bond polarization have no noticeable influence on the stabilities of conformers of 32ilences. In such cases, the relative stability of a specific conformer is determined by the steric demand of the structure and not by the reversed polarization effect.

## 1.2.2 Disilenes

### 1.2.2.1 The discovery and synthesis of disilene

The convincing proof for the formation of the disilene was obtained by G.J.D. Peddle and D.N. Roark in 1972 during their analysis on the pyrolysis of 7,8-disilabicycloocta-2,5-diene to tetramethyldisilene by way of a reverse Diels - Alder reaction (Roark and Peddle 1972). The highly unstable disilene could be trapped using naphthalene or anthracene (Scheme 1.8) (Carberry and West 1969; Strating et al. 1969). However, the incessant attempts to isolate the disilene even in deep cooled matrix were failed (Gaspar Peter P. 1978; Gusel'nikov, Nametkin, and Vdovin 1975; M. Ishikawa 1978). Meanwhile, in 1980, M. Ishikawa and M. Kumada reported the transient formation of silylenes; the Silicon analogue of carbenes, in the photolytic decomposition of polysilanes (Mitsuo Ishikawa and Kumada 1981). Trapping of the dimethylsilylene ( $\text{Me}_2\text{Si}:$ ) in argon matrix below 10 K allowed its detection of it by electronic and IR spectra (Arrington et al. 1984; Conlin and Gill 1983; Drahnak, Michl, and West 1979; Steele and Weber 1982). The research group of R. West, University of Wisconsin resulted in the groundbreaking achievement of the fabrication of a stable disilene molecule, tetramesityldisilene. The photolytic conversion of 2,2-bis(mesityl)hexamethyltrisilane in a solution of hydrocarbon generated Tetramesityldisilene. The intermediate silylene formed was dimerised to form tetramesityldisilene, which is precipitated as a bright yellow crystalline solid (Scheme 1.9) (Gaspar and West 1998; West, Fink, and Michl 1981).



**Scheme 1.8**

Photolysis of 2,2- bis(mesityl)hexamethyltrisilane led to the discovery of a stable disilene

### 1.2.2.2 Structure of Disilenes

The structure of tetramesityl disilene, the first ever synthesised compound carrying a silicon-silicon double bond, was explored by the West group themselves by X-ray crystallographic method, immediately after the successful synthesis of the compound. The molecule has a two-fold axis of symmetry which is passing perpendicular to the Si = Si double bond. The well-established geometry of alkenes confirmed the planar structure of them, which is a direct result of the trigonal planar alignment of the  $sp^2$  hybridised orbitals of the central carbon atom. The Si = Si double bond, the bond distance is  $2.16 \text{ \AA}$  in this molecule, against the C = C distance in ethylene which is  $1.34 \text{ \AA}$  (Boudjouk, Han, and Anderson 1982; Fink et al. 1983).

In tetramesityl disilene, the two doubly bonded silicon atoms and the four carbon atoms of the mesityl groups connected to them appears to be lie approximately in the same plane. A close analysis confirms that, the plane containing the C–Si– C bond forms a bend of angle  $\theta = 18^\circ$  with the bond connecting the two Si nuclei. The mesitylene groups attached to Si(2) bent upwards through the angle  $\theta$ , whereas the mesitylene groups connected to Si(1) bent downwards through the same angle. The resulting trans-bent geometry effects the pyramidalization of the Si atom in the structure and the angle  $\theta$  is called pyramidalization angle. Also, the planes containing the first C–Si–C and the second C–Si–C of tetramesityl disilene are not parallel; they make a twist angle of five degree (Figure 1.2) (Goldberg et al. 1986; Grev, Schaefer, and Gaspar 1991; Harding and Goddard 1978).

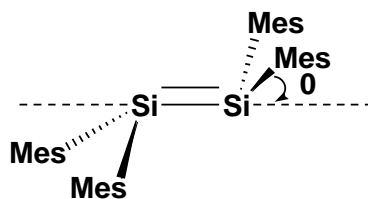


**Figure 1.2** Structure of disilene

The theoretical explanation for the elevation of the C–Si–C plane from the Si=Si double bond line by angle  $\theta$  is based on the singlet – triplet energy gap of the silylene moieties involved in the formation of the disilene. For the simplicity of treatment, the disilene can be viewed as the aggregate of two  $R_2Si:$  diradicals joined through a double bond (Harding and Goddard 1978; Leopold, Murray, and Lineberger 1984).

### 1.2.3 Silylene

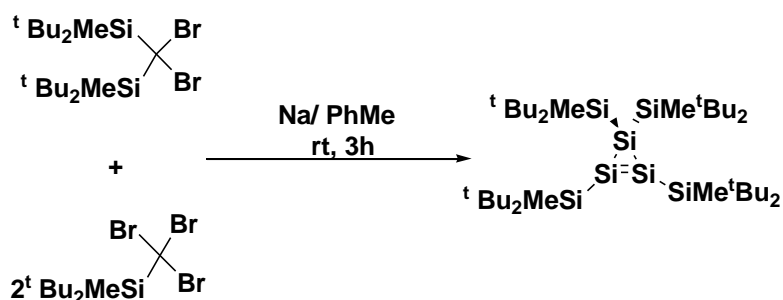
According to the energy status of the system, silylene can remain either in the triplet or in the singlet state. Contrary to the general trend and expectation, the singlet state is found to be more stable than the triplet state in silylenes. The singlet level of silylene occupies a position 21kcal/mol lower than the triplet state. The greater stability of singlet state relative to the triplet state is found to be prevalent in silicon and higher congeners of the group 14 (Carter and Goddard 1986; Driess and Grützmacher 1996; Malrieu and Trinquier 1989; Power 1999; Trinquier and Malrieu 1987).

### 1.2.4 Cyclotrisilene

#### 1.2.4.1 Synthesis

Successful synthesis of partial alkene analogue of silicon: the silene  $R_2Si=CR_2$ , and exact alkene analogue of silicon, the disilene  $R_2Si=SiR_2$  attracted the synthetic chemists to deeply explore on the possible synthesis of unsaturated compounds of heavier 14 group elements, mainly that of silicon. The elaborated search came up with verity of novel methods to synthesize differently substituted silenes and disilenes with substantially improved stability and highly desired property modulations. A breakthrough in this direction was the synthesis of a stable cyclotrisilene by Ichinohe and co-workers in 1999. They have synthesized a  $SiMe_2^tBu$  substituted cyclotrisilene, from a reaction mixture of 2,2-dibromo-1,1,3,3-tetra(tert-butyl)-1,3-dimethyltrisilane and 2,2,2-tribromo-1,1-di(tert-butyl)-1-methyldisilane with sodium in toluene (Ichinohe, Matsuno, and Sekiguchi 1999).



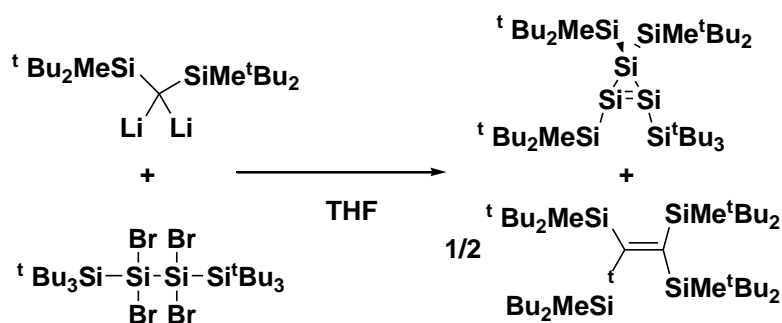


**Scheme 1.9**

Reaction between 2,2,2-tribromo-1,1-di(tert-butyl)-1-methyldisilane and 2,2-dibromo-1,1,3,3-tetra(tert-butyl)-1,3-dimethyltrisilane: formation of the first stable cyclotrisilene.

The selection of protecting groups is the most important criterion in the synthesis of strained ring compounds such as cyclotrisilene. As explained in the previous sections, silicon-silicon multiple bonds are largely stabilised by heavy sterically demanding functional groups. Quantum mechanical calculations proved that electropositive substituents such as silyl groups largely reduce the ring strain of cyclotrisilene (Ichinohe, Fukaya, and Sekiguchi 1998; Kira, Iwamoto, and Kabuto 1996; Nagase 1993; Sekiguchi et al. 1995; Wiberg et al. 1998).

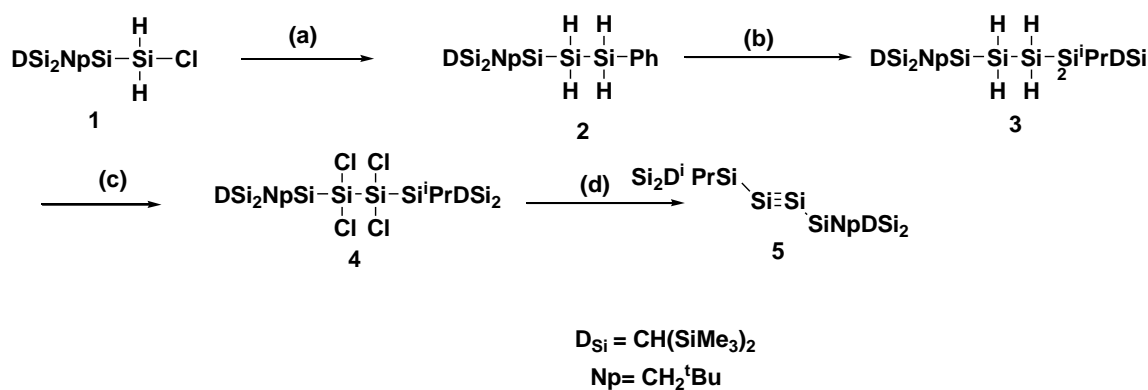
Sekiguchi and his co-workers developed a method to synthesise a highly crowded cyclotrisilene by the reaction of substituted dilithiosilane with substituted 1,2-dibromotetrasilane at a ratio of 2:1 in THF (Murata, Ichinohe, and Sekiguchi 2010). During this reaction, the second equivalent of dilithiosilane acts as a reductant.



**Scheme 1.10**

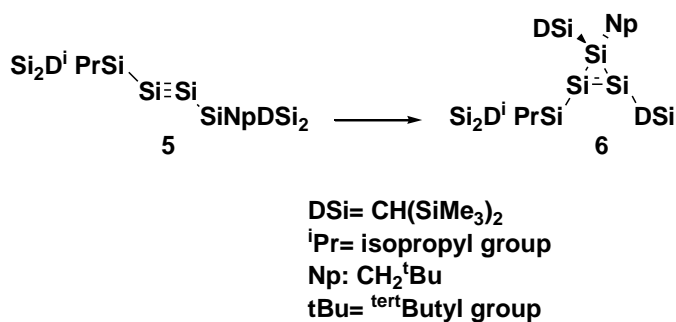
Reaction of  $({}^t\text{Bu}_2\text{MeSi})_2\text{SiLi}_2$  with  ${}^t\text{Bu}_3\text{SiBr}_2\text{SiBr}_2\text{Si}{}^t\text{Bu}_3$  led to the generation of a highly crowded stable cyclotrisilene

Y. Murata and colleagues reported a step-wise formation of cyclotrisilene starting from  $\text{DSi}_2\text{NpSiSiH}_2\text{Cl}$  (**1**) [ $\text{DSi} = \text{CH}(\text{SiMe}_3)_2$  and  $\text{Np} = \text{CH}_2{}^t\text{Bu}$ ] when kept at room temperature for overnight (Murata, Ichinohe, and Sekiguchi 2010).



**Scheme 1.11**

Slow isomerisation of the disilyne **5** in solution at room temperature generated cyclotrisilene **6** as the only product.



**Scheme 1.12**

Step-wise synthesis of cyclotrisilene (**6**) from  $\text{Dsi}_2\text{NpSiSiH}_2\text{Cl}$  (**1**)

### 1.2.4.2 Structure

The molecular structure of  $\text{SiMe}_2^t\text{Bu}$  substituted cyclotrisilene (**I**) has been confirmed by X-ray crystallography (Figure 1.3) (Ichinohe et al. 1999). The crystal structure revealed that, crystallographically, the molecule has no symmetry. The geometry around the  $\text{Si}=\text{Si}$  double bond is not planar, as obtained by the sum of the bond angles of the unsaturated silicon atoms ( $357.58^\circ$  for Si1 and  $358.18^\circ$  for Si2). Probably because of the eclipsed arrangement of the two bulky  $^t\text{Bu}_2\text{MeSi}$  substituents attached to the silicon atoms, the geometry of cyclotrisilene has a twisted  $\text{Si}=\text{Si}$  double bond.

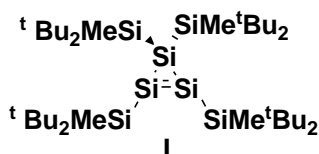


**Figure 1.3**

Structure cyclotrisilene synthesised by Ichinohe et al. 1999

The Si4-Si1-Si2-Si5 torsional angle is  $31.98^\circ$ . The length of Si-Si bond of **I** is  $2.138\text{\AA}$ , which is one of the shortest distances among the reported Si=Si double-bonds ( $2.138 \pm 2.261\text{\AA}$ ). The lengths of Si-Si single bonds in **I**, especially the bond distances between the saturated silicon atom in the three-membered ring and the substituents ( $2.401\text{\AA}$  for Si3-Si6 and  $2.403\text{\AA}$  for Si3-Si7), are observed to be somewhat elongated than the usual Si-Si bond ( $2.34\text{\AA}$ ). The ring formed by the three Si atoms is nearly an isosceles triangle and the bond angles are  $62.8^\circ$ ,  $63.3^\circ$ , and  $53.9^\circ$ .

Cyclisation of molecules bring in strain energy in to the cyclic systems. Thus, when propane is converted to cyclopropane, the molecule possesses strain energy of  $27.5\text{kcal/mole}$ . This is due to change of the bond angle around the carbon atom from the normal  $sp^3$  hybridisation angle,  $109^\circ 28'$  to the acute angle  $60^\circ$  of the triangular geometry of the cyclic molecule. Introduction of a double bond into the cyclic system enhances the strain energy of it, since the  $sp^2$  atoms that forms the double bond has the inherent bond angle  $120^\circ$ , which is still wider than the tetrahedral angle. The energy required to distort the bond angle to  $60^\circ$  from  $120^\circ$  would be greater than that is required from  $109^\circ 28'$ . Thus, strain energy of cyclopropene molecule is  $53.8\text{ kcal/mole}$  (Geiseler 1970; Hengge and Janoschek 1995; Naruse, Ma, and Inagaki 2001). Surprisingly, B3LYP/6-31G(d)//B3LYP/6-311++G(3df,2p) level calculations proved that the energy due to ring strain of the unsaturated cyclotrisilene ( $34.5\text{kcal/mol}$ ) is slightly lower and notable than the ring strain energy of the saturated cyclotrisilane ( $35.5\text{ kcal/mol}$ ). Naruse. Y et al., using the orbital phase theory, postulated that this phenomenon, which terribly contradicts the observations associated with carbon analogues, is due to the delocalisation of electrons of the Si = Si  $\pi$  bond through the sigma antibonding ( $\sigma^*$ ) orbitals of the Si-H bond (Gimarc and Zhao 1997; Iwamoto et al. 2000; Naruse, Ma, and Inagaki 2001).

### 1.3 Conclusion

The initial segment of this Chapter was the introduction to theoretical background of the computational methods that are frequently used in the analysis carried out in computational chemistry. A summarised account of the Hartree-Fock method which is the fundamental of the computational chemistry techniques such as the Post HF methods, electronic structure methods, Hybrid QM-MM methods, Density Functional Theory and some specific electronic properties is given. The second part of Chapter 1 describes silicon chemistry, specifically oriented on multivalent compounds of silicon. Multivalent silicon compounds are rather new to the synthetic field and opened immense opportunities and challenges in the research scenario. The history of invention, methods of formation and structural details of silene, disilene and cyclotrisilene are briefly described. Reductive approaches the successful method of choice for the formation of multiply bonded silicon compounds. In the Si=C double bond, the electron arrangement is remain in a polarized way ( $\text{Si}^{\delta+}=\text{C}^{\delta-}$ ). Silenes are found to be naturally polarized ( $\text{Si}^{\delta+}=\text{C}^{\delta-}$ ) or reverse polarized ( $\text{Si}^{\delta-}=\text{C}^{\delta+}$ ), depending on the substituents attached to it. Theoretical analysis and the data generated from experiments showed that the “reversed polarity” of silene bond (C=Si) have a significant influence in controlling the stability as well as reactivity of silences. The data gathered on substituted silenes clearly indicated that the chemical and physical properties of silenes can be modified predictably, by the correct selection of the substituents. The effect of substituents is found to be more pronounced when placed over the silicon atom of the silene bond. The steric bulk of the substituents also play an equally important role in providing kinetic stability to silicon multiple bond compounds.

## Reference

- Allen, Leland C., and Arnold M. Karo. 1960. "Basis Functions for Ab Initio Calculations." *Reviews of Modern Physics* 32(2): 275–85. <https://link.aps.org/doi/10.1103/RevModPhys.32.275>.
- Apeloig, Yitzhak, and Miriam Karni. 1984. "Substituent Effects on the Carbon-Silicon Double Bond. Monosubstituted Silenes." *Journal of the American Chemical Society* 106(22): 6676–82. <https://pubs.acs.org/doi/abs/10.1021/ja00334a036>.
- Arrington, Charles A., Kenneth A. Klingensmith, Robert West, and Josef Michl. 1984. "Polarized Infrared Spectroscopy of Matrix-Isolated Dimethylsilylene and 1-Methylsilene." *Journal of the American Chemical Society* 106(3): 525–30.
- Attila Szabo, and Neil S. Ostlund. 1989. *Modern Quantum Chemistry: Introduction to Advanced Electronic Structure*. 1st ed. New York: McGraw-Hill.
- Avakyan, Vitaly G., Stephan L. Guselnikov, and Leonid E. Gusel'nikov. 2003. "Classical Planar Doubly Bonded Si-Substituted Silenes—a Boundary System between Olefins and Heavier Group 14 Analogs." *Journal of Organometallic Chemistry* 686(1–2): 257–71.
- Bartlett, Rodney J., and David M. Silver. 1975. "Some Aspects of Diagrammatic Perturbation Theory." *International Journal of Quantum Chemistry* 9(9 S): 183–98.
- Becke, A. D. 1988. "Density-Functional Exchange-Energy Approximation with Correct Asymptotic Behavior." *Physical Review A* 38(6): 3098–3100. <https://link.aps.org/doi/10.1103/PhysRevA.38.3098>.
- Becke, Axel D. 1993. "A New Mixing of Hartree-Fock and Local Density-Functional Theories." *The Journal of Chemical Physics* 98(2): 1372–77.
- Bendikov, Michael, Sabine Ruth Quadt, Oded Rabin, and Yitzhak Apeloig. 2002. "Addition of Nucleophiles to Silenes. A Theoretical Study of the Effect of Substituents on Their Kinetic Stability." *Organometallics* 21(19): 3930–39. <https://pubs.acs.org/doi/10.1021/om0202571>.
- Born, M., and R. Oppenheimer. 1927. "Born Oppenheimer." *Annalen Der Physik* (20): 457–84.
- Bouckaert, L. P., R. Smoluchowski, and E. Wigner. 1936. "Theory of Brillouin Zones and Symmetry Properties of Wave Functions in Crystals." *Physical Review* 50(1): 58–67. <https://link.aps.org/doi/10.1103/PhysRev.50.58>.
- Boudjouk, Philip, Byung Hee Han, and Kevin R. Anderson. 1982. "Sonochemical and Electrochemical Synthesis of Tetramesityldisilene." *Journal of the American Chemical Society* 104(18): 4992–93.
- Boudjouk, Philip, and Leo H. Sommer. 1973. "Photochemical Generation of an Intermediate Containing a Silicon-Carbon Double Bond or Its Equivalent from 1,1-Diphenylsilylacetylobutane." *Journal of the Chemical Society, Chemical Communications* (2): 54.
- Bowen, J. Phillip, and Norman L. Allinger. 1991. "Molecular Mechanics: The Art and Science of Parameterization." 2: 81–97.
- Boyd, Donald B., and Kenny B. Lipkowitz. 1982. "Molecular Mechanics: The Method and Its Underlying Philosophy." *Journal of Chemical Education* 59(4): 269–74.
- Boys, S F, and Proc R Soc Lond A. 1950. "Electronic Wave Functions - I. A General Method of Calculation for the Stationary States of Any Molecular System." *Proceedings of the Royal Society of London. Series A. Mathematical and Physical Sciences* 200(1063): 542–54.
- Bradaric, Christine J., and William J. Leigh. 1997. "Substituent Effects on the Reactivity of the Silicon–Carbon Double Bond. Arrhenius Parameters for the Reaction of 1,1 -Diarylsilenes with

- Alcohols and Acetic Acid.” *Canadian Journal of Chemistry* 75(10): 1393–1402. <http://www.nrcresearchpress.com/doi/10.1139/v97-167>.
- Breidung, Jürgen, and Walter Thiel. 1998. “Anharmonic Force Field and Spectroscopic Constants of Silene: An Ab Initio Study.” *Theoretical Chemistry Accounts* 100(1–4): 183–90.
- Brook, A. G. et al. 1982. “Stable Solid Silaethylenes.” *Journal of the American Chemical Society* 104(21): 5667–72. <https://pubs.acs.org/doi/abs/10.1021/ja00385a019>.
- Brook, A. G., R. K.M.R. Kallury, and Y. C. Poon. 1982. “Attempted Stabilization of Silaethylenes with Aryl or Trifluoromethyl Groups.” *Organometallics* 1(7): 987–94.
- Brook, Adrian G. et al. 1981. “A Solid Silaethene: Isolation and Characterization.” *Journal of the Chemical Society, Chemical Communications* (4): 191. <http://xlink.rsc.org/?DOI=c39810000191>.
- Butler, N. 1962. “Thermal Decomposition of Octafluorocyclobutanel.”
- Carberry, Edward, and Robert West. 1969. “111.’ The.” 223(10): 5440–46.
- Carter, Emily A., and William A. Goddard. 1986. “Relation between Singlet-Triplet Gaps and Bond Energies.” *Journal of Physical Chemistry* 90(6): 998–1001.
- Chedekel, M. R., M. Skoglund, R. L. Kreeger, and H. Shechter. 1976. “Solid State Chemistry. Discrete Trimethylsilylmethylene.” *Journal of the American Chemical Society* 98(24): 7846–48.
- Christopher J. Cramer. 2002. *Essentials of Computational Chemistry*. 2nd ed. England: John Wiley & Sons Ltd.
- Čížek, Jiří. 1966. “On the Correlation Problem in Atomic and Molecular Systems. Calculation of Wavefunction Components in Ursell-Type Expansion Using Quantum-Field Theoretical Methods.” *The Journal of Chemical Physics* 45(11): 4256–66. <https://pubs.aip.org/jcp/article/45/11/4256/211247/On-the-Correlation-Problem-in-Atomic-and-Molecular>.
- Clementi, Enrico, and A. D. McLean. 1964. “Atomic Negative Ions.” *Physical Review* 133(2A): A419–23. <https://link.aps.org/doi/10.1103/PhysRev.133.A419>.
- Conlin, Robert T., and Russel S. Gill. 1983. “Thermal Fragmentation of Silacyclobutane. Formation of Silylene, Methylsilylene, and Silene.” *Journal of the American Chemical Society* 105(3): 618–19.
- Cramer, Christopher J., Frederic J. Dulles, Joey W. Storer, and Sharon E. Worthington. 1994. “Full Valence Complete Active Space SCF, Multireference CI, and Density Functional Calculations of 1A1—3B1 Singlet—Triplet Gaps for the Valence-Isoelectronic Series BH-2, CH2, NH+2, AlH-2, SiH2, PH+2, GaH-2, GeH2, and AsH+2.” *Chemical Physics Letters* 218(5–6): 387–94. <https://linkinghub.elsevier.com/retrieve/pii/0009261494000301>.
- Dinur, Uri, and Arnold T. Hagler. 1991. “New Approaches to Empirical Force Fields.” In , 99–164. <https://onlinelibrary.wiley.com/doi/10.1002/9780470125793.ch4>.
- Ditchfield, R., W. J. Hehre, and J. A. Pople. 1971. “Self-Consistent Molecular-Orbital Methods. IX. An Extended Gaussian-Type Basis for Molecular-Orbital Studies of Organic Molecules.” *The Journal of Chemical Physics* 54(2): 720–23.
- Doll, Jim, and David L. Freeman. 1994. “Monte Carlo Methods in Chemistry.” *IEEE Computational Science and Engineering* 1(1): 22–32.
- Drahnak, Timothy J., Josef Michl, and Robert West. 1979. “Dimethylsilylene, (CH3)2Si.” *Journal of the American Chemical Society* 101(18): 5427–28.

- Driess, Matthias, and Hansjörg Grützmacher. 1996. "Main Group Element Analogues of Carbenes, Olefins, and Small Rings." *Angewandte Chemie (International Edition in English)* 35(8): 828–56.
- Dunning, Thom H. 1970. "Gaussian Basis Functions for Use in Molecular Calculations. I. Contraction of (9s5p) Atomic Basis Sets for the First-Row Atoms." *The Journal of Chemical Physics* 53(7): 2823–33. <https://pubs.aip.org/jcp/article/53/7/2823/450810/Gaussian-Basis-Functions-for-Use-in-Molecular>.
- Dykstra, Clifford E. 1988. "Efficient Calculation of Electrically Based Intermolecular Potentials of Weakly Bonded Clusters." *Journal of Computational Chemistry* 9(5): 476–87. <https://onlinelibrary.wiley.com/doi/10.1002/jcc.540090506>.
- Eklöf, Anders M., Tamaz Guliashvili, and Henrik Ottosson. 2008. "Relation between the  $\pi$ -Contribution to Reversed Si=C Bond Polarization and the Reaction Profile for the Thermolytic Formation of Silenes." *Organometallics* 27(20): 5203–11. <https://pubs.acs.org/doi/10.1021/om800477j>.
- El-Sayed, Ibrahim et al. 2002. "Evidence for Formation of Silenes Strongly Influenced by Reversed SiC Bond Polarity." *Organic Letters* 4(11): 1915–18. <https://pubs.acs.org/doi/10.1021/ol025920w>.
- Feller, David, and Ernest R. Davidson. 1990. "Basis Sets for Ab Initio Molecular Orbital Calculations and Intermolecular Interactions." In , 1–43. <https://onlinelibrary.wiley.com/doi/10.1002/9780470125786.ch1>.
- Fink, Mark J. et al. 1983. "The X-Ray Crystal Structure of Tetramesityldisilene." *Journal of the Chemical Society, Chemical Communications* (18): 1010.
- Flowers, M. C., and L. E. Gusel'nikov. 1968. "Correction to Paper Entitled 'a Kinetic Study of the Gas-Phase Thermal Decomposition of 1, 1-Dimethyl-1-Silacyclobutane.'" *J. Chem. Soc. B* 0(0): 1396–1396.
- Fock, V. 1930. "Näherungsmethode Zur Lösung Des Quantenmechanischen Mehrkörperproblems." *Zeitschrift für Physik* 61(1–2): 126–48. <http://link.springer.com/10.1007/BF01340294>.
- Foresman, James B., Martin Head-Gordon, John A. Pople, and Michael J. Frisch. 1992. "Toward a Systematic Molecular Orbital Theory for Excited States." *The Journal of Physical Chemistry* 96(1): 135–49. <https://pubs.acs.org/doi/abs/10.1021/j100180a030>.
- Frank Jensen. 1999. *Introduction to Computational Chemistry*. 2nd ed. England: John Wiley & Sons Ltd.
- Gaspar P. P., and R West. 1998. *2 The Chemistry of Organic Silicon Compounds*. eds. Zvi Rappoport and Yitzhak Apeloig. New York: John Wiley and Sons.
- Gaspar Peter P. 1978. *1 Reactive Intermediates. 7. Silylenes*. eds. M. Jones and RA Moss. New York: Wiley.
- Geiseler, G. 1970. "J. D. Cox Und G. Pilcher: Thermochemistry of Organic and Organometallic Compounds. Academic Press, London and New York 1970. 643 Seiten. Preis: 170s." *Berichte der Bunsengesellschaft für physikalische Chemie* 74(7): 727–727. <https://onlinelibrary.wiley.com/doi/10.1002/bbpc.19700740727>.
- Gerberich, H. R., and W. D. Walters. 1961. "The Thermal Decomposition of Trans-1,2-Dimethylcyclobutane 1,2." *Journal of the American Chemical Society* 83(24): 4884–88. <https://pubs.acs.org/doi/abs/10.1021/ja01485a003>.
- Gimarc, Benjamin M., and Ming Zhao. 1997. "Strain and Resonance Energies in Main-Group Homoatomic Rings and Clusters." *Coordination Chemistry Reviews* 158: 385–412.

- Goldberg, David E. et al. 1986. "Subvalent Group 4B Metal Alkyls and Amides. Part 9. Germanium and Tin Alkene Analogues, the Dimetallenes  $M_2R_4$  [ $M = \text{Ge or Sn, } R = \text{CH}(\text{SiMe}_3)_2$ ]: X-Ray Structures, Molecular Orbital Calculations for  $M_2H_4$ , and Trends in the Series  $M_2R'_4$  [ $M = \text{C, Si, Ge, or Sn; } R' = \text{R, Ph, } C_6H_2Me_3$  -2,4,6, or  $C_6H_3Et_2$  -2,6]." *J. Chem. Soc., Dalton Trans.* (11): 2387–94.
- Grev, Roger S., Henry F. Schaefer, and Peter P. Gaspar. 1991. "In Search of Triplet Silylenes." *Journal of the American Chemical Society* 113(15): 5638–43.
- Gusel'nikov, L. E., V. G. Avakyan, and S. L. Gusel'nikov. 2001. "Effect of the Electronic Structure of Substituents at the Silicon Atom on the Structure and Bond Energies of Methylhydrosilanes and Silenes." *Russian Journal of General Chemistry* 71(12): 1933–41.
- Gusel'Nikov, L. E., and M. C. Flowers. 1967. "The Thermal Decomposition of 1,1-Dimethyl-1-Silacyclobutane and Some Reactions of an Unstable Intermediate Containing a Silicon–Carbon Double Bond." *Chem. Commun. (London)* (17): 864–65. <http://xlink.rsc.org/?DOI=C19670000864>.
- Gusel'nikov, L. E., N. S. Nametkin, and V. M. Vdovin. 1975. "Unstable Silicon Analogs of Unsaturated Compounds." *Accounts of Chemical Research* 8(1): 18–25. <https://pubs.acs.org/doi/abs/10.1021/ar50085a003>.
- Hall. 1951. "The Molecular Orbital Theory of Chemical Valency VIII. A Method of Calculating Ionization Potentials." *Proceedings of the Royal Society of London. Series A. Mathematical and Physical Sciences* 205(1083): 541–52. <https://royalsocietypublishing.org/doi/10.1098/rspa.1951.0048>.
- Harding, Lawrence B., and William A. Goddard. 1978. "Methylene: Ab Initio Vibronic Analysis and Reinterpretation of the Spectroscopic and Negative Ion Photoelectron Experiments." *Chemical Physics Letters* 55(2): 217–20.
- Hengge, Edwin, and Rudolf Janoschek. 1995. "Homocyclic Silanes." *Chemical Reviews* 95(5): 1495–1526.
- Ichinohe, Masaaki et al. 1999. 38 Molecular Spectra and Molecular Structure *Synthesis, Characterization, and Crystal Structure of Cyclotrisilene: A Three-Membered Ring Compound with a Si–Si Double Bond*\*\*.. Van Nostrand Reinhold.
- Ichinohe, Masaaki, Norihisa Fukaya, and Akira Sekiguchi. 1998. "Synthesis and Structure of Cyclotrigermanium Salt of the Tetrakis{3,5-Bis(Trifluoromethyl)Phenyl}borate Anion. A Stable Free Germyl Cation in the Condensed Phase." *Chemistry Letters* 27(10): 1045–46.
- Ichinohe, Masaaki, Tadahiro Matsuno, and Akira Sekiguchi. 1999. "Synthesis, Characterization, and Crystal Structure of Cyclotrisilene: A Three-Membered Ring Compound with a Si–Si Double Bond." *Angewandte Chemie International Edition* 38(15): 2194–96. [https://onlinelibrary.wiley.com/doi/10.1002/\(SICI\)1521-3773\(19990802\)38:15%3C2194::AID-ANIE2194%3E3.0.CO;2-L](https://onlinelibrary.wiley.com/doi/10.1002/(SICI)1521-3773(19990802)38:15%3C2194::AID-ANIE2194%3E3.0.CO;2-L).
- Ishikawa, M. 1978. "Photolysis of Organopolysilanes. Generation and Reactions of Silicon-Carbon Double-Bonded Intermediates." *Pure and Applied Chemistry* 50(1): 11–18. <https://www.degruyter.com/document/doi/10.1351/pac197850010011/html>.
- Ishikawa, Mitsuo, and Makoto Kumada. 1981. "Photochemistry of Organopolysi/Anes." 19(14).
- Iwamoto, Takeaki, Makoto Tamura, Chizuko Kabuto, and Mitsuo Kira. 2000. "A Stable Bicyclic Compound with Two Si=Si Double Bonds." *Science* 290(5491): 504–6. <https://www.science.org/doi/10.1126/science.290.5491.504>.
- James J. P. Stewart. 1990. "MOPAC: A Semiempirical Molecular Orbital Program." *Journal of Computer-Aided Molecular Design* 4: 1–103.



- John A. Pople, and David L. Beveridge. 1970. *Approximate Molecular Orbital Theory*. NEW YORK: McGRAW-HILL BOOK COMPANY.
- Kira, Mitsuo, Takeaki Iwamoto, and Chizuko Kabuto. 1996. "The First Stable Cyclic Disilene." 7863(c): 10303–4.
- Kohn, W., and L. J. Sham. 1965. "Self-Consistent Equations Including Exchange and Correlation Effects." *Physical Review* 140(4A): A1133–38. <https://link.aps.org/doi/10.1103/PhysRev.140.A1133>.
- Krishnan, R., J. S. Binkley, R. Seeger, and J. A. Pople. 1980. "Self-Consistent Molecular Orbital Methods. XX. A Basis Set for Correlated Wave Functions." *The Journal of Chemical Physics* 72(1): 650–54. <https://pubs.aip.org/jcp/article/72/1/650/971433/Self-consistent-molecular-orbital-methods-XX-A>.
- Lee, Chengteh, Weitao Yang, and Robert G. Parr. 1988. "Development of the Colle-Salvetti Correlation-Energy Formula into a Functional of the Electron Density." *Physical Review B* 37(2): 785–89. <https://link.aps.org/doi/10.1103/PhysRevB.37.785>.
- Leigh, William J., Rabah Boukherroub, and Corinna Kerst. 1998. "Substituent Effects on the Reactivity of the Silicon–Carbon Double Bond. Resonance, Inductive, and Steric Effects of Substituents at Silicon on the Reactivity of Simple 1-Methylsilenes." *Journal of the American Chemical Society* 120(37): 9504–12.
- Leigh, William J et al. 2008. "Substituent Effects on Silene Reactivity — Reactive Silenes from Photolysis of Phenylated Tri- and Tetrasilanes." *Canadian Journal of Chemistry* 86(12): 1105–17. <http://www.nrcresearchpress.com/doi/10.1139/v08-165>.
- Leopold, D. G., K. K. Murray, and W. C. Lineberger. 1984. "Laser Photoelectron Spectroscopy of Vibrationally Relaxed CH<sub>2</sub>: A Reinvestigation of the Singlet–Triplet Splitting in Methylene." *The Journal of Chemical Physics* 81(2): 1048–50. <https://pubs.aip.org/jcp/article/81/2/1048/218501/Laser-photoelectron-spectroscopy-of-vibrationally>.
- Mal'tsev, A. K., V. N. Khabashesku, and O. M. Nefedov. 1976. "Stabilization and Direct Spectroscopic Observation of Molecules with an Unsaturated Carbon-Silicon Bond." *Bulletin of the Academy of Sciences of the USSR Division of Chemical Science* 25(5): 1165–1165.
- Malrieu, Jean Paul, and Georges Trinquier. 1989. "Trans Bending at Double Bonds. Occurrence and Extent." *Journal of the American Chemical Society* 111(15): 5916–21.
- Miller, John H, and Hugh P Kelly. 1971. "+lr»-R." : 480–84.
- Miracle, Gary E., Jared L. Ball, Douglas R. Powell, and Robert West. 1993. "The First Stable 1-Silaallene." *Journal of the American Chemical Society* 115(24): 11598–99. <https://pubs.acs.org/doi/abs/10.1021/ja00077a069>.
- Møller, Chr., and M. S. Plesset. 1934. "Note on an Approximation Treatment for Many-Electron Systems." *Physical Review* 46(7): 618–22. <https://link.aps.org/doi/10.1103/PhysRev.46.618>.
- Morkin, Tracy L., and William J. Leigh. 2001. "Substituent Effects on the Reactivity of the Silicon–Carbon Double Bond." *Accounts of Chemical Research* 34(2): 129–36. <https://pubs.acs.org/doi/10.1021/ar960252y>.
- Murata, Yoshitaka, Masaaki Ichinohe, and Akira Sekiguchi. 2010. "Unsymmetrically Substituted Disilyne Dsi<sub>2</sub><sup>i</sup> PrSi—Si≡Si—SiNpDsi<sub>2</sub> (Np = CH<sub>2</sub><sup>t</sup> Bu): Synthesis and Characterization." *Journal of the American Chemical Society* 132(47): 16768–70.
- Nagase, S. 1993. "Theoretical Study of Heteroatom-Containing Compounds. From Aromatic and Polycyclic Molecules to Hollow Cage Clusters." *Pure and Applied Chemistry* 65(4): 675–82.

<https://www.degruyter.com/document/doi/10.1351/pac199365040675/html>.

- Naruse, Yuji, Jing Ma, and Satoshi Inagaki. 2001. "Relaxation of Ring Strain by Introduction of a Double Bond." *Tetrahedron Letters* 42(37): 6553–56.
- Ottosson, Henrik. 2003. "Zwitterionic Silenes: Interesting Goals for Synthesis?" *Chemistry – A European Journal* 9(17): 4144–55. <https://chemistry-europe.onlinelibrary.wiley.com/doi/10.1002/chem.200204583>.
- Ottosson, Henrik, and Anders M. Eklöf. 2008. "Silenes: Connectors between Classical Alkenes and Nonclassical Heavy Alkenes." *Coordination Chemistry Reviews* 252(12–14): 1287–1314. <https://linkinghub.elsevier.com/retrieve/pii/S0010854507001452>.
- Pauli, W. 1925. "Über Den Zusammenhang Des Abschlusses Der Elektronengruppen Im Atom Mit Der Komplexstruktur Der Spektren." *Zeitschrift für Physik* 31(1): 765–83. <http://link.springer.com/10.1007/BF02980631>.
- Perdew, John P. et al. 1992. "Atoms, Molecules, Solids, and Surfaces: Applications of the Generalized Gradient Approximation for Exchange and Correlation." *Physical Review B* 46(11): 6671–87. <https://link.aps.org/doi/10.1103/PhysRevB.46.6671>.
- Peter Atkins, and Julio de Paula. 2006. *Physical Chemistry*. 8th ed. New York: W. H. Freeman & Co.
- Pople, J. A., R. Krishnan, H. B. Schlegel, and J. S. Binkley. 1978. "Electron Correlation Theories and Their Application to the Study of Simple Reaction Potential Surfaces." *International Journal of Quantum Chemistry* 14(5): 545–60. <https://onlinelibrary.wiley.com/doi/10.1002/qua.560140503>.
- Pople, John A., J. Stephen Binkley, and Rolf Seeger. 1976. "Theoretical Models Incorporating Electron Correlation." *International Journal of Quantum Chemistry* 10(10 S): 1–19.
- Power, Philip P. 1999. " $\pi$ -Bonding and the Lone Pair Effect in Multiple Bonds between Heavier Main Group Elements." *Chemical Reviews* 99(12): 3463–3504.
- Rapaport, D. C. 2004. *The Art of Molecular Dynamics Simulation*. Cambridge University Press. <https://www.cambridge.org/core/product/identifier/9780511816581/type/book>.
- Rauhut, Guntram, and Peter Pulay. 1995. "Transferable Scaling Factors for Density Functional Derived Vibrational Force Fields." *Journal of Physical Chemistry* 99(10): 3093–3100.
- Roark, D. N., and G. J. D. Peddle. 1972. "Reactions of 7,8-Disilabicyclo[2.2.2]Octa-2,5-Dienes. Evidence for the Transient Existence of a Disilene." *Journal of the American Chemical Society* 94(16): 5837–41.
- Roothaan, C. C. J. 1951. "New Developments in Molecular Orbital Theory." *Reviews of Modern Physics* 23(2): 69–89. <https://link.aps.org/doi/10.1103/RevModPhys.23.69>.
- Sakamoto, Kenkichi, Jun Ogasawara, Hideki Sakurai, and Mitsuo Kira. 1997. "The First Silatriafulvene Derivative: Generation, Unusually Low Reactivity toward Alcohols, and Isomerization to Silacyclobutadiene." *Journal of the American Chemical Society* 119(14): 3405–6. <https://pubs.acs.org/doi/10.1021/ja970083s>.
- Sekiguchi, Akira et al. 1995. "Cyclotrimerenes: A New Unsaturated Ring System." *Journal of the American Chemical Society* 117(30): 8025–26.
- Slater, J. C. 1930. "Atomic Shielding Constants." *Physical Review* 36(1): 57–64. <https://link.aps.org/doi/10.1103/PhysRev.36.57>.
- Steele, Kent P., and William P. Weber. 1982. "Mass Spectrometry of Allyloxy Di- and Trimethylsilanes." *Organic Mass Spectrometry* 17(5): 222–28.
- Stewart, Robert F. 1970. "Small Gaussian Expansions of Slater-Type Orbitals." *The Journal of*

- Chemical Physics* 52(1): 431–38. <https://pubs.aip.org/jcp/article/52/1/431/85134/Small-Gaussian-Expansions-of-Slater-Type-Orbitals>.
- Strating, J., B. Zwanenburg, A. Wagenaar, and A.C. Udding. 1969. “Evidence for the Expulsion of Bis-CO from Bridged  $\alpha$ -Diketones.” *Tetrahedron Letters* 10(3): 125–28.
- Thomas, L. H. 1927. “The Calculation of Atomic Fields.” *Mathematical Proceedings of the Cambridge Philosophical Society* 23(5): 542–48. [https://www.cambridge.org/core/product/identifier/S0305004100011683/type/journal\\_article](https://www.cambridge.org/core/product/identifier/S0305004100011683/type/journal_article).
- Tim Clark. 1985. *A Handbook of Computational Chemistry: A Practical Guide to Chemical Structure and Energy Calculations*. New York: John Wiley & Sons.
- Trinquier, Georges, and Jean-Paul Malrieu. 1987. “{keine Sn-Sn-Geometriedaten} Nonclassical Distortions at Multiple Bonds.” *Journal of the American Chemical Society* 109: 5303–15.
- Veszprémi, Tamás et al. 1998. “An Ab Initio MO Study of Structure and Reactivity of 4-Silatriafulvene.” *Journal of the American Chemical Society* 120(10): 2408–14. <https://pubs.acs.org/doi/10.1021/ja971925q>.
- Weiner, Paul K., and Peter A. Kollman. 1981. “AMBER: Assisted Model Building with Energy Refinement. A General Program for Modeling Molecules and Their Interactions.” *Journal of Computational Chemistry* 2(3): 287–303.
- West, Robert, Mark J. Fink, and Josef Michl. 1981. “Tetramesityldisilene, a Stable Compound Containing a Silicon-Silicon Double Bond.” *Science* 214(4527): 1343–44. <https://www.science.org/doi/10.1126/science.214.4527.1343>.
- Wiberg, Nils et al. 1998. “Diiodotetrasupersilylcyclotetrasilene (TBu<sub>3</sub>Si)<sub>4</sub>Si<sub>4</sub>I<sub>2</sub> – Eine Verbindung Mit Ungesättigtem Si<sub>4</sub>-Ring.” *Angewandte Chemie* 110(20): 3030–33.
- Woon, David E., and Thom H. Dunning. 1993. “Gaussian Basis Sets for Use in Correlated Molecular Calculations. III. The Atoms Aluminum through Argon.” *The Journal of Chemical Physics* 98(2): 1358–71.
- Zhao, Yan, and Donald G. Truhlar. 2008. “The M06 Suite of Density Functionals for Main Group Thermochemistry, Thermochemical Kinetics, Noncovalent Interactions, Excited States, and Transition Elements: Two New Functionals and Systematic Testing of Four M06-Class Functionals and 12 Other Function.” *Theoretical Chemistry Accounts* 120(1–3): 215–41. <https://link.springer.com/10.1007/s00214-007-0310-x>.



# Chapter 2:

## Substituent effects on the dimerization reaction of silenes: the di-radical and the zwitter-ion reaction pathways

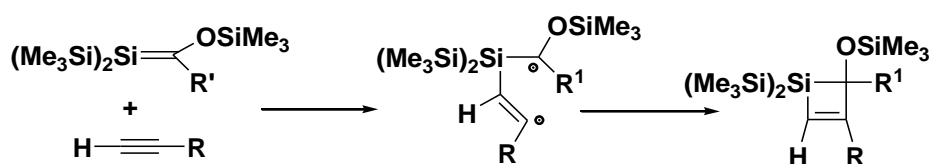
---

### 2.1 Introduction

The Si=C double bond is an intrinsically reactive bonding arrangement that has gained a great deal of experimental and theoretical attention over the past few decades (Baines 2013; Eklöf, Guliashvili, and Ottosson 2008; Ottosson and Eklöf 2008). Most of the silenes have only transient existence; that too the gas phase or in solution. They react in nascent state itself with oxygen or other nucleophiles due to their instability. When other reactive substrates are absent, they undergo self-dimerization. Successful attempts to synthesize isolable silenes primarily require a protective measure to safe guard it from the self-dimerization tendency. The principal tool for this purpose is the use of bulky substituents. This kind of steric stabilization of the silenes is purely kinetic in nature and is to be augmented with components that are capable in enhancing the thermodynamic stabilization of the molecule. For this purpose, synthetic chemists usually made use of substituents such as trialkylsilyl group at the Si atom and alkoxy- and (or) alkyl-substituents at the C atom of the C=Si bond. It is well established that such substitution patterns lead to marked reductions in the natural ( $\delta^+ \text{Si}=\text{C}^{\delta-}$ ) polarity associated with the Si=C double bond, slowing the normally diffusion-controlled dimerization reaction and reversing its normal (head-to-tail) regiochemistry (Apeloig and Karni 1984).

Silenes freely react with nucleophilic substrates including a mines, carboxylic acids, alcohols, water and alkoxy silanes due to their prominent electrophilic character and the reaction is typical [1,2]-addition in nature. Aldehydes and ketones react with silenes in the [2 + 2]-cycloaddition and/or ene-addition fashion. However, dienes and alkenes and undergo [4 + 2]-cycloaddition and/ or ene-addition, [2 + 2] with the silenes. In the absence of such reagents, they easily undergo dimerization, usually by head-to-tail [2 + 2]-cycloaddition (Bernardi et al. 1994; Brook and Baines 1986; Gusel'nikov and Nametkin 1979; Gusel'nikov, Nametkin, and Vdovin 1975; Morkin and Leigh 2001). The high electro negativity deference

of 0.7 in the Pauling scale between the Si and C atoms made the C=Si bond in silene remarkably polar. Therefore, the reactions of silenes with nucleophiles are highly region-specific. The addition of alkynes to Brook silenes,  $(\text{Me}_3\text{Si})_2\text{Si}=\text{CR}(\text{OSiMe}_3)$ , is a well-known regio-elective reaction of relatively nonpolar silenes that typically yields silacyclobutenes (Hajgató et al. 2002; Hardwick and Baines 2011; Pavelka et al. 2015; Takahashi, Veszprémi, and Kira 2004; Hiromasa Tanaka et al. 2012; Veszprémi et al. 2001). An exclusive theoretical exploration of the detailed mechanism of the addition reaction of alkynes with silenes was done by Milnes et al. They studied the different possible reaction pathways and their energetics of the addition reactions of silenes with terminal alkynes. The energetics of the biradical, zwitter-ion, and concerted pathways were computed and arrived at the conclusion that diradical pathways is significantly more favored (Milnes, Jennings, and Baines 2006; Milnes, Pavelka, and Baines 2010; Pavelka et al. 2015). In view of the importance of addition of alkynes to silenes in the chemistry of silicon compounds, Baines et al. undertook an experimental study of the mechanism of the cycloaddition of alkynes to Brook silences (Milnes, Jennings, and Baines 2006). They utilized a series of cyclopropyl alkynes which they have developed as mechanistic probes of the reaction. They arrived at the conclusion that a 1,4-diradical is involved in the addition reaction which is schematically represented below (scheme 2.1).

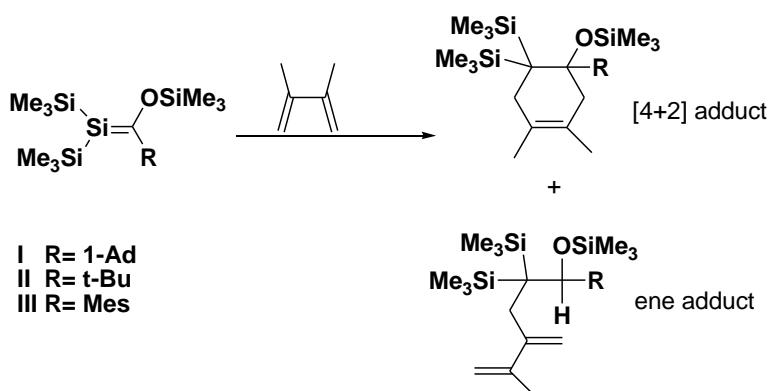


**Scheme 2.1**

Addition of alkynes to silene; the diradical pathway

Silenes readily undergo addition reaction with dienes also. Both  $[4 + 2]$  and  $[2 + 2]$  cycloadditions, as well as ene reactions, can occur between silenes and dienes, and which of these reaction routes is followed depends largely on the extent of the Si=C double bond polarity (A. G. Brook et al. 1987; Seidl, Grev, and Schaefer 1992). The silene molecule  $(\text{Me}_3\text{Si})_2\text{Si}=\text{C}(\text{OSiMe}_3)\text{R}$  with the R= 1-Ad (**I**) and R=t-Bu (**II**) produced both the ene and  $[4 + 2]$  addition products during reactions with the dien; 2,3-dimethyl-1,3-butadiene (Scheme 2.2). The relative amounts of the  $[4 + 2]$  addition product and the ene addition product is in the ratio 1.5:1 for both silenes **I** and **II**, and the collective yields were very high; more than

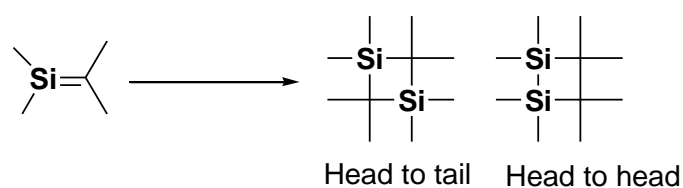
98%. In contrast, [2 + 2] cycloadducts were found in higher yields than the [4 + 2] cycloadducts in reactions between  $(\text{Me}_3\text{Si})_2\text{Si}=\text{C}(\text{OSiMe}_3)\text{R}$  silene **III** and 1,3-butadiene (scheme 2.2) (Brook et al. 1987).



**Scheme 2.2**

The [4+2] cyclo-addition and ene-addition of silenes to dienes

As already mentioned, silenes ( $\text{R}_2\text{Si}=\text{CR}_2$ ) readily undergo self-dimerization reaction, particularly in the absence of other reacting partners. The dimerization tendency is particularly augmented by the relatively smaller size of substituents attached to the carbon and silicon atoms, facilitating the steric environment conducive for the process (Apeloig et al. 1998; Brook et al. 1982; Ottosson and Eklöf 2008). The self-addition could be in either of the two possible fashions: head-to-tail or head-to-head coupling (Seidl, Grev, and Schaefer 1992; Venturini et al. 1998). A general schematic representation of these two modes of dimerization is given below (Scheme 2.3) (A. G. Brook et al. 1982).



**Scheme 2.3**

The head-to-tail and head-to-head modes of dimerization of silenes

The fundamental driving force operating in the inclination for the dimerization reaction of silenes is the dipolar nature of the C-Si bond ( $\delta^+\text{Si}=\text{C}\delta^-$ ) (Apeloig and Karni 1984). Obviously, factors such as properly designed electronic effects of substituents that can reduce polarity of the C=Si bond or even cause reversal of it as an extreme influence, reduce the tendency for dimerization significantly (Guliashvili et al. 2010; Miracle et al. 1993). The

larger size of the substituents considerably augments the inertia towards dimerization. This principle is successfully being used in the synthesis of silenes (Brook et al. 1981).

The nature of polarisation itself ( $\delta^+ \text{Si}=\text{C}^{\delta-}$ ) suggests an increased tendency of silenes toward head-to-tail coupling than head-to-head coupling during the dimerization reaction. As far as the parent silene is concerned, the head-to-tail dimerization reaction proceeds through a significantly stabilised pathway culminating in a well stabilised product. Even though the natural drive of the original charge separation of the silene could be to direct the dimerization reaction to proceed in a path generating a dimer resulting from the head-to-tail coupling, the substituents attached to the carbon and silicon of the silene could significantly affect the bond polarity and there for, the mode of the coupling also. The modulation in the bond polarity of the C=Si bond by the substituents profoundly affects the entire course of the dimerization reaction; even a reversal in the direction of coupling, resulting in the generation of the head-to-head coupled product could be turned up as an extreme gesture (Guliashvili et al. 2010; Leigh et al. 1999; Leigh, Boukherroub, and Kerst 1998; Sakamoto et al. 1997).

## 2.2 Objectives

- Understanding the possible reaction pathways and the energetics of the head-to-tail coupling reactions of silenes, resulting in the formation of 1,3-disilacyclobutanes.
- Analysis of the effect of substituents on the mechanism and free energy profile for the dimerization of monosubstituted ( $\text{RHSi}=\text{CH}_2$ ,  $\text{H}_2\text{Si}=\text{CHR}$ ) and disubstituted ( $\text{RHSi}=\text{CHR}$ ) silenes.

## 2.3 Computational Methods

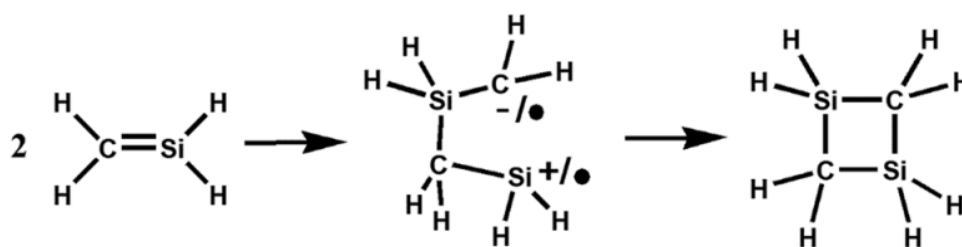
B3LYP/6-31G(d,p) level of density functional theory using Gaussian 16 suite of programs is employed in the present study to perform the computations. Minimas were ascertained by the method of IR frequency analysis, and the saddle points were located by a single imaginary frequency. To obtain intermediates and transition states possessing the singlet diradicals character, the broken-symmetry-spin-unrestricted B3LYP was used. To verify the consistency of out puts, all of calculations were also repeated at the PW6B95D3/6-311++G(d,p) level of theory also (due to convergence difficulties, the diradicals were excluded). The energy values are found to be consistent with B3LYP/6-31G(d,p) calculation. Therefore, the presented discussion on the study is exclusively based on the results generated from the B3LYP/6-31G(d,p) level calculations.



## 2.4 Results and Discussion

In the present study, we chose to analyze the reaction pathways and energetics of the head-to-tail coupling reactions of silenes resulting in the formation of 1,3-disilacyclobutanes. The unsubstituted parent silene,  $\text{H}_2\text{Si}=\text{CH}_2$  is chosen as the reference molecule of the investigation. The reaction pathways and energetics of the dimerization of the mono-substituted and disubstituted silenes were examined deeply and the results generated were compared with those of the unsubstituted silene to elucidate the effect of substituent on the reaction. Monosubstituted silenes with substituent on the silicon atom ( $\text{RHSi}=\text{CH}_2$ ) are designated as H-CSi-R, monosubstituent on carbon ( $\text{H}_2\text{Si}=\text{CHR}$ ) are designated as R-CSi-H and disubstituted silenes with one R each on both C and Si ( $\text{RHSi}=\text{CHR}$ ) as R-CSi-R. The substituents (R) chosen are  $-\text{CH}_3$ ,  $-\text{SiH}_3$ ,  $-\text{OH}$ ,  $-\text{CN}$  and  $-\text{F}$ ; span a range of electronic properties.

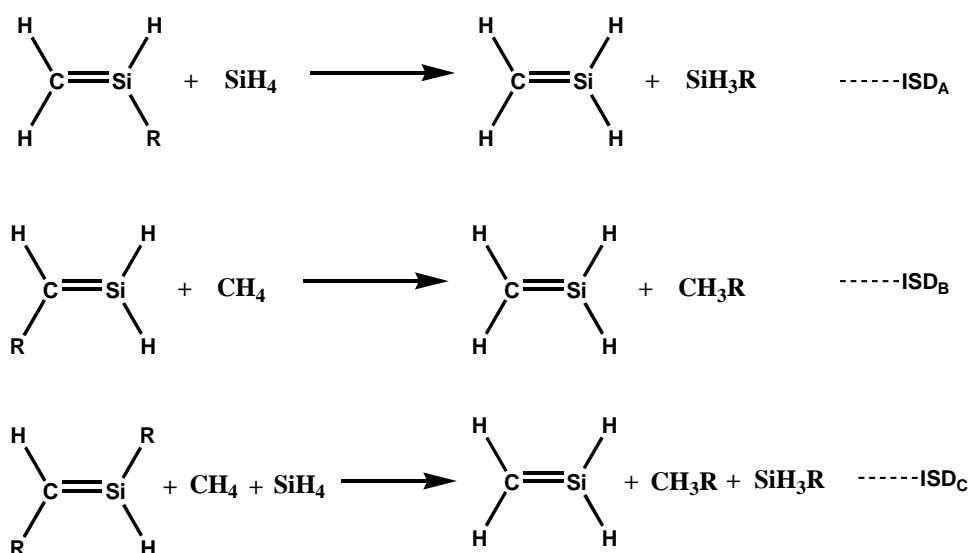
The  $-\text{OH}$  group is a strong  $\pi$ -electron donor, because of the unshared electron pair on the oxygen atom, but is a weak  $\sigma$ -acceptor. The  $-\text{CN}$  group on the other hand is a strong  $\pi$ -acceptor and also an equally powerful  $\sigma$ -acceptor. The  $-\text{SiH}_3$  exerts a much milder electronic effect, it is a weak  $\pi$ -acceptor and a weak  $\sigma$ -donor. The  $-\text{CH}_3$  group is a weak  $\pi$ - and  $\sigma$ -donor, while  $-\text{F}$  is a strong  $\sigma$ -acceptor and a weak  $\pi$ -donor (Apeloig and Karni 1984). Theoretical investigations support a pathway involving a 1,4-diradical as intermediate for the dimerization reaction of silenes resulting in the formation of 1,3-disilacyclobutane. This conclusion corroborated by experimental investigations. Various possibilities such as concerted mechanism and head-to-head dimerization to form 1,2-disilacyclobutane via a diradical intermediate have also been reported (Gusel'nikov, Avakyan, and Gusel'nikov 2002; Seidl, Grev, and Schaefer 1992; Venturini et al. 1998). In the present study, we have investigated the head-to-tail mode of the dimerization reaction of the silenes only, yielding 1,3-disilacyclobutane (1,3-D) as product. Two pathways, viz; zwitter-ion intermediate pathway (ZW) and the diradical pathway (DR) have been calculated to analyze whether the course of the reaction changes with substituents and to understand substituent effects on energetic (Scheme 2.4) (Milnes, Pavelka, and Baines 2010; Pavelka et al. 2015). We have scrutinized the energetics involved in both of these pathways outlined for the dimerization with all the investigated molecules to enable a comparison of the mechanisms. The effect of the substituents with divergent electronic properties on the reaction course and energetics of the coupling reaction is the thrust area of the investigation.



**Scheme 2.4**

The zwitter-ion intermediate pathway (ZW) and the diradical intermediate pathway (DR) for the head-to-tail dimerization of the parent silene.

In the present investigation we have used isodesmic reactions to understand the stabilizing/destabilizing effects of substituents in silences (Apeloig and Karni 1984). Following isodesmic reaction schemes were used in the analysis.



**Scheme 2.5**

Isodesmic reaction scheme used for the analysis

In the displayed examples, ISD represent difference in energy of the -R bond when it is part of the respective silene system and corresponding alkane or silane. A positive ISD ( $\sum_{H_f} \text{products} - \sum_{H_f} \text{reactants}$ ) indicates a lower stability of the substituted silene and a negative value indicates a higher stability. We have calculated the ISD values for different substituted silenes used in the present work and is tabulated in Table 2.1

**Table 2.1** Isodesmic reaction energy values

	Free energy a. u	Free energy a. u	Free energy a. u			
R	R-CSi-H	H-CSi-R	R-CSi-R	ISD <sub>A</sub> kcal/mol	ISD <sub>B</sub> kcal/mol	ISD <sub>C</sub> kcal/mol
H	-329.925405	-329.925405	-329.925405	0	0	0

Me	-369.214723	-369.227163	-408.515422	0.62751	-1.60078	-0.30873
SiH <sub>3</sub>	-620.617505	-620.615313	-911.307286	-0.76619	-5.16315	-5.54091
OH	-405.125159	-405.180917	-480.374409	0.983308	-2.88027	7.882153
CN	-422.177662	-422.180844	-514.429348	0.7687	-6.57379	-5.48255
F	-429.151413	-429.226644	-528.446372	1.853037	-0.41353	8.830321

The values listed in the Table 2.1 shows primarily that, the electronic characteristics of the substituent atoms or groups attached to the silene molecule have no decisive role in deciding the thermodynamic stability of it. Both electron-pushing and electron-pulling substituents on carbon end of the silene bond impart a mild additional stabilization to silene. This is specifically true with the substituents -SiH<sub>3</sub> and -CN. Moreover, placing the substituents on the silicon atom of the C=Si bond also failed to provide any noticeable improvement on the thermodynamic stability of the silenes. However, in the disubstituted systems R-CSi-R,  $\pi$ -donating groups and atoms like -OH and -F contribute a marginal stabilization to the molecule, whereas the other group helps to enhance the thermodynamic stability to a small extent.

### 2.4.1 Molecular electrostatic potential and polarity of the C=Si in silenes

The molecular electrostatic potential (MESP) at a point specify by the position vector  $(x,y,z)$  in the premises of a particle may be defined as ‘the force acting on a positive test charge (a proton) located at  $p$ , through the electrical charge cloud generated through the electrons and nuclei of the molecule’. The magnitude of molecular electrostatic potential (MESP) at an atom in a molecule is found to be convenient and precise parameter to arrive at the substituent effects on a molecule. It also serves to determine the control of the substituent over the reactivity of the molecule (Dimitrova, Ilieva, and Galabov 2003; Suresh, Remya, and Anjalikrishna 2022). MESP is calculated at the carbon nucleus ( $V_C$ ) and silicon nucleus ( $V_{Si}$ ) of all the silene systems (R-CSi-H, H-CSi-R and R-CSi-R) are presented in Table 2.2, along with the C-Si bond lengths of the corresponding silene.

**Table 2.2** H-CSi-R: Mono substituent on Si, R-CSi-H: Mono substituent on C, R-CSi-R: One substituent each on C and Si.  $V_C$ : MSEP at C,  $V_{Si}$ : MSEP at Si.

Substituent (R)	H-CSi-R			R-CSi-H			R-CSi-R		
	$r_{(C=Si)}$ Å	MESP at nucleus		$r_{(C=Si)}$ Å	MESP at nucleus		$r_{(C=Si)}$ Å	MESP at nucleus	
		$V_C$ a.u.	$V_{Si}$ a.u.		$V_C$ a.u.	$V_{Si}$ a.u.		$V_C$ a.u.	$V_{Si}$ a.u.
-H	1.71	-14.7477	-49.2402	1.71	-14.7477	-49.2402	1.71	-14.7477	-49.2402

-CH <sub>3</sub>	1.71	-14.7631	-49.2459	1.72	-14.7408	-49.2495	1.71	-14.7555	-49.2539
-SiH <sub>3</sub>	1.72	-14.7468	-49.2455	1.71	-14.7485	-49.2272	1.72	-14.7489	-49.2339
-OH	1.69	-14.7641	-49.2148	1.77	-14.6792	-49.2591	1.77	-14.6924	-49.2321
-CN	1.71	-14.7208	-49.1944	1.72	-14.6955	-49.1976	1.72	-14.6718	-49.1557
-F	1.69	-14.7499	-49.1935	1.73	-14.6608	-49.2361	1.71	-14.6643	-49.1863

The extent of the charge separation on the C=Si bond, owing to the electro negativity difference between the two atoms and the electron displacement effects produced by the substituents on it are reflected in the calculated  $V_C$  and  $V_{Si}$  values. The MESP data at the carbon and silicon nuclei of a silene ( $V_C$  and  $V_{Si}$ ) varies with the electron withdrawing or donating capability of the substituents connected to them. The change in the MESP values is caused by the electron density displacements at the respective carbon and silicon centres by the different electronic effects of the substituents such as inductive, mesomeric, hyper conjugative etc (Takahashi, Veszprémi, and Kira 2004). The inductive effect of the substituents is more visible on the Si atom in R-C=Si-H, where the substituent is connected to the C nucleus of the silene. Silenes with strong  $\pi$ -donating groups on carbon are generally known to possess polarity reversal (Apeloig and Karni 1984; El-Sayed et al. 2002; Ottosson 2003). Polarity reversal in the C=Si bond in HO-CSi-H is obvious from the measure of the MSEP values  $V_{Si}$  and  $V_C$  on the silicon and carbon atoms: -49.2591 a.u and -14.6792 a.u. respectively. The corresponding values on the silicon and carbon atoms of H-CSi-H are -49.2402 a. u and -14.7477 a. u respectively. It can be seen that, in R-CSi-H systems the measure of  $V_{Si}$  is maximum when the substituent R = -OH. Hence, the magnitude of the molecular electrostatic potential at the Si nucleus of the silene molecule can be taken as a good parameter to assess the reversal of the polarity R-CSi-H systems. Further, an elongation of the C-Si bond length amounting to 0.06 Å in HO-CSi-H (C-Si bond length 1.77 Å) compared to the unsubstituted H-CSi-H (C-Si bond length 1.71 Å) is also point to the reversal of polarity. A perusal of the MSEP table given above will reveals that the extension of the C-Si bond length to 1.77 Å is manifested in the disubstituted HO-CSi-OH also. Obviously, this indicates the polarity reversal in HO-CSi-OH too as is further evident from the corresponding  $V_{Si}$  value of -49.2321 compared to -49.2148 a.u. in the monosubstituted H-CSi-OH (Apeloig and Karni 1984).

## 2.4.2 Dimerization - The zwitter-ion pathway

### Dimerization of H-CSi-H

The structural parameters and the relative energy values associated with the transition states, intermediates and product involved in the dimerization process of the reference molecule (unsubstituted silene,  $\text{H}_2\text{C}=\text{SiH}_2$ ) through the zwitter-ion pathway is calculated. The structure of intermediates, transition states and product located and the corresponding energy values arrived at are depicted in Figure. 2.1.

The two silene molecules undergoing the dimerization reaction oriented to a dispersion complex (Z-1) initially, with a relative energy 7.70 kcal/mol. The dipolar nature associated with the silene molecules facilitates the orientation of the individual molecules in the dispersion complex. Natural charge values ( $q$ ) of carbon and silicon nuclei in the silene molecule are  $q_{\text{C}} = -1.08$  and  $q_{\text{Si}} = 0.90$  respectively and the C-Si bond distance is 1.71 Å. Z-1 is advanced to a transition state Z-TS1, in which a strong attraction among the silicon nucleus of the first silene molecule and the carbon nucleus of the second is developed ( $r_{\text{C-Si}} = 2.68$  Å). The formation of the transition state, Z-TS1 affected the measure of natural charges over the C and Si atoms of both the molecules. A slight elongation is observed with the C-Si bond also ( $r_{\text{C-Si}} = 1.72$  Å). The activation energy involved in the formation of the transition state Z-TS1 is 3.67 kcal/mol (The symbol “ $\Delta G\#1$ ” will be used for indicating the first activation barrier in further discussion) and the relative energy of the structure is 11.37 kcal/mol.

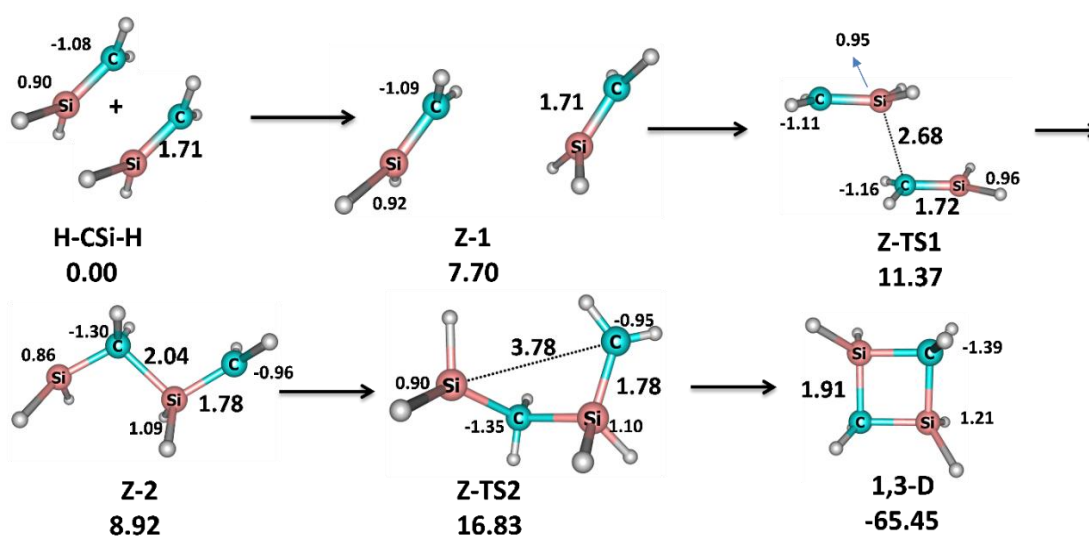


**Figure 2.1** Intermediates and transition states located for the dimerization of H-CSi-H via zwitter-ion pathway. Relative free energies are given in kcal/ mol and bond lengths in Å. Natural charges are also shown.

The activated complex Z-TS1 is progressed to zwitter-ionic intermediate Z-2 by the firming of the intermolecular C-Si bond ( $r_{C-Si} = 2.04\text{\AA}$ ). The measures of natural charges on Si1, C1, Si2 and C2 respectively are 0.86, -1.30, 1.09, and -0.96. This indicates the zwitter – ionic nature of Z-2. The bond distance Si-C bond of the silene is extended from  $1.71\text{\AA}$  to  $1.78\text{\AA}$  and the newly formed C-Si bond length is  $2.04\text{\AA}$ .

The intermediate Z-2 is advanced to another transition state, Z-TS2 through the rotation with respect to the newly formed intramolecular C-Si bond. The process involves an activation energy of 7.91 kcal/mol (Symbol “ $\Delta G\#2$ ” will be used to denote the second activation barrier in the proceeding discussion) and the relative energy of the of the second activated complex is 16.83 kcal/mol. The natural charges over the atoms also changed in accordance with the structural changes of the system and the intra molecular C-Si bond length remains unchanged ( $r_{C-Si} = 1.78\text{\AA}$ ). The transition state Z-TS2 advanced to the product 1,3-D. The process is highly exothermic indicating the better stability of the dimer. The high exoergicity of 65.45 kcal/mol of the dimerization reaction resulting in the formation of 1,3-D suggests the feasibility of the reaction in ambient reaction conditions.

To understand the role of substituent effect on the dimerization reaction of silenes, the reactions of monosubstituted (R-CSi-H and H-CSi-R) and the di substituted silene (R-CSi-R) were subjected to the mechanistic analysis. For all the silenes with substituents, the general mechanism followed exactly the same pattern as that of  $H_2C=SiH_2$ . The free energy of all the intermediates, transition states and products formed in the dimerization reaction of R-CSi-H, H-CSi-R and R-CSi-R are listed in Table 2.3

**Table 2.3** Relative free energy values (in kcal/mol) of intermediates and transition states involved in the dimerization of R-CSi-H, H-CSi-R and R-CSi-R via zwitter-ion pathway

Silene	Substituent (R)	Z-1	Z-TS1	Z-2	Z-TS2	1,3-D
$H_2C=SiH_2$	-H	7.70	11.37	8.92	16.83	-65.45
R-CSi-H	-CH <sub>3</sub>	6.70	14.79	12.28	20.19	-56.53
	-SiH <sub>3</sub>	7.87	14.35	13.75	19.07	-59.12
	-OH	-0.96	9.08	-1.26	10.89	-50.57
	-CN	-1.28	15.00	13.99	20.28	-53.46
	-F	7.07	12.24	7.10	14.63	-56.85
H-CSi-R	-CH <sub>3</sub>	5.99	11.82	10.56	16.38	-65.06
	-SiH <sub>3</sub>	6.22	13.55	12.73	18.5	-60.19
	-OH	0.82	4.42	-3.31	6.73	-74.36
	-CN	5.84	10.41	6.57	12.23	-70.47

	-F	-	-	-	-	-
R-CSi-R	-CH <sub>3</sub>	6.34	14.58	12.13	21.52	-56.00
	-SiH <sub>3</sub>	6.82	15.26	14.82	22.12	-52.05
	-OH	1.38	5.26	-14.96	-4.38	-68.84
	-CN	-15.36	12.99	10.16	19.28	-53.51
	-F	5.59	10.04	-8.45	4.26	-75.41

For all the monosubstituted R-CSi-H systems, the high exoergicity and low energy of activations (<18 kcal/mol) of the dimerization reactions show that it is practicable under ambient conditions. Measures of the activation energies,  $\Delta G\#1$  and  $\Delta G\#2$  for the strongly electron withdrawing F substituted F-CSi-H differ from those of electron donating CH<sub>3</sub> and SiH<sub>3</sub> substituted H<sub>3</sub>C-CSi-H and H<sub>3</sub>Si-CSi-H by only <3 kcal/mol. This observation indicates that the characteristics of substituents on carbon does not create any significant influence on silene reactivity in the dimerization process. Moreover, the values of the first and second activation energies  $\Delta G\#1$  and  $\Delta G\#2$  of H<sub>2</sub>C=SiH<sub>2</sub> differ by only ~3 kcal/mol compared to that of the substituted silenes F-CSi-H, (CH<sub>3</sub>)-CSi-H and (SiH<sub>3</sub>)-CSi-H. This shows that, irrespective the electronic nature, the effect of substituents on the dimerization of the monosubstituted R-CSi-H is only marginal.

The relatively elevated activation energy barrier of 16.28kcal/mol for NC-CSi-H ( $\Delta G\#1$ ) is resulted from the N-Si interaction in Z-1. The greater barrier heights of  $\Delta G\#1$  and  $\Delta G\#2$  of HO-CSi-H (10.04 and 12.15 kcal/mol) evolved from the hydrogen-bond interactions in the dispersion complex Z-1 and the intermediate Z-2. The intermediates and transition states formed during the dimerization process of HO-CSi-H and NC-CSi-H are given in figures 2.2 and 2.3. The calculated energy value shows that strong hydrogen-bond interactions in the intermediates and transition states significantly stabilize the free energy profile of the monosubstituted HO-CSi-H. However, even though perceptible enough, the polarity reversal of the C=Si bond in HO-CSi-H did not makes any significant change to the barrier heights.

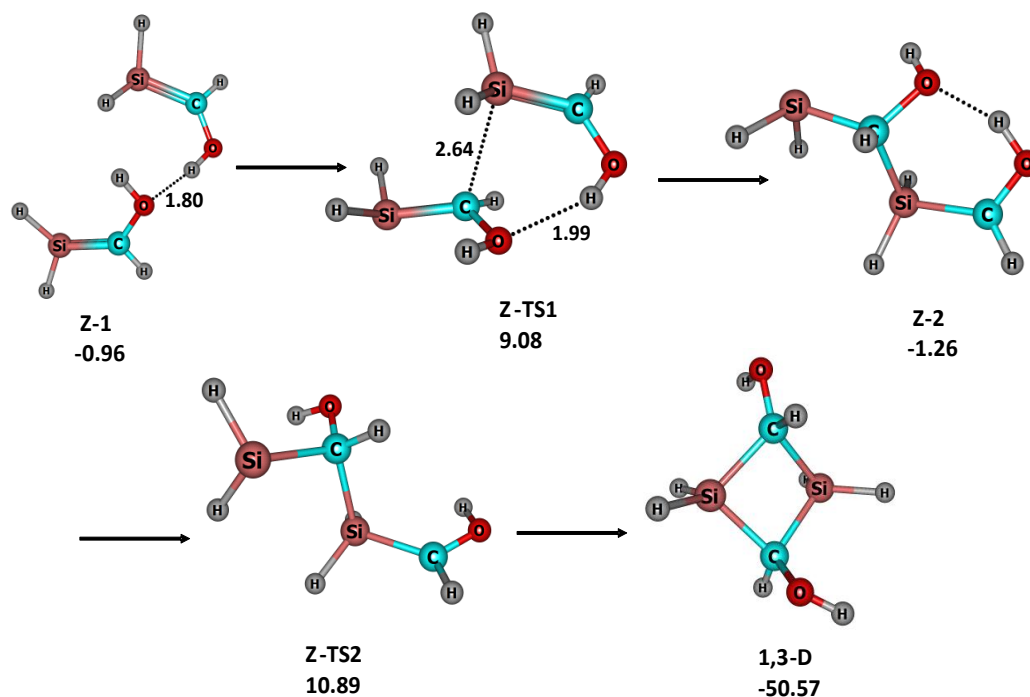


**Figure 2.2** Intermediates and transition states located for the dimerization of HO-CSi-H via Zwitter-ion pathway. Relative free energies are given in kcal/mol and bond lengths in Å. A reactant complex with totally separated silenes could not be optimized.

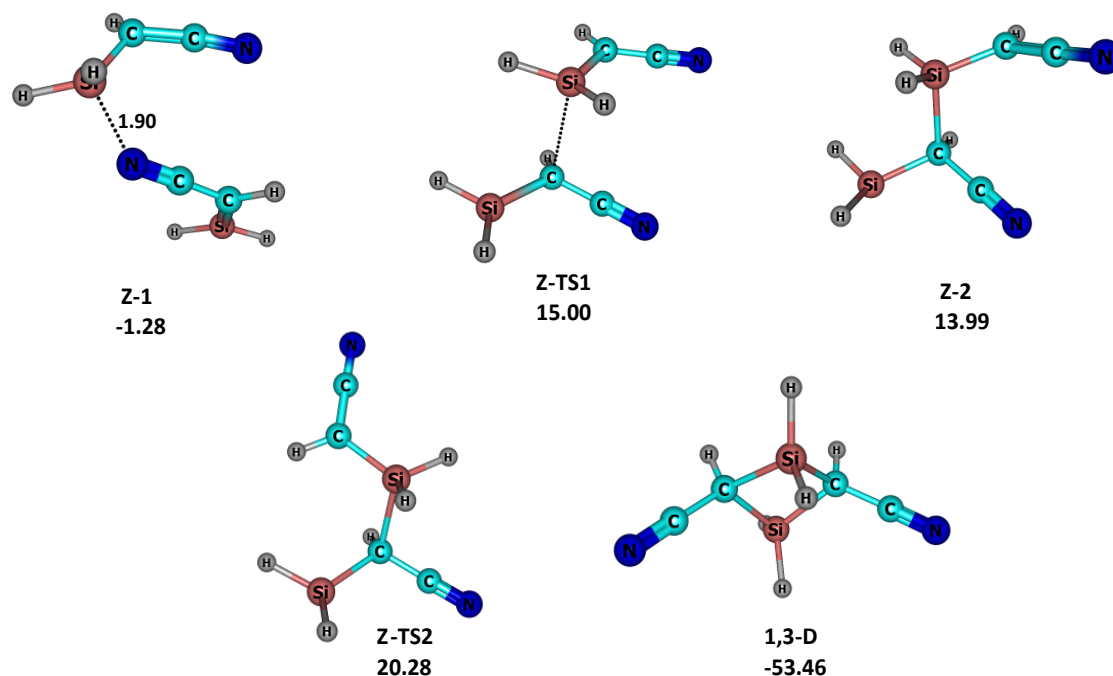


**Figure 2.3** Intermediates and transition states located for the dimerization of NC-CSi-H via Zwitter-ion pathway. Relative free energies are given in kcal/mol and bond lengths in Å. A reactant complex with totally separated silenes could not be optimized.



The free energy profile diagram enabling the comparison of the energetics of the dimerization of the monosubstituted silene R-CSi-His given in Figure 2.4

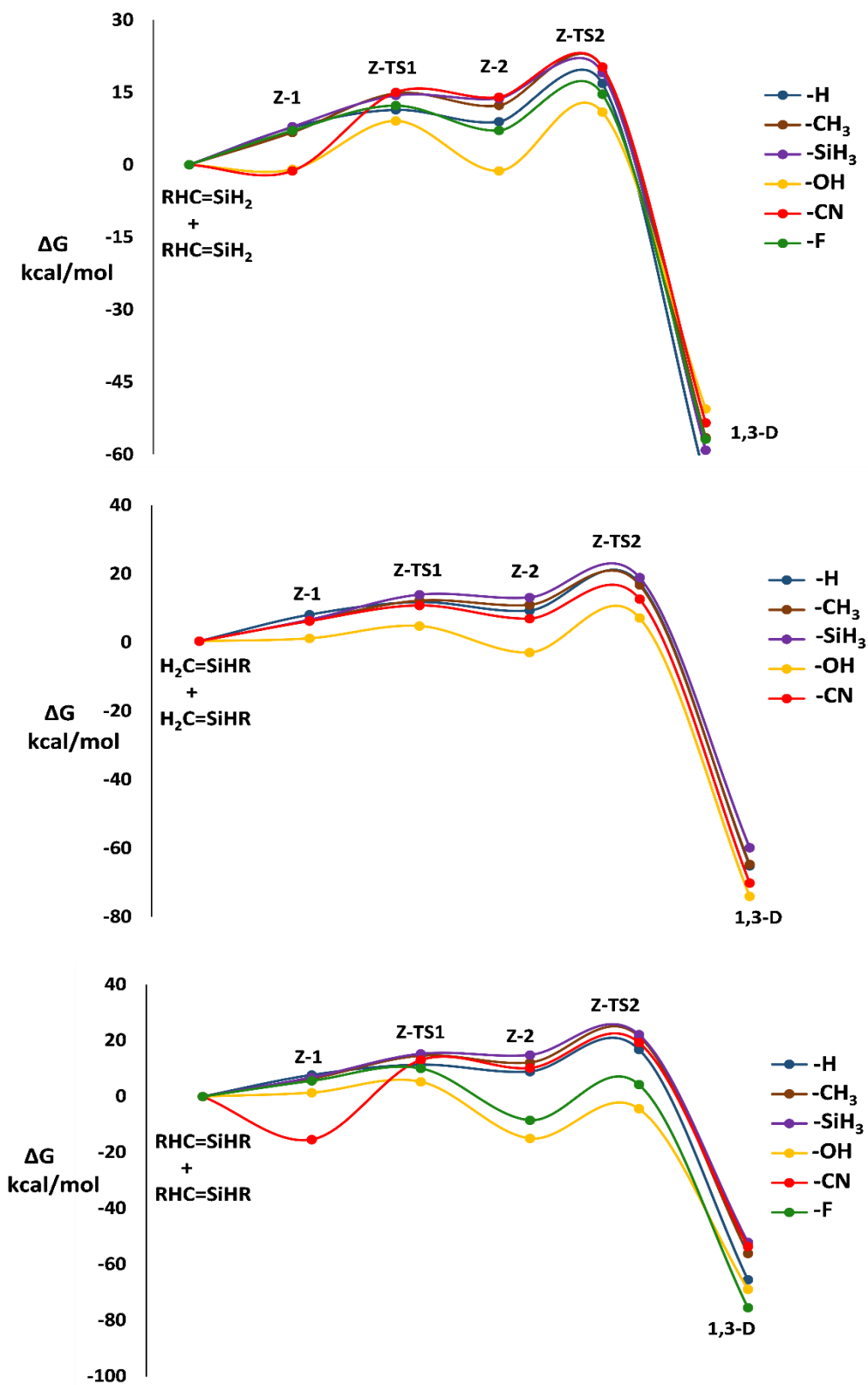


**Figure 2.4** Comparative free energy profile diagram for the dimerization of R-CSi-H, H-CSi-R and R-CSi-R via zwitter-ionic pathway.

As far as the Si substituted H-CSi-R silenes are concerned, the dispersion complex (Z-1) and the transition state for the formation of zwitter-ion (Z-TS1) could not be located for H-CSi-F due to strong Si-F attraction. Relative free energy values listed in table 2.3 of the dimerization of the H-CSi-R through the zwitter-ionic pathway indicate that the interference of the substituents in the dimerization process is more prominent when they are placed on the Si nucleus of the silene than on C nucleus (R-CSi-H). An enhanced stabilization is provided to the free energy profile of the dimerization of H-CSi-R by the appropriate substituents than that is extended to the C- substituted counterparts; R-CSi-H. The reduction in the first activation energy  $\Delta G\#1$  of the dimerization for H-CSi-OH and H-CSi-CN compared to electron donating substituents is clearly observable. This can be attributed to the enhanced polarity of the C-Si bond in the -OH and -CN substituted H-CSi-R. However, the second activation energy values  $\Delta G\#2$  of all H-CSi-R silenes are nearly the same ( $\sim 5.45$  kcal/mol) except for H-CSi-OH (10.04 kcal/mol). The significantly higher value of  $\Delta G\#2$  of H-CSi-OH originates from the H-bond interactions in the intermediate Z-2. The formation of the transition state Z-TS2 involves the rotation with respect to the C-Si bond, which is not solely controlled by the electronic effect of substituents. Figure 2.6 depicts Z-TS2 of all H-CSi-R systems. The H-bond interactions in H-CSi-OH resulted in comparatively low relative energy values of Z-1, Z-TS1 and Z-2 of and a general stabilization of its reaction profile.

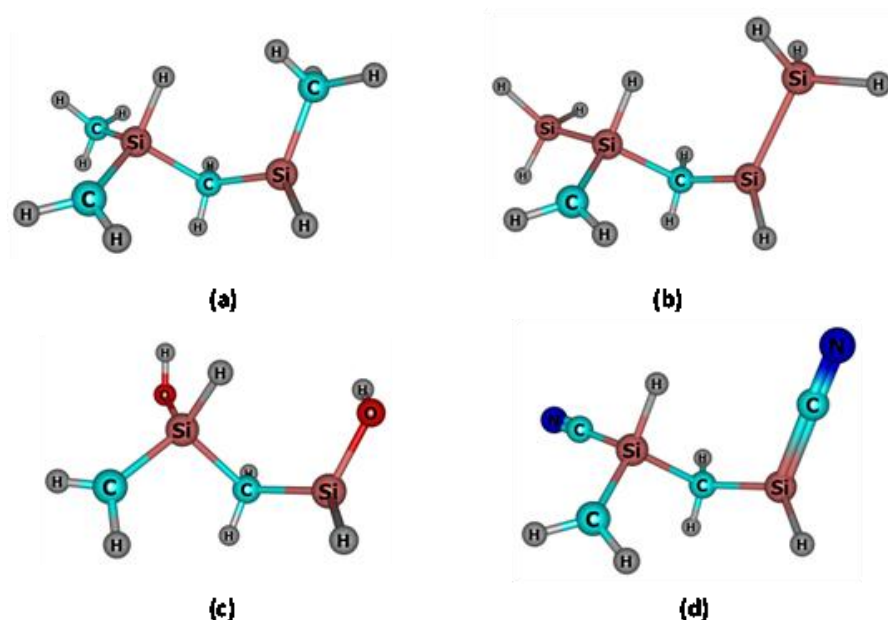


**Figure 2.5** Z-TS2 of (a) H-CSi-CH<sub>3</sub>, (b) H-CSi-SiH<sub>3</sub> (c) H-CSi-OH and (d) H-CSi-CN

The steric and electronic effects of substituents when present on both carbon and silicon of silenes (R-CSi-R) did not cause any significant change on the free energy profile of

the dimerization reaction compared to that of mono-substituted silenes. The R-CSi-R with electron donating groups had slightly higher values for  $\Delta G\#1$  and  $\Delta G\#2$  values compared to that of the monosubstituted systems. The exceptionally high value of  $\Delta G\#1$  for the disubstituted NC-CSi-CN resulted from the N-Si interactions in the reactant complex (Z-1). The magnitude of the second activation energy  $\Delta G\#2$  of NC-CSi-CN is also higher than its monosubstituted counterparts. Even though the magnitude of  $\Delta G\#1$  is nearly the same for both F-CSi-F and F-CSi-H, the extend of the second activation barrier  $\Delta G\#2$  for the formation of the dimer 1,3-Dof F-CSi-F is greater. The  $\Delta G\#1$  and  $\Delta G\#2$  values of both the disubstituted OH-CSi-OH and H-CSi-OH are almost the same. However, these values are and higher for HO-CSi-H system. In general, a better stabilization of the free energy profile has been observed with the -OH substituted systems in both mono- and disubstituted cases; mainly due to the H-bonding interactions.

To compare the free energy values using a different basis set, we have calculated the energetics of the dimerization reaction of the R-CSi-H, H-CSi-R and R-CSi-R via the zwitter -ionic path way at PW6B95D3/6-311++G(d,p). The results are given in Table 2.4

**Table 2.4** Relative free energy values (in kcal/mol) of intermediates and transition states involved in the dimerization of R-CSi-H, H-CSi-R and R-CSi-R via zwitter-ion pathway calculated at PW6B95D3/6-311++G(d,p)

Silene	Substituent (R)	Unbound silene	Z-1	Z-TS1	Z-2	Z-TS2	1,3-D
H <sub>2</sub> C=SiH <sub>2</sub>	-H	0.00	7.26	8.05	7.10	14.01	-70.77
R-CSi-H	-CH <sub>3</sub>	0.00	5.56	10.20	8.36	16.76	-64.99
	-SiH <sub>3</sub>	0.00	5.42	7.37	7.08	12.74	-69.38
	-OH	0.00	1.68	8.57	-1.07 1.43	11.18	-57.23
	-CN	0.00	-60.80	11.28	10.98	16.44	-61.58
	-F	0.00	2.00	10.29	6.76	13.54	-63.87
H-CSi-R	-CH <sub>3</sub>	0.00		7.10	6.66	12.07	-71.29
	-SiH <sub>3</sub>	0.00	6.00	8.17	7.96	13.48	-67.42
	-OH	0.00	-3.13	3.74	-3.13	7.69	-75.39
	-CN	0.00	4.58	6.09	3.91	9.56	-76.36
	-F	-					
R-CSi-R	-CH <sub>3</sub>	0.00	5.35	7.56	6.23	15.46	-65.97
	-SiH <sub>3</sub>	0.00			2.82	11.48	-65.63
	-OH	0.00	1.20	1.96	-17.43	-3.77	-74.78
	-CN	0.00			5.80	14.84	-62.56
	-F	0.00	5.15	6.82	-7.25	5.30	-74.78

Even though, marginal difference in the corresponding values of each species can be made out, the general trend in the variation of energy is same as that perceived at B3LYP/6-

31G(d,p) basis set. This is true with individual reactions and the gradation in energy values among different silenes.

### 2.4.3 The diradical pathway

The intermediates, transition states and the product located during the dimerization reaction of the unsubstituted silene H-CSi-H through the diradical pathway are given in Fig. 2.6, along with the relative energy values.

Energy values and the structures of the primary dispersion intermediate D-1 and the first transition state D-TS1 evolved in the diradical pathway are found to be exactly identical to those observed in the zwitter-ion pathway (Z-1 and Z-TS1 respectively). As the reaction progress from the first activated complex (D-TS1/Z-TS1), the two mechanisms part ways. In the diradical pathway, intermediate evolved from the transition state D-TS1, (D-2) is a diradical, contrary to the zwitter-ionic intermediate (Z-2) formed in the zwitter-ionic mechanism. The Mulliken spin densities of the end C and Si of the diradical intermediate D-1 are calculated to be 1.00 and 0.89, respectively. The relative energy value of D-2 is -6.95 kcal/mol. The corresponding intermediate species emerged in the zwitter-ion pathway of the reaction is Z-2 and its relative energy is 8.92 kcal/mol. The large difference in the energy values of these intermediates (15.87 kcal/mol) clearly demonstrates that the diradical intermediate D-2 is a lot more stable than the zwitter-ionic counterpart, Z-1. The activation barrier ( $\Delta G^\ddagger$ ) for the cyclization process of the intermediate, leading to the formation of the tetragonal dimerised product is only 1.13 kcal/mol in the diradical pathway. The corresponding energy value in the zwitter-ionic pathway is 7.91 kcal/mol, which is considerably greater. It is evident that the diradical character significantly stabilizes the intermediate D-2 (relative energy -6.95 kcal/mol) and the transition state D-TS2 (relative energy -5.82 kcal/mol) compared to the corresponding zwitter-ion intermediate Z-2 (relative energy 8.92 kcal/mol) and the zwitter-ionic transition state Z-TS2 (relative energy 16.83 kcal/mol).

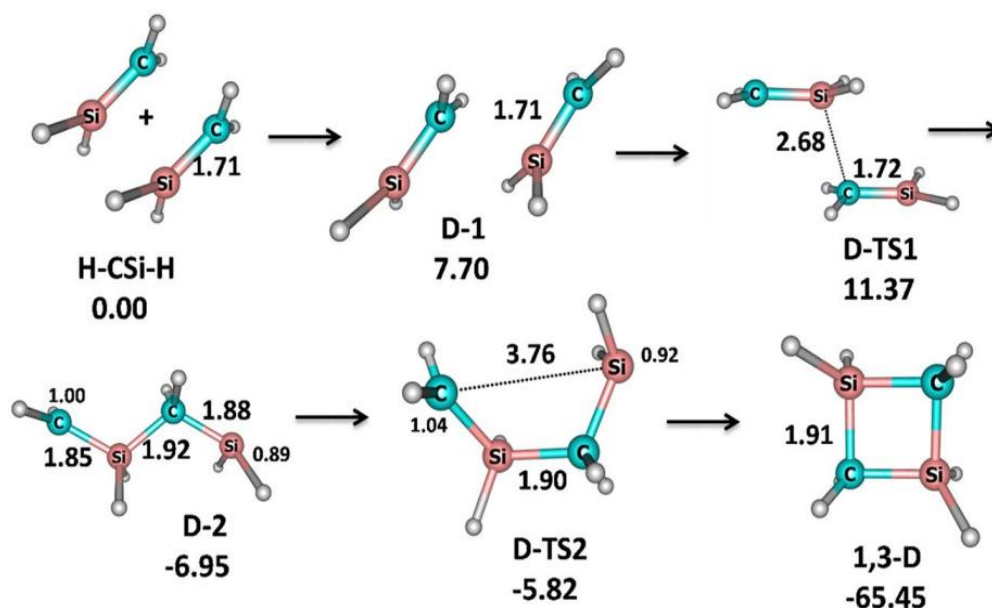


**Figure 2.6** Intermediates and transition states located for the trimerization of H-CSi-H via diradical pathway. Relative free energies are given in kcal/mol and bond lengths in Å

The energetics for the dimerization via the diradical pathway for all the monosubstituted R-CSi-H, H-CSi-R and the disubstituted R-CSi-R systems have been calculated and is presented in Table 2.5. Comparative free energy profile diagrams for each type of the system are depicted in Figure 2.7.

**Table 2.5** Relative free energy values (in kcal/mol) of intermediates and transition states involved in the dimerization of R-CSi-H, H-CSi-R and R-CSi-R via diradical pathway

Silene	Substituent (R)	D-1	D-TS1	D-2	D-TS2	1,3-D
H <sub>2</sub> C=SiH <sub>2</sub>	-H	7.70	11.37	-6.95	-5.82	-65.45
R-CSi-H	-CH <sub>3</sub>	6.70	14.79	-2.68	0.03	-56.53
	-SiH <sub>3</sub>	7.87	14.35	-0.41	1.94	-59.12
	-OH	-0.96	9.08	-10.22	-4.26	-50.57
	-CN	-1.28	13.39	-2.94	0.33	-53.46
	-F	7.07	12.24	-8.92	-5.16	-59.12
H-CSi-R	-CH <sub>3</sub>	5.99	11.82	-4.38	-2.39	-65.06
	-SiH <sub>3</sub>	6.22	12.46	-3.72	0.46	-60.19
	-OH	0.82	4.42	-15.14	-10.90	-74.36
	-CN	5.84	10.41	-10.27	-8.45	-70.47
	-F	-	-	-	-	-
R-CSi-R	-CH <sub>3</sub>	6.34	14.58	-0.79	0.90	-56.00
	-SiH <sub>3</sub>	6.82	18.37	3.35	5.37	-52.52
	-OH	4.58	8.67	-21.27	-16.61	-68.84
	-CN	-15.36	13.40	-4.29	-2.33	-53.51
	-F	5.59	10.04	-24.88	-21.95	-75.41

For all systems, transition state for the first C-Si bond formation (D-1), is the same as that of the zwitter-ion pathway (Z-1). The energy profile through the diradical pathway shows a substantial increase in stabilization compared to the zwitter ionic pathway in the further progress of the reaction to the formation of the diradical intermediate (D-2). A comparison of the relative energies of intermediates formed during the dimerization through the diradical pathway, D-1 with the corresponding intermediate formed in the zwitter-ionic pathway, displayed in Tables 2.5 and 2.3 respectively reveal that the relative energy of with the former is much lower. This observation is valid for all the monosubstituted R-CSi-H, H-CSi-R and the disubstituted R-CSi-R systems.

It is further observed that, the presence of a substituent on Si (H-CSi-R) offers better stabilization of D-2 compared to that on C (R-CSi-H). Also, the  $\pi$ -donating substituents (-OH, -F) are found to be better candidates for the stabilization of diradical intermediate. Also, contrary to the observation in the zwitter-ionic pathway, the evolution of the intermediate D-2 from the dispersion complex D-1 is largely exothermic in the diradical pathway, except for the NC-CSi-CN. The odd behavior in the energy transformation associated with the conversion of D-1 to D-2 in the case of the disubstituted NC-CSi-CN is emanated from the N-Si interactions in the reactant complex (Z-1).

The magnitudes of the second activation energy  $\Delta G\#2$  range from 1- 6 kcal/mol for R-CSi-R systems in the diradical pathway of dimerization. A perusal of the calculated values of  $\Delta G\#2$  reveals that, a generalization based on the electronic effect of substituents on the second activation energy cannot be arrived at. The most perceptible observation is the magnificent stabilization provided by the substituent -OH for both the monosubstituted HO-CSi-H, H-CSi-OH and the disubstituted HO-CSi-OH systems. This is primarily due to the hydrogen-bonds developed by the -OH group. The stabilization of the carbon and Silicon radical centers in the intermediate D-2 and the transition state D-TS2 by the strongly  $\pi$ -donating -OH group is also equally contributing to this stabilization. Among the substituents employed, the least stabilization to the free energy profile is provided by the electron donating -SiH<sub>3</sub> group. In general, the diradical mechanism is the preferred pathway for the dimerization of silenes, irrespective of the electronic nature of substituents on the C or Si atom. Substituent effect is more prominent when it is present on the Si atom of the silene molecule. The  $\pi$ -donating and electron withdrawing substituents make the silenes more reactive towards dimerization than electron donating groups.

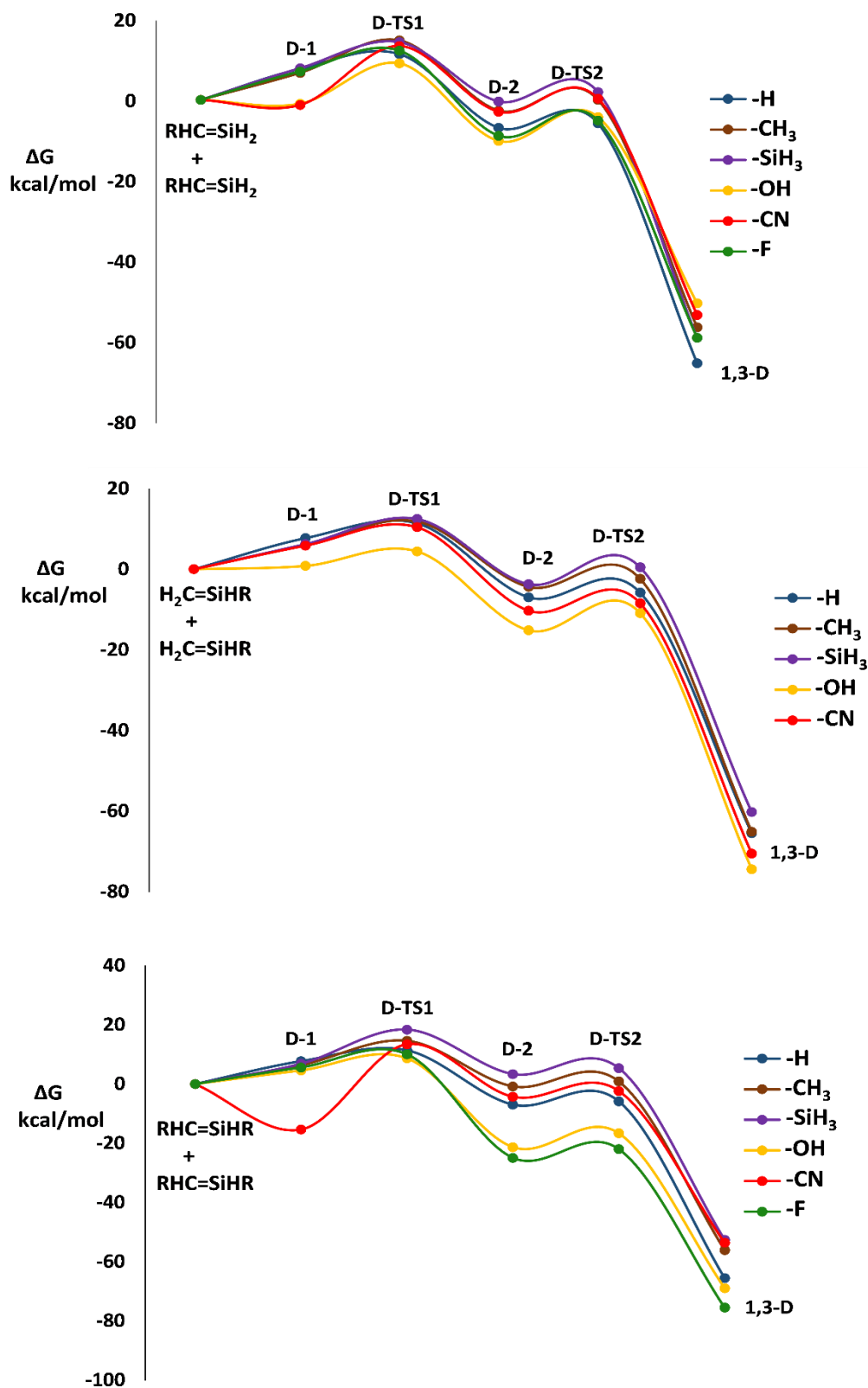


**Figure 2.7** Comparative free energy profile diagram for the dimerization of R-CSi-H, H-CSi-R and R-CSi-R via diradical formation.

## 2.5 Conclusion

The dimerization reaction of silenes is an exothermic process with fairly low activation energy ( $< 20$  kcal/mol) and is therefore, feasible under ambient condition. As far as mono substituted silenes R-CSi-H and H-CSi-R are concerned, the substituents are more effective in promoting the dimerization when the substituent is attached to Si than to C. Electron donating substituents,  $-CH_3$  and  $-SiH_3$  destabilise the dimerization reaction in both the mono substituted and disubstituted systems in comparison with the dimerization process of the unsubstituted silene. Electron withdrawing substituents stabilize the dimerization of silenes; especially when they are attached to the Si atom. The electron withdrawing and  $\pi$  donating substituent  $-OH$  is found to be the most effective among the five substituents attempted. The H-bond formation at the intermediate stages of the reaction by the  $-OH$  substituent has an active role in stabilising the reaction. The course of dimerization of silenes is found to be more stabilised in the diradical pathway than the zwitter-ionic pathway. Therefore, it can safely comprehend that the dimerization reaction of silenes prefers a diradical pathway over the zwitter-ionic pathway. Relative free energy values of intermediates and transition states involved in the dimerization of R-CSi-H, H-CSi-R and R-CSi-R via zwitter-ion pathway is calculated at PW6B95D3/6-311++G(d,p) also. Even though, marginal difference in the corresponding values of each species can be made out, the general trend in the variation of energy is same as that perceived at B3LYP/6-31G(d,p) basis set. This is true with individual reactions and the gradation in energy values among different silenes.



## Reference

- Apeloig, Y., Bravo-Zhivotovskii, D., Zharov, I., Panov, V., Leigh, W. J., & Sluggett, G. W. (1998). Thermal and Photochemical [2+2] Cycloreversion of a 1,2-Disilacyclobutane and a 1,2-Digermacyclobutane. *Journal of the American Chemical Society*, *120*(7), 1398–1404. <https://doi.org/10.1021/ja9729600>
- Apeloig, Y., & Karni, M. (1984). Substituent effects on the carbon-silicon double bond. Monosubstituted silenes. *Journal of the American Chemical Society*, *106*(22), 6676–6682. <https://doi.org/10.1021/ja00334a036>
- Baines, K. M. (2013). Brook silenes: inspiration for a generation. *Chemical Communications*, *49*(57), 6366. <https://doi.org/10.1039/c3cc42595a>
- Bernardi, F., Bottoni, A., Olivucci, M., Venturini, A., & Robb, M. A. (1994). Ab initio MC-SCF study of thermal and photochemical [2 + 2] cycloadditions. *Journal of the Chemical Society, Faraday Transactions*, *90*(12), 1617. <https://doi.org/10.1039/ft9949001617>
- Brook, A. G., Abdesaken, F., Gutekunst, B., Gutekunst, G., & Kallury, R. K. (1981). A solid silaethene: Isolation and characterization. *Journal of the Chemical Society, Chemical Communications*, *4*, 191–192. <https://doi.org/10.1039/c39810000191>
- Brook, A. G., & Baines, K. M. (1986). *Silenes* (pp. 1–44). [https://doi.org/10.1016/S0065-3055\(08\)60571-7](https://doi.org/10.1016/S0065-3055(08)60571-7)
- Brook, A. G., Nyburg, S. C., Abdesaken, F., Gutekunst, B., Gutekunst, G., Krishna, R., Kallury, M. R., Poon, Y. C., Chang, Y. M., & Winnie, W. N. (1982). Stable solid silaethylenes. *Journal of the American Chemical Society*, *104*(21), 5667–5672. <https://doi.org/10.1021/ja00385a019>
- Brook, A. G., Vorspohl, K., Ford, R. R., Hesse, M., & Chatterton, W. J. (1987). Reactions of stable silenes with dienes and alkenes: [2 + 2], [2 + 4] and ene reactions. *Organometallics*, *6*(10), 2128–2137. <https://doi.org/10.1021/om00153a017>
- Dimitrova, V., Ilieva, S., & Galabov, B. (2003). Electrostatic potential at nuclei as a reactivity index in hydrogen bond formation. Complexes of ammonia with C–H, N–H and O–H proton donor molecules. *Journal of Molecular Structure: THEOCHEM*, *637*(1–3), 73–80. [https://doi.org/10.1016/S0166-1280\(03\)00402-0](https://doi.org/10.1016/S0166-1280(03)00402-0)
- Eklöf, A. M., Guliashvili, T., & Ottosson, H. (2008). Relation between the  $\pi$ -Contribution to Reversed Si=C Bond Polarization and the Reaction Profile for the Thermolytic Formation of Silenes. *Organometallics*, *27*(20), 5203–5211. <https://doi.org/10.1021/om800477j>
- El-Sayed, I., Guliashvili, T., Hazell, R., Gogoll, A., & Ottosson, H. (2002). Evidence for Formation of Silenes Strongly Influenced by Reversed SiC Bond Polarity. *Organic Letters*, *4*(11), 1915–1918. <https://doi.org/10.1021/ol025920w>
- Guliashvili, T., Tibbelin, J., Ryu, J., & Ottosson, H. (2010). Unsuccessful attempts to add alcohols to transient 2-amino-2-siloxy-silenes - leading to a new benign route for base-free alcohol protection. *Dalton Transactions*, *39*(39), 9379. <https://doi.org/10.1039/c0dt00323a>
- Gusel'nikov, L. E., Avakyan, V. G., & Guselnikov, S. L. (2002). Effect of Geminal Substitution at Silicon on 1-Sila- and 1,3-Disilacyclobutanes' Strain Energies, Their 2+2 Cycloreversion Enthalpies, and SiC  $\pi$ -Bond Energies in Silenes. *Journal of the American Chemical Society*, *124*(4), 662–671. <https://doi.org/10.1021/ja011287i>
- Gusel'nikov, L. E., & Nametkin, N. S. (1979). Formation and properties of unstable intermediates containing multiple p.pi.-p.pi. bonded Group 4B metals. *Chemical Reviews*, *79*(6), 529–577. <https://doi.org/10.1021/cr60322a004>

- Gusel'nikov, L. E., Nametkin, N. S., & Vdovin, V. M. (1975). Unstable silicon analogs of unsaturated compounds. *Accounts of Chemical Research*, 8(1), 18–25. <https://doi.org/10.1021/ar50085a003>
- Hajgató, B., Takahashi, M., Kira, M., & Veszprémi, T. (2002). The Mechanism of 1,2-Addition of Disilene and Silene: Hydrogen Halide Addition Part 2; for Part 1 see: T. Veszprémi, M. Takahashi, B. Hajgató, M. Kira, *J. Am. Chem. Soc.* 2001, 123, 6629. *Chemistry - A European Journal*, 8(9), 2126. [https://doi.org/10.1002/1521-3765\(20020503\)8:9<2126::AID-CHEM2126>3.0.CO;2-2](https://doi.org/10.1002/1521-3765(20020503)8:9<2126::AID-CHEM2126>3.0.CO;2-2)
- Hardwick, J. A., & Baines, K. M. (2011). Addition of Nitriles to Two Brook Silenes. *Organometallics*, 30(10), 2831–2837. <https://doi.org/10.1021/om200182q>
- Leigh, W. J., Boukherroub, R., & Kerst, C. (1998). Substituent Effects on the Reactivity of the Silicon–Carbon Double Bond. Resonance, Inductive, and Steric Effects of Substituents at Silicon on the Reactivity of Simple 1-Methylsilenes. *Journal of the American Chemical Society*, 120(37), 9504–9512. <https://doi.org/10.1021/ja981435d>
- Leigh, W. J., Kerst, C., Boukherroub, R., Morkin, T. L., Jenkins, S. I., Sung, K., & Tidwell, T. T. (1999). Substituent Effects on the Reactivity of the Silicon–Carbon Double Bond. Substituted 1,1-Dimethylsilenes from Far-UV Laser Flash Photolysis of  $\alpha$ -Silylketenes and (Trimethylsilyl)diazomethane. *Journal of the American Chemical Society*, 121(20), 4744–4753. <https://doi.org/10.1021/ja984277z>
- Milnes, K. K., Jennings, M. C., & Baines, K. M. (2006). Addition of Cyclopropyl Alkynes to a Brook Silene: Definitive Evidence for a Biradical Intermediate. *Journal of the American Chemical Society*, 128(7), 2491–2501. <https://doi.org/10.1021/ja057596g>
- Milnes, K. K., Pavelka, L. C., & Baines, K. M. (2010). Reactivity of a Polar Silene toward Terminal Alkynes: Preference for C–H Insertion over Cycloaddition. *Organometallics*, 29(22), 5972–5981. <https://doi.org/10.1021/om100756p>
- Miracle, G. E., Ball, J. L., Powell, D. R., & West, R. (1993). The first stable 1-silaallene. *Journal of the American Chemical Society*, 115(24), 11598–11599. <https://doi.org/10.1021/ja00077a069>
- Morkin, T. L., & Leigh, W. J. (2001). Substituent Effects on the Reactivity of the Silicon–Carbon Double Bond. *Accounts of Chemical Research*, 34(2), 129–136. <https://doi.org/10.1021/ar960252y>
- Ottosson, H. (2003). Zwitterionic Silenes: Interesting Goals for Synthesis? *Chemistry – A European Journal*, 9(17), 4144–4155. <https://doi.org/10.1002/chem.200204583>
- Ottosson, H., & Eklöf, A. M. (2008). Silenes: Connectors between classical alkenes and nonclassical heavy alkenes. *Coordination Chemistry Reviews*, 252(12–14), 1287–1314. <https://doi.org/10.1016/j.ccr.2007.07.005>
- Pavelka, L. C., Hanson, M. A., Staroverov, V. N., & Baines, K. M. (2015). Mechanism of the addition of alkynes to silenes and germenes: A density functional study. *Canadian Journal of Chemistry*, 93(1), 134–142. <https://doi.org/10.1139/cjc-2014-0256>
- Sakamoto, K., Ogasawara, J., Sakurai, H., & Kira, M. (1997). The First Silatriafulvene Derivative: Generation, Unusually Low Reactivity toward Alcohols, and Isomerization to Silacyclobutadiene. *Journal of the American Chemical Society*, 119(14), 3405–3406. <https://doi.org/10.1021/ja970083s>
- Seidl, E. T., Grev, R. S., & Schaefer, H. F. (1992). Mechanistic, structural, and vibrational aspects of the dimerization of silaethylene. *Journal of the American Chemical Society*, 114(10), 3643–3650. <https://doi.org/10.1021/ja00036a011>
- Suresh, C. H., Remya, G. S., & Anjalikrishna, P. K. (2022). Molecular electrostatic potential analysis: A powerful tool to interpret and predict chemical reactivity. *WIREs Computational Molecular*

*Science*, 12(5). <https://doi.org/10.1002/wcms.1601>

- Takahashi, M., Veszprémi, T., & Kira, M. (2004). 1,2-Addition Reaction of Monosubstituted Disilenes: An Ab Initio Study. *Organometallics*, 23(24), 5768–5778. <https://doi.org/10.1021/om049418m>
- Tanaka, H., Shiota, Y., Hori, K., Naka, A., Ishikawa, M., & Yoshizawa, K. (2012). Substituent Effects in Thermal Reactions of a Silene with Silyl-Substituted Alkynes: A Theoretical Study. *Organometallics*, 31(13), 4737–4747. <https://doi.org/10.1021/om300310g>
- Venturini, A., Bernardi, F., Olivucci, M., Robb, M. A., & Rossi, I. (1998). Dimerization of Silaethylene: Computational Evidence for a Novel Mechanism for the Formation of 1,3-Disilacyclobutane via a 1,2 Approach. *Journal of the American Chemical Society*, 120(8), 1912–1913. <https://doi.org/10.1021/ja973472v>
- Veszprémi, T., Takahashi, M., Hajgató, B., & Kira, M. (2001). The Mechanism of 1,2-Addition of Disilene and Silene. 1. Water and Alcohol Addition. *Journal of the American Chemical Society*, 123(27), 6629–6638. <https://doi.org/10.1021/ja0040823>



# Chapter 3

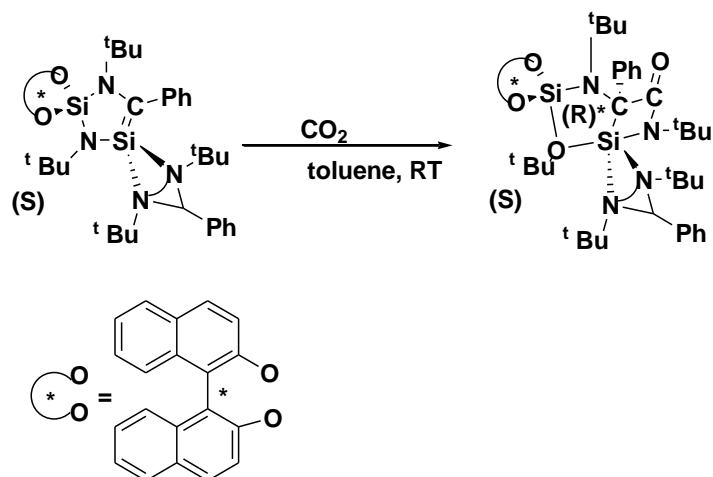
## Substituent effects on the addition of small molecules (NH<sub>3</sub>, NO, CO) to silene and silene-silylene isomerization

---

### 3.1 Introduction

Even though the number of stable silenes steadily expanded with time by making use of the stability imparted by different substituents of varying steric and electronic capabilities, studies relating to their interactions in bond activation processes, specially that involving small molecules are few. Recently, activation of small molecules such as H<sub>2</sub>O, NH<sub>3</sub>, CO, CO<sub>2</sub>, NO, H<sub>2</sub>, O<sub>2</sub> etc via insertion into the multiple bonds of heavier members of group 14 have been reported in many cases (Adrian G Brook and Michael A Brook 1996; Gaspar P. P. and West 1998; Gerhard Raabe and Josef Michl 1989; Morkin, Owens, and Leigh 2001). These small molecules are inherently very stable and activating their pretty strong bonds for the desired chemical process requires particularly appropriate catalysts. Silenes are proposed to be a possible option for the small molecule activation, due their high reactivity and possibility of modulation of the polarity of the C=Si double bond by the proper selection of substituents. The primary challenge in the usage of silenes in the activation reactions is the avoidance of the cleavage of the C–Si bond of the silene altogether and secondly, achieving reversibility of the reaction, i.e., regeneration of the multiple bonds as a key step for any future catalytic application (Chu and Nikonov 2018; Sugahara et al. 2018; Weetman and Inoue 2018; L. Zhao et al. 2012).

Roesky et al. isolated the first chiral cyclic silene, which can activate small molecules such as elemental sulphur (S<sub>8</sub>), CO<sub>2</sub>, and HCl (Sun et al. 2022). CO<sub>2</sub> being the most challenging green-house gas, development of a molecular system involving some main group elements that can be effectively used for the activation of it is the ardent enthusiasm of several synthetic chemists. Roesky et al explored the reaction of CO<sub>2</sub> with chiral silene molecule (**I**) they have synthesised. Stirring a toluene solution of silene **I** under CO<sub>2</sub> atmosphere at room temperature led complete absorption of CO<sub>2</sub> by equivalent quantity of **I** (Scheme 3.1) (Sun et al. 2022).



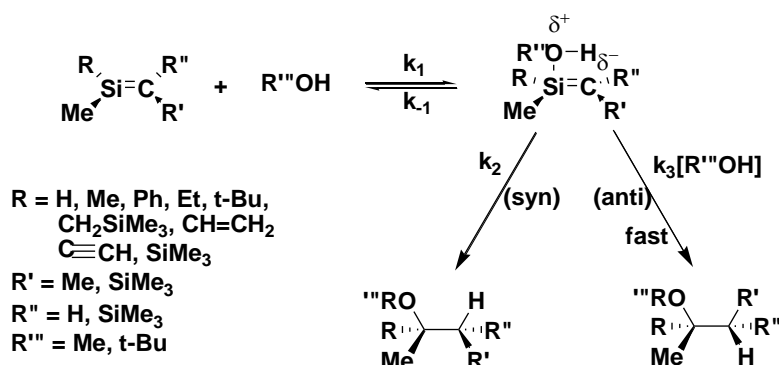
**Scheme 3.1**

CO<sub>2</sub> activation by the chiral silene **I**

Silenes are highly electrophilic owing to their inherently polar constitution. The Si atom of the selenic bond carries the positive polarity and is the site of the attack by nucleophilic substrates such as water, alcohols, amines, and other electron rich species. Reaction of alcohols with naturally polarized silenes is found to be preceded by the initial shaping of a complex structure followed by an intra-molecular transfer of a proton from the oxygen atom of the alcohol to the carbon atom of the silene. However, further investigations revealed that an intermolecular proton transfer can compete with the intra-molecular pathway. Bendikov et al revealed yet another mechanism for addition of alcohols to silenes (Auner et al. 2000; Bendikov et al. 2002; Rappoport and Apeloig 1998; Takeaki, Kabuto, and Kira 1984). Burk et al. 1996; Sakamoto et al. revealed that the substituent which are successful in influencing the polarity of the C-Si bond of silene are critically effective in modifying the activation properties of it also (Burk, Abboud, and Koppel 1996; Sakamoto et al. 1997; Schriver, Fink, and Gordon 1987; Takahashi, Sakamoto, and Kira 2001; Veszprémi et al. 1998).

The fastest reactions of silenes with nucleophiles are those with simple alcohols and amines so that these are the most used trapping reaction for transient silences (Bradaric & Leigh, 1996; Sakamoto et al. 1997). The reaction proceeds through a stepwise mechanism involving initial nucleophilic attack at positively polarised silicon to form a  $\sigma$ -bonded complex, which proceeds to product by proton transfer from oxygen to the silenic carbon (Bradaric & Leigh, 1996; Sakamoto et al. 1997). Leigh and co-workers precisely studied the mechanism of addition of alcohols to several transient silenes using nanosecond flash-laser

photolysis (Auner et al. 2000; Bendikov et al. 2002; Bradaric and Leigh 1996; Rappoport and Apeloig 1998; Sakamoto et al. 1997; Schriver, Fink, and Gordon 1987; Takahashi, Sakamoto, and Kira 2001; Veszprémi et al. 1998). The conclusions arrived at from these studies led to the proposal of the mechanism depicted in Scheme 3.2, where a complex is reversibly formed between the silene and alcohol in the initial part of the reaction. The second step is the rate-determining one, during which a proton transfer from the attacking alcohol or from a second alcohol molecule takes place (Bradaric and Leigh 1996).



**Scheme 3.2**

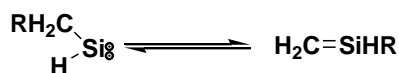
Addition of alcohols to silene

The addition of H<sub>2</sub>O and NH<sub>3</sub> follows a similar mechanism.

### The silene-silylene rearrangement

The relative stability between silylenes and the corresponding silenes and the barrier separating the two species is a matter of debate for a long time (Gaspar and West 1998; Hideki Sakurai 1989; Kira 2012; Schaefer 1982). The theoretical studies regarding the structures of the silene **IIa** and its methyl derivative **Ia** conducted by S. Ishida et al revealed that **Ia** and **IIa** are energetically very close. However, the barrier height for the isomerisation is very high (40 kcal mol<sup>-1</sup>) (Boatz and Gordon 1990; Grev et al. 1988; Ishida, Iwamoto, and Kira 2009). Though, the results obtained for the difference in energy between silene and the corresponding silylene depends strongly on the computational methods and basis sets; it is generally agreed that silylene **Ia** is 3 - 4 kcal mol<sup>-1</sup> more stable than silene **2a** (Boatz and Gordon 1990; Grev et al. 1988). Effect of substituents on the energy difference and the barrier heights are known to be significant (Hideki Sakurai 1989). Nagase and Kudo (Takeaki, Kabuto, and Kira 1984) have found that silene **IIIb** is 10.3 kcal mol<sup>-1</sup> more stable than silylene **Ib** at the MP3/6-31G\* level, whereas the isomerization between **IIa** and **Ia** is

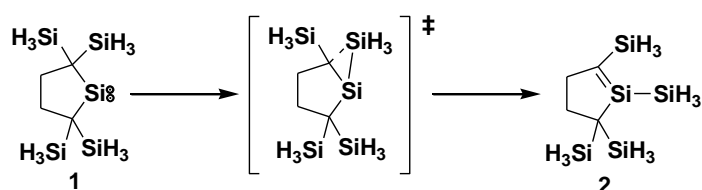
almost thermoneutral. Isomerisation between **IIc** and **Ic** is also calculated to be nearly thermoneutral. The energy barrier heights for the isomerization of **Ia**, **Ib**, and **Ic** to **IIa**, **IIb**, and **IIc** are found to be 43.0, 44.4, and 24.8 kcal mol<sup>-1</sup> respectively. This clearly demonstrates that the measure of the activation energy required for the 1,2- silyl transfer is significantly lower than the activation energy demand of 1,2-hydrogen and 1,2-methyl migrations.



### Scheme 3.3

The silene-silylene isomerisation

Even though, elaborate and systematic theoretical studies of silylene-silene isomerization are available in plenty, experimental evidence for the isomerization is rare. Few studies such as that made by Conlin, R.T et al (Conlin and Wood 1981) proposed that silene-to-silylene isomerization occurs during the high-temperature thermolysis of silacyclobutanes and polysilanes. In recent past, S. Ishida et al (Ishida, Iwamoto, and Kira 2009) reported that silylene **1** isomerizes into the corresponding silene **2** slowly at room temperature in solution. On keeping a solution of the silylene **1** in hexane solution at room temperature in sealed NMR tube protected from light, it isomerizes irreversibly into a single product quantitatively and is identified as silene **2**. The presence of the unshared pair of electrons the silicon atom of Silylene**1** is made it less stable than the silene **2** by around 3 kcal mol<sup>-1</sup>.



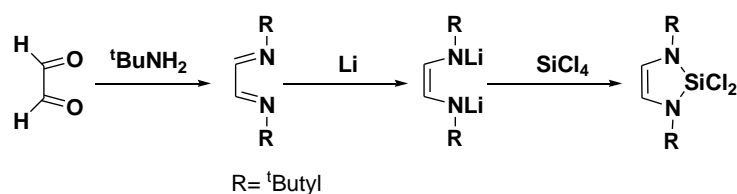
### Scheme 3.4

The silene-silylene isomerisation (reported by S. Ishida et al. 2009)

The silicon counterparts to carbenes of organic chemistry are known as silylenes. Like carbenes they also carry a lone pair of electrons. They can be represented as R<sub>2</sub>Si:. The



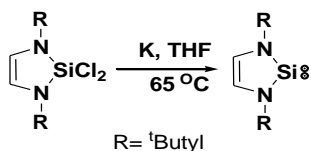
importance of silylenes in silicon chemistry is more prominent than the significance of carbenes in organic chemistry. The key intermediates in many thermal and photochemical reactions of organosilicon compounds are silylenes (West and Denk 1996). The pathfinders of unsaturated silicon compound synthesis, the well versed organo-silicon research group of Robert West, University of Wisconsin, had created the remarkable breakthrough in the silylene synthesis also (Denk et al. 1994; Dieck and Zettlitzer 1987; R. West and Denk 1996; Zettlitzer, Dieck, and Stamp 1986). Inspired by the transformation of 1,3,4,5-tetramethylimidazolium chloride in to a carbene, they have synthesised a similar imidazole type compound with the apex carbon replaced with silicon by the following sequence of reactions (Scheme 3.3) (West and Denk 1996).



**Scheme 3.5**

Preparation of the precursor 1,3-Diaza-2,2-dichloro-2-sila-4-cyclopentene for silylene synthesis

The 1,3-Diaza-2,2-dichloro-2-sila-4-cyclopentene thus obtained was subjected the dehalogenation under extremely vigorous conditions: refluxing with molten potassium metal in THF for three days (Scheme 3.2) (Denk et al. 1994; West and Denk 1996).

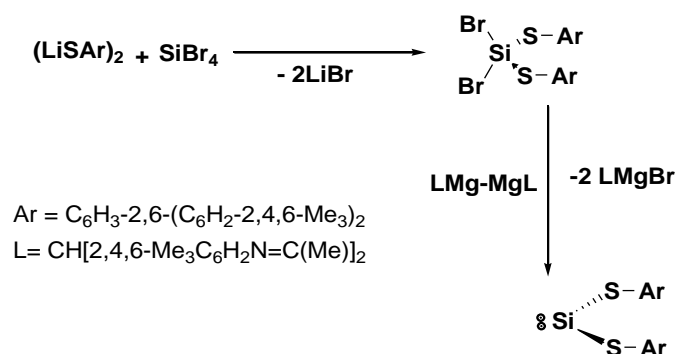


**Scheme 3.6**

Preparation of the first (cyclic) silylene from 1,3-Diaza-2,2-dichloro-2-sila-4-cyclopentene

Laborious efforts to synthesize acyclic silylenes, isolable at ambient temperature, have been unsuccessful till 2012. In 2012 in the Journal of the American Chemical Society, two leading research groups in silicon chemistry have independently reported the first ever synthesis, isolation and structural characterization of two different types of acyclic silylenes, quiet stable at ambient temperature (Protchenko et al. 2012; Rekken et al. 2012). In one of these communications, Power and co-workers, announced the formation and isolation of a bis (aryl-thio)-substituted silylene, through a gentle reduction of the respective silicon (IV)

precursor  $(RS)_2SiBr_2$  by Jones's Mg(I)–Mg(I) complex (Rekken et al. 2012) (Scheme 3.5) (Akkari-El Ahdab et al. 2001; Asay, Jones, and Driess 2011; Bonyhady et al. 2009; Ellison, Ruhlandt- Senge, and Power 1994).



**Scheme 3.7**

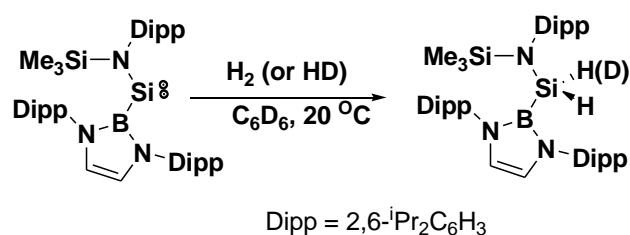
Synthesis of the stable acyclic (aryl-thio) substituted silylene

It is observed that the newly synthesised acyclic silylene is remarkably stable up to 146 °C.

Independently, Protchenko, A. V et al. describe in their communication a ground breaking solution for activating  $H_2$  by a stable acyclic silylene even at 0 °C (Ellison, Ruhlandt- Senge, and Power 1994; Akkari-El Ahdab et al. 2001; Filippou, Chernov, and Schnakenburg 2009; Li et al. 2011; Segawa, Yamashita, and Nozaki 2006; Yao et al. 2007). Apeloig and co-workers reported the synthesis of stable geometrical isomers of  $(tBu_2MeSi)(tBuMe_2Si)Si=CH(Ad)$  and the mechanistic analysis of the isomerization revealed the intermediate formation of silylene (Zborovsky et al. 2019).

The thermodynamic stability of silylenes is achieved mainly by the  $\pi$  electron donation of the adjacent atoms, to the  $P_\pi$  orbital of the central Si atom (Rekken et al. 2012). The kinetic stability is provided by the steric protection of the heavy substituents connected to the adjacent atoms (Ellison, Ruhlandt- Senge, and Power 1994; Rekken et al. 2012). The catalytic activity of acyclic silylenes is found to be much greater than the cyclic silylenes, due to the smaller L-Si-L angle and the diminished HOMO-LUMO gap (Asay et al. 2011; Rekken et al. 2012; Bertrand and Reed 1994; Igau et al. 1988; Shan, Yao, and Driess 2020). Even isolable silylenes are highly reactive and can dissociate most stable covalent bonds in molecules like  $H_2$ , CO,  $CO_2$ ,  $N_2O$ ,  $O_2$ ,  $NH_3$ ,  $H_2O$ , ethylene and  $P_4$ . Traditionally, almost all these catalytic processes were achieved by transition metal complexes only.

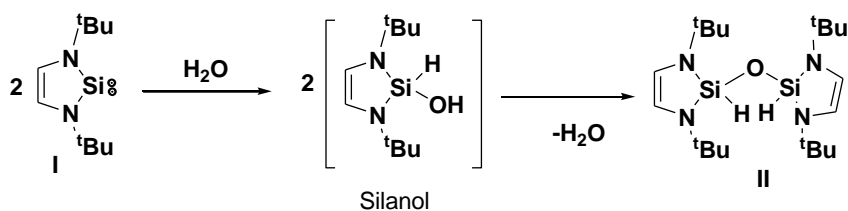
The first two-coordinate acyclic silylene, stable at ambient temperatures was reported by Jones et al in 2012. The stability of the silylene was achieved using the strong electron donating substituent  $B(N\text{Dipp}CH)_2$  (Dipp = 2,6- $i$ Pr $_2$ C $_6$ H $_3$ ) that provide sample steric protection also. This acyclic silylene undergoes spontaneous oxidative addition of  $H_2$ , being the first example of experimentally observed dihydrogen activation by a silylene (Protchenko et al. 2012) (Scheme 3.6).



**Scheme 3.8**

Hydrogen activation by silylene

Several examples can be cited to show that silylenes are powerful enough to break the strong O-H bond of water (Ghadwal et al. 2011; Hadlington, Driess, and Jones 2018; Meltzer et al. 2010; Mo et al. 2017). West and co-workers revealed that the first isolable N-heterocyclic silylene **I** inserts into O-H bonds of  $H_2O$  quite easily (Haaf et al. 1998; Haaf, Schmedake, and West 2000). The disiloxane **II** can be prepared by the reaction between the silylene **I** and water. The analogous silanol compound is proposed to be an intermediate, which rapidly self-condenses to the product **II** (Scheme 3.7) (Haaf, Schmedake, and West 2000).



**Scheme 3.9**

O-H bond activation by silylene

## 3.2 Objectives

1. Computational analysis to explore the reaction pathways and energetics of small molecule (NH<sub>3</sub>, CO, NO) addition to silene.
2. Effect of substituents on the reactivity of mono-substituted and di-substituted silences towards small molecule activation is explored.
3. Computational analysis of the energetics and mechanism for the isomerization of silene to silylenes and the effect of substituents on the energetics and mechanism of silene-silylene isomerization.

## 3.3 Computational methods

All calculations were carried out at the B3LYP/6-31G(d,p) level of density functional theory using the Gaussian 16 suite of programs. Minimas were confirmed by IR frequency analysis, and saddle points were characterized by a single imaginary frequency. All calculations were also performed at the PW6B95D3/6-311++G(d,p) level of theory, however, the energy values are consistent with B3LYP/6-31G(d,p) calculation. Hence, the present discussion is solely based on B3LYP/6-31G(d,p) level calculations.

## 3.4 Results and discussion

Mono-substituted silences with substituent on carbon (represented as HRC=SiH<sub>2</sub>), mono-substituted silences with substituent on silicon (represented as H<sub>2</sub>C=SiRH) and disubstituted silene with a substituent on both carbon and silicon (represented as HRC=SiRH) were taken for the analysis with substituents (R) -CH<sub>3</sub>, -SiH<sub>3</sub>, -OH, -CN and -F. The addition reaction of these silenes with small molecules such as NH<sub>3</sub>, NO and CO is carried out.

### 3.4.1 NH<sub>3</sub>: The N-H bond activation

#### NH<sub>3</sub> - N-H activation

The reaction scheme calculated for the N-H activation in ammonia by the parent silene H-C<sub>Si</sub>-H is depicted in Figure 3.1 along with the relative energy values. The silene and the NH<sub>3</sub> molecule initially form a reactant complex (Si<sub>l</sub>-NH<sub>3</sub>-RNT) by a nucleophilic interaction between the lone pair on the nitrogen and the π\*-orbital of the C-Si bond ( $r_{Si-N} =$

2.27 Å). The formation of the reactant complex is endothermic by 3.73 kcal/mol. Weakening of the N-H bond oriented towards the carbon nuclei of the silene leading to the formation of new C-H bond resulted in the formation of the transition state Sil-NH<sub>3</sub>-TS. The activation barrier associated with the formation of Sil-NH<sub>3</sub>-TS is 8.5 kcal/mol. The transition state Sil-NH<sub>3</sub>-TS corresponds to C-Si  $\pi$  - N-H $\sigma^*$  interaction leading to the formation of two new bonds, viz; Si-N ( $r_{\text{Si-N}} = 1.93$  Å) and C-H ( $r_{\text{C-H}} = 1.71$  Å). These bond formations are culminated in the weakening of N-H ( $r_{\text{N-H}} = 1.19$  Å) and C=Si bonds ( $r_{\text{C-Si}} = 1.79$  Å). The transition state Sil-NH<sub>3</sub>-TS transformed to the product Sil-NH<sub>3</sub>-PDT, which is a silamine. The overall exothermicity of the reaction 50 kcal/mol coupled with the low activation energy 12.23 kcal/mol, suggests that the reaction would be feasible at ambient conditions.

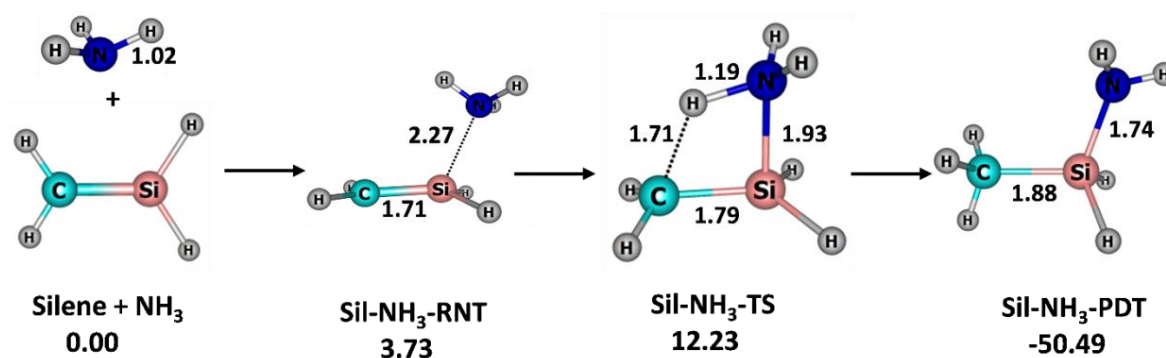


**Figure 3.1** Reaction scheme for N-H activation by H-CSi-H. Relative free energies are given in kcal/mol and bond lengths in Å.

The N-H activation in ammonia by the mono- and di- substituted silenes; R-CSi-H, H-CSi-R and R-CSi-R were also explored. The primary observation is that, the introduction of substituents on C and Si did not change the reaction pathway of the N-H activation process. The free energy profile diagrams for the N-H activation by R-CSi-H, H-CSi-R and R-CSi-R are given in Figure 3.2, and the energy values are presented in Table 3.1. It is clearly perceptible that, in each of the three types of silenes, stronger electrostatic Si-N interaction is established in the silenes with greater positive charge on Si nucleus ( $\text{low } V_{\text{Si}}$ ), and hence the formation of the reactant complex Sil-NH<sub>3</sub>-RNT is turned out to be exothermic. The bond distances  $r_{\text{Si-N}}$  of such reactant complexes are significantly shorter ( $r_{\text{Si-N}} = \sim 2.09$  Å) than the corresponding value of the parent silene ( $r_{\text{Si-N}} = 2.27$  Å). In such systems, the formation of Sil-NH<sub>3</sub>-RNT occurs through a transition state, but the activation barrier is only  $\sim 2$  kcal/mol and not included in the discussion. From the reactant complex Sil-NH<sub>3</sub>-RNT, the activation barrier for N-H activation is  $\sim 10$  kcal/mol irrespective of the electronic nature of

substituents and the position of substitution. A better stabilization of the free energy profile is encountered with the electron withdrawing and  $\pi$ -donating substituents in the monosubstituted H-CSi-R and the disubstituted R-CSi-R systems. The high exothermicity of the reactions involving the substituted and the unsubstituted silenes and the low energy barrier imply the potential of silenes in the activation of N-H bonds.

**Table 3.1** Relative free energy values of intermediates and transition states involved in the N-H activation by R-CSi-H, H-CSi-R and R-CSi-R

Silene	Substituent (R)	Silene + NH <sub>3</sub>	Sil-NH <sub>3</sub> -RNT	Sil-NH <sub>3</sub> -TS	Sil-NH <sub>3</sub> -PDT
H <sub>2</sub> C=SiH <sub>2</sub>	-H	0.00	3.73	12.23	-50.49
R-CSi-H	-CH <sub>3</sub>	0.00	5.31	16.79	-46.78
	-SiH <sub>3</sub>	0.00	-1.46	9.38	-45.47
	-OH	0.00	7.31	19.03	-44.91
	-CN	0.00	-6.32	6.31	-45.25
	-F	0.00	4.46	16.38	-48.21
H-CSi-R	-CH <sub>3</sub>	0.00	4.55	12.78	-50.77
	-SiH <sub>3</sub>	0.00	4.88	14.88	-46.83
	-OH	0.00	-1.97	7.48	-57.31
	-CN	0.00	-1.57	9.06	-55.91
	-F	0.00	-3.90	4.73	-62.84
R-CSi-R	-CH <sub>3</sub>	0.00	6.04	17.02	-47.30
	-SiH <sub>3</sub>	0.00	1.11	12.06	-41.62
	-OH	0.00	-0.14	10.02	-56.21
	-CN	0.00	-9.60	3.54	-49.63
	-F	0.00	-1.89	5.06	-62.94

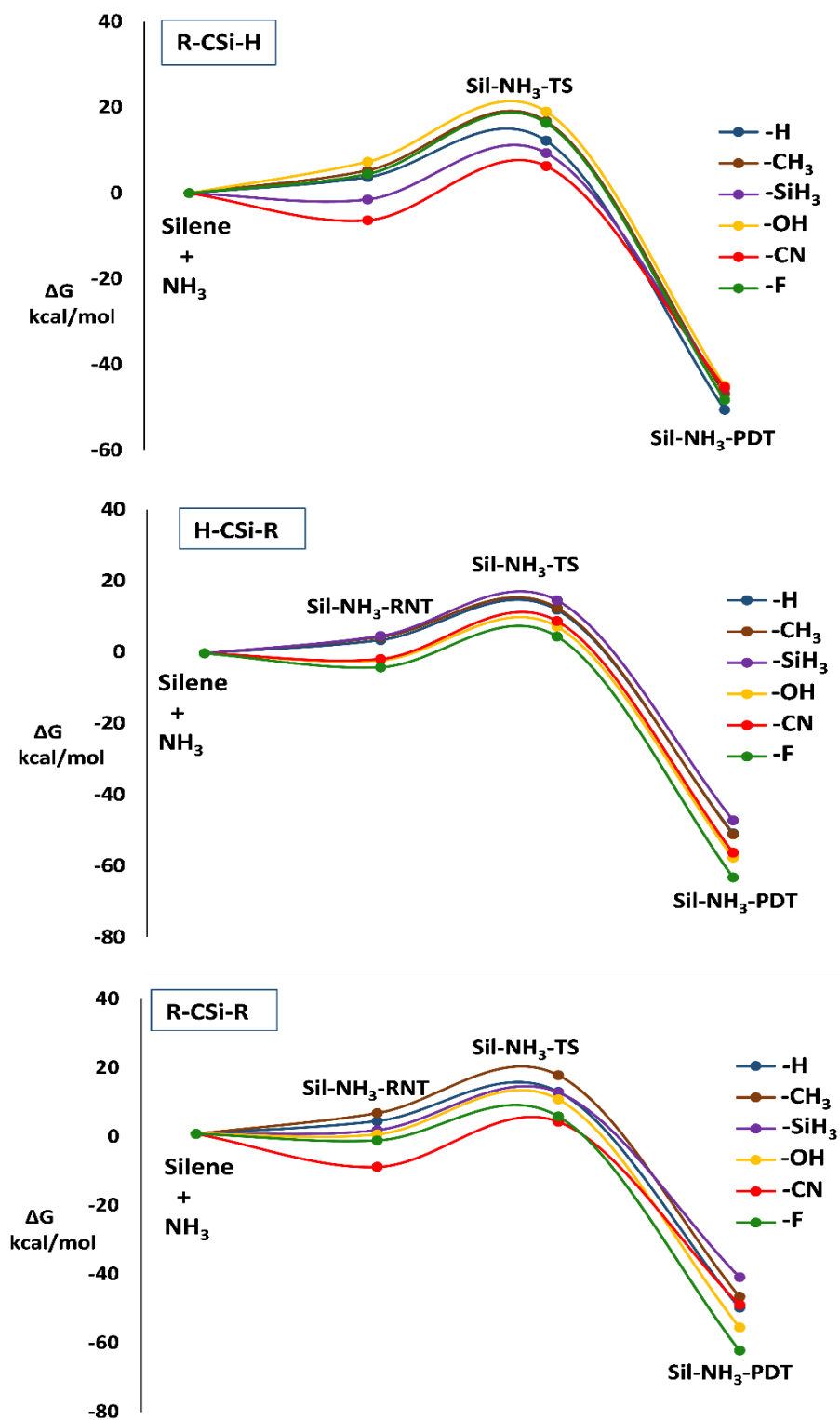


**Figure 3.2** Comparative free energy profiles for N-H activation by R-CSi-H, H-CSi-R and R-CSi-R

To estimate the difference in the calculated values using a different basis sets, we have calculated the energetics of the N-H activation reaction of the R-CSi-H, H-CSi-R and R-CSi-R at PW6B95D3/6-311++G(d,p). The results are given in Table 3.2

**Table 3.2** Relative energy values of intermediates and transition states involved in the N-H activation by R-CSi-H, H-CSi-R and R-CSi-R calculated at PW6B95D3/6-311++G(d,p)

Silene	Substituent (R)	Silene + NH <sub>3</sub>	Sil-NH <sub>3</sub> -RNT	Sil-NH <sub>3</sub> -TS	Sil-NH <sub>3</sub> -PDT
H <sub>2</sub> C=SiH <sub>2</sub>	-H	0.00	2.88	10.92	-48.14
R-CSi-H	-CH <sub>3</sub>	0.00	4.98	15.30	-47.09
	-SiH <sub>3</sub>	0.00	-1.99	8.12	-45.90
	-OH	0.00	6.86	17.70	-45.00
	-CN	0.00	-7.39	5.21	-45.00
	-F	0.00	3.64	13.94	-50.11
H-CSi-R	-CH <sub>3</sub>	0.00	3.06	11.19	-50.27
	-SiH <sub>3</sub>	0.00	3.65	13.17	-46.59
	-OH	0.00	-3.04	7.48	-56.10
	-CN	0.00	-2.61	7.90	-55.31
	-F	0.00	-5.46	4.71	-60.82
R-CSi-R	-CH <sub>3</sub>	0.00	5.39	15.20	-47.96
	-SiH <sub>3</sub>	0.00	0.01	10.22	-42.46
	-OH	0.00	-2.18	8.98	-56.49
	-CN	0.00	-11.76	2.44	-50.23
	-F	0.00	-2.98	3.33	-63.15

Even though, marginal difference in the corresponding values of each species can be made out, the general trend in the variation of energy is same as that perceived atB3LYP/6-31G(d,p) basis set. This is true with individual reactions and the gradation in energy values among different silenes.

### 3.4.2 NO: N-O bond activation

Figure 3.3 depicts the calculated reaction scheme for the addition of H-CSi-H with NO along with the relative energy values. Addition of NO to silenes initiates with the formation of a weakly bonded van der Waals reactant complex Sil-NO-RNT, which possess a relative free energy 4.26 kcal/mol. Strong electrostatic attraction between electropositive Si of the silene molecule and electronegative oxygen atom of the nitric oxide molecule leads to Si-O bond formation with the bond length  $r_{\text{Si-O}} = 1.73 \text{ \AA}$ . The Si-O bond formation is associated with the cleavage of the C-Si  $\pi$ -bond ( $r_{\text{C-Si}} = 1.83 \text{ \AA}$ ) generating Sil-NO-INT1 via the transition state Sil-NO-TS1. The activation barrier for the formation of the intermediate Sil-NO-INT1 is 14 kcal/mol. The rupture of the C-Si  $\pi$ -bond, leading to the formation of Sil-NO-INT1, makes the carbon nuclei a radical center with spin density 1.01. Accordingly, the nitrogen atom gets a spin density of 1.71. The radical nature of C and N eases the C-N bond formation resulted in the silene-NO adduct, Sil-NO-PDT through the transition state Sil-NO-



TS2. The magnitude of the second activation barrier is 3.21 kcal/mol. Free rotation of the -CH<sub>2</sub> group towards O-N in Sil-NO-TS2 is contributed to the low activation barrier of the C-N bond formation, along with the radical nature of the participating atoms. The overall reaction is exothermic by ~22 kcal/mol. The rate determining step of the NO activation process is the formation of the intermediate Sil-NO-INT1 from the van der Waals reactant complex Sil-NO-RNT.

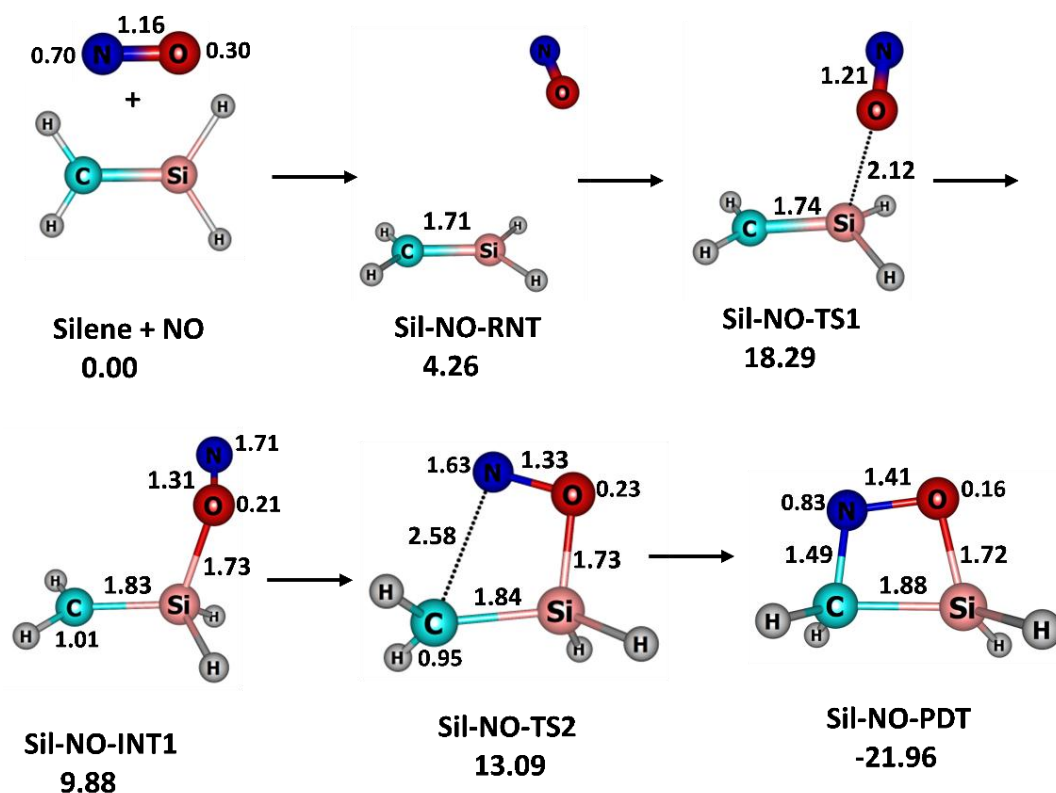


**Figure 3.3** Calculated reaction scheme for the NO addition to H-C-Si-H. Relative free energy values in kcal/mol, bond lengths in Å and Mulliken spin density in a.u

**Table 3.3** Relative free energy values of intermediates and transition states involved in the addition of NO to R-CSi-H, H-CSi-R and R-CSi-R

Silene	Substituent (R)	Silene + NO	Sil-NO-RNT	Sil-NO-TS1	Sil-NO-INT1	Sil-NO-TS2	NO-PDT
H <sub>2</sub> C=SiH <sub>2</sub>	-H	0.00	4.26	18.29	9.88	13.09	-21.96
R-CSi-H	-CH <sub>3</sub>	0.00	5.62	17.06	6.72	10.58	-22.42
	-SiH <sub>3</sub>	0.00	4.22	18.14	11.57	14.40	-17.08
	-OH	0.00	5.20	15.05	2.13	5.71	-24.20
	-CN	0.00	4.55	16.06	7.34	11.91	-13.00
	-F	0.00	3.66	16.82	4.91	8.39	-25.78
	-CH <sub>3</sub>	0.00	5.15	16.42	7.58	10.33	-25.04

H-CSi-R	-SiH <sub>3</sub>	0.00	3.94	19.94	12.61	16.15	-19.46
	-OH	0.00	5.82	14.80	2.87	5.39	-31.57
	-CN	0.00	4.49	18.66	9.61	12.35	-22.55
	-F	0.00	5.24	13.90	0.90	3.09	-32.45
R-CSi-R	-CH <sub>3</sub>	0.00	5.49	14.99	3.91	7.42	-26.09
	-SiH <sub>3</sub>	0.00	5.01	20.83	15.85	17.40	-14.78
	-OH	0.00	3.14	9.37	-7.48	-6.48	-37.29
	-CN	0.00	4.52	15.72	7.14	10.82	-13.91
	-F	0.00	4.65	12.06	-7.17	-5.25	-39.50

The relative free energy values of the intermediates, transition states, and products involved in NO addition to the monosubstituted silenes R-CSi-H, H-CSi-R and the disubstituted silenes R-CSi-R are calculated and presented in Table 3.3. The comparative free energy profile diagrams are given in Figure 3.4. It is found that, the relative energy values of the reactant complex (Sil-NO-RNT) are nearly the same for all systems. However, the position and the nature of substituent are decisive in deciding the magnitude of the activation barrier leading to the formation of the intermediate Sil-NO-INT1. Electron donating as well as electron withdrawing substituents on carbon nucleus of the silene suppress the activation barrier for the formation of the intermediate Sil-NO-INT1 slightly, compared to the corresponding barrier height of the parent silene H-CSi-H. Among the R-CSi-H systems, the lowest barrier height is encountered with HO-CSi-H (9.85 kcal/mol) and the highest with H<sub>3</sub>Si-CSi-H (13.92 kcal/mol). Considering the H-CSi-R systems, both H-CSi-SiH<sub>3</sub> and H-CSi-CN molecules showed an increase in activation energy for the formation of Sil-NO-INT1 compared to that of the unsubstituted H-CSi-H. Despite that, both H-CSi-OH and H-CSi-F molecules exhibit lower activation energy than that of carbon substituted counterparts. A further lowering of the activation barrier is identified with -OH and -F substituted R-CSi-R. But, the introduction of -SiH<sub>3</sub> substituents on both C and Si atoms (H<sub>3</sub>Si-CSi-SiH<sub>3</sub>) increases the activation barrier compared to the parent silene, H-CSi-H.

For all systems, the formation of Sil-NO-INT1 is the rate limiting step. The activation barrier for the formation of the second activated complex Sil-NO-TS2 ranges from 1 to 4.5 kcal/mol. In general, -CH<sub>3</sub>, -OH and -F substituents stabilize the free energy profile in all three types of silenes. The stabilization is more significant with -OH and -F groups when in the disubstituted R-CSi-R systems. The -SiH<sub>3</sub> and -CN substituents have little impact while in R-CSi-H, but -SiH<sub>3</sub> is destabilizing in H-CSi-R and R-CSi-R whereas -CN is stabilizing with the latter two systems. Overall reaction is exothermic for all systems. The relative energy values of intermediates and transition states support the feasibility of NO addition to silenes in ambient reaction conditions.

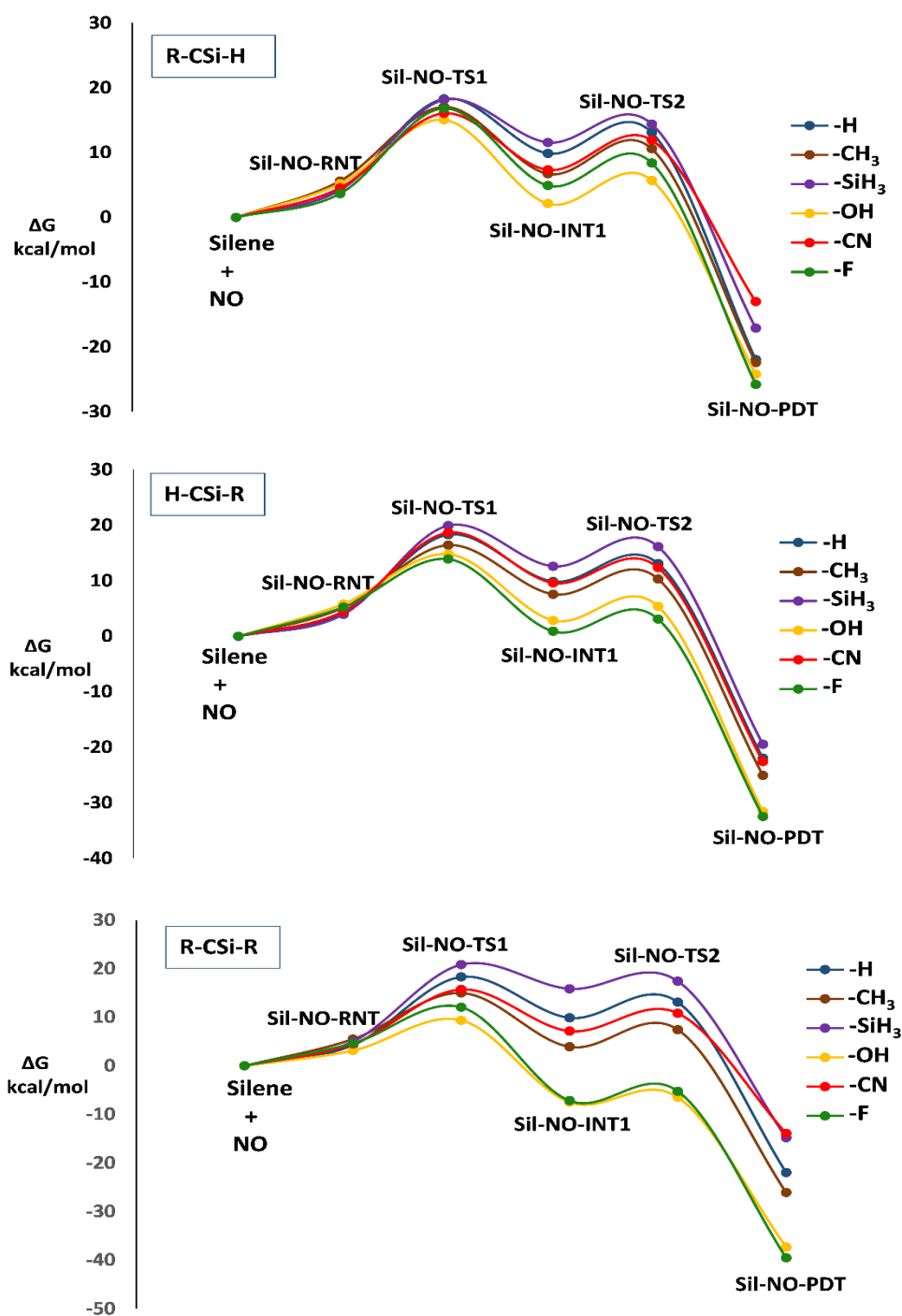


**Figure 3.4** Comparative free energy profile for NO activation by R-CSi-H, H-CSi-R and R-CSi-R

To estimate the difference in the calculated values using a different basis sets, we have calculated the energetics of the N-O activation reaction of the R-CSi-H, H-CSi-R and R-CSi-R at PW6B95D3/6-311++G(d,p). The results are given in Table 3.4

**Table 3.4** Relative energy values of intermediates and transition states involved in the addition of NO to R-CSi-H, H-CSi-R and R-CSi-R calculated at PW6B95D3/6-311++G(d,p)

Silene	Substituent (R)	Silene + NO	Sil-NO-RNT	Sil-NO-TS1	Sil-NO-INT1	Sil-NO – TS2	NO-PDT
H <sub>2</sub> C=SiH <sub>2</sub>	-H	0.00	4.13	20.19	13.36	16.68	-19.89
R-CSi-H	-CH <sub>3</sub>	0.00			6.56	36.39	-21.09
	-SiH <sub>3</sub>	0.00	6.27	20.05	14.99	17.97	-15.57
	-OH	0.00	4.17	16.89	4.69	6.70	-22.51
	-CN	0.00	4.46	18.21	11.34	15.78	-11.01
	-F	0.00					
H-CSi-R	-CH <sub>3</sub>	0.00	7.14	18.45	11.02	36.75	-22.81
	-SiH <sub>3</sub>	0.00			7.05	41.66	-17.36
	-OH	0.00	4.38	12.12	-4.56	-3.27	-35.48
	-CN	0.00			4.84	38.79	-19.89
	-F	0.00	5.12	16.81	6.59	29.87	-27.73
R-CSi-R	-CH <sub>3</sub>	0.00	5.68	16.46	17.64	34.19	-24.80
	-SiH <sub>3</sub>	0.00	4.81	21.47	16.35	20.24	-13.56
	-OH	0.00	4.38	12.12	-4.56	-3.27	-35.48

Even though, marginal difference in the corresponding values of each species can be made out, the general trend in the variation of energy is same as that perceived at B3LYP/6-31G(d,p) basis set. This is true with individual reactions and the gradation in energy values among different silenes.

### 3.4.3 CO: C-O bond activation

Figure 3.5 demonstrates the calculated reaction scheme for the addition of H<sub>2</sub>C=SiH<sub>2</sub> with CO and the relative energy values.

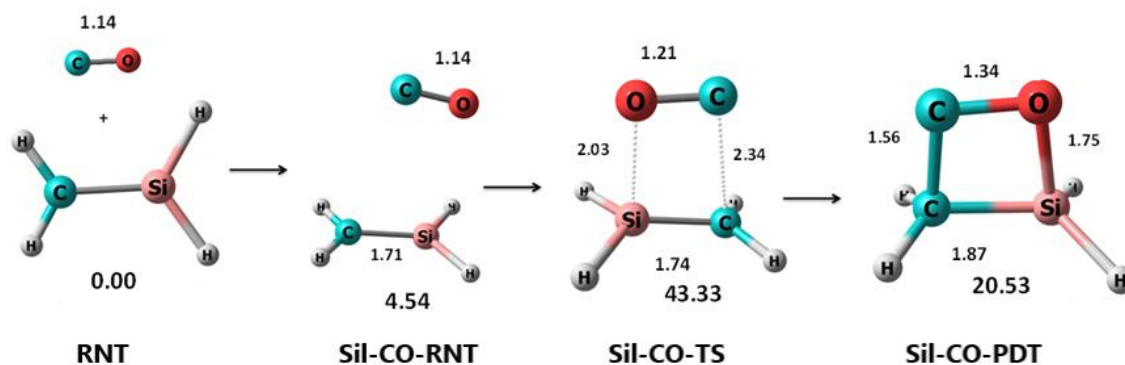


**Figure 3.5** Calculated reaction scheme for the CO addition to H<sub>2</sub>C= SiH<sub>2</sub>. Relative free energy values in kcal/mol and bond lengths in Å.

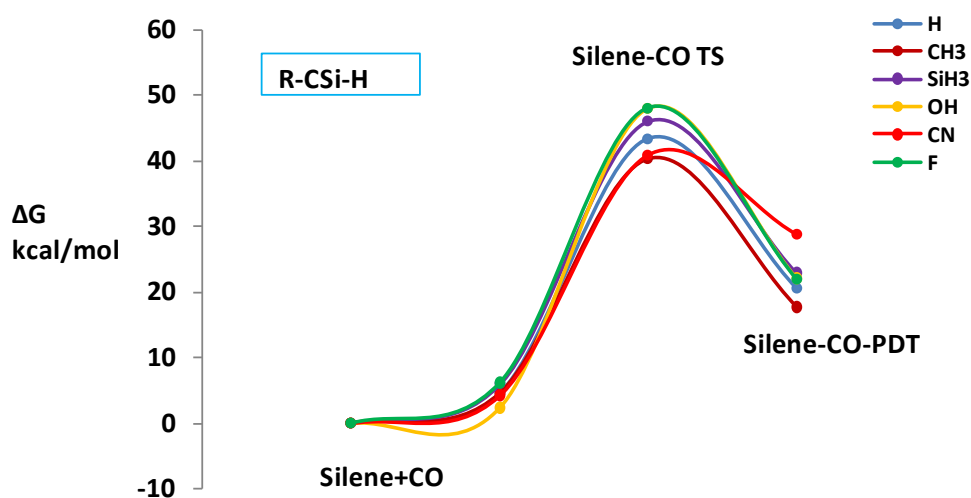
The addition of CO to the silenes initiated with the formation of a weakly bonded van der Waals reactant complex Sil-CO-RNT, having a relative free energy is 4.54kcal/mol. The reaction is progressed to the four-membered ring transition state Sil-CO-TS by the emergence of an electrostatic attraction between the positively polarized selenic Si atom and negatively polarized oxygen atom of carbon monoxide leading to the buildup of a strong Si-O interaction ( $r_{\text{Si-O}} = 2.34 \text{ \AA}$ ) and an associated weakening of the Si-C bond ( $r_{\text{C-Si}} = 1.74 \text{ \AA}$ ). An interaction between the negatively polarized silenic carbon atom and positively polarized carbon atom of the carbon monoxide molecule also developed at this stage of the reaction ( $r_{\text{C-C}} = 2.03 \text{ \AA}$ ). The relative energy of Sil-CO-TS is 43.33 kcal/mol and the barrier height is for the transformation of Sil-CO-RNT to Sil-CO-TS is 37.79 kcal/mol. The formation of the four-membered ring product is endothermic by 20.53 kcal/mol. The rather high activation energy and the endothermic nature of the reaction indicate that the CO addition to silene is not feasible under normal laboratory conditions.

**Table 3.5** Relative free energy values of intermediates and transition states involved in the addition of CO to R-CSi-H, H-CSi-R and R-CSi-R

Silene	Substituent (R)	Silene + CO	Sil-CO-RNT	Sil-CO-TS	Sil-CO-PDT
H <sub>2</sub> C=SiH <sub>2</sub>	-H	0.00	4.54	43.33	20.53
R-CSi-H	-CH <sub>3</sub>	0.00	4.54	40.39	17.75
	-SiH <sub>3</sub>	0.00	5.90	45.97	22.88
	-OH	0.00	2.29	48.07	22.09
	-CN	0.00	4.20	40.87	28.80
	-F	0.00	6.13	48.05	21.91
H-CSi-R	-CH <sub>3</sub>	0.00	4.54	40.39	17.75
	-SiH <sub>3</sub>	0.00	5.90	45.97	22.88
	-OH	0.00	3.46	32.89	10.94
	-CN	0.00	4.48	43.51	20.32
	-F	0.00	4.82	32.71	10.60
R-CSi-R	-CH <sub>3</sub>	0.00	4.67	41.85	18.63
	-SiH <sub>3</sub>	0.00	4.15	44.49	25.63
	-OH	0.00	4.00	34.05	8.23
	-CN	0.00	4.30	41.01	28.29
	-F	0.00	4.82	33.88	8.21

The relative free energy values of the reactive intermediates, transition states, and products involved in CO addition to the mono-substituted silences (R-CSi-H and H-CSi-R) and the di-substituted silene (R-CSi-R) is calculated and presented in Table 3.5. The comparative free energy profile diagrams are given in Figure 3.6. The relative energy value

of the reactant complex Sil-CO-RNT is considerably reduced in the -OH substituted systems; especially in the HO-CSi-H molecule. The activation energy for the formation of the transition state Sil-CO-TS is more for all R-CSi-H systems, except for the -SiH<sub>3</sub> and -CN substituted systems compared to the parent silene H-CSi-H. Regarding the H-CSi-R systems, the -OH and -F substituted molecules exhibit a considerable decrease in the activation energy ( $\square 11$  kcal/mol) for the formation of Sil-CO-TS. This decrease in the activation energy is maintained almost nearly at the same value by these substituents in the disubstituted R-CSi-R system also. Other substituents made no significant impact on the activation energy value in comparison with that of the unsubstituted molecule in any of the substituted systems. Another noticeable substituent effect is the large decrease in the endothermicity of the CO addition reaction by the -OH and -F substituents in the monosubstituted H-CSi-R and the disubstituted R-CSi-R systems. Both substituents reduced the endothermicity by  $\square 10$  kcal/mol in the H-CSi-R system and  $\square 12$  kcal/mol in the R-CSi-R systems. These observations indicate that, the CO addition to silences becomes nearly feasible under ambient conditions with -OH and -F substituted H-CSi-R and R-CSi-R systems.



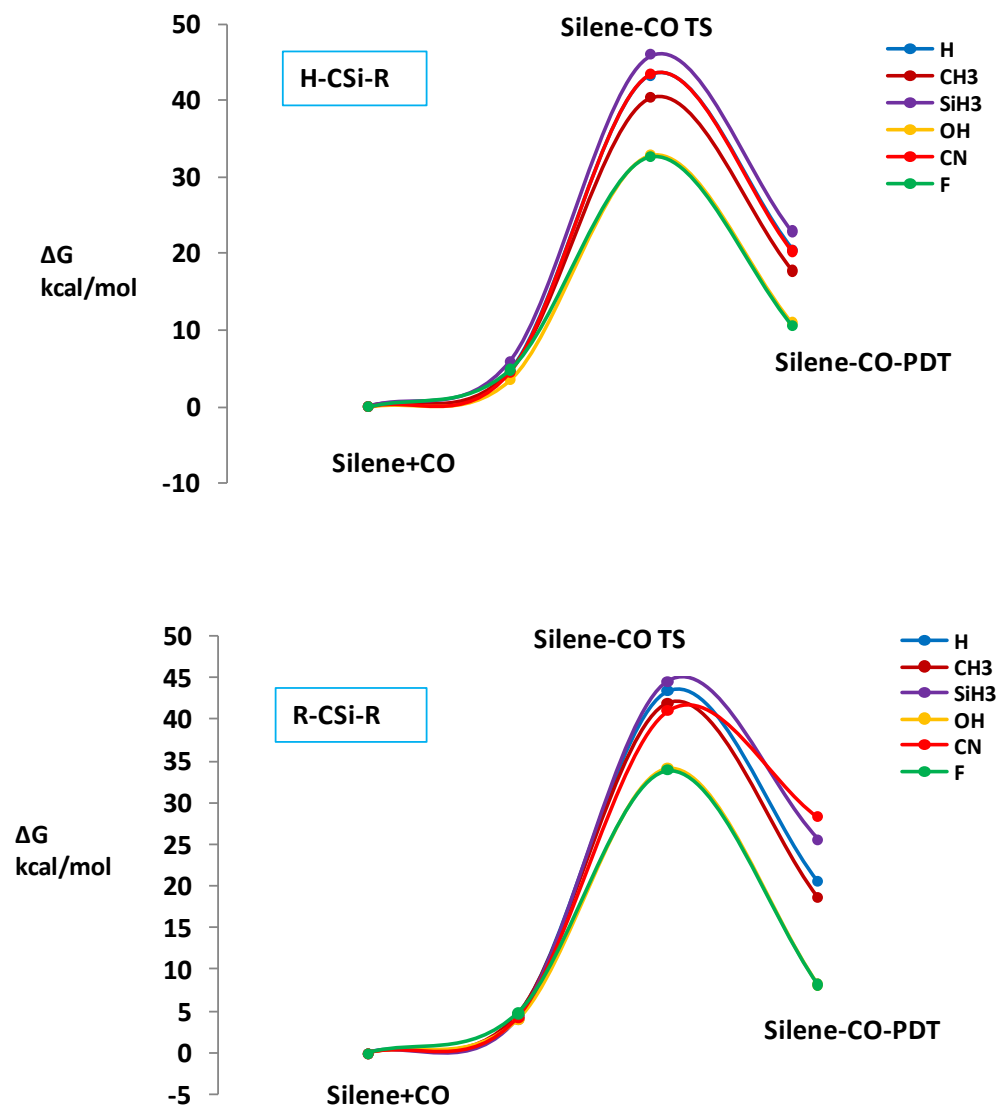


**Figure 3.6** Comparative free energy profile for CO activation by R-CSi-H, H-CSi-R and R-CSi-R

To estimate the difference in the calculated values using a different basis sets, we have calculated the energetics of the C-O activation reaction of the R-CSi-H, H-CSi-R and R-CSi-R at PW6B95D3/6-311++G(d,p). The results are given in Table 3.6

**Table 3.6** Relative energy values of intermediates and transition states involved in the addition of CO to R-CSi-H, H-CSi-R and R-CSi-R calculated at PW6B95D3/6-311++G(d,p)

Silene	Substituent (R)	Silene + CO	Sil-CO-RNT	Sil-CO-TS	Sil-CO-PDT
H <sub>2</sub> C=SiH <sub>2</sub>	-H	0.00	4.77	43.49	21.13
R-CSi-H	-CH <sub>3</sub>	0.00	4.39	44.85	21.65
	-SiH <sub>3</sub>	0.00	5.63	41.49	23.22
	-OH	0.00	4.48	47.71	21.96
	-CN	0.00	3.83	41.22	29.40

	-F	0.00	4.19	47.42	21.78
H-CSi-R	-CH <sub>3</sub>	0.00	6.13	40.39	18.41
	-SiH <sub>3</sub>	0.00	4.45	39.93	23.29
	-OH	0.00	6.39	35.41	14.46
	-CN	0.00	4.76	44.15	21.78
	-F	0.00	5.06	34.89	13.88
R-CSi-R	-CH <sub>3</sub>	0.00	3.94	40.99	18.11
	-SiH <sub>3</sub>	0.00	4.99	4350	25.03
	-OH	0.00	5.53	35.49	9.17
	-CN	0.00	5.52	41.65	29.29
	-F	0.00	4.92	35.42	10.11

Even though, marginal difference in the corresponding values of each species can be made out, the general trend in the variation of energy is same as that perceived at B3LYP/6-31G(d,p) basis set. This is true with individual reactions and the gradation in energy values among different silenes also.

### 3.4.4 The silene-silylene rearrangement

Energetics for the rearrangement of silene to silylene via 1,2- H migration has been calculated for the parent silene, H-CSi-H. The structures and energy values are given in Figure 9. The silene-silylene rearrangement is the result of a 1,2- H migration. This migration takes place through a transition state silylene-TS in which a strong C-H interaction is developed by the associated weakening of the Si-H ( $r_{\text{Si-H}} = 1.58 \text{ \AA}$ ) and Si-C bonds ( $r_{\text{Si-C}} = 1.80 \text{ \AA}$ ). The activation barrier for H-migration is 35.92 kcal/mol and the rearrangement is feebly endothermic by 0.74 kcal/mol. The relatively high activation barrier and endothermic nature of the reaction indicate that the reaction is not feasible under normal conditions.

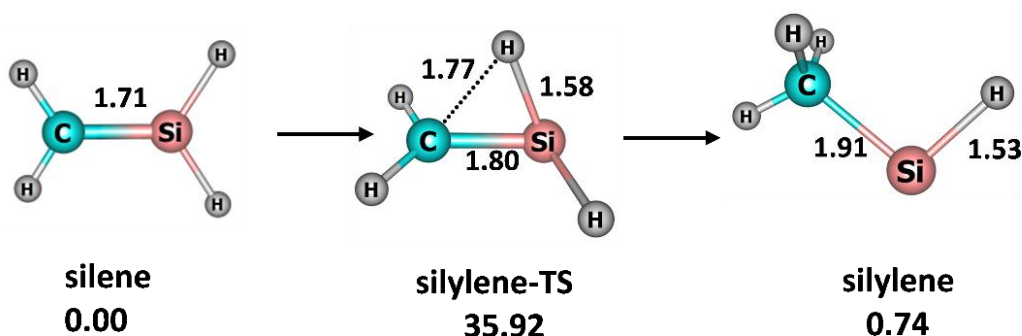


**Figure 3.7** Reaction scheme for silene-silylene rearrangement. Relative free energy values in kcal/mol and bond lengths in Å.

The relative energy value of the transition states, intermediates and products involved in the silene-silylene rearrangement of in R-CSi-H, H-CSi-R and R-CSi-R systems were calculated and is presented in table 3.7. The energy profile diagrams are displayed in figure

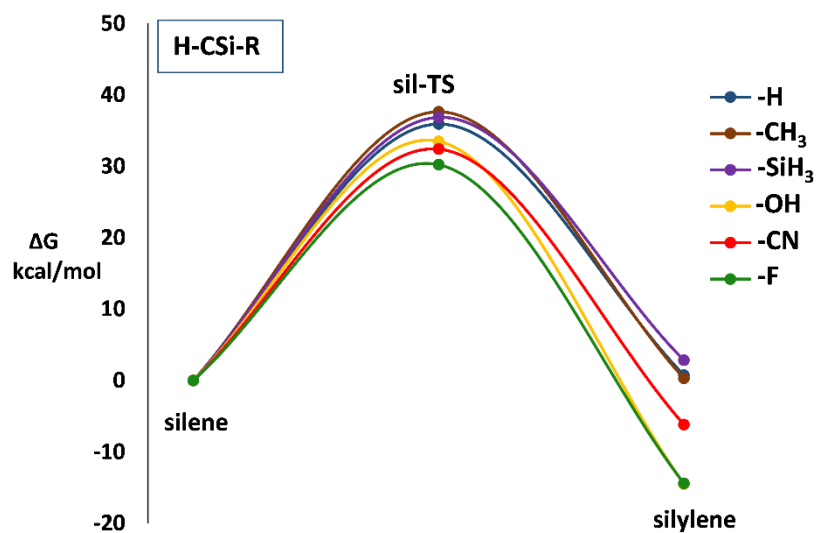
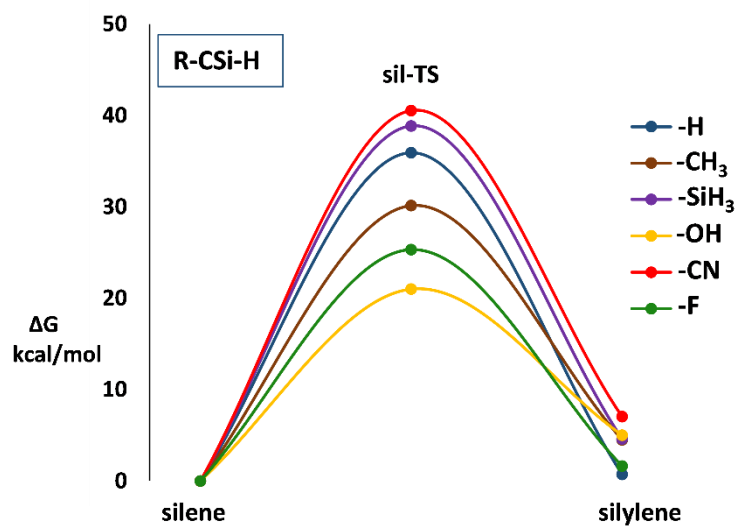


3.8. Introduction of substituents on carbon (R-CSi-H) did not make any noticeable change to the endothermicity of the rearrangement. The effect of substituents on the energy barrier for the 1,2 -H migration is quite significant. Electron donating -SiH<sub>3</sub> and electron withdrawing -CN increased the activation barrier (38.86 kcal/mol and 40.54 kcal/mol respectively) in the R-CSi-H system, whereas -OH and -F groups lowered the barrier height substantially (21.0 and 25.32 kcal/mol respectively). Even though, not as profound as observed with -OH and -F groups, the -CH<sub>3</sub> substitution also resulted in a decrease of the barrier height in H<sub>3</sub>C-CSi-H molecule. However, the monosubstitution on Si atom of the selenic bond (H-CSi-R) is failed to produce any noticeable alteration in the energy barrier, irrespective of the electronic nature of the substituent. The presence of electron withdrawing substituents on Si makes the reaction strikingly exothermic. The rearrangement accomplished by H-CSi-OH and H-CSi-F are exothermic by 14.51 and 14.43 kcal/mol respectively. The exothermicity can be assumed to be as due to the stability attained by the silylene owing to the  $\pi$ -donation to Si by these substituents. Regarding the disubstituted systems R-CSi-R, the activation energy the -OH and -F substituted molecules is still lower than that observed with the R-CSi-H systems (15.65 kcal/mol and 18.40 kcal/mol respectively). Interestingly, the activation energy of these systems falls in to the workable limit. Exothermicity is observed with the  $\pi$ -donating and electron withdrawing substituents in the R-CSi-R system also. The low activation energy and exothermicity of the rearrangement in R-CSi-R system suggests that, the simultaneous presence of  $\pi$ -donating substituents such as -OH and -F on Si and C nuclei of the silene would favor the 1,2 – H migration in them, allowing the formation of stable silylenes.

**Table 3.7** Relative free energy values of intermediates and transition states involved in the silene-silylene rearrangement of R-CSi-H, H-CSi-R and R-CSi-R

Silene	Substituent (R)	silene	silylene-TS	silylene
H <sub>2</sub> C=SiH <sub>2</sub>	-H	0.00	35.92	0.74
R-CSi-H	-CH <sub>3</sub>	0.00	30.14	4.52
	-SiH <sub>3</sub>	0.00	38.86	4.61
	-OH	0.00	21.00	5.03
	-CN	0.00	40.54	7.04
	-F	0.00	25.32	1.64
H-CSi-R	-CH <sub>3</sub>	0.00	37.63	0.29
	-SiH <sub>3</sub>	0.00	36.86	2.84
	-OH	0.00	33.49	-14.51
	-CN	0.00	32.41	-6.18
	-F	0.00	30.22	-14.43
	-CH <sub>3</sub>	0.00	33.45	3.11

R-CSi-R	-SiH <sub>3</sub>	0.00	41.46	5.93
	-OH	0.00	15.65	-14.29
	-CN	0.00	36.34	-0.02
	-F	0.00	18.40	-15.45



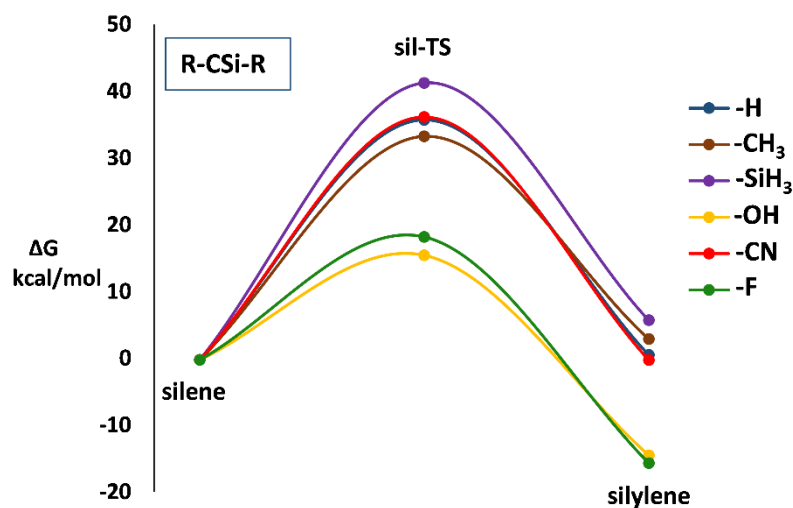


**Figure 3.8** Comparative free energy profile for the silene-silylene rearrangement in R-CSi-H, H-CSi-R and R-CSi-R.

To estimate the difference in the calculated values using a different basis sets, we have calculated the energetics of the silene-silylene rearrangement of the R-CSi-H, H-CSi-R and R-CSi-R at PW6B95D3/6-311++G(d,p). The results are given in Table 3.16

**Table 3.8** Relative energy values of intermediates and transition states involved in the silene-silylene rearrangement of R-CSi-H, H-CSi-R and R-CSi-R calculated at PW6B95D3/6-311++G(d,p)

Silene	Substituent (R)	silene	silylene-TS	silylene
H <sub>2</sub> C=SiH <sub>2</sub>	-H	0.00	36.01	2.26
R-CSi-H	-CH <sub>3</sub>	0.00	31.63	4.61
	-SiH <sub>3</sub>	0.00	38.61	0.95
	-OH	0.00	13.39	5.11
	-CN	0.00	38.40	7.43
	-F	0.00	22.13	1.48
	H-CSi-R	-CH <sub>3</sub>	0.00	37.60
-SiH <sub>3</sub>		0.00	36.08	3.96
-OH		0.00	34.65	-11.84
-CN		0.00	32.06	-5.11
-F		0.00	30.83	-13.25
R-CSi-R	-CH <sub>3</sub>	0.00	33.03	3.43
	-SiH <sub>3</sub>	0.00	40.13	1.45
	-OH	0.00	16.37	-14.28
	-CN	0.00	35.84	-0.20
	-F	0.00	18.87	-17.01

Even though, marginal difference in the corresponding values of each species can be made out, the general trend in the variation of energy is same as that perceived at B3LYP/6-31G(d,p) basis set.

### 3.5 Conclusion

The effect of substituents  $R = \text{CH}_3, \text{SiH}_3, \text{OH}, \text{CN}$  and  $\text{F}$  on the small molecule activation reaction of  $\text{H-CSi-H}$  is examined. The substituted silenes examined are  $\text{R-CSi-H}$ ,  $\text{H-CSi-R}$  and  $\text{R-CSi-R}$  and the small molecules tried were  $\text{NH}_3$ ,  $\text{NO}$  and  $\text{CO}$ . Silene is found to be extremely effective in  $\text{N-H}$  and  $\text{N-O}$  activation process. The reaction is taking place at the expense of low activation energy and is highly exothermic for the parent silene.  $\sigma$ -withdrawing and  $\pi$ -donating substituents  $-\text{OH}$  and  $-\text{F}$  are found to be effective in promoting the activation process by largely stabilizing the reaction pathway and increasing the exothermicity of the reaction. The substituents are found to be more effective in  $\text{H-CSi-R}$  and  $\text{R-CSi-R}$ . The  $\text{CO}$  addition reaction of the parent silene requires relatively high activation energy and is endothermic in nature. The  $\text{OH}$  and  $\text{F}$  substituents are found to be profoundly effective in stabilizing the energy profile of the  $\text{CO}$  addition reaction and reducing the endothermicity, especially in  $\text{H-CSi-R}$  and  $\text{R-CSi-R}$ .

As far as the 1,2-H migration of silene generating silylene rearrangement is concerned, the introduction of substituents on carbon did not make any change on the endothermicity of the reaction but showed a significant effect on the energy barrier. Electron donating  $-\text{SiH}_3$  and electron withdrawing  $-\text{CN}$  increased the activation barrier while  $-\text{CH}_3$ ,  $-\text{OH}$  and  $-\text{F}$  groups lowered the barrier height. A notable decrease in the barrier height is seen with the presence of  $\pi$ -donating substituents  $-\text{OH}$  and  $-\text{F}$  which can be attributed to the polarity reversal in  $\text{HO-CSi-H}$  and  $\text{F-CSi-H}$ . It can be understood that  $\pi$ -donation to  $\text{Si}$  could make the silylene more stable. When  $-\text{OH}$  or  $-\text{F}$  substituents present on both  $\text{C}$  and  $\text{Si}$  ( $\text{R-CSi-R}$ ), the rearrangement proceeds with low activation energy and becomes even exothermic. In general, the presence of  $\pi$ -donating substituents on  $\text{Si}$  would favor the 1,2-H migration in silenes to form stable silylene and make the rearrangement workable under ambient conditions.

## Reference

- Adrian G Brook, & Michael A Brook. (1996). *Advances in Organometallic Chemistry* (Vol. 39). New York, Academic Press.
- Akkari-El Ahdab, A., Rima, G., Gornitzka, H., & Barrau, J. (2001). Synthesis and characterization of 2,4,6-tris((dimethylamino)methyl)phenoxy silicon compounds. *Journal of Organometallic Chemistry*, 636(1–2), 96–107. [https://doi.org/10.1016/S0022-328X\(01\)01053-1](https://doi.org/10.1016/S0022-328X(01)01053-1)
- Asay, M., Jones, C., & Driess, M. (2011). N -Heterocyclic Carbene Analogues with Low-Valent Group 13 and Group 14 Elements: Syntheses, Structures, and Reactivities of a New Generation of Multitalented Ligands. *Chemical Reviews*, 111(2), 354–396. <https://doi.org/10.1021/cr100216y>
- Auner, N., Grobe, J., Müller, T., & Rathmann, H. W. (2000). Transient Silenes and Their Dimethyl- d 6 Ether Donor Complexes from the Gas-Phase Pyrolysis of Siletanes ., *Organometallics*, 19(18), 3476–3485. <https://doi.org/10.1021/om0002778>
- Bendikov, M., Quadt, S. R., Rabin, O., & Apeloig, Y. (2002). Addition of Nucleophiles to Silenes. A Theoretical Study of the Effect of Substituents on Their Kinetic Stability. *Organometallics*, 21(19), 3930–3939. <https://doi.org/10.1021/om0202571>
- Bertrand, G., & Reed, R. (1994).  $\lambda^3$ -Phosphinocarbenes  $\lambda^5$ -phosphaacetylenes. *Coordination Chemistry Reviews*, 137, 323–355. [https://doi.org/10.1016/0010-8545\(94\)03005-B](https://doi.org/10.1016/0010-8545(94)03005-B)
- Boatz, J. A., & Gordon, M. S. (1990). Predicted enthalpies of formation for silaethylene, disilene, and their silylene isomers. *The Journal of Physical Chemistry*, 94(19), 7331–7333. <https://doi.org/10.1021/j100382a001>
- Bonyhady, S. J., Green, S. P., Jones, C., Nembenna, S., & Stasch, A. (2009). A Dimeric Magnesium(I) Compound as a Facile Two- Center/Two- Electron Reductant. *Angewandte Chemie International Edition*, 48(16), 2973–2977. <https://doi.org/10.1002/anie.200900331>
- Bradaric, C. J., & Leigh, W. J. (1996). Arrhenius Parameters for the Addition of Nucleophiles to the Silicon–Carbon Double Bond of 1,1-Diphenylsilene. *Journal of the American Chemical Society*, 118(37), 8971–8972. <https://doi.org/10.1021/ja9620346>
- Burk, P., Abboud, J.-L. M., & Koppel, I. A. (1996). Aromaticity of Substituted Cyclopropenes: A Theoretical Study. *The Journal of Physical Chemistry*, 100(17), 6992–6997. <https://doi.org/10.1021/jp953279s>
- Chu, T., & Nikonov, G. I. (2018). Oxidative Addition and Reductive Elimination at Main-Group Element Centers. *Chemical Reviews*, 118(7), 3608–3680. <https://doi.org/10.1021/acs.chemrev.7b00572>
- Conlin, R. T., & Wood, D. L. (1981). Evidence for the isomerization of 1-methylsilene to dimethylsilylene. *Journal of the American Chemical Society*, 103(7), 1843–1844. <https://doi.org/10.1021/ja00397a046>
- Denk, M., Lennon, R., Hayashi, R., West, R., Belyakov, A. V., Verne, H. P., Haaland, A., Wagner, M., & Metzler, N. (1994). Synthesis and Structure of a Stable Silylene. *Journal of the American Chemical Society*, 116(6), 2691–2692. <https://doi.org/10.1021/ja00085a088>
- Dieck, H. T., & Zettlitzer, M. (1987). Darstellung und Reaktionen N - silylierter En- diamine, II [2 +

2]- Cycloadditionen: Synthese von  
1,4- Diamino- 1,3- butadien- 2,3- dicarbonsäure- Derivaten. *Chemische Berichte*, 120(5),  
795–801. <https://doi.org/10.1002/cber.19871200518>

Ellison, J. J., Ruhlandt- Senge, K., & Power, P. P. (1994). Synthesis and Characterization of Thiolato Complexes with Two- Coordinate Iron(  $\text{II}$  ). *Angewandte Chemie International Edition in English*, 33(11), 1178–1180. <https://doi.org/10.1002/anie.199411781>

Filippou, A. C., Chernov, O., & Schnakenburg, G. (2009). SiBr 2 (Idipp): A Stable N- Heterocyclic Carbene Adduct of Dibromosilylene. *Angewandte Chemie International Edition*, 48(31), 5687–5690. <https://doi.org/10.1002/anie.200902431>

Gaspar P. P., & West, R. (1998). *The Chemistry of Organic Silicon Compounds* (Zvi Rappoport & Yitzhak Apeloig (Eds.); Vol. 2). John Wiley and Sons.

Gerhard Raabe, & Josef Michl. (1989). *The Chemistry of Organic Silicon Compounds* (Saul Patai & Zvi Rappoport (Eds.); 1st ed., Vol. 1). John Wiley & Sons.

Ghadwal, R. S., Azhakar, R., Roesky, H. W., Pröpper, K., Dittrich, B., Klein, S., & Frenking, G. (2011). Donor–Acceptor-Stabilized Silicon Analogue of an Acid Anhydride. *Journal of the American Chemical Society*, 133(44), 17552–17555. <https://doi.org/10.1021/ja206702e>

Grev, R. S., Scuseria, G. E., Scheiner, A. C., Schaefer, H. F., & Gordon, M. S. (1988). Relative energies of silaethylene and methylsilylene. *Journal of the American Chemical Society*, 110(22), 7337–7339. <https://doi.org/10.1021/ja00230a010>

Haaf, M., Schmedake, T. A., & West, R. (2000). Stable Silylenes. *Accounts of Chemical Research*, 33(10), 704–714. <https://doi.org/10.1021/ar950192g>

Haaf, M., Schmiedl, A., Schmedake, T. A., Powell, D. R., Millevolte, A. J., Denk, M., & West, R. (1998). Synthesis and Reactivity of a Stable Silylene. *Journal of the American Chemical Society*, 120(49), 12714–12719. <https://doi.org/10.1021/ja9733999>

Hadlington, T. J., Driess, M., & Jones, C. (2018). Low-valent group 14 element hydride chemistry: towards catalysis. *Chemical Society Reviews*, 47(11), 4176–4197. <https://doi.org/10.1039/C7CS00649G>

Hideki Sakurai. (1989). *The Chemistry of Organic Silicon Compounds* (Zvi Rappoport, Yitzhak Apeloig, & Saul Patai (Eds.); Vol. 2). John Wiley & Sons.

Igau, A., Grutzmacher, H., Baceiredo, A., & Bertrand, G. (1988). Analogous .alpha.,.alpha.'-bis-carbenoid, triply bonded species: synthesis of a stable .lambda.3-phosphino carbene-.lambda.5-phosphaacetylene. *Journal of the American Chemical Society*, 110(19), 6463–6466. <https://doi.org/10.1021/ja00227a028>

Ishida, S., Iwamoto, T., & Kira, M. (2009). Isomerization of an Isolable Silylene into a Silene via 1,2-Silyl Migration. *Organometallics*, 28(3), 919–921. <https://doi.org/10.1021/om800692b>

Kira, M. (2012). Bonding and structure of disilenes and related unsaturated group-14 element compounds. *Proceedings of the Japan Academy Series B: Physical and Biological Sciences*, 88(5), 167–191. <https://doi.org/10.2183/pjab.88.167>

Li, J., Stasch, A., Schenk, C., & Jones, C. (2011). Extremely bulky amido-group 14 element chloride complexes: Potential synthons for low oxidation state main group chemistry. *Dalton Transactions*, 40(40), 10448. <https://doi.org/10.1039/c1dt10678c>

- Meltzer, A., Inoue, S., Präsang, C., & Driess, M. (2010). Steering S–H and N–H Bond Activation by a Stable N-Heterocyclic Silylene: Different Addition of H<sub>2</sub>S, NH<sub>3</sub>, and Organoamines on a Silicon(II) Ligand versus Its Si(II)→Ni(CO)<sub>3</sub> Complex. *Journal of the American Chemical Society*, *132*(9), 3038–3046. <https://doi.org/10.1021/ja910305p>
- Mo, Z., Szilvási, T., Zhou, Y., Yao, S., & Driess, M. (2017). An Intramolecular Silylene Borane Capable of Facile Activation of Small Molecules, Including Metal-Free Dehydrogenation of Water. *Angewandte Chemie International Edition*, *56*(13), 3699–3702. <https://doi.org/10.1002/anie.201700625>
- Protchenko, A. V., Birjkumar, K. H., Dange, D., Schwarz, A. D., Vidovic, D., Jones, C., Kaltsoyannis, N., Mountford, P., & Aldridge, S. (2012). A Stable Two-Coordinate Acyclic Silylene. *Journal of the American Chemical Society*, *134*(15), 6500–6503. <https://doi.org/10.1021/ja301042u>
- Rappoport, Z., & Apeloig, Y. (Eds.). (1998). *The Chemistry of Organic Silicon Compounds* (Vol. 2). Wiley. <https://doi.org/10.1002/0470857250>
- Rekken, B. D., Brown, T. M., Fettinger, J. C., Tuononen, H. M., & Power, P. P. (2012). Isolation of a Stable, Acyclic, Two-Coordinate Silylene. *Journal of the American Chemical Society*, *134*(15), 6504–6507. <https://doi.org/10.1021/ja301091v>
- Sakamoto, K., Ogasawara, J., Sakurai, H., & Kira, M. (1997). The First Silatriafulvene Derivative: Generation, Unusually Low Reactivity toward Alcohols, and Isomerization to Silacyclobutadiene. *Journal of the American Chemical Society*, *119*(14), 3405–3406. <https://doi.org/10.1021/ja970083s>
- Schaefer, H. F. (1982). The silicon-carbon double bond: a healthy rivalry between theory and experiment. *Accounts of Chemical Research*, *15*(9), 283–290. <https://doi.org/10.1021/ar00081a003>
- Schriver, G. W., Fink, M. J., & Gordon, M. S. (1987). Ab initio calculations on some C<sub>3</sub>SiH<sub>4</sub> isomers. *Organometallics*, *6*(9), 1977–1984. <https://doi.org/10.1021/om00152a024>
- Segawa, Y., Yamashita, M., & Nozaki, K. (2006). Boryllithium: Isolation, Characterization, and Reactivity as a Boryl Anion. *Science*, *314*(5796), 113–115. <https://doi.org/10.1126/science.1131914>
- Shan, C., Yao, S., & Driess, M. (2020). Where silylene–silicon centres matter in the activation of small molecules. *Chemical Society Reviews*, *49*(18), 6733–6754. <https://doi.org/10.1039/D0CS00815J>
- Sugahara, T., Guo, J., Sasamori, T., Nagase, S., & Tokitoh, N. (2018). Regioselective Cyclotrimerization of Terminal Alkynes Using a Digermyne. *Angewandte Chemie International Edition*, *57*(13), 3499–3503. <https://doi.org/10.1002/anie.201801222>
- Sun, X., Hinz, A., Kucher, H., Gamer, M. T., & Roesky, P. W. (2022). Stereoselective Activation of Small Molecules by a Stable Chiral Silene. *Chemistry – A European Journal*, *28*(55). <https://doi.org/10.1002/chem.202201963>
- Takahashi, M., Sakamoto, K., & Kira, M. (2001). Substituent effects on inversion motion of 4-silatriafulvene derivatives: An ab initio MO study. *International Journal of Quantum Chemistry*, *84*(2), 198–207. <https://doi.org/10.1002/qua.1322>
- Takeaki, I., Kabuto, C., & Kira, M. (1984). The First Stable Cyclotrisilene. *Angew. Chem., Int. Ed. Engl.*, *56*(2), 886–887. <https://doi.org/10.1021/ja983623>

- Tracy L. Morkin, Thomas R. Owens, & William J. Leigh. (2001). *The Chemistry of Organic Silicon Compounds* (Zvi Rappoport & Yitzhak Apeloig (Eds.); 1st ed., Vol. 3). John Wiley & Sons.
- Veszprémi, T., Takahashi, M., Ogasawara, J., Sakamoto, K., & Kira, M. (1998). An ab Initio MO Study of Structure and Reactivity of 4-Silatriafulvene. *Journal of the American Chemical Society*, *120*(10), 2408–2414. <https://doi.org/10.1021/ja971925q>
- Weetman, C., & Inoue, S. (2018). The Road Travelled: After Main- Group Elements as Transition Metals. *ChemCatChem*, *10*(19), 4213–4228. <https://doi.org/10.1002/cctc.201800963>
- West, R., & Denk, M. (1996). Stable silylenes: synthesis, structure, reactions. *Pure and Applied Chemistry*, *68*(4), 785–788. <https://doi.org/10.1351/pac199668040785>
- Yao, S., Brym, M., van Wüllen, C., & Driess, M. (2007). From a Stable Silylene to a Mixed- Valent Disiloxane and an Isolable Silaformamide–Borane Complex with Considerable Silicon–Oxygen Double- Bond Character. *Angewandte Chemie*, *119*(22), 4237–4240. <https://doi.org/10.1002/ange.200700398>
- Zborovsky, L., Kostenko, A., Bravo- Zhivotovskii, D., & Apeloig, Y. (2019). Mechanism of the Thermal Z⇌E Isomerization of a Stable Silene; Experiment and Theory. *Angewandte Chemie*, *131*(41), 14666–14670. <https://doi.org/10.1002/ange.201907864>
- Zettlitzer, M., Dieck, H. tom, & Stamp, L. (1986). Reaktionen N-silylierter Endiamine, I Übergangsmetallkomplexe von 1,3-Diaza-2-sila-4-cyclopentenen / Reactions of N-Silated Endiamines, I Transition Metal Complexes of 1,3-Diaza-2-sila-4-cyclopentenes. *Zeitschrift Für Naturforschung B*, *41*(10), 1230–1238. <https://doi.org/10.1515/znb-1986-1008>
- Zhao, L., Huang, F., Lu, G., Wang, Z.-X., & Schleyer, P. von R. (2012). Why the Mechanisms of Digermyne and Distannyne Reactions with H<sub>2</sub> Differ So Greatly. *Journal of the American Chemical Society*, *134*(21), 8856–8868. <https://doi.org/10.1021/ja300111q>



# Chapter 4

## Reactions of 1,2,3,3-tetramethyl cyclotrisilene with propylene, phenylacetylene, trimethylsilylacetylene, formaldehyde and benzaldehyde

---

### 4.1 Introduction

Ever since the landmark inventions of silene (Adrian G. Brook et al. 1981) and disilene (West, Fink, and Michl 1981) in 1981, the course of silicon chemistry emphasised on the synthesis of novel unsaturated compounds of silicon. One of the major curiosities was to obtain silicon analogue of cyclopropene; cyclotrisilene ( $\text{Si}_3\text{H}_4$ ), which is remarkably unstable (Al-Rubaiey and Walsh 1994; Becerra and Walsh 1994; Erwin, Ring, and O'Neal 1985; Rogers et al. 1987). Efforts in this direction hit the target as Iwamoto et.al. (1999) achieved a stable solid derivative of the heavily substituted cyclotrisilene for the first time (Figure 4.1) (Takeaki Iwamoto, Chizuko Kabuto, and Mitsuo Kira\* 1999).

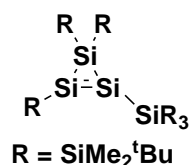
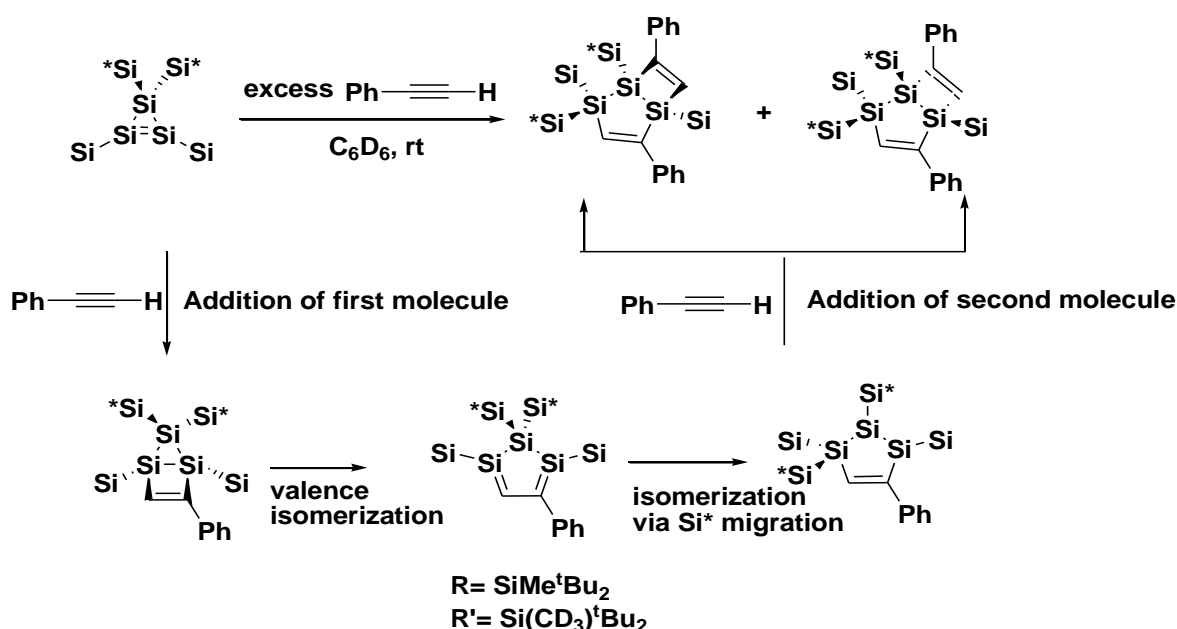


**Figure 4.1** First stable cyclotrisilene synthesised by Iwamoto et.al. (1999)

It is apparent that, the heavy substituents attached to the Si atoms impart kinetic stability to the strained cyclotrisilene ring by suppressing the thermodynamically favoured formation of saturated dimers or oligomers (Fischer and Power 2010; Präsang and Scheschkewitz 2016; Ya. Lee and Sekiguchi 2010). Thenceforth, a fair collection of cyclotrisilenes, brilliantly designed for sterically and electronically balanced stabilisation, were prepared by the exuberant effort of enthusiastic researchers across the globe (Leszczyńska et al. 2012; Lee, Yasuda, and Sekiguchi 2007; Uchiyama et al. 2007; Iwamoto et al. 2000; Ichinohe et al. 1999). Whatever may be the substituents attached, all of the cyclotrisilenes are generally highly reactive; which may be a blessing in disguise, qualifying their use as a synthetic rudiment for wide variety of products.

The interaction of cyclotrisilenes with unsaturated molecules advances primarily in two pathways: The  $\pi$ -addition reactions of unsaturated substrates to the silicon - silicon double bond of the cyclotrisilene in the general [2+2] fashion, generating a pentagonal product bearing no Si - Si double bond. Phenyl acetylene enters [2+2] addition reaction with cyclotrisilene which is basically a  $\pi$ -addition reaction (Tanaka et al. 2011; Lee, Ichinohe, and Sekiguchi 2001; Fukaya, Ichinohe, and Sekiguchi 2000; Lee et al. 2000). The reaction initiates by the  $\pi$ -addition of phenyl acetylene to the C=Si bond in the silacyclo ring, followed by an isomerisation leading to the ring expansion. The pentagonal ring product further isomerises by the migration of a substituent to generate a better stabilised product. This primary pentagonal product undergoes one more [2+2] addition reaction with a fresh molecule of phenyl acetylene, generating the final bicyclic product which can have two conformers (Scheme 4.1) (Lee, Ichinohe, and Sekiguchi 2001).

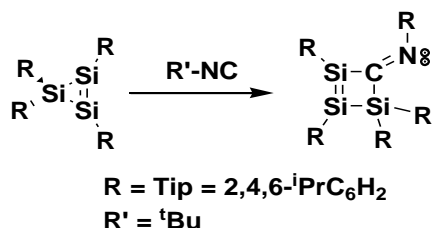


**Scheme 4.1**

Formation of a  $\pi$ -addition product between a cyclotrisilene molecule and an unsaturated reactant

The second type of reaction is the  $\sigma$ -insertion of the substrate into one of the endocyclic silicon - silicon single bonds, resulting in the ring expansion with the formation of a product with a Si - Si double bond (Ohmori et al. 2013; Cowley et al. 2013; Lee, Ichinohe, and Sekiguchi 2001). This type of ring expansion reactions of cyclotrisilene,

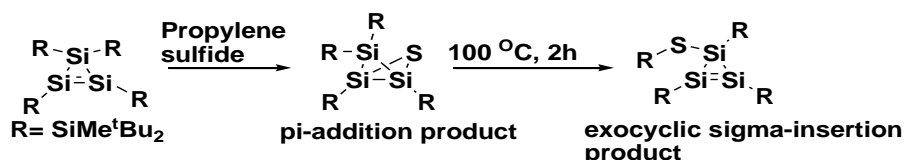
leading to the formation of a four-membered ring product with a Si-Si double bond in the ring, is classified as  $\sigma$ -insertion reaction (H. Zhao et al. 2018). Y. Ohmori et al reported the reactions of alkyl and aryl isocyanides with cyclotrisilenes generating the tetragonal disilenes with an exocyclic imine functionality in potential conjugation with the Si=Si double bond (Scheme 4.2) (Ohmori et al. 2013). In this reaction, the substrate isocyanide breaks a Si-Si  $\sigma$ -bond of the cyclotrisilene molecule and sandwiched itself between the two Si atoms, leaving the Si-Si double bond untouched, generating the four-membered ring  $\sigma$ -insertion product.



**Scheme 4.2**

Formation of an  $\sigma$ -insertion product between a cyclotrisilene molecule and an isocyanide.

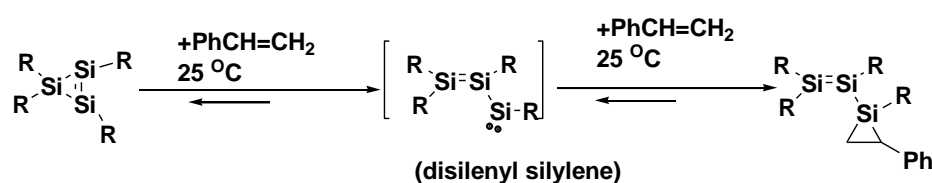
There are reported reactions of a third category, in which the unsaturated reactant find place between a ring Si atom of the cyclotrisilene and its substituent (exocyclic -  $\sigma$  insertion) (Cowley et al. 2013; Ichinohe et al. 1999; Lee, Yasuda, and Sekiguchi 2007; Leszczyńska et al. 2012; Robinson et al. 2015). Only limited examples of reactions of this class are reported with cyclotrisilenes. Insertion of a sulphur atom between one of the cyclic silicon atoms ( $sp^3$  Si atom) of the cyclotrisilene ring and one of the substituents attached to it, observed by Lee et al., is an interesting example (Lee et al. 2015). They found that, when cyclotrisilene molecule with the substituent  $R = \text{SiMe}^t\text{Bu}_2$  is made to react with propylene sulphide, the  $\pi$ -addition product, thiatrisilabicyclo-[1.1.0] butane is obtained as the primary product. When this bicyclic product is heated at  $100^\circ\text{C}$  for two hours, it is isomerised to the S exocyclic  $\sigma$ -inserted product (Scheme 4.3) (Lee et al. 2015).



**Scheme 4.3**

Formation of an exocyclic  $\sigma$ -insertion product between a cyclotrisilene molecule and an unsaturated reactant.

Even though the carbon analogues of the cyclotrisilene readily undergo ring opening reactions, it is not common with the silicon counterpart (Lee, Yasuda, and Sekiguchi 2007). However, the reaction between cyclotrisilene, substituted with  $R = \text{Tip} = 2,4,6\text{-}i\text{Pr}_3\text{C}_6\text{H}_2$  and styrene (phenylethene) even at room temperature, produced a momentous outcome: disilyl-substituted silirane is obtained as an orange powder in good yield (Abersfelder and Scheschkewitz 2008; Lee, Yasuda, and Sekiguchi 2007; Rodriguez et al. 2011; Wendel et al. 2017; H. Zhao et al. 2018). Zhao H. et al., proposed a mechanistic course for this reaction involving the intermediary of a disilyl silylene; which is the result of the ring opening of the cyclotrisilene (H. Zhao et al. 2018).



**Scheme 4.4**

Formation of disilyl silylene (intermediate) between a cyclotrisilene molecule and an unsaturated reactant

Therefore, one can expect four distinct interplays between an unsaturated reagent and cyclotrisilenes on their encounter (H. Zhao et al. 2018). Even though the products formed in the first three types reactions are not totally rare, the product evolved from the ring opening of cyclotrisilene is a fascinating one. It is an acyclic bifunctional entity with three Si atoms, carrying a silicon - silicon double bond and a lone pair on the third Si atom: a disilyl silylene (Ohmori et al. 2013; H. Zhao et al. 2018). This silylene, Si analogue of carbene, possess superior potentials in small molecule activation, a property which has got infinite importance in industrial and research areas. Silylenes are found to activate rigorously small molecules, possessing stable non-polar chemical bonds of quiet higher strength such as H<sub>2</sub>, CO<sub>2</sub>, N<sub>2</sub>O, O<sub>2</sub>, H<sub>2</sub>O, CH<sub>4</sub>, C<sub>2</sub>H<sub>4</sub> and NH<sub>3</sub> (Chu and Nikonov 2018; Fischer and Power 2010; Hadlington, Driess, and Jones 2018; Shan, Yao, and Driess 2020; Weetman and Inoue 2018; Yadav, Saha, and Sen 2016).

## 4.2 Objectives

- Computational investigation of possible interactions of 1,2,3,3-tetramethyl cyclotrisilene,  $c\text{-Si}_3\text{Me}_4$  (**I**) with five substrates possessing multiple bonds is conducted.
- The substrates employed are phenylacetylene ( $\text{C}_6\text{H}_5\text{-C}\equiv\text{CH}$ ; **R1**), propylene ( $\text{CH}_3\text{-C}\equiv\text{CH}$ ; **R2**), trimethylsilylacetylene ( $((\text{CH}_3)_3\text{Si-C}\equiv\text{CH}$ ; **R3**), benzaldehyde ( $\text{C}_6\text{H}_5\text{-HC=O}$ ; **R'1**) and formaldehyde ( $\text{H}_2\text{C=O}$ ; **R'2**).
- Four reaction path ways;  $\pi$ -addition,  $\sigma$ -insertion, ring opening and exocyclic  $\sigma$ -insertion were explored and the energetics and mechanisms were studied systematically.

## 4.3 Computational Methods

All calculations were carried out at the M06-2X/6-311G(d,p) level of density functional theory using the Gaussian 16 suite of programs. Transition states were optimized by using the Synchronous Transit-Guided Quasi-Newton (STQN) method implemented in Gaussian 16. Minima were ascertained by the IR frequency analysis, and the saddle points were characterized by a single imaginary frequency. The solvent effects (benzene) were accounted by single point calculation at SMD-M06-2X/6-311+G(d,p) level and the single point energy was corrected by adding the thermal correction to Gibbs free energy obtained from the gas phase calculation (at 298.15 K).

## 4.4 Results and Discussion

We have carried out a detailed computational analysis of the reaction between substituted cyclotrisilene ( $c\text{-Si}_3\text{R}_4$ ) and substrates carrying multiple bonds. As a model system for cyclotrisilene, 1,2,3,3-tetramethyl cyclotrisilene,  $c\text{-Si}_3\text{Me}_4$  (**I**) is chosen and the substrates are phenylacetylene ( $\text{C}_6\text{H}_5\text{-C}\equiv\text{CH}$ ; **R1**), propylene ( $\text{CH}_3\text{-C}\equiv\text{CH}$ ; **R2**), trimethylsilylacetylene ( $((\text{CH}_3)_3\text{Si-C}\equiv\text{CH}$ ; **R3**), benzaldehyde ( $\text{C}_6\text{H}_5\text{-HC=O}$ ; **R'1**) and formaldehyde ( $\text{H}_2\text{C=O}$ ; **R'2**).

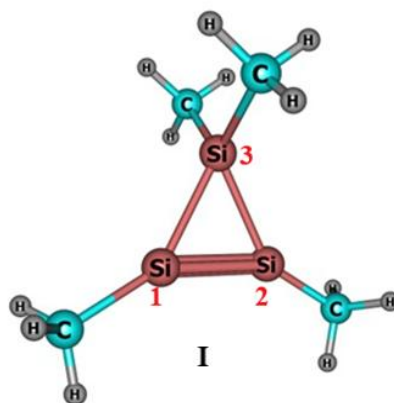
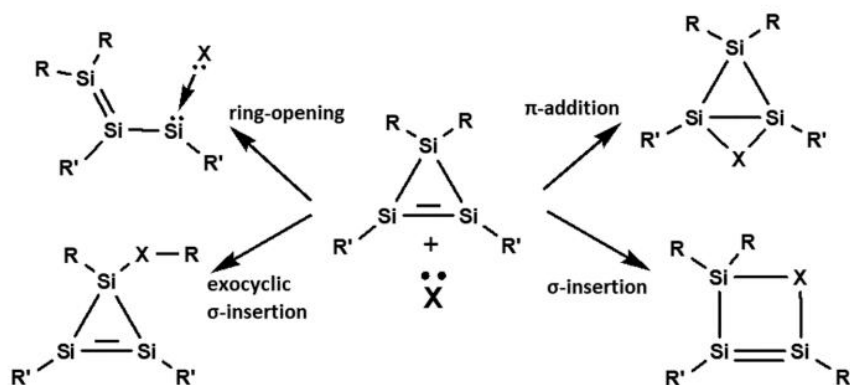


**Figure 4.2** 1,2,3,3-tetramethyl cyclotrisilene ( $c\text{-Si}_3\text{Me}_4$ ; **I**)

It is evident that, the reactants bear two different functional groups carrying multiple bonds (alkynyl or carbonyl) and substituents attached to the functional groups are phenyl, methyl or trimethylsilyl groups. This allows the following explorations on the reactions:

1. To investigate the difference in the interaction between **I** and the functional groups ( $\text{C}\equiv\text{CH}$  /  $\text{-C=O}$ ).
2. To analyse the difference in the effect of the substituents attached to the functional group on the reactions ( $\text{-Ph}$  /  $\text{-Me}$  /  $\text{-TMS}$ ).

We have scrutinised the reaction profiles of all the four possible pathways viz.,  $\pi$ -addition,  $\sigma$  – insertion, exocyclic  $\sigma$  – insertion and ring opening reactions of **I** with the substrates **R1**, **R2**, **R3**, **R'1** & **R'2** to understand the energetics and mechanisms (Scheme 4.5).



**Scheme 4.5**

Four possible reaction pathways of cyclotrisilene

## 4.4.1 Reaction pathways of $\text{c-Si}_3\text{Me}_4$ (**I**) with $\text{C}_6\text{H}_5\text{-C}\equiv\text{CH}$ (**R1**)

### 4.4.1.1 $\pi$ -addition

A direct  $2\pi + 2\pi$  addition pathway forming a four membered ring could not be located, but a two-step reaction pathway has been identified for the reaction between the acetylenic group of **R1** and the silenyl part of **I**. The Intermediates and transitions states located are presented in Figure 4.3. The three Si atoms of **I** are denoted as  $\text{Si}_{(1)}$ ,  $\text{Si}_{(2)}$  and  $\text{Si}_{(3)}$ .

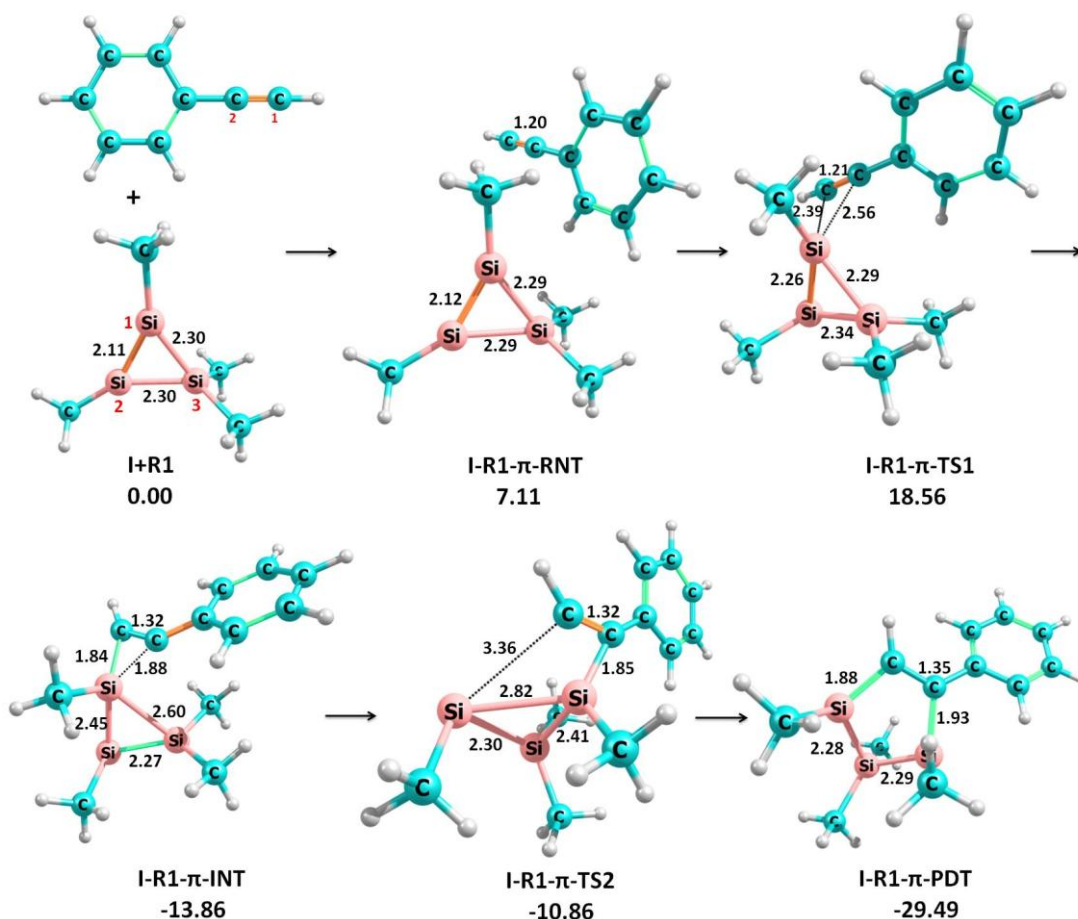


**Figure 4.3** Intermediates and transitions states involved in the  $\pi$ -addition pathway of **I** and **R1**. Relative free energies are given in kcal/mol and bond lengths in Å

The reaction initiates with the formation of a reactant dispersion complex having an appropriate orientation, between **I** and **R1** (I-R1- $\pi$ -RNT), bearing relative energy 7.11 kcal/mol. This dispersion complex is proceeded to a transition state I-R1- $\pi$ -TS1, in which both the methyl groups of silenyl moiety (attached to  $\text{Si}_{(1)}$  and  $\text{Si}_{(2)}$ ) moves out from the cyclotrisilene plane and the  $\pi$ -electron cloud of the alkyne interacts with one of the unsaturated Si atoms ( $\text{Si}_{(1)}$ ). Among the acetylenic carbon atoms, the  $\text{C}_{(1)}$  keeps a closer approach to the  $\text{Si}_{(1)}$  (2.39 Å), as it is more electron rich than the one connected to the electron withdrawing phenyl group. Formation of this transition state is associated with a

considerable weakening of the  $\text{Si}_{(1)}=\text{Si}_{(2)}$  double bonds indicated by the elongation of the bond distance from 2.12 Å to 2.26 Å.

**I-R1- $\pi$ -TS1** progressed to the intermediate **I-R1- $\pi$ -INT**. Strong bonding interaction between the acetylene group of **R1** and  $\text{Si}_{(1)}$  ( $r_{\text{C-Si}_{(1)}} = 1.84 \text{ \AA}$  and  $1.88 \text{ \AA}$ ) of **I** in **I-R1- $\pi$ -INT** lead to the weakening of both  $\text{Si}_{(1)}-\text{Si}_{(2)}$  double bond ( $r_{\text{Si}_{(1)}=\text{Si}_{(2)}} = 2.45 \text{ \AA}$ ) and  $\text{Si}_{(1)}-\text{Si}_{(3)}$  single bond ( $r_{\text{Si}_{(1)}-\text{Si}_{(3)}} = 2.60 \text{ \AA}$ ). The stress release of the system associated with the loosening of the bonds of the cyclotrisilene ring and the energy of formation of the  $\text{Si}_{(1)}-\text{C}_{(1)}$  bond made this step considerably exoergic as evidenced by the relative energy of **I-R1- $\pi$ -INT** (-13.86 kcal/mol). The activation energy required for the formation of **I-R1- $\pi$ -INT1** is 18.56 kcal/mol. **I-R1- $\pi$ -INT** advanced to the second transition state, **I-R1- $\pi$ -TS2**. At this stage of the reaction, the addition of alkynyl group to the  $\text{Si}_{(1)}-\text{Si}_{(2)}$  bond occurs, leading to the formation of the final product is realised. In **I-R1- $\pi$ -TS2**,  $\text{Si}_{(1)}-\text{Si}_{(2)}$  double bond is fully broken ( $r_{\text{Si}_{(1)}-\text{Si}_{(2)}} = 2.83 \text{ \AA}$ ) and the product, **I-R1- $\pi$ -PDT** located is a five membered ring ( $r_{\text{Si}_{(1)}-\text{Si}_{(2)}} = 2.72 \text{ \AA}$ ), consistent with the experimental observations (Lee et al. 2000; Ya. Lee et al. 2001). The Si-Si bond length in the five membered ring is less than the normal Si-Si single bond length ( $r_{\text{Si}_{(1)}-\text{Si}_{(3)}} = 2.28 \text{ \AA}$   $r_{\text{Si}_{(2)}-\text{Si}_{(3)}} = 2.29 \text{ \AA}$ ). The activation barrier for the second step is 3.00 kcal/mol and the overall reaction is exoergic by 29.49 kcal/mol. The free energy changes associated with the reaction profile suggests the thermodynamic and kinetic feasibility of the reaction at ordinary laboratory conditions.

#### 4.4.1.2 $\sigma$ -insertion

The Intermediates and transition states located for  $\sigma$ -insertion reaction between **I** and **R1** is represented in Figure 4.4.



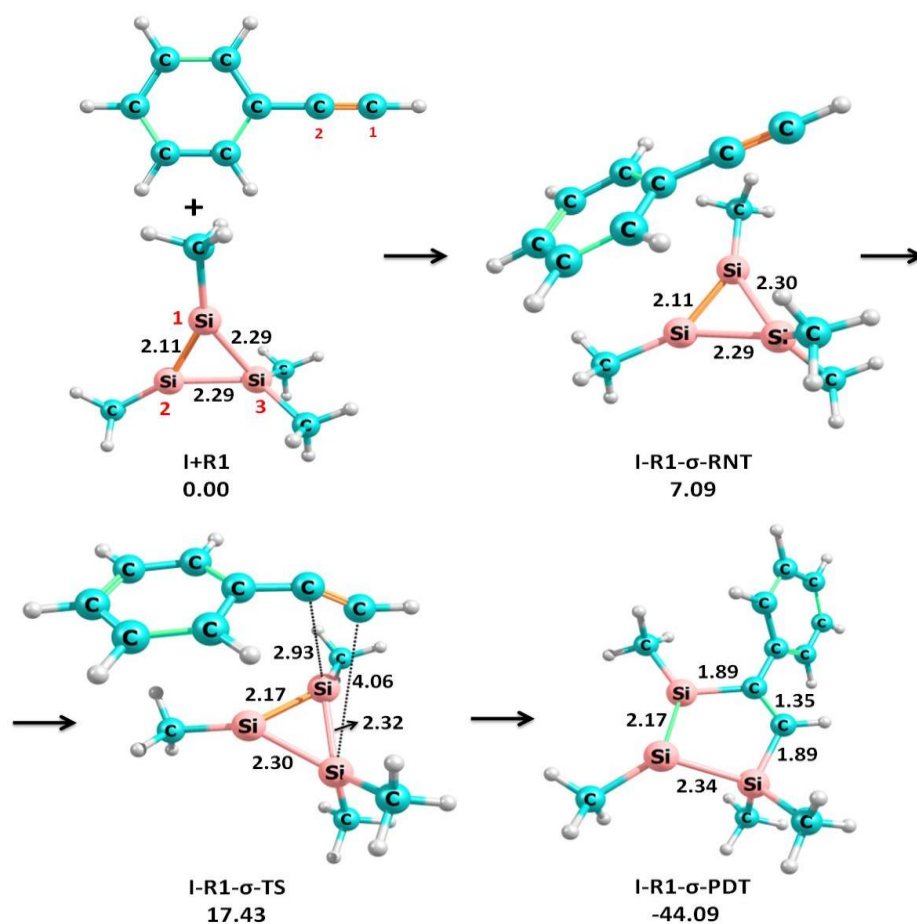


**Figure 4.4** Intermediates and transition states involved in the  $\sigma$ -insertion pathway of **I** + **R1**. Relative free energies are given in kcal/mol and bond lengths in Å

It is reported that the angular strain in the cyclotrisilene molecule made it susceptible to rather unexpected reactions such as  $\sigma$ -insertion of a substrate between the ring Si atoms. In the present investigation, the  $\sigma$ -insertion of acetylenic group of **R1** into the  $Si_{(1)}-Si_{(3)}$  single bond of **I** is found to be a single step process. This insertion is initiated by the formation of the reactant dispersion complex, **I-R1- $\sigma$ -RNT** possessing a relative energy 7.09 kcal/mol. **I-R1- $\sigma$ -RNT** proceeds to a transition state, **I-R1- $\sigma$ -TS** in which  $Si_{(1)}-Si_{(3)}$  bond is slightly elongated ( $r_{Si_{(1)}-Si_{(3)}} = 2.32$  Å) and the acetylenic group is oriented along  $Si_{(1)}-Si_{(3)}$  bond. **I-R1- $\sigma$ -TS** is transformed to the final product **I-R1- $\sigma$ -PDT** which is pentagonal shaped. The activation barrier for the  $\sigma$ -insertion is 17.4 kcal/mol and the reaction is exoergic by 44.09 kcal/mol. In, **I-R1- $\sigma$ -PDT**, the  $Si_{(1)}-Si_{(2)}$  bond keeps the double bond nature ( $r_{Si_{(1)}-Si_{(2)}} = 2.17$  Å) and  $Si_{(2)}-Si_{(3)}$  bond is a normal single bond ( $r_{Si_{(2)}-Si_{(3)}} = 2.34$  Å). High exoergic value and a moderate activation barrier can be attributed to the release of strain associated with the three membered cyclotrisilene ring along with the stability associated with the well-defined structure of the product.

### 4.4.1.3 Ring opening

The intermediates and transitions states located for the ring opening reaction between **I** and **R1** is represented in Figure 4.5

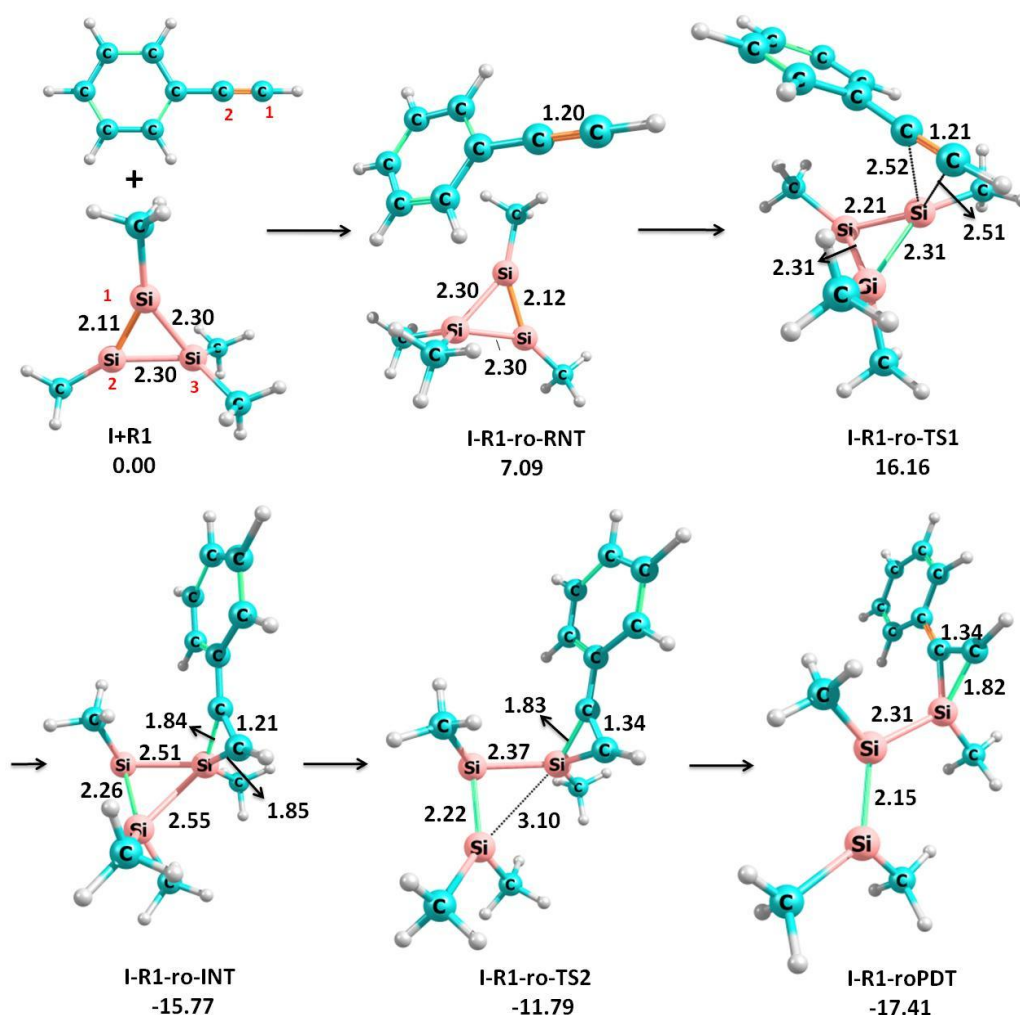


**Figure 4.5** Intermediates and transitions states involved in the ring opening reaction pathway of **I**+ **R1**. Relative free energies are given in kcal/mol and bond lengths in Å

The course of the ring opening reaction between **I** and **R1** is very much similar to that of  $\pi$ -addition reaction (Figure 4.3). The initially formed reactant dispersion complex (**I-R1-ro-RNT**) with relative energy 7.09 kcal/mol led to the transition state (**I-R1-ro-TS1**), which corresponds to the attack on a tricoordinate Si atom ( $\text{Si}_{(1)}$ ) of the trisilene ring by the  $\pi$ -electron cloud of the acetylene group. In the intermediate **I-R1-ro-INT1**, the acetylenic group strongly binds to  $\text{Si}_{(1)}$  which lead to the elongation of  $\text{Si}_{(1)}\text{-Si}_{(2)}$  and  $\text{Si}_{(1)}\text{-Si}_{(3)}$  bonds. The formation of the intermediate **I-R1-ro-INT1** is exoergic by 15.77 kcal/mol, and the activation barrier is 16.16 kcal/mol. The complete cleavage of  $\text{Si}_{(1)}\text{-Si}_{(3)}$  occurs in the transition state **I-R1-ro-TS2**, leading to the ring-opened product **I-R1-ro-PDT**. The activation barrier is 3.98 kcal/mol, and the overall reaction is exoergic by 17.41 kcal/mol. The ring-opened product

represents a disilene ( $r\text{Si}_{(2)}\text{-Si}_{(3)} = 2.149 \text{ \AA}$ ) with a silylene moiety stabilized by the coordination of acetylenic group.

#### 4.4.1.4 Exocyclic sigma insertion

The Intermediates and transitions states located for the exocyclic  $\sigma$ -insertion reaction between **I** and **R1** is represented in Figure 4.6

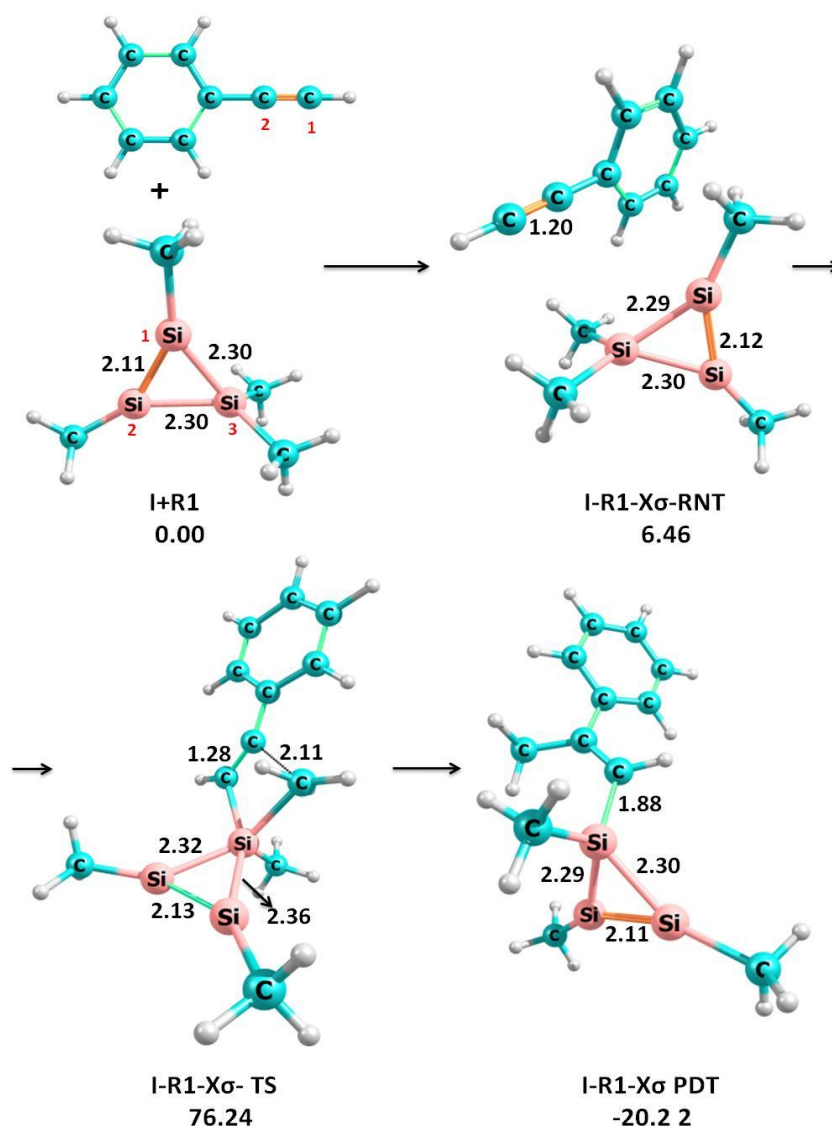


**Figure 4.6** Intermediates and transitions states involved in the exocyclic  $\sigma$ -insertion reaction pathway of **I** + **R1**. Relative free energies are given in kcal/mol and bond lengths in Å

In the exocyclic  $\sigma$ -insertion, the acetylene group of **R1** inserts into the bond between  $\text{sp}^3$  Si atom of the cyclotrisilene ring and a substituent ( $\text{Si}_{(3)}\text{-CH}_3$ ) of **I**. The initially formed reactant dispersion complex **I-R1-x $\sigma$ -RNT** has a relative energy 6.46kcal/mol. The reactant complex advanced to an activated complex **I-R1-x $\sigma$ -TS1** which can directly transform to the

product, **I-R1-x $\sigma$ -PDT**. The overall reaction being exoergic by 20.2 kcal/mol, the reaction is kinetically impossible at ambient conditions due to a high activation barrier of 76.2 kcal/mol.

Free energy profile diagrams of the four reaction pathways between **I** and **R1** are given in Figure 4.7

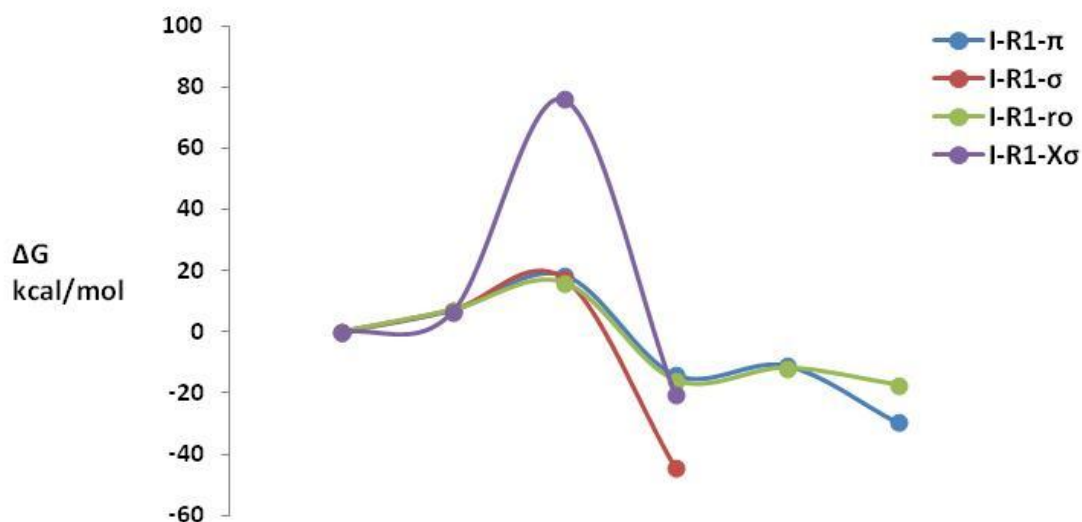


**Figure 4.7** Comparative free energy profile diagram for the different reaction pathways between **I** + **R1**

Out of the four reaction pathways between **I** and **R1** demonstrated above, the  $\sigma$ -insertion reaction and the exocyclic  $\sigma$ -insertion reactions are direct conversion of the reactants to products. The other two; the  $\pi$ -addition reaction and the ring opening reaction, are found to be two-step processes. Even though, both  $\pi$ -addition and  $\sigma$ -insertion reactions yield similar pentagonal products, the one that is generated in the former is slightly less stable. This is due to the ambiguous partial double bonds existing between the three adjacent silicon atoms of the  $\pi$ -addition product. Energetics of the four possible reaction pathways between **I** and **R1** suggest that the  $\pi$ -addition,  $\sigma$ -insertion, and ring opening reactions are feasible under normal conditions whereas the exocyclic  $\sigma$ -insertion is kinetically not feasible. Among the  $\pi$ -addition,  $\sigma$ -insertion, and ring-opening reactions,  $\sigma$ -insertion has a better feasibility due to its higher exoergic nature. Further, the existence of three competitive pathways suggests that the reaction can be made to proceed through the desired pathway by fine-tuning the steric and electronic nature of cyclotrisilene and the substrate.

## 4.4.2 Reaction pathways of $c\text{-Si}_3\text{Me}_4(\mathbf{I})$ and $\text{CH}_3\text{-C}\equiv\text{CH}(\mathbf{R2})$

### 4.4.2.1 $\pi$ -addition

As observed with  $\mathbf{I}$  and  $\mathbf{R1}$ , a direct  $2\pi + 2\pi$  addition pathway, generating a four membered ring addition product could not be located in this case also. Instead, a two step reaction pathway has been identified for the  $\pi$ -addition reaction between the acetylenic group of  $\mathbf{R2}$  and the silenyl part of  $\mathbf{I}$ . The intermediates and transitions states located are presented in Figure 4.8

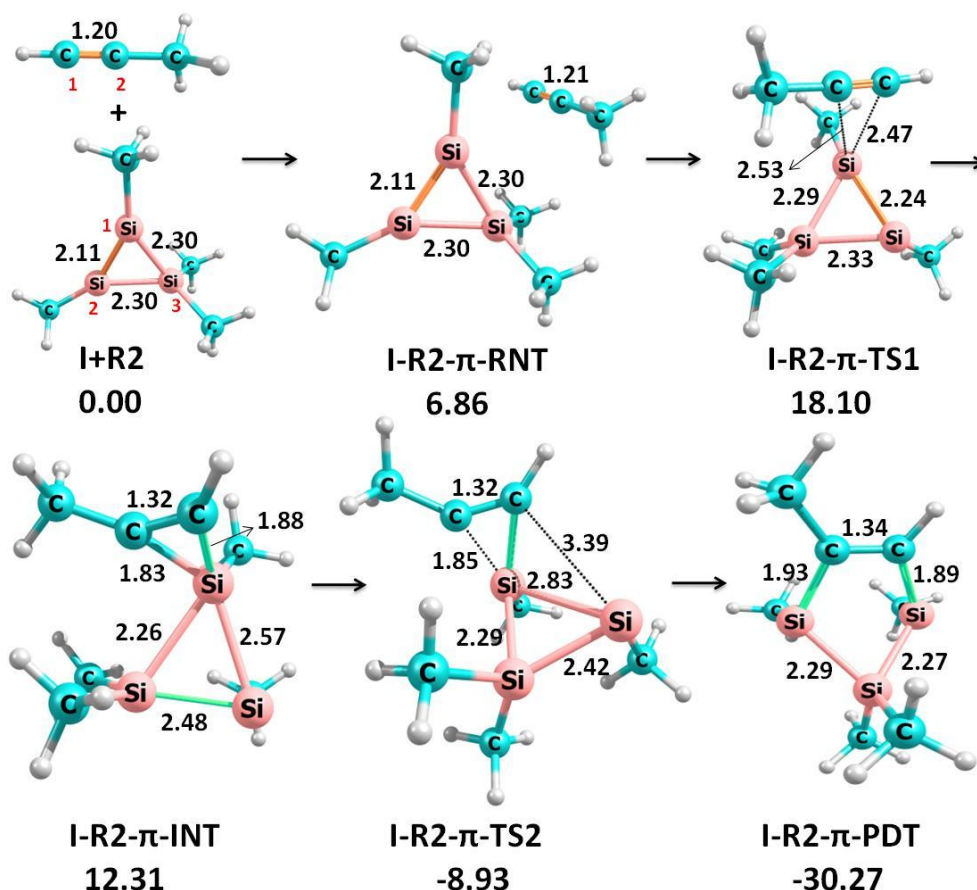


**Figure 4.8** Intermediates and transitions states involved in the  $\pi$ -addition pathway of  $\mathbf{I} + \mathbf{R2}$ . Relative free energies are given in kcal/mol and bond lengths in Å.

The  $\pi$ -addition reaction between  $\mathbf{I}$  and  $\mathbf{R2}$  commenced by the formation of a reactant complex  $\mathbf{I-R2-}\pi\text{-RNT}$  with a relative energy 6.86 kcal/mol which proceeds to the formation of an intermediate  $\mathbf{I-R2-}\pi\text{-INT}$  (12.31 kcal/mol), via the transition state  $\mathbf{I-R2-}\pi\text{-TS1}$ . In  $\mathbf{I-R2-}\pi\text{-INT}$ , the acetylenic group is bonded to  $\text{Si}_{(1)}$  and the necessary electron density being made available from the trisilene ring by the elongation of the Si-Si bonds ( $r_{\text{Si}_{(1)}\text{-Si}_{(2)}} = 2.57$  Å,  $r_{\text{Si}_{(2)}\text{-Si}_{(3)}} = 2.48$  Å). The activation energy required for the formation of  $\mathbf{I-R2-}\pi\text{-INT}$  is 18.10 kcal/mol.



The reaction is advanced further from **I-R2- $\pi$ -INT** to the new activated complex **I-R2- $\pi$ -TS2**, which corresponds to the addition of acetylenic group to Si<sub>(1)</sub>-Si<sub>(2)</sub> bond ( $r_{\text{Si}(1)\text{-Si}(2)} = 3.39\text{\AA}$ ). The Si<sub>(1)</sub>-Si<sub>(2)</sub> bond continue its degradation as indicated by the further weakened bond;  $r_{\text{Si}(1)\text{-Si}(2)} = 2.83\text{\AA}$ . The second activated complex is converted to the pentagonal final product, **I-R2- $\pi$ -PDT** with an activation barrier of 21.24 kcal/mol. In **I-R2- $\pi$ -PDT**, both the Si-Si bonds exhibits a partial double bond nature; ( $r_{\text{Si}(1)\text{-Si}(3)} = 2.29\text{\AA}$ ,  $r_{\text{Si}(2)\text{-Si}(3)} = 2.27\text{\AA}$ ). The exoergic value of 30.27 kcal/mol supports the feasibility of the  $\pi$ -addition reaction between **I** and **R2** under ambient conditions.

#### 4.4.2.2 $\sigma$ -insertion

The Intermediates and transitions states located for the  $\sigma$ -insertion reaction between **I** and **R2** is represented in Figure 4.9

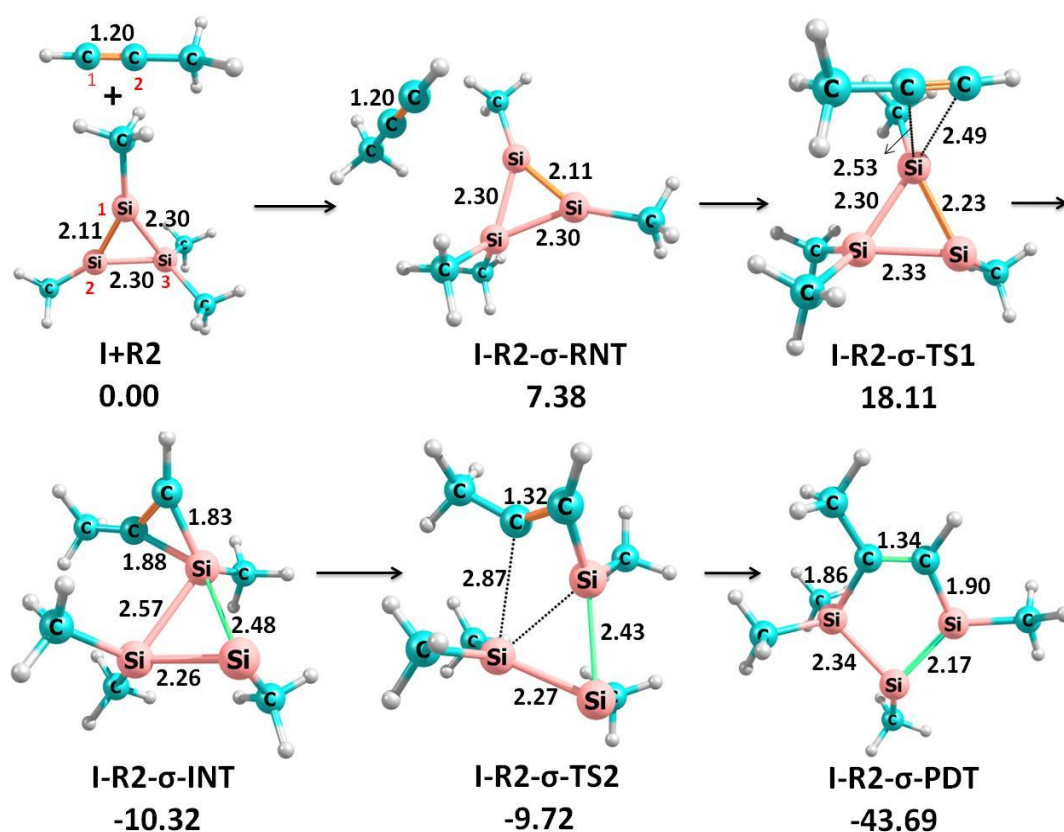


**Figure 4.9** Intermediates and transitions states involved in the  $\sigma$ -insertion pathway of **I** + **R2**. Relative free energies are given in kcal/mol and bond lengths in  $\text{\AA}$

During the  $\sigma$ -insertion reaction between **I** and **R2**, the initially formed reaction complex **I-R2- $\sigma$ -RNT**, with relative energy 7.38 kcal/mol is transformed to an activated complex **I-R2- $\sigma$ -TS1**. The activated complex is characterized by a weakened Si<sub>(1)</sub>-Si<sub>(2)</sub> double bond ( $r_{\text{Si}(1)\text{-Si}(2)} = 2.33\text{\AA}$ ) and a strong interaction-buildup between the

acetylenic carbon atoms of **R2** with the tricoordinate Si<sub>(1)</sub> of **I** ( $r_{\text{Si}_{(1)}-\text{C}_{(1)}} = 2.49 \text{ \AA}$ ,  $r_{\text{Si}_{(1)}-\text{C}_{(2)}} = 2.53 \text{ \AA}$ ). The transition state **I-R2- $\sigma$ -TS1** is advanced to the intermediate **I-R2- $\sigma$ -INT**, with a noticeably low relative energy -10.32 kcal/mol. The activation energy required for the formation of **I-R2- $\sigma$ -INT** is 18.11 kcal/mol. The downturn of the energy in the course of the reaction during the formation of the **I-R2- $\sigma$ -INT** is principally due the relaxation in the ring strain of the cyclotrisilene moiety in it, as is evidenced from the extended bond distances ( $r_{\text{Si}_{(1)}-\text{Si}_{(2)}} = 2.48 \text{ \AA}$ ,  $r_{\text{Si}_{(1)}-\text{Si}_{(3)}} = 2.57 \text{ \AA}$ ). The partial double bond nature of the Si<sub>(2)</sub>-Si<sub>(3)</sub> linkage ( $r_{\text{Si}_{(2)}-\text{Si}_{(3)}} = 2.26 \text{ \AA}$ ) and the linkages of Si<sub>(1)</sub> with carbon atoms satisfies the valency requirement of the trisilene ring of **I-R2- $\sigma$ -INT**.

The intermediate, **I-R2- $\sigma$ -INT** is progressed to the second transition state, **I-R2- $\sigma$ -TS2** in which the carbon nucleus of **R2** changed its linkage from Si<sub>(1)</sub> to Si<sub>(3)</sub> of **I** ( $r_{\text{Si}_{(3)}-\text{C}} = 2.87 \text{ \AA}$ ) and progressed to the pentagonal shaped product, through an exoergic process (33.37 kcal/mol) the activation energy is only 0.60 kcal/mol. The low activation energy and the high exoergicity of the  $\sigma$ -insertion reaction (43.69 kcal/mol) between **I** and **R2** suggests that, it is achievable under ambient conditions.

#### 4.4.2.3 Ring opening

The intermediates and transition states located for the ring opening reaction between **I** and **R2** is represented in Figure 4.10

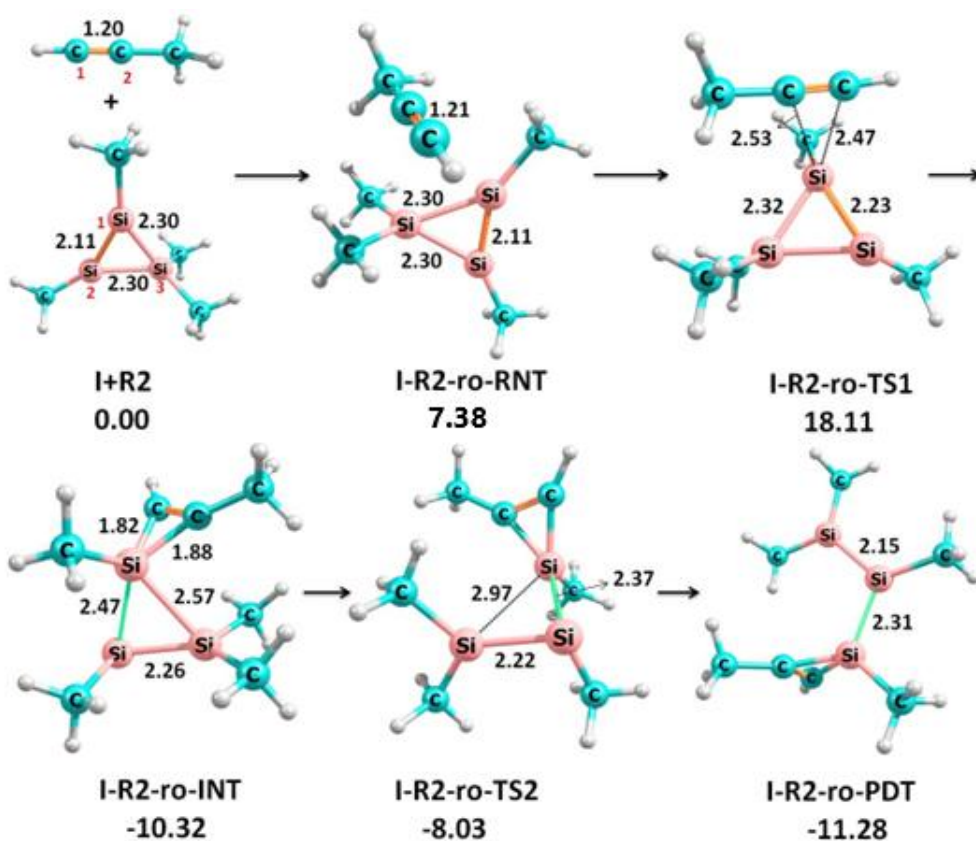


**Figure 4.10** Intermediates and transition states involved in the ring opening pathway of **I** + **R2**. Relative free energies are given in kcal/mol and bond lengths in Å.

The ring opening reaction between **I** and **R2** follows a mechanistic pathway exactly same as that of the  $\sigma$ -insertion reaction between the two up to the formation of the intermediate **I-R2-ro-INT** (**I-R2-ro-INT** is labeled as **I-R2- $\sigma$ -INT** in  $\sigma$ -insertion reaction).

**I-R2- $\sigma$ -INT** progressed to the second transition state **I-R2-ro-TS2**, in which the  $\text{Si}_{(1)}\text{-Si}_{(3)}$  bond loosened to a significant extent ( $r_{\text{Si}_{(1)}\text{-Si}_{(3)}} = 2.97 \text{ \AA}$ ) and the  $\text{Si}_{(2)}\text{-Si}_{(3)}$  bond transformed to a double bond ( $r_{\text{Si}_{(2)}\text{-Si}_{(3)}} = 2.22 \text{ \AA}$ ). The completion of the  $\text{Si}_{(1)}\text{-Si}_{(3)}$  bond cleavage resulted in the ring-opened product. The activation barrier is 2.29 kcal/mol, and the overall reaction is exoergic by 11.28 kcal/mol. The low activation energy and the exoergic nature of the ring opening reaction between **I** and **R2** indicate that it is achievable under ambient conditions.



#### 4.4.2.4 Exocyclic $\sigma$ -insertion

The Intermediates and transitions states located for the exocyclic  $\sigma$ -insertion reaction between **I** and **R2** is represented in Figure 4.11

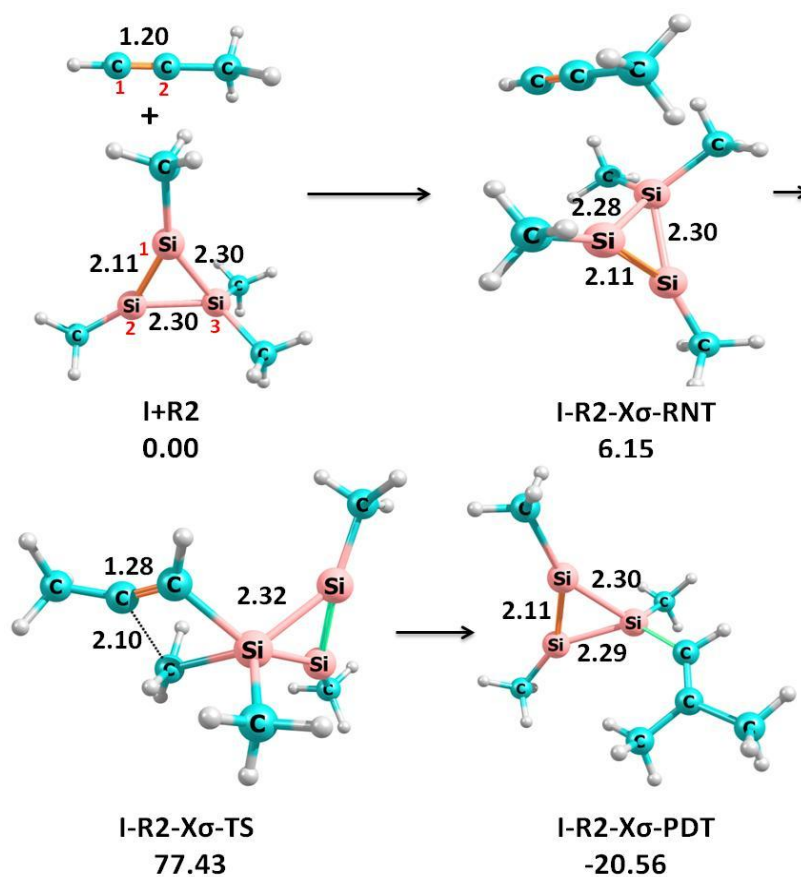


**Figure 4.11** Intermediates and transitions states involved in the exocyclic  $\sigma$ -insertion pathway of **I** + **R2**. Relative free energies are given in kcal/mol and bond lengths in Å.

In the exocyclic  $\sigma$ -insertion, the acetylenic part of **R2** inserts into the bond between the  $sp^3$  Si atom and one of the substituents ( $Si_{(3)}-CH_3$ ) of **I**. The initially formed reactant complex **I-R2-x $\sigma$ -RNT** has a relative energy 6.15 kcal/mol. The reactant complex progressed to activated complex **I-R2-x $\sigma$ -TS** which can directly transform to the product **I-R2-x $\sigma$ -PDT**. Despite the overall reaction being exoergic by 20.56 kcal/mol, the reaction is kinetically impossible at ambient conditions due to a high activation barrier of 77.43 kcal/mol.

Free energy profile diagrams of the four reaction pathways between **I** and **R2** are given in Figure 4.12

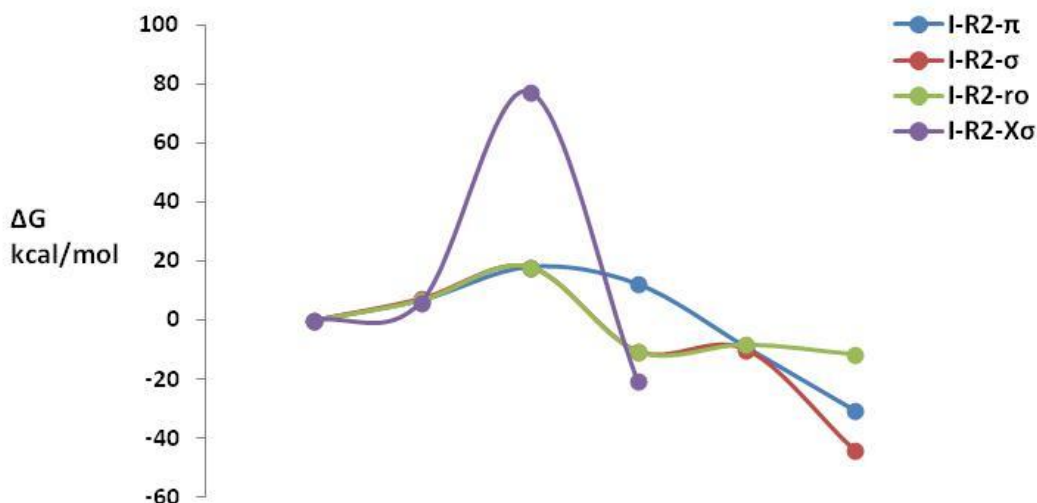


**Figure 4.12** Comparative free energy profile diagram for the different reaction pathways between **I** + **R2**

Out of the four reaction pathways between **I** and **R2** demonstrated above, all except the exocyclic  $\sigma$ -insertion reaction are two-step processes. The exocyclic  $\sigma$ -insertion reaction is a direct single-step process. Even though, both  $\pi$ -addition and  $\sigma$ -insertion reactions yield similar pentagonal products, the one that is generated in the former is less stable (-30.29 and -43.69 kcal/mol respectively). This is due to the partial double bonds existing between the silicon atoms of the  $\pi$ -addition product. A perusal of the energetics of the four reaction pathways between **I** and **R2** suggests that the three pathways, viz.,  $\pi$ -addition,  $\sigma$ -insertion, and ring-opening reactions, are competitive, with a slight advantage to the  $\sigma$ -insertion reaction.

### 4.4.3 Reaction pathways of **c-Si<sub>3</sub>Me<sub>4</sub> (I)** with **(CH<sub>3</sub>)<sub>3</sub>Si-C $\equiv$ CH(R3)**

#### 4.4.3.1. $\pi$ -addition

A two-step reaction pathway has been identified for the  $\pi$ -addition reaction between the acetylenic group of **R3** and the silenyl part of **I**. The intermediates and transition states located are presented in Figure 4.13.

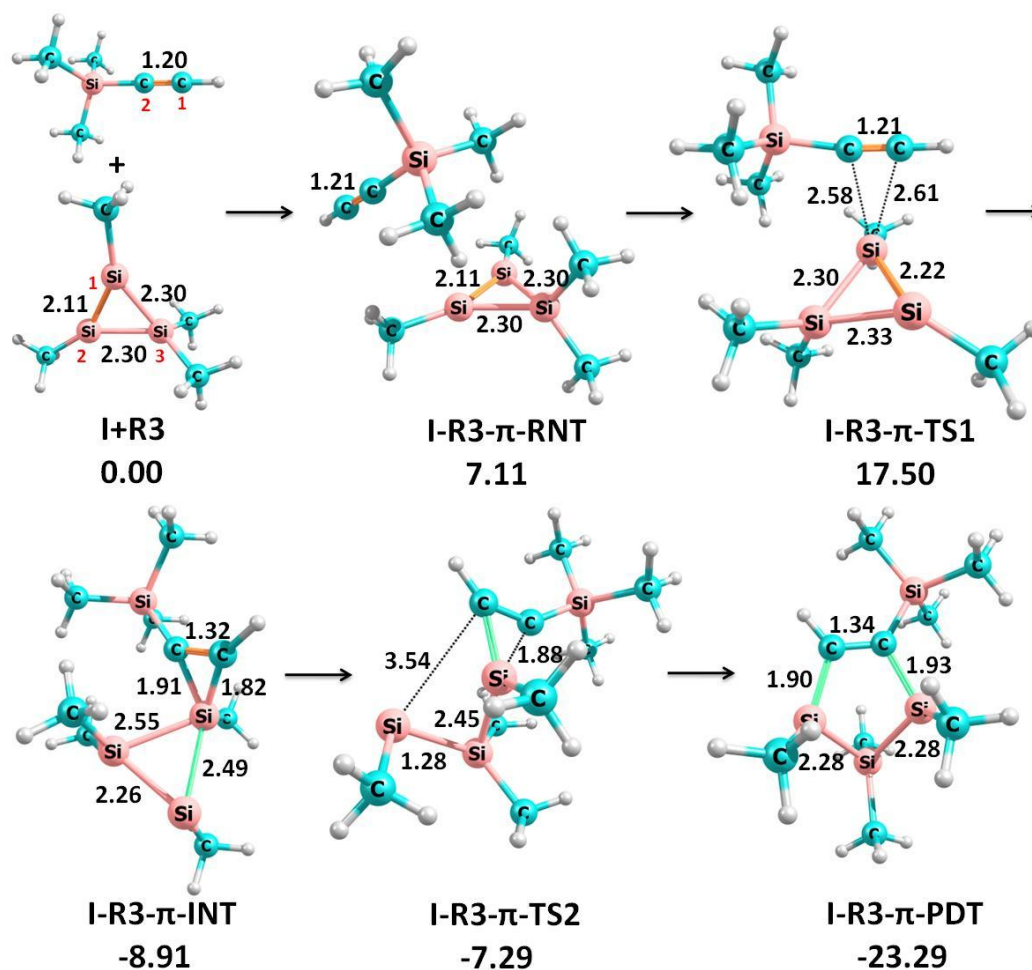


**Figure 4.13** Intermediates and transitions states involved in the  $\pi$ -addition pathway of **I** + **R3**. Relative free energies are given in kcal/mol and bond lengths in Å.

At the onset of the reaction, a reactant dispersion complex is formed between **I** and **R3** (**I-R3- $\pi$ -RNT**) with relative energy 7.11 kcal/mol. The dispersion complex is advanced to the formation of a transition state **I-R3- $\pi$ -TS1**, here both methyl groups of silenyl moiety ( $\text{Si}_{(1)}$  and  $\text{Si}_{(2)}$ ) moves out from the cyclotrisilene plane and the  $\pi$ -electron cloud of the alkyne interacts with one of the unsaturated Si atoms ( $\text{Si}_{(1)}$ ). Both of the acetylenic carbon atoms develop almost an equal association with the  $\text{Si}_{(1)}$  ( $r_{\text{Si}_{(1)}-\text{C}_{(1)}} = 2.61 \text{ \AA}$ ,  $r_{\text{Si}_{(1)}-\text{C}_{(2)}} = 2.58 \text{ \AA}$ ) in **I-R3- $\pi$ -TS1**. Formation of **I-R3- $\pi$ -TS1** is associated with a considerable weakening of the  $\text{Si}_{(1)}-\text{Si}_{(2)}$  double bond indicated by the extension of the bond distance from 1.12 Å to 2.22 Å. **I-R3- $\pi$ -TS1** is advanced to an intermediate **I-R3- $\pi$ -INT** (-8.91 kcal/mol). The activation energy required for the formation of **I-R3- $\pi$ -INT** is 17.50 kcal/mol. Strong bonding interaction of the acetylenic group of **R3** with the ring silicon atom  $\text{Si}_{(1)}$  of **I** ( $r_{\text{Si}_{(1)}-\text{C}_{(1)}} = 1.82 \text{ \AA}$ ,  $r_{\text{Si}_{(1)}-\text{C}_{(2)}} = 1.91 \text{ \AA}$ ) in **I-R3- $\pi$ -INT** led to the weakening of both  $\text{Si}_{(1)}-\text{Si}_{(2)}$  double bond ( $r_{\text{Si}_{(1)}-\text{Si}_{(2)}} = 2.49 \text{ \AA}$ ) and  $\text{Si}_{(1)}-\text{Si}_{(3)}$  single bond ( $r_{\text{Si}_{(1)}-\text{Si}_{(3)}} = 2.55 \text{ \AA}$ ). The intermediate, **I-R3- $\pi$ -INT** progressed to the second transition state **I-R3- $\pi$ -TS2**. This stage of the reaction

corresponds to the addition of acetylenic group to  $\text{Si}_{(1)}\text{-Si}_{(2)}$  bond, paving way to the formation of the final product. In **I-R3- $\pi$ -TS2**,  $\text{Si}_{(1)}\text{-Si}_{(2)}$  bond is fully broken and the product located is a five membered ring, **I-R3- $\pi$ -PDT**. The Si-Si bond length in **I-R3- $\pi$ -PDT** is less than the normal Si-Si single bond length ( $r_{\text{Si}_{(1)}\text{-Si}_{(3)}} = 2.28 \text{ \AA}$ ,  $r_{\text{Si}_{(2)}\text{-Si}_{(3)}} = 2.28 \text{ \AA}$ ). The activation barrier is 1.62 kcal/mol, and the overall reaction is exoergic by 23.29 kcal/mol. The energy value suggests the feasibility of the reaction under ambient conditions.

#### 4.4.3.2 $\sigma$ -insertion

The intermediates and transitions states located for the exocyclic  $\sigma$ -insertion reaction between **I** and **R3** is represented in Figure 4.14

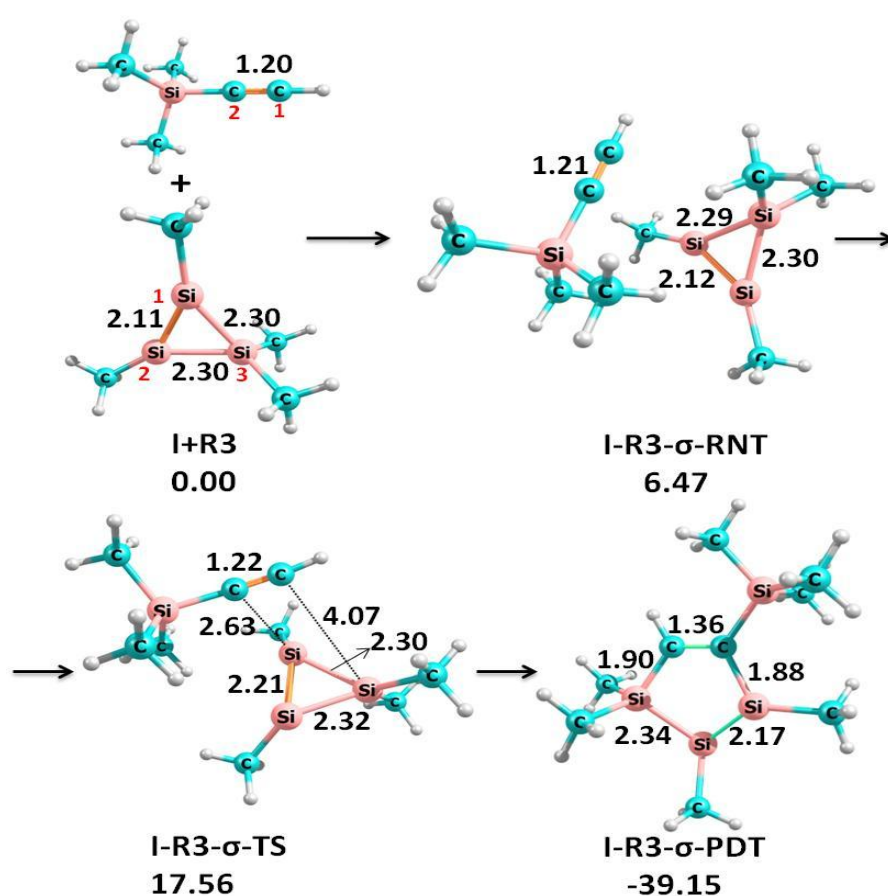


**Figure 4.14** Intermediates and transitions states involved in the  $\sigma$ -insertion pathway of **I** and **R3**. Relative free energies are given in kcal/mol and bond lengths in  $\text{\AA}$

The  $\sigma$ -insertion of acetylenic group of **R3** into the  $\text{Si}_{(1)}\text{-Si}_{(3)}$  single bond of **I** is initiated with the formation of the reactant dispersion complex **I-R3- $\sigma$ -RNT** possessing relative energy 6.47 kcal/mol. It is proceeded to a transition state, **I-R3- $\sigma$ -TS** in which the acetylenic group is oriented along  $\text{Si}_{(1)}\text{-Si}_{(3)}$  bond. **I-R3- $\sigma$ -TS** transformed directly to the pentagonal product, **I-R3- $\sigma$ -PDT** by the rupture of the  $\text{Si}_{(1)}\text{-Si}_{(3)}$  bond and the insertion of

the acetylenic group across it. The activation barrier for the formation of **I-R3- $\sigma$ -PDT** is 17.56 kcal/mol and the overall reaction is exoergic by 39.15 kcal/mol. The high exoergic value and a moderate activation barrier can be attributed to the release of ring strain associated with the cyclotrisilene and the well-defined structure of the product. The exoergic nature and low activation energy value support the feasibility of the reaction under ambient conditions.

#### 4.4.3.3 Ring opening

The intermediates and transition states located for the ring opening reaction between **I** and **R3** is represented in Figure 4.15

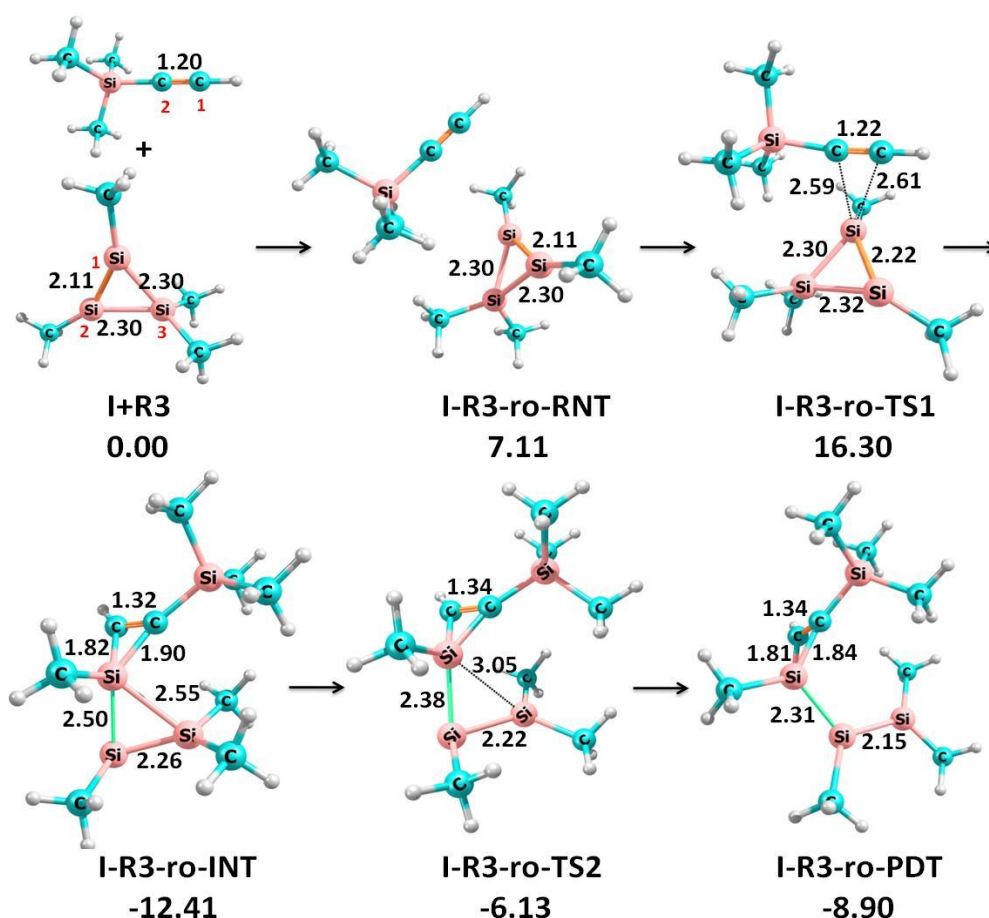


**Figure 4.15** Intermediates and transition states involved in the ring opening reaction pathway of **I** + **R3**. Relative free energies are given in kcal/mol and bond lengths in Å

The course of the ring opening reaction between **I** and **R3** is very much similar to that of  $\pi$ -addition reaction. The initially formed reactant dispersion complex (**I-R3-ro-RNT**) with a relative energy 7.11 kcal/mol is transformed to transition state, **I-R3-ro-TS1**. This transition state represents the attack on the tricoordinate Si atom ( $\text{Si}_{(1)}$ ) of the trisilene ring by the  $\pi$ -electron cloud of the acetylenic group ( $r_{\text{Si}_{(1)}-\text{C}_{(1)}} = 2.61 \text{ \AA}$ ,  $r_{\text{Si}_{(1)}-\text{C}_{(2)}} = 2.59 \text{ \AA}$ ,  $r_{\text{Si}_{(1)}-\text{Si}_{(2)}} = 2.22$

Å). The transition state is further advanced to the intermediate **I-R3-ro-INT**, in which the acetylenic group strongly bound to the Si<sub>(1)</sub>, which lead to the elongation of Si<sub>(1)</sub>-Si<sub>(2)</sub> and Si<sub>(1)</sub>-Si<sub>(3)</sub> bonds ( $r_{\text{Si}_{(1)}-\text{Si}_{(2)}} = 2.50 \text{ \AA}$ ,  $r_{\text{Si}_{(1)}-\text{Si}_{(3)}} = 2.55 \text{ \AA}$ ,  $r_{\text{Si}_{(1)}-\text{C}_{(1)}} = 1.82 \text{ \AA}$ ,  $r_{\text{Si}_{(1)}-\text{C}_{(2)}} = 1.90 \text{ \AA}$ ). The formation of the intermediate **I-R3-ro-INT** is exoergic by 12.41 kcal/mol and transformation involves an activation barrier of 16.30 kcal/mol.

**I-R3-ro-INT** is advanced to the second transition state **I-R3-ro-TS2** by the weakening of the Si<sub>(1)</sub>-Si<sub>(3)</sub> bond ( $r_{\text{Si}_{(1)}-\text{Si}_{(3)}} = 3.05 \text{ \AA}$ ). Significant changes in the remaining Si-Si bond distances of the cyclotrisilene moiety is also associated with it ( $r_{\text{Si}_{(1)}-\text{Si}_{(2)}} = 2.38 \text{ \AA}$ ,  $r_{\text{Si}_{(2)}-\text{Si}_{(3)}} = 2.22 \text{ \AA}$ ). The complete cleavage of Si<sub>(1)</sub>-Si<sub>(3)</sub> bond in the transition state **I-R3-ro-TS2** directed the course of the reaction to the formation of the ring opened product, **I-R3-ro-PDT**. The highest activation barrier of the ring opening reaction between **I** and **R3** is 16.30 kcal/mol and the overall reaction is exoergic by 8.90 kcal/mol. The ring opened product is a disilylenyl silylene ( $r_{\text{Si}_{(2)}-\text{Si}_{(3)}} = 2.15 \text{ \AA}$ ) with a silylene moiety stabilized by the coordination with the acetylenic group. The low activation energy and exoergic nature of the ring opening reaction between **I** and **R3** suggests that it is workable under ambient conditions.

#### 4.4.3.4 Exocyclic $\sigma$ -insertion

The intermediates and transition states located for the exocyclic  $\sigma$ -insertion reaction between **I** and **R3** is represented in Figure 4.16.

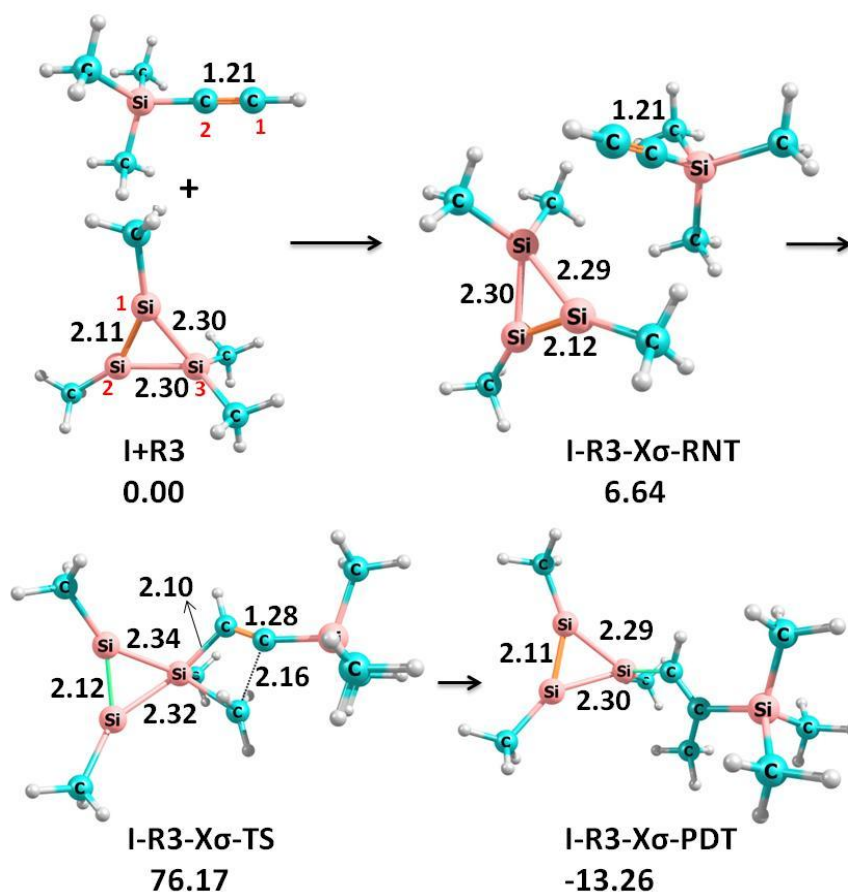


**Figure 4.16** Intermediates and transition states involved in the exocyclic  $\sigma$ -insertion reaction pathway of **I** and **R3**. Relative free energies are given in kcal/mol and bond lengths in Å

In the exocyclic  $\sigma$ -insertion, the acetylene part of **R3** inserts into the bond between  $sp^3$  Si atom of **I** and a methyl substituent ( $Si_{(3)}-CH_3$ ). The initially formed reactant dispersion complex **I-R3-x $\sigma$ -RNT** has a relative energy 6.64 kcal/mol. The reactant complex changed to an activated complex **I-R3-x $\sigma$ -TS** which is directly converted to the product **I-R3-x $\sigma$ -PDT**. The overall reaction being exoergic by 13.26 kcal/mol, the reaction is kinetically impossible at ambient conditions due to a high activation barrier of 76.17 kcal/mol.

Free energy profile diagrams of the four reaction pathways between **I** and **R3** are given in Figure 4.17



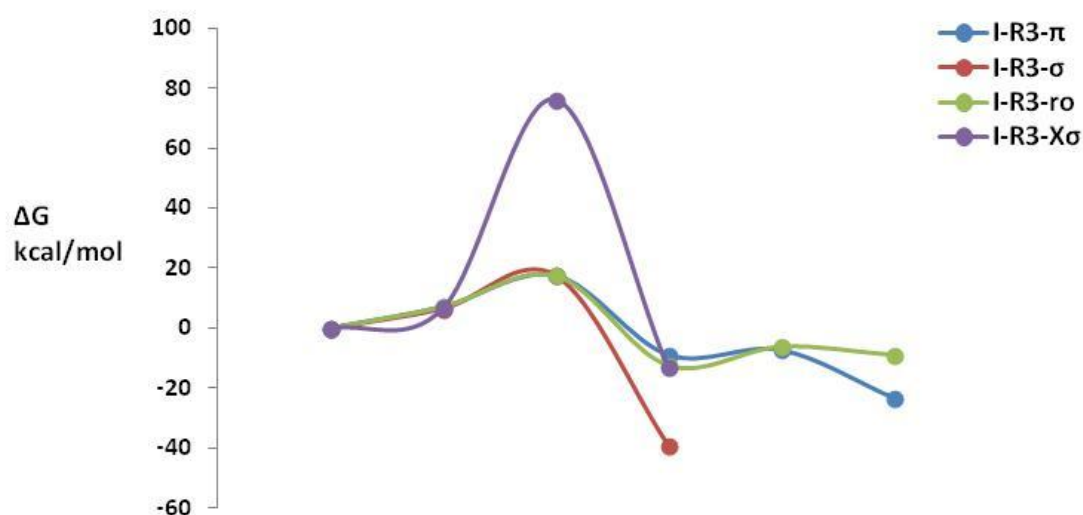


**Figure 4.17** Comparative free energy profile diagram for the different reaction pathways between **I** and **R3**

As observed with **I** and **R2**, the  $\pi$ -addition reaction and ring opening reaction between **I** and **R3** also proceed via a two-step processes. The remaining two, the  $\sigma$ -insertion reaction and exocyclic  $\sigma$ -insertion are direct, single-step processes. The energetics of the four possible reaction pathways between **I** and **R3** suggests that; the  $\pi$ -addition,  $\sigma$ -insertion, and ring opening reactions are feasible under ambient conditions whereas the exocyclic  $\sigma$ -insertion reaction is kinetically not accessible.

A comparison of the four classes of the reactions pathways analysed between the substrates **R1**, **R2** and **R3** with **I**, primarily illustrate that all of them are exoergic. The  $\sigma$ -insertion reaction is the most exoergic irrespective of the substrates, followed by the  $\pi$ -addition reaction. For **R1** and **R2**, the magnitudes of exoergic of  $\pi$ -addition and  $\sigma$ -insertion reactions are almost similar, whereas the values are comparatively low for **R3**. Eventhough much lesser in magnitude, the ring opening reactions are also exoergic. The exoergic nature of the exocyclic  $\sigma$ -insertion reaction is unbeneficial as it is inaccessible owing to the formidable energy barrier (>75 kcal/mol). Regarding all the substrates, the activation energies of the  $\pi$ -addition,  $\sigma$ -insertion and ring opening reactions are calculated to be in the moderate range of 17 - 19 kcal/mol. The low activation energy values and the exoergic nature of these three classes of the reactions of **R1**, **R2** and **R3** with **I** strongly support their feasibility under ambient conditions. Further, it is clear that the steric and electronic changes associated with substrates do not cause a significant change to the mechanism and energetics of the reactions.



## 4.4.4 Reaction pathways between $c\text{-Si}_3\text{Me}_4$ (**I**) + $\text{C}_6\text{H}_5\text{-CHO}$ (**R'1**)

### 4.4.4.1 $\pi$ -addition

As observed in the reaction between **I** and **R1**, a two-step reaction pathway has been identified for the reaction between the carbonyl group of **R'1** and the silenyl part of **I**. Intermediates and transition states located for the reaction is represented in Figure 4.18

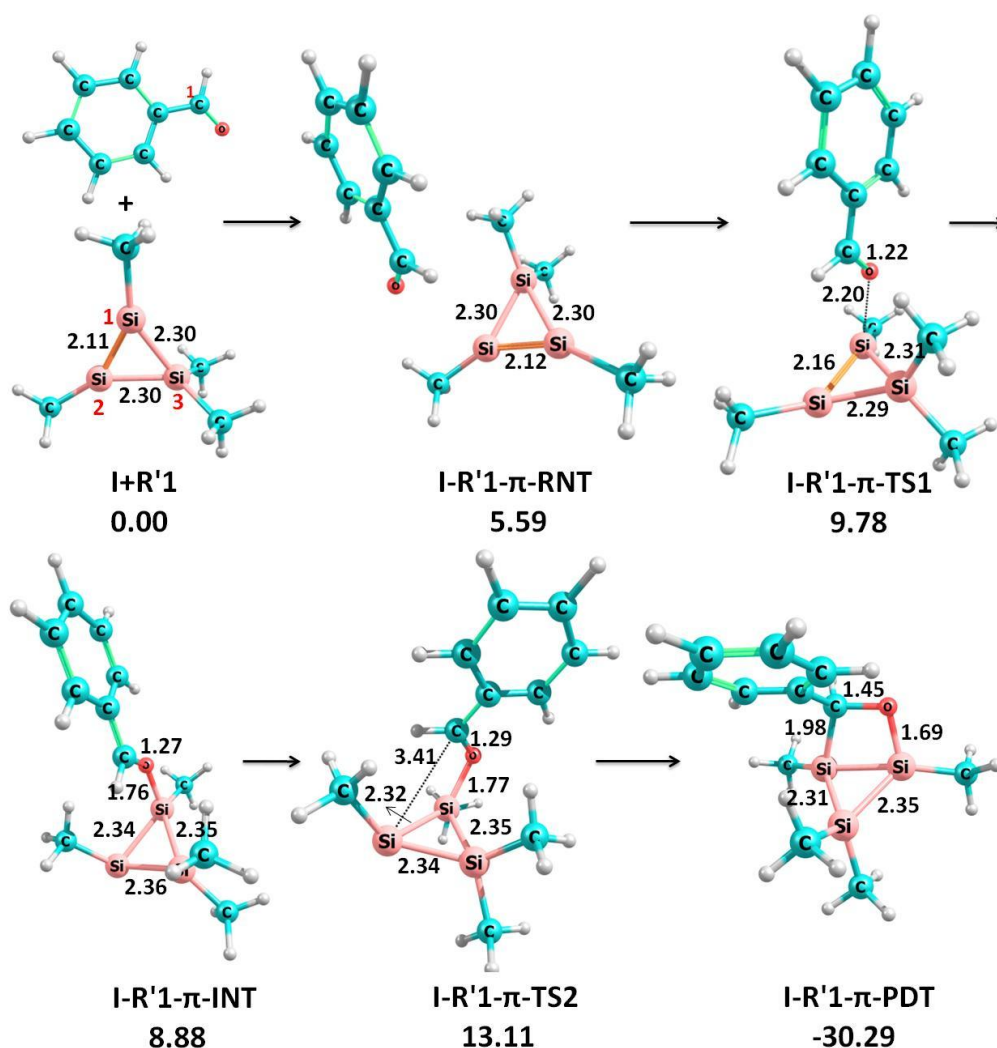


**Figure 4.18** Intermediates and transition states involved in the  $\pi$ -addition reaction pathway of **I** + **R'1**. Relative free energies are given in kcal/mol and bond lengths in Å

The formation of the reactant dispersion complex between **I** and **R'1** (**I-R'1- $\pi$ -RNT**), with relative energy 5.59 kcal/mol marked the beginning of the  $\pi$ -addition reaction. **I-R'1- $\pi$ -RNT** is progressed to the transition state **I-R'1- $\pi$ -TS1** in which the carbonyl oxygen of **R'1** initiates a bonding interaction with one of the electron rich silenyl silicon atoms of **I**,  $\text{Si}_{(1)}$  ( $r_{\text{O-Si}_{(1)}} = 2.20$  Å). This interaction is followed by a slight elongation of the  $\text{Si}_{(1)}=\text{Si}_{(2)}$  double bond ( $r_{\text{Si}_{(1)}=\text{Si}_{(2)}} = 2.16$  Å). **I-R'1- $\pi$ -TS1** is advanced to an intermediate, **I-R'1- $\pi$ -INT** with

the full rupture of the  $\pi$ -bond between  $\text{Si}_{(1)}$  and  $\text{Si}_{(2)}$  ( $r_{\text{Si}_{(1)}-\text{Si}_{(2)}} = 2.35 \text{ \AA}$ ) and formation of a  $\text{Si}_{(1)}-\text{O}$  bond ( $r_{\text{Si}_{(1)}-\text{O}} = 1.76 \text{ \AA}$ ). The activation barrier for the formation of the intermediate **I-R'1- $\pi$ -INT** is 9.78 kcal/mol.

Further progress of the  $\pi$ -addition reaction is marked by the formation of **I-R'1- $\pi$ -TS2** from **I-R'1- $\pi$ -INT**. During this step of the reaction, a strong interaction between  $\text{Si}_{(2)}$  of **I** and carbonyl carbon of **R'1** is developed ( $r_{\text{C}_{(1)}-\text{Si}_{(2)}} = 3.41 \text{ \AA}$ ). **I-R'1- $\pi$ -TS2** is transformed to the  $\pi$ -addition product, **I-R'1- $\pi$ -PDT** by the formation of the  $\text{C}_{(1)}-\text{Si}_{(2)}$  bond ( $r_{\text{C}_{(1)}-\text{Si}_{(2)}} = 1.98 \text{ \AA}$ ). The associated activation energy is 4.23 kcal/mol. The product is a bicyclic housane-shaped one with a bridging  $\text{Si}_{(1)}-\text{Si}_{(2)}$  bond ( $r_{\text{Si}_{(1)}-\text{Si}_{(2)}} = 2.31 \text{ \AA}$ ). The product formation is characterized by the elongation of the  $\text{C}_{(1)}-\text{O}$  bond of **R'1** ( $r_{\text{C}_{(1)}-\text{O}} = 1.45 \text{ \AA}$ ) and further shortening of the  $\text{O}-\text{Si}_{(1)}$  bond ( $r_{\text{O}-\text{Si}_{(1)}} = 1.69 \text{ \AA}$ ). Formation of the product is remarkably exoergic as evidenced by the relative energy of the product, **I-R'1- $\pi$ -PDT** (-30.30 kcal/mol). The low activation barriers and the exoergic value 30.30 kcal/mol strongly support the practicability of the  $\pi$ -addition reaction between **I** and **R'1**.

#### 4.4.4.2 $\sigma$ -insertion

The intermediates and transition states located for  $\sigma$ -insertion reaction between **I** and **R'1** is represented in Figure 4.19

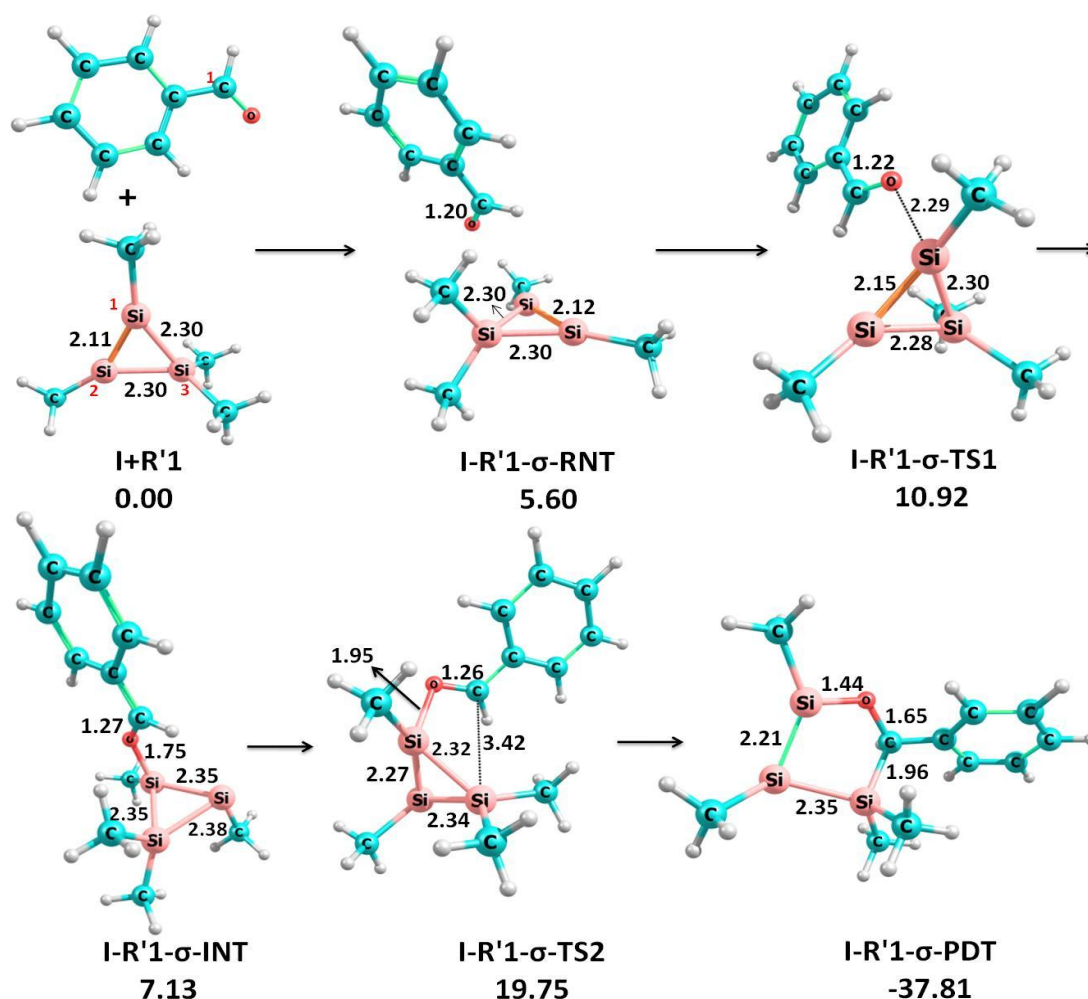


**Figure 4.19** Intermediates and transition states involved in the  $\sigma$ -insertion reaction pathway of **I + R'1**). Relative free energies are given in kcal/mol and bond lengths in Å.

The  $\sigma$ -insertion reaction between **I** and **R'1** is a two-step process. The reaction is initiated by the formation of the reactant dispersion **I-R'1- $\sigma$ -RNT**, which passes through the transition state **I-R'1- $\sigma$ -TS1**, to form the intermediate **I-R'1- $\sigma$ -INT**. The activation energy required for the formation of **I-R'1- $\sigma$ -INT** 10.92 kcal/mol and the transformation is endoergic by 7.13 kcal/mol. The intermediate, **I-R'1- $\sigma$ -INT** is characterized by the completed cleavage of the disilyl  $\pi$ -bond ( $r_{\text{Si}(1)\text{-Si}(2)} = 2.35\text{\AA}$ ) and the formation of the  $\text{Si}(1)\text{-O}$  bond ( $r_{\text{Si}(1)\text{-O}} = 1.75\text{\AA}$ ).

**I-R'1- $\sigma$ -INT** is progressed to the second transition state **I-R'1- $\sigma$ -TS2**, which corresponds to the bond formation between carbonyl carbon and  $\text{Si}(3)$ . In **I-R'1- $\sigma$ -TS2**, the  $\text{C-Si}(3)$  bond length is  $3.42\text{\AA}$ , whereas the  $r_{\text{O-Si}(1)}$  is weakened to  $1.95\text{\AA}$  compared with  $1.71\text{\AA}$  in the intermediate, **I-R'1- $\sigma$ -INT**. **I-R'1- $\sigma$ -TS2** is transformed to the  $\sigma$ -insertion product, **I-R'1- $\sigma$ -PDT** with a relative energy  $-37.81$  kcal/mol, demonstrating a high exoergic value of the

reaction. The activation barrier involved in this transformation is 12.62 kcal/mol. The product is a pentagonal-ring structured one with  $r\text{Si}_{(1)}\text{-Si}_{(2)} = 2.21\text{\AA}$ , indicating the continuing double bond nature of it. The low activation energy and the high exoergic value (-37.81 kcal/mol) ensures the easy attainment of the  $\sigma$ -insertion reaction between **I** and **R'1** at ordinary laboratory conditions.

#### 4.4.4.3 Ring opening

The intermediates and transitions states located for ring opening reaction between **I** and **R'1** is represented in Figure 4.20

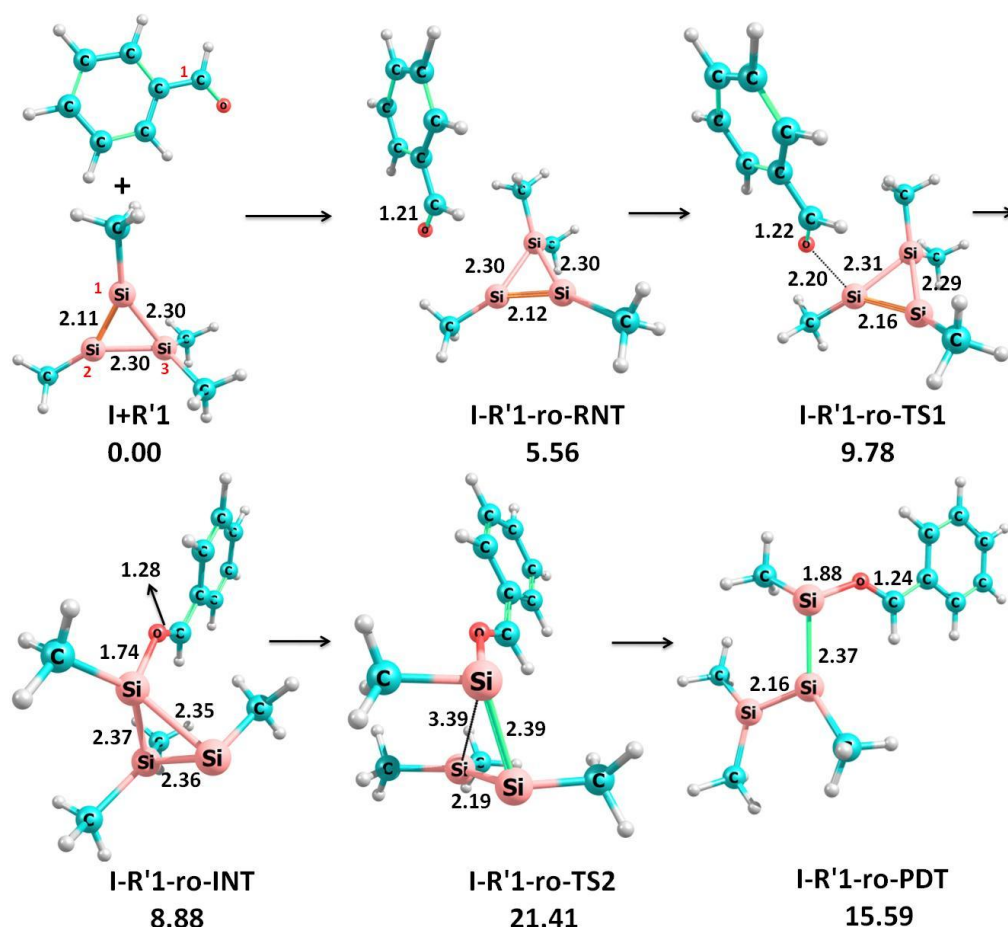


**Figure 4.20** Intermediates and transitions states involved in the ring opening reaction pathway of **I** + **R'1**. Relative free energies are given in kcal/mol and bond lengths in  $\text{\AA}$ .

The ring opening reaction between **I** and **R'1** begin with the formation of a reactant dispersion complex **I-R'1-ro-RNT** which is transformed to a transition state **I-R'1-ro-TS1**, in which a strong  $\text{Si}_{(1)}\text{-O}$  bonding interaction is initiated. The evolution of the  $\text{O-Si}_{(1)}$  interaction ( $r\text{O-Si}_{(1)} = 2.20\text{\AA}$ ) is associated with a partial weakening of the  $\text{Si}_{(1)}\text{=Si}_{(2)}$  double bond ( $r\text{Si}_{(1)}\text{=Si}_{(2)} = 2.16\text{\AA}$ ). **I-R'1-ro-TS1** is progressed to the intermediate **I-R'1-ro-INT**

(8.88kcal/mol) and the activation energy involved is 9.78 kcal/mol. The breaking of the Si<sub>(1)</sub>-Si<sub>(2)</sub>  $\pi$ -bond ( $r_{\text{Si}(1)\text{-Si}(2)} = 2.37 \text{ \AA}$ ) and the formation of the O-Si<sub>(1)</sub> bond ( $r_{\text{O-Si}(1)} = 1.74 \text{ \AA}$ ) is achieved during this part of the ring opening reaction.

The intermediate **I-R'1-ro-INT** converted to the second transition state **I-R'1-ro-TS2**, the attainment of which involves the rupture of Si<sub>(1)</sub>-Si<sub>(3)</sub> bond. The completion of the rupture of the Si<sub>(1)</sub>-Si<sub>(3)</sub> bond results in the formation of the ring opened product, **I-R'1-ro-PDT**. The activation barrier is 12.53 kcal/mol, the overall reaction endoergic by 15.59 kcal/mol. Even though the activation barriers are moderate, the endoergic nature of the ring opening reaction between **I** and **R'1** makes it not feasible under ambient conditions.

#### 4.4.4.4 Exocyclic sigma insertion

The intermediates and transition states located for the exocyclic sigma insertion reaction between **I** and **R'1** is represented in Figure 4.21

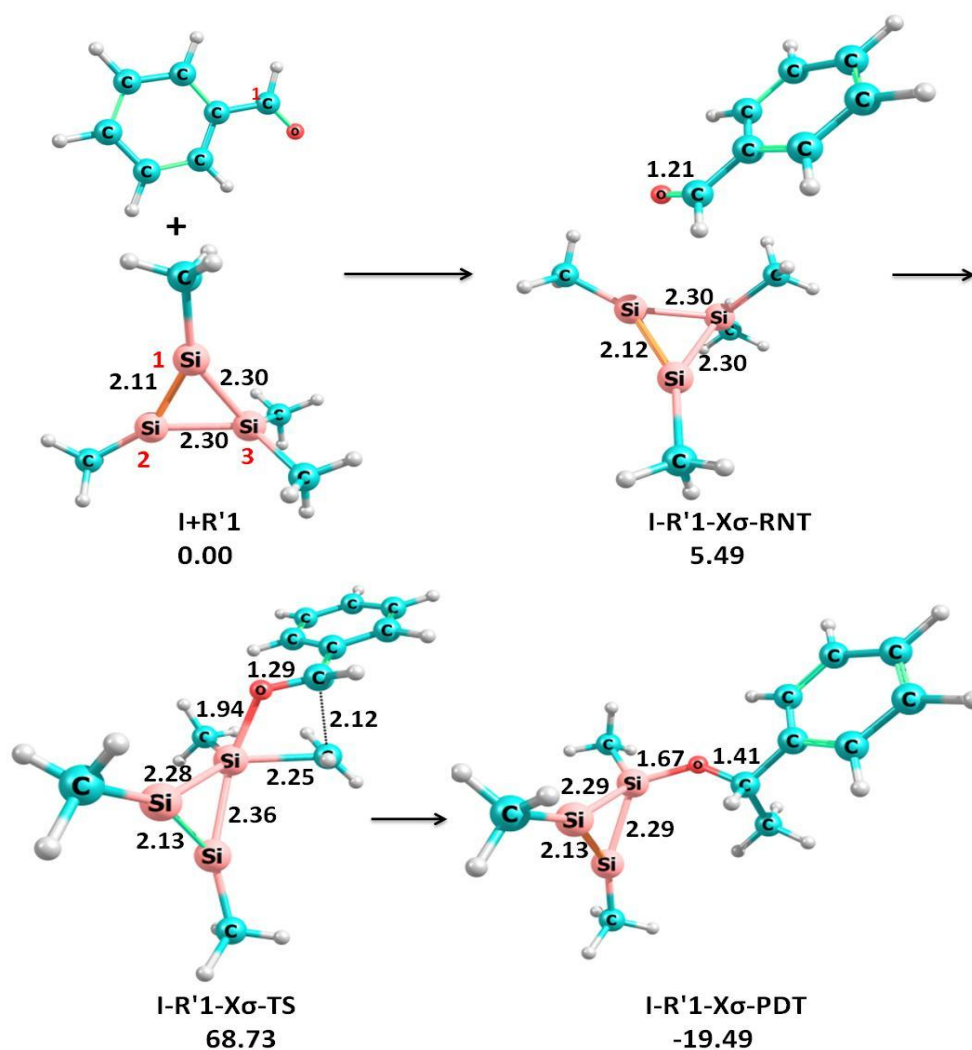


**Figure 4.21** Intermediates and transition states involved in the exocyclic  $\sigma$ -insertion reaction pathway of **I** + **R'1**. Relative free energies are given in kcal/mol and bond lengths in Å.

During the exocyclic  $\sigma$ -insertion reaction between **I** and **R'1**, the carbonyl group inserts into an exocyclic  $\text{Si}_{(3)}\text{-C}_{(1)}$  bond. Even though this reaction is exoergic by 19.50kcal/mol, it is kinetically not attainable under ambient conditions due the exorbitant activation energy of 68.73 kcal/mol.

Free energy profile diagrams of the four reaction pathways between **I** and **R'1** are given in Figure 4.22

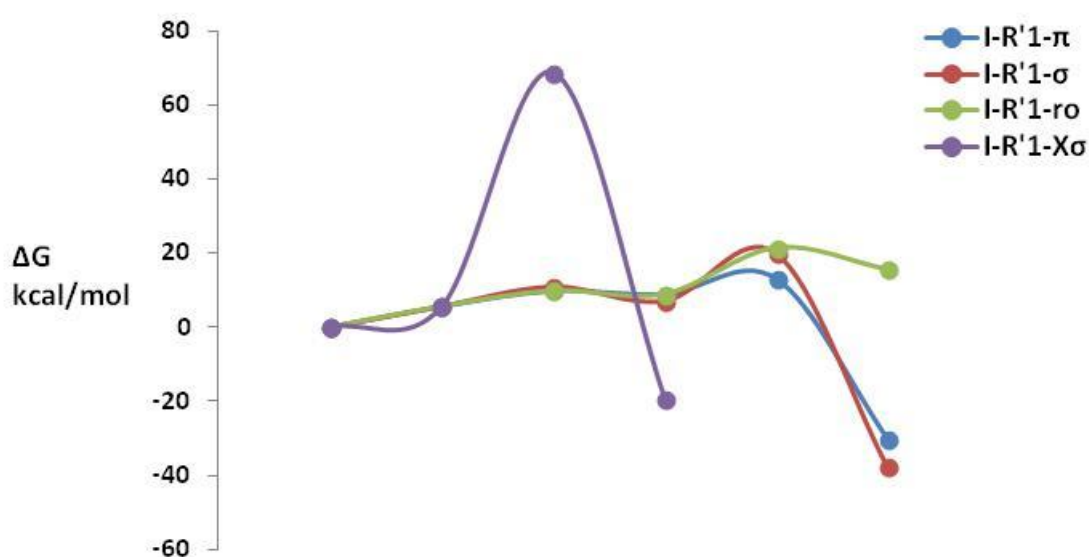


**Figure 4.22** Comparative free energy profile diagram for the different reaction pathways between **I** + **R'1**

Out of the four reaction pathways between **I** and **R'1**, all except the exocyclic  $\sigma$ -insertion reaction passed through two intermediates and two transition states, before arriving at the end-product. The bicyclic nature of the  $\pi$ -addition product enhanced the ring strain in it and therefore, it is slightly higher in energy than the  $\sigma$ -insertion product, which is monocyclic. The relative energy values observed in the reaction pathways confirms that, both  $\pi$ -addition and  $\sigma$ -insertion reactions between **I** and **R'1** are feasible under ambient conditions. Even though not too high, the ring opening reaction is endoergic; probably due to the insufficiency in the stabilization mechanism existing in the system. Even though the activation energy is in the workable limit the practicability of the ring opening reaction between **I** and **R'1** requires stabilization by the coordination of a base with silylene moiety.

The exocyclic  $\sigma$ -insertion reaction between **I** and **R'1** is found to be exoergic to a good extent, but is non-practicable under ambient conditions due the huge activation energy barrier of the reaction.

#### 4.4.5 Reaction pathways between **c-Si<sub>3</sub>Me<sub>4</sub>** (**I**) and formaldehyde (**R'2**)

##### 4.4.5.1 $\pi$ -addition

A direct single-step reaction pathway ( $2\pi + 2\pi$  addition) has been located for the  $\pi$ -addition reaction between the carbonyl group of **R'2** and the disilyl part of **I**. Intermediates and transitions states located for the reaction is represented in Figure 4.23

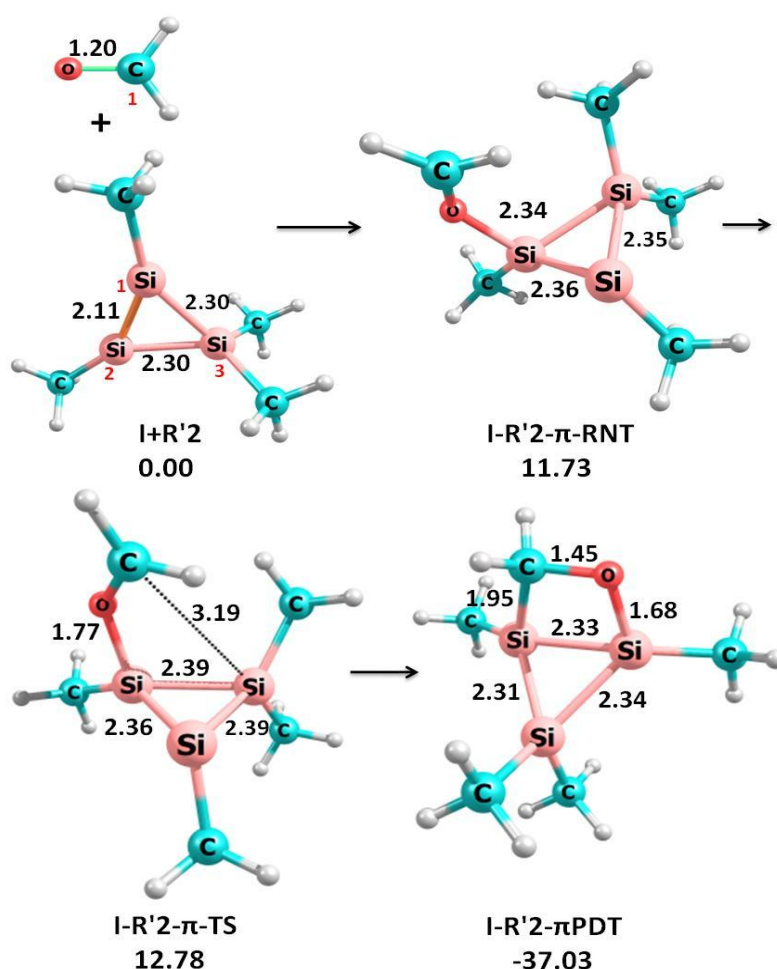


**Figure 4.23** Intermediates and transitions states involved in the  $\pi$ -addition reaction pathway of **I** and **R'2**. Relative free energies are given in kcal/mol and bond lengths in Å

The  $\pi$ -addition reaction between **I** and **R'2** takes place in a single step by the direct  $\pi$ -addition of carbonyl group with the disilyl part of **I**. In the transition state **I-R'2- $\pi$ -TS**, the  $-\text{CO}$  group is oriented along Si-Si double bond and the O-Si<sub>(1)</sub> and C<sub>(1)</sub>-Si<sub>(2)</sub> bonding



interaction initiates ( $r_{\text{O-Si}_{(1)}} = 2.46 \text{ \AA}$ ,  $r_{\text{C}_{(1)}\text{-Si}_{(2)}} = 3.19 \text{ \AA}$ ). Further, the O-Si<sub>(1)</sub> bond formation is associated with the weakening of the  $\pi$ -bond between the Si<sub>(1)</sub> and Si<sub>(2)</sub>. The transition state is directly transformed to the product **I-R'2- $\pi$ -PDT** and the activation barrier is 12.78 kcal/mol. The product is a bicyclic housane - shaped one with relative energy -37.03 kcal/mol. The bridging Si-Si bond characterizes the standard  $\pi$ -addition nature of the reaction. The low activation energy and high exoergic value of the  $\pi$ -addition reaction between **I** and **R'2** predicts its practicability under normal laboratory conditions.

#### 4.4.5.2 $\sigma$ -insertion

The intermediates and transitions states located for  $\sigma$ -insertion reaction between **I** and **R'2** is represented in Figure 4.24

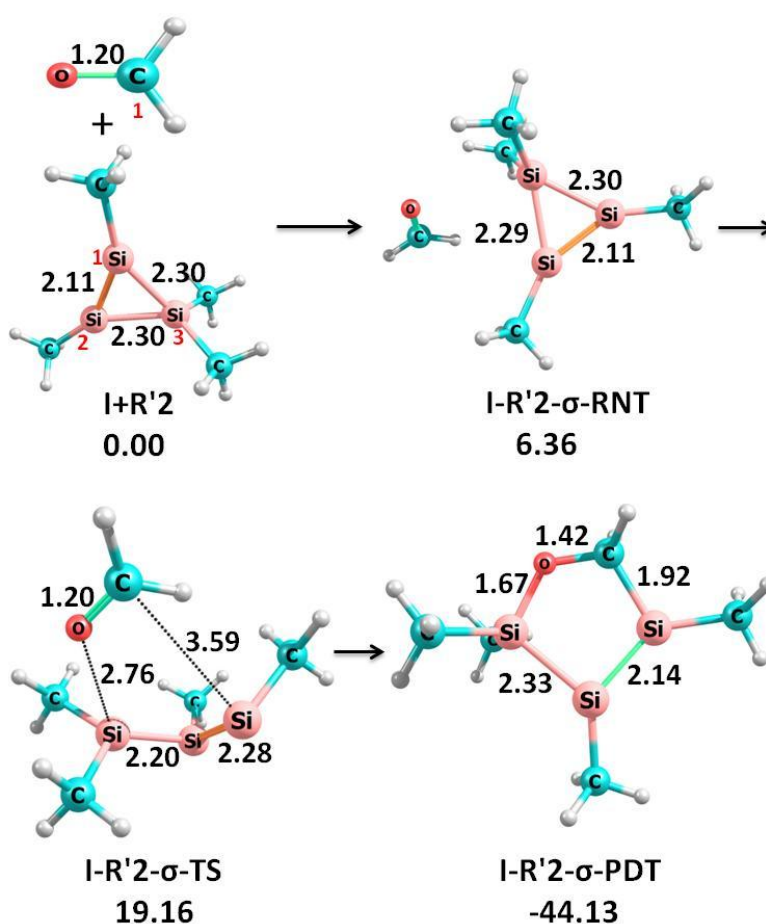


**Figure 4.24** Intermediates and transitions states involved in the  $\sigma$ -insertion reaction pathway of **I** and **R'2**. Relative free energies are given in kcal/mol and bond lengths in Å.

The  $\sigma$ -insertion reaction between **R'2** and the cyclotrisilene **I** is also a direct single-step process. The dispersion complex, **I-R'2- $\sigma$ -RNT** is progressed to the activated complex **I-R'2- $\sigma$ -TS**, in which strong C<sub>(1)</sub>-Si<sub>(1)</sub> and O-Si<sub>(3)</sub> interactions are developed between the



carbonyl group of **R'2** and cyclotrisilene moiety of **I** ( $r_{\text{O-Si}(3)} = 2.76 \text{ \AA}$ ,  $r_{\text{C}(1)\text{-Si}(1)} = 3.59 \text{ \AA}$ ). **I-R'2- $\sigma$ -TS** is transformed to the  $\sigma$ -insertion product, **I-R'2- $\sigma$ -PDT** with a relative energy -44.13 kcal/mol, indicating the high exoergic value of the reaction. The activation energy for the formation of the product is 19.16 kcal/mol. The product is a pentagonal ring-structured one with  $r_{\text{Si}(1)\text{-Si}(2)} = 2.14 \text{ \AA}$  confirming the double bond nature of this bond. The moderate value of the total activation energy (19.16 kcal/mol) and the high exoergic value (-44.13 kcal/mol) of the  $\sigma$ -insertion reaction between **I** and **R'2** support the attainment of it at ambient laboratory conditions.

#### 4.4.5.3 Ring opening

The Intermediates and transitions states located for ring opening reaction between **I** and **R'2** is represented in Figure 4.25

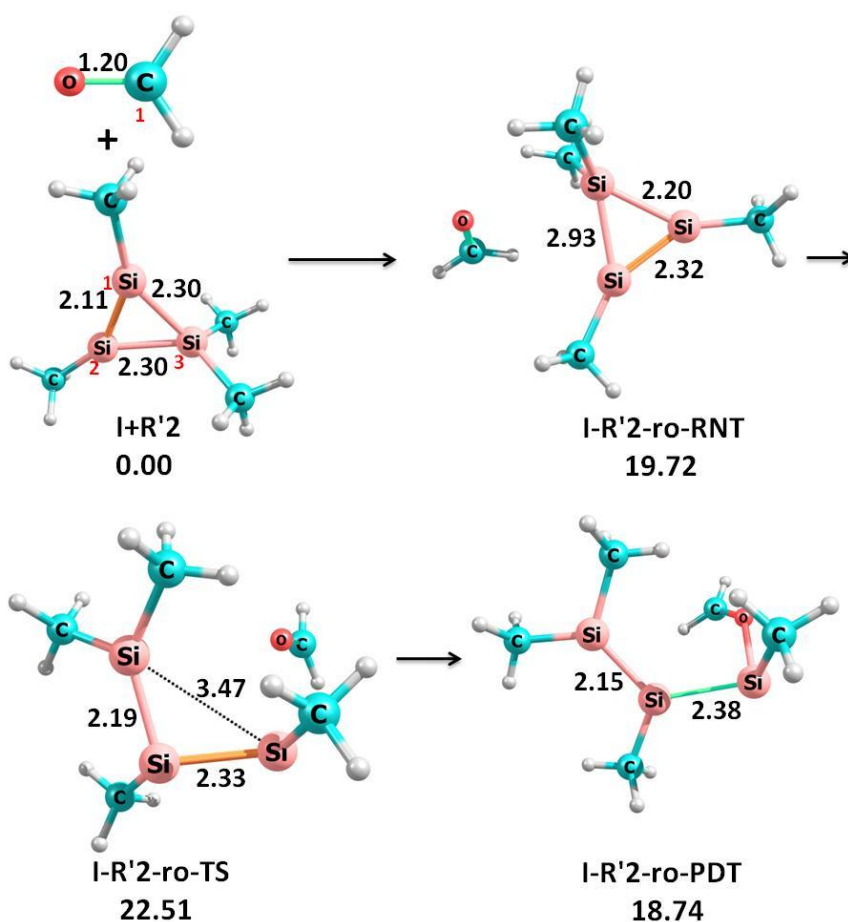


**Figure 4.25** Intermediates and transitions states involved in the ring opening reaction pathway of **I** and **R'2**. Relative free energies are given in kcal/mol and bond lengths in Å.

The ring opening reaction between **I** and **R'2** also is initiated by the formation of dispersion complex **I-R'2-ro-RNT** which is advanced to the transition state **I-R'2-ro-TS**. The

major change noticeable during the formation of the transition state is the thorough weakening of the  $\text{Si}_{(1)}\text{-Si}_{(3)}$  bond ( $r_{\text{Si}_{(1)}\text{-Si}_{(3)}} = 3.47 \text{ \AA}$ ) and an associated strengthening of the  $\text{O-Si}_{(1)}$  bond between **I** and **R'2** ( $r_{\text{O-Si}_{(1)}} = 2.53 \text{ \AA}$ ). **I-R'2-ro-TS** is advanced to the ring opened product, **I-R'2-ro-PDT** the activation barrier is 22.51 kcal/mol. The product is a disilyl silylene. The instability of **I-R'2-ro-PDT** is evident from its endoergic nature (18.74 kcal/mol). Even though the activation energy barrier is in the workable limit, the endoergic nature of the ring opening reaction between **I** and **R'2** makes it not feasible under ambient conditions.

#### 4.4.5.4 Exocyclic $\sigma$ -insertion

The intermediates and transitions states located for exocyclic  $\sigma$ -insertion reaction between **I** and **R'2** is represented in Figure 4.26

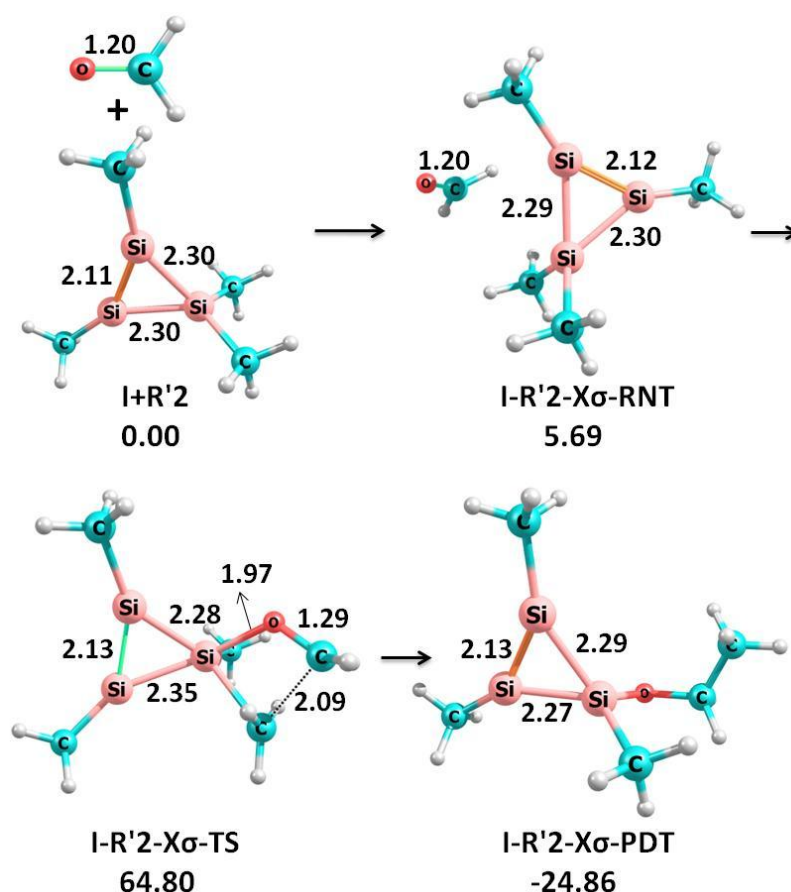


**Figure 4.26** Intermediates and transitions states involved in the exocyclic  $\sigma$ -insertion reaction pathway of **I** and **R'2**. Relative free energies are given in kcal/mol and bond lengths in  $\text{\AA}$ .

The exocyclic  $\sigma$ -insertion pathway between **I** and **R'2** also is a direct single step process. The reaction is initiated by the formation of a reactant dispersion complex **I-R'2-x $\sigma$ -**

**RNT** possessing a relative energy 5.69 kcal/mol. The dispersion complex **I-R'2-xσ-RNT** progressed to a transition state, **I-R'2-xσ-TS** in which the carbonyl oxygen established a strong interaction with the tetra coordinate silicon atom of the cyclotrisilene ( $r_{\text{O-Si}(3)} = 1.97 \text{ \AA}$ ). The carbonyl carbon of **R'2** also developed an interaction with the carbon atom of one of the methyl groups attached to the  $\text{sp}^3$  silicon atom **I**. The transition state developed in to the product in which the methyl group migrated to the carbonyl carbon of **R'2** and the carbonyl oxygen remain connected to the tetra-coordinate silicon atom of **I**. Even though the reaction is appearing to be achievable thermodynamically due to the exoergic nature (-24.86 kcal/mol), the exorbitant activation energy (64.80 kcal/mol) denies its kinetic feasibility.

Free energy profile diagrams of the four reaction pathways between **I** and **R'1** are given in Figure 4.27

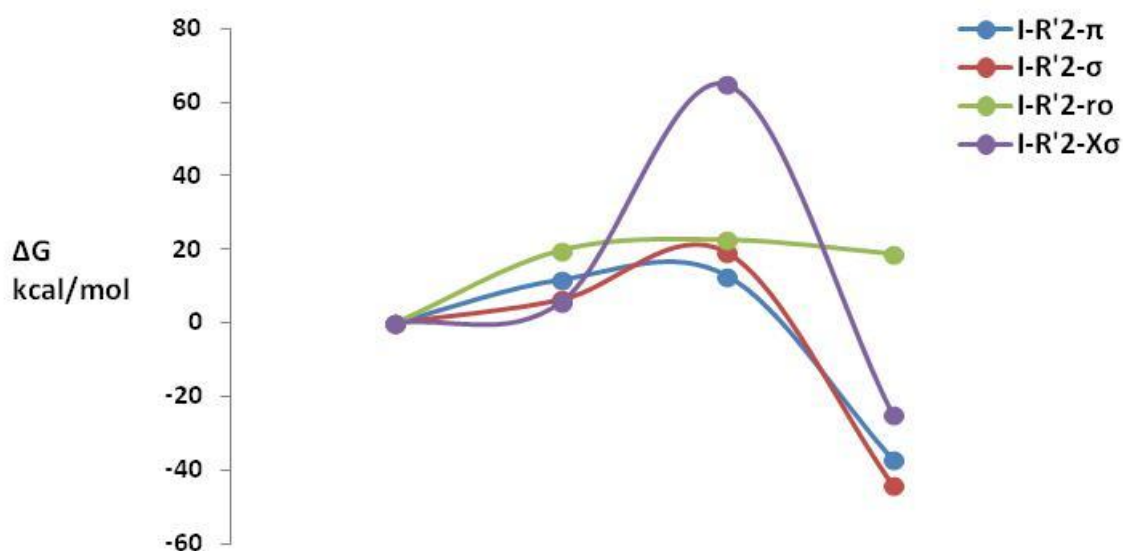


**Figure 4.27** Comparative free energy profile diagram for the different reaction pathways between **I** and **R'2**

All the four reaction pathways between **I** and **R'2** are direct single-step process, primarily due to the small size of the formaldehyde molecule, enabling its easy access to the close vicinity of the cyclotrisilene molecule. All the reaction pathways except the ring opening reaction are exoergic. The exoergic value is highest with the  $\sigma$ -insertion reaction. Except for the exocyclic  $\sigma$ -insertion reaction, the activation barriers are in the workable limit for all the classes of the reactions. However, the endoergic nature of the ring-opening reaction disapproves its feasibility under normal laboratory conditions. The  $\pi$ -addition and  $\sigma$ -insertion

reactions possess low activation barriers and high exoergic nature, indicating their easy accessibility under ordinary laboratory conditions.

A comparison of the reactivity of the alkynes (**R1**, **R2** and **R3**) and aldehydes (**R'1** and **R'2**) towards **I** shows that, for both class of the substrates the  $\sigma$ -insertion and  $\pi$ -addition reaction pathways are well stabilized and are feasible under ambient conditions. However, the ring opening reactions involving aldehydes are considerably endoergic and are not feasible under ambient conditions. It is worth mentioning that ring opening pathway is competitive with the  $\pi$ -addition and  $\sigma$ -insertion reactions for alkynes. It implies that a non-polar functional group is necessary for the stabilization of the ring-opened product. Even though, the energy barrier of the exocyclic  $\sigma$ -insertion reaction is  $\approx 10$  kcal/mol lesser for the reactions involving aldehydes than those involving alkynes, it is nowhere near to the workable range.

## 4.5 Conclusion

We have made a thorough computational exploration of the possible interactions of **R1**, **R2**, **R3**, **R'1** and **R'2** with the cyclotrisilene **I**. Four reaction path ways;  $\pi$ -addition,  $\sigma$ -insertion, ring opening and exocyclic  $\sigma$ -insertion were identified and the energetics and mechanisms were studied systematically. The former three substrates (**R1**, **R2** & **R3**) are acetylenes carrying different substituents and the latter two (**R'1** & **R'2**) are aldehydes with different substituents. Regarding all the five substrates investigated, the  $\pi$ -addition the  $\sigma$ -insertion reactions are found to follow a better stabilized reaction path. Even though the activation energy required for both these classes of reactions are almost same with the three alkynes **R1**, **R2** and **R3**, the exoergicity is found to be slightly greater for the  $\sigma$ -insertion reactions. This can be attributed to the well-defined pentagonal structure of the product generated. The  $\sigma$ -insertion reaction is a single step process except for that involving **R1** among acetylenes, whereas the  $\pi$ -addition is a two-stage process for all the three alkynes. Even though less exothermic, the ring opening reactions of the alkynes are feasible under ambient conditions due to the low activation energy barrier. The ring opening reaction is found to follow the most stabilized course with **R3** among the three acetylenes. Regarding the aldehydes, all the four categories of reactions of **R'2** with **I** are direct single-step processes; probably due to the smaller size of the substrate. The ring opening reactions of **I** with the carbonyl compounds are endothermic. The activation barrier is also relatively higher in comparison with the ring opening reactions of the alkynes. Generally, reactions of **I** with

alkynes follow a more stabilized path than that with carbonyl compounds. The exocyclic  $\sigma$ -insertion reaction pathway is found to be associated with formidable energy barrier in all the five investigated cases. Even though, the magnitude of activation energy is slightly lower with the reaction involving aldehydes, the value is nowhere near in the practicability range of the reaction under ordinary laboratory conditions. As a conclusion, it can be arrived at the postulation that, by proper selection of the substituents on the substrates based on their electronic and steric capabilities, the reaction with the cyclotrisilene **I** can be driven through the desired pathway.

## Reference

- Abersfelder, Kai, and David Scheschkewitz. 2008. "Syntheses of Trisila Analogues of Allyl Chlorides and Their Transformations to Chlorocyclotrisilanes, Cyclotrisilanides, and a Trisilaindane." *Journal of the American Chemical Society* 130(12): 4114–21. <https://pubs.acs.org/doi/10.1021/ja711169w>.
- Al-Rubaiey, N., and R. Walsh. 1994. "Gas-Phase Kinetic Study of the Prototype Silylene Addition Reaction  $\text{SiH}_2 + \text{C}_2\text{H}_4$  over the Temperature Range 298–595 K. An Example of a Third-Body Mediated Association." *The Journal of Physical Chemistry* 98(20): 5303–9. <https://pubs.acs.org/doi/abs/10.1021/j100071a021>.
- Becerra, R., and R. Walsh. 1994. "Gas- phase Kinetic Study of the Silylene Addition Reaction to Acetylene and Acetylene- d 2 over the Temperature Range 291–613 K." *International Journal of Chemical Kinetics* 26(1): 45–60. <https://onlinelibrary.wiley.com/doi/10.1002/kin.550260107>.
- Brook, Adrian G. et al. 1981. "A Solid Silaethene: Isolation and Characterization." *Journal of the Chemical Society, Chemical Communications* (4): 191. <http://xlink.rsc.org/?DOI=c39810000191>.
- Chu, Terry, and Georgii I. Nikonov. 2018. "Oxidative Addition and Reductive Elimination at Main-Group Element Centers." *Chemical Reviews* 118(7): 3608–80. <https://pubs.acs.org/doi/10.1021/acs.chemrev.7b00572>.
- Cowley, Michael J., Volker Huch, Henry S. Rzepa, and David Scheschkewitz. 2013. "Equilibrium between a Cyclotrisilene and an Isolable Base Adduct of a Disilanyl Silylene." *Nature Chemistry* 5(10): 876–79.
- Erwin, J. W., M. A. Ring, and H. E. O'Neal. 1985. "Mechanism and Kinetics of the Silane Decomposition in the Presence of Acetylene and in the Presence of Olefins." *International Journal of Chemical Kinetics* 17(10): 1067–83.
- Fischer, Roland C., and Philip P. Power. 2010. " $\pi$ -Bonding and the Lone Pair Effect in Multiple Bonds Involving Heavier Main Group Elements: Developments in the New Millennium." *Chemical Reviews* 110(7): 3877–3923. <https://pubs.acs.org/doi/10.1021/cr100133q>.
- Fukaya, Norihisa, Masaaki Ichinohe, and Akira Sekiguchi. 2000. "New Fused Bicyclic Cyclotrigermanes from Cycloaddition Reactions of Cyclotrigermene." *Angewandte Chemie* 39(21): 3881–84. [https://onlinelibrary.wiley.com/doi/10.1002/1521-3773\(20001103\)39:21%3C3881::AID-ANIE3881%3E3.0.CO;2-3](https://onlinelibrary.wiley.com/doi/10.1002/1521-3773(20001103)39:21%3C3881::AID-ANIE3881%3E3.0.CO;2-3).
- Hadlington, Terrance J., Matthias Driess, and Cameron Jones. 2018. "Low-Valent Group 14 Element Hydride Chemistry: Towards Catalysis." *Chemical Society Reviews* 47(11): 4176–97. <http://xlink.rsc.org/?DOI=C7CS00649G>.
- Ichinohe, Masaaki et al. 1999. 38 Molecular Spectra and Molecular Structure *Synthesis, Characterization, and Crystal Structure of Cyclotrisilene: A Three-Membered Ring Compound with a Si Å Si Double Bond\*\**. Van Nostrand Reinhold.
- Iwamoto, Takeaki, Makoto Tamura, Chizuko Kabuto, and Mitsuo Kira. 2000. "A Stable Bicyclic Compound with Two Si=Si Double Bonds." *Science* 290(5491): 504–6.
- Lee, Vladimir Ya. et al. 2000. "The First Three-Membered Unsaturated Rings Consisting of Different Heavier Group 14 Elements: 1-Disilagermirene with a SiSi Double Bond and Its Isomerization to a 2-Disilagermirene with a SiGe Double Bond." *Journal of the American Chemical Society* 122(37): 9034–35. <https://pubs.acs.org/doi/10.1021/ja001551s>.
- Lee, Vladimir Ya., Hiroyuki Yasuda, and Akira Sekiguchi. 2007. "Interplay of  $\text{EnE}^3\text{-NC}$  Valence Isomers (E,  $\text{E}^3 = \text{Si, Ge}$ ): Bicyclo[1.1.0]Butanes with Very Short Bridging Bonds and Their

- Isomerization to Alkyl-Substituted Cyclopropenes.” *Journal of the American Chemical Society* 129(9): 2436–37.
- Lee, Vladimir Ya, Masaaki Ichinohe, and Akira Sekiguchi. 2001. “Reaction of 1-Disilagermirene with Benzaldehyde: An Unexpected Combination of Cycloaddition and Insertion Pathways.” *Chemistry Letters* 30(7): 728–29. <https://academic.oup.com/chemlett/article/30/7/728/7404027>.
- Leszczyńska, Kinga et al. 2012. “Reversible Base Coordination to a Disilene.” *Angewandte Chemie International Edition* 51(27): 6785–88. <https://onlinelibrary.wiley.com/doi/10.1002/anie.201202277>.
- Ohmori, Yu et al. 2013. “Functionalized Cyclic Disilenes via Ring Expansion of Cyclotrisilenes with Isocyanides.” *Organometallics* 32(6): 1591–94. <https://pubs.acs.org/doi/10.1021/om400054u>.
- Präsang, Carsten, and David Scheschkewitz. 2016. “Reactivity in the Periphery of Functionalised Multiple Bonds of Heavier Group 14 Elements.” *Chemical Society Reviews* 45(4): 900–921.
- Robinson, Thomas P., Michael J. Cowley, David Scheschkewitz, and Jose M. Goicoechea. 2015. “Phosphide Delivery to a Cyclotrisilene.” *Angewandte Chemie International Edition* 54(2): 683–86.
- Rodriguez, Ricardo et al. 2011. “Reversible Binding of Ethylene to Silylene–Phosphine Complexes at Room Temperature.” *Angewandte Chemie International Edition* 50(44): 10414–16. <https://onlinelibrary.wiley.com/doi/10.1002/anie.201105097>.
- Rogers, D. S., K. L. Walker, M. A. Ring, and H. E. O’Neal. 1987. “Silylene Reactions with Ethylene and Butadiene: Mechanism and Kinetics.” *Organometallics* 6(11): 2313–18. <https://pubs.acs.org/doi/abs/10.1021/om00154a008>.
- Shan, Changkai, Shenglai Yao, and Matthias Driess. 2020. “Where Silylene–Silicon Centres Matter in the Activation of Small Molecules.” *Chemical Society Reviews* 49(18): 6733–54. <http://xlink.rsc.org/?DOI=D0CS00815J>.
- Takeaki Iwamoto, Chizuko Kabuto, and Mitsuo Kira\*. 1999. “The First Stable Cyclotrisilene.” *J. Am. Chem. Soc.* 121: 886–87.
- Tanaka, Hiroaki et al. 2011. “Synthesis and Striking Reactivity of an Isolable Tetrasilyl-Substituted Trisilaallene.” *Organometallics* 30(13): 3475–78. <https://pubs.acs.org/doi/10.1021/om200405e>.
- Uchiyama, Kei et al. 2007. “Thermal and Photochemical Cleavage of SiSi Double Bond in Tetrasila-1,3-Diene.” *Journal of the American Chemical Society* 129(35): 10638–39. <https://pubs.acs.org/doi/10.1021/ja0741473>.
- Weetman, Catherine, and Shigeyoshi Inoue. 2018. “The Road Travelled: After Main- Group Elements as Transition Metals.” *ChemCatChem* 10(19): 4213–28. <https://chemistry-europe.onlinelibrary.wiley.com/doi/10.1002/cctc.201800963>.
- Wendel, Daniel et al. 2017. “From Si(II) to Si(IV) and Back: Reversible Intramolecular Carbon–Carbon Bond Activation by an Acyclic Iminosilylene.” *Journal of the American Chemical Society* 139(24): 8134–37. <https://pubs.acs.org/doi/10.1021/jacs.7b05136>.
- West, Robert, Mark J. Fink, and Josef Michl. 1981. “Tetramesityldisilene, a Stable Compound Containing a Silicon-Silicon Double Bond.” *Science* 214(4527): 1343–44.
- Ya. Lee, Vladimir, Tadahiro Matsuno, Masaaki Ichinohe, and Akira Sekiguchi. 2001. “Interconversion of Cyclotrimetallenes and Dihalocyclotrimetallanes Consisting of Group 14 Elements.” *Heteroatom Chemistry* 12(4): 223–26.
- Ya. Lee, Vladimir, and Akira Sekiguchi. 2010. *Organometallic Compounds of Low-Coordinate Si, Ge, Sn and Pb: From Phantom Species to Stable Compounds*. J. Wiley & Sons, Ltd.,

Yadav, Sandeep, Sumana Saha, and Sakya S. Sen. 2016. "Compounds with Low-Valent P-Block Elements for Small Molecule Activation and Catalysis." *ChemCatChem* 8(3): 486–501. <https://chemistry-europe.onlinelibrary.wiley.com/doi/10.1002/cctc.201501015>.

Zhao, Hui et al. 2018. "Disilyl Silylene Reactivity of a Cyclotrisilene." *Angewandte Chemie International Edition* 57(9): 2445–49.



# Chapter 5

## Reactions of 1,2-bis(trimethylsilyl)-3,3-dimethyl cyclotrisilene with propylene, phenyl acetylene, trimethylsilylacetylene, formaldehyde and benzaldehyde

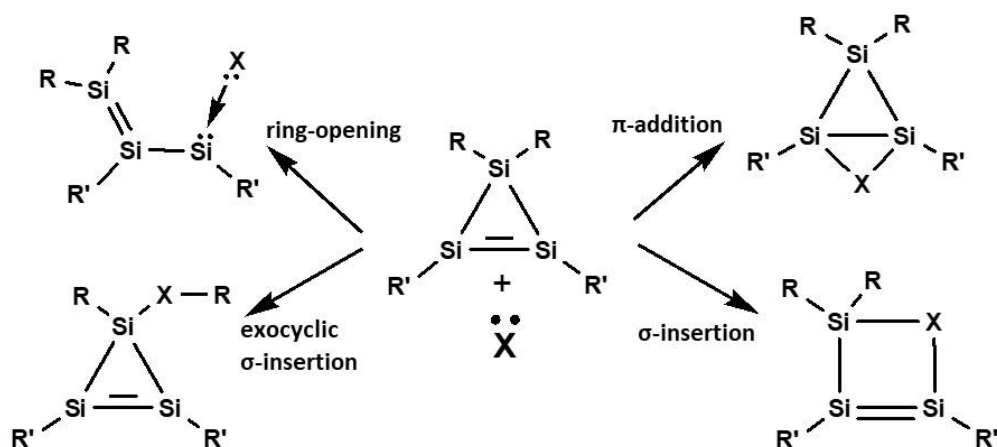
---

### 5.1 Introduction

The chemistry of silicon multiple bonds has expanded dramatically in the past few decades (Scheschkewitz 2009). Even functionalized disilenes ( $\text{Si}=\text{Si}$ ) and silenes ( $\text{Si}=\text{C}$ ) are becoming increasingly available and present tremendous promise as synthetic tools for the transfer of intact silicon-containing double-bond moieties (Scheschkewitz 2011; Sekiguchi and Lee 2003). Conversely, small, unsaturated silacycles (Kira, Iwamoto, and Kabuto 1996) are relatively rare due to their difficulty in synthesis. To date, the few stable examples have been prepared by the reduction of halosilanes (Ichinohe M et al. 2005; Wiberg et al. 2001) reactions of metallosilyl reagents (Abersfelder, Güclü, and Scheschkewitz 2006; Leszczyńska et al. 2012), cycloadditions of disilynes with alkenes (Kinjo et al. 2007; Lee, Yasuda, and Sekiguchi 2007), and thermal or photochemical interconversions (Lee et al. 2008; Uchiyama et al. 2007). Cyclotrisilenes are predominant among them. They are attractive reaction precursors: the incorporation of the silicon-containing double bond into the highly strained three-membered ring allows for functionalizing interventions via ring opening, addition and other type of interactions (Power 1999). The relatively shallow energy profile of this species with silicon-silicon multiple bond manifest the easy polarizability of the electron density, which makes disilenes susceptible to coordination by strong Lewis bases (Fukaya, Ichinohe, and Sekiguchi 2000; Lee et al. 2000; Sekiguchi, Kinjo, and Ichinohe 2004). In addition, the enhanced reactivity arising from the combination of a highly reactive metal–metal double bond and a highly strained three-membered ring skeleton in one molecule, gives access to new cyclic and bicyclic compounds by addition and cycloaddition reactions (Hajgató et al. 2002; Kira and Iwamoto 2006; Lee et al. 2000)

In the previous chapter (Chapter 4) we have carried out a detailed computational analysis of interaction between substituted cyclotrisilene ( $\text{C}-\text{Si}_3\text{R}_4$ ) and molecules carrying multiple bonds. As explained in chapter 4, one can expect four distinct reaction pathways

between an unsaturated reagent and cyclotrisilenes on their encounter. The reactions are categorized as  $\pi$ -addition,  $\sigma$ -insertion, exocyclic  $\sigma$ -insertion and ring opening processes (scheme 5.1).



**Scheme 5.1**

Four distinct reaction pathways that can be expected between cyclotrisilene and an unsaturated substrate on their encounter

To understand the role of steric and electronic effects of substituents on the reactivity of cyclotrisilenes and to get a more realistic picture of the possible reactions, we have analyzed the reactions of 1,2,3,3-tetramethyl cyclotrisilene  $C-(CH_3)_4$  with different substrates possessing multiple bonds and the results are displayed in chapter 4. Interaction with five substrates; three alkynes and two aldehydes were discussed there. In this chapter, we are discussing the results generated in the reactions of the same five substrates with 1,2-bis(trimethylsilyl)-3,3-dimethylcyclotrisilene,  $C-Si_3Me_2(SiMe_3)_2$ , (**II**). The difference in the effect of substituents on the cyclotrisilene molecule (**I** and **II**) over the four types of interactions, viz;  $\pi$ -addition,  $\sigma$ -insertion, ring opening and exocyclic  $\sigma$ -insertion is an additional area of discussion of this chapter.

## 5.2 Objectives

- Computational exploration of possible interactions of 1,2-bis(trimethylsilyl)-3,3-dimethylcyclotrisilene,  $c-Si_3Me_2(SiMe_3)_2$ , (**II**) with five substrates possessing multiple bonds is conducted.
- The substrates employed are phenylacetylene ( $C_6H_5-C\equiv CH$ ; **R1**), propylene ( $CH_3-C\equiv CH$ ; **R2**), trimethylsilylacetylene ( $(CH_3)_3Si-C\equiv CH$ ; **R3**), benzaldehyde ( $C_6H_5-HC=O$ ; **R'1**) and formaldehyde ( $H_2C=O$ ; **R'2**).

- Four reaction path ways;  $\pi$ -addition,  $\sigma$ -insertion, ring opening and exocyclic  $\sigma$ -insertion were explored and the energetics and mechanisms were studied systematically.

### 5.3 Computational Methods

All calculations were carried out at the M06-2X/6-311G(d,p) level of density functional theory using the Gaussian 16 suite of programs. Transition states were optimized by using the Synchronous Transit-Guided Quasi-Newton (STQN) method implemented in Gaussian 16. Minima were ascertained by the IR frequency analysis, and the saddle points were characterized by a single imaginary frequency. The solvent effects (benzene) were accounted by single point calculation at SMD-M06-2X/6-311+G(d,p) level and the single point energy was corrected by adding the thermal correction to Gibbs free energy obtained from the gas phase calculation (at 298.15 K).

### 5.4 Results and discussion

In this chapter, the reactions of 1,2-bis(trimethylsilyl)-3,3-dimethylcyclotrisilene (*c*-Si<sub>3</sub>Me<sub>2</sub>(SiMe<sub>3</sub>)<sub>2</sub>, **II**) with the reactants bearing multiple bonds are discussed.

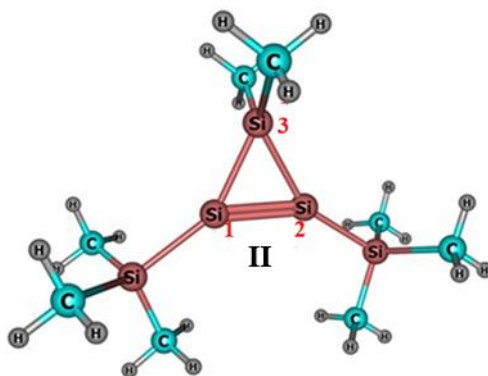


**Figure 5.1** 1,2-bis(trimethylsilyl)-3,3-dimethylcyclotrisilene;**II**

Here also, the reactants used are phenylacetylene (C<sub>6</sub>H<sub>5</sub>-C≡CH; **R1**), propylene (CH<sub>3</sub>-C≡CH; **R2**), trimethylsilyl acetylene ((CH<sub>3</sub>)<sub>3</sub>Si-C≡CH; **R3**), benzaldehyde (C<sub>6</sub>H<sub>5</sub>-HC=O; **R'1**) and formaldehyde (H<sub>2</sub>C=O; **R'2**). As observed in the reaction between **I** and multiple bonded substrates, the reaction between *c*-Si<sub>3</sub>Me<sub>2</sub>(SiMe<sub>3</sub>)<sub>2</sub> molecule (**II**) and a reactant also expected to proceed through any one of the four reaction pathways;  $\pi$ -**addition**,  $\sigma$  – **insertion**, **exocyclic**  $\sigma$  – **insertion** and **ring opening**. We have scrutinised the reaction

profiles of all these pathways between **II** and **R1**, **R2**, **R3**, **R'1** & **R'2** to understand the energetics and mechanisms.

## 5.4.1 Reaction pathways of **c-Si<sub>3</sub>Me<sub>2</sub>(SiMe<sub>3</sub>)<sub>2</sub>(II)** with **C<sub>6</sub>H<sub>5</sub>-C≡CH (R1)**

### 5.4.1.1 $\pi$ -addition

A direct  $2\pi + 2\pi$  addition pathway giving rise to a four membered ring could not be located in this case also. However, a two-step reaction pathway has been identified in the reaction between the acetylenic part of **R1** and the silenyl part of **II**. The intermediates and transitions states located are presented in Figure 5.2

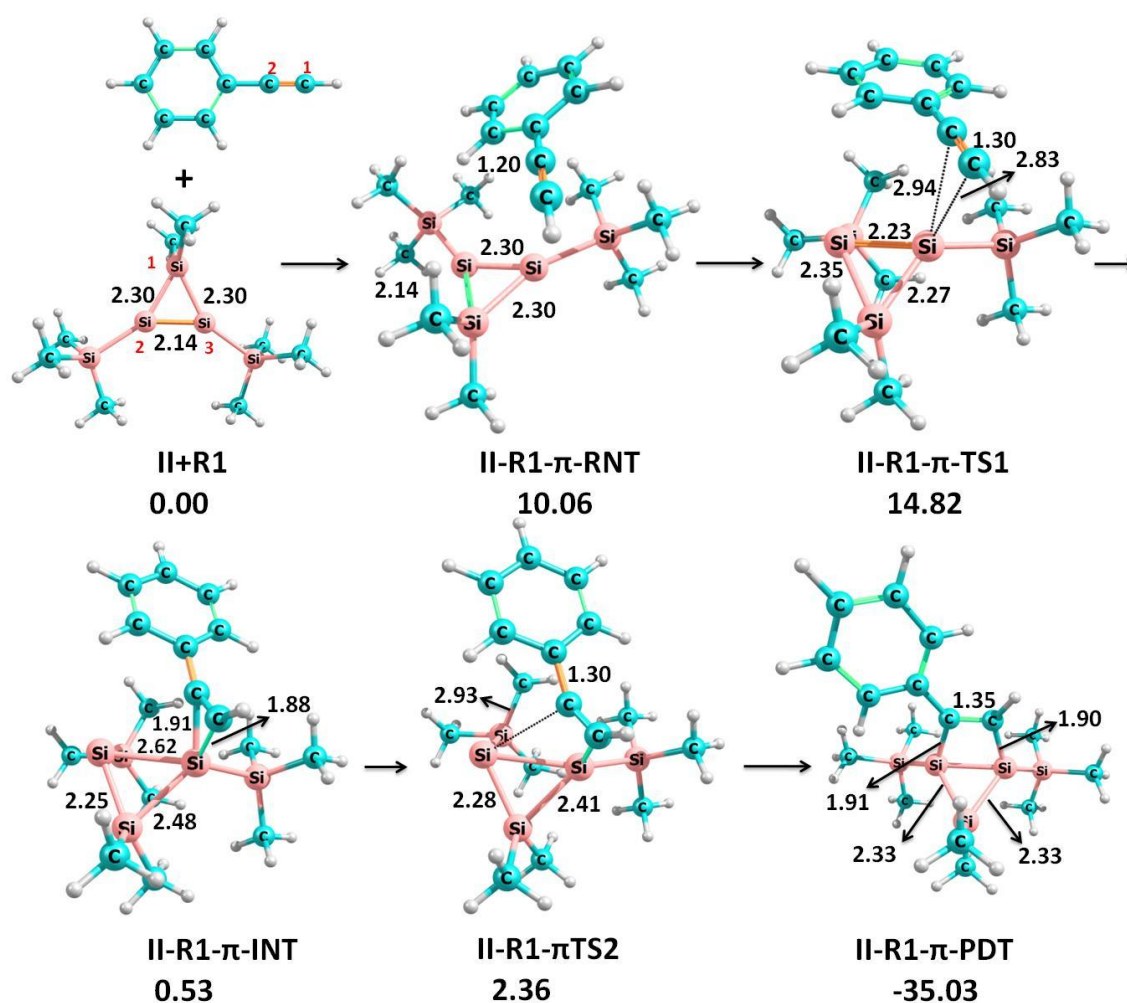


**Figure 5.2** Intermediates and transitions states involved in the  $\pi$ -addition pathway **II** and **R1**. Relative free energies are given in kcal/mol and bond lengths in Å

The initially formed the reactant complex (**II-R1- $\pi$ -RNT**) passed through a transition state **II-R1- $\pi$ -TS1** to form the intermediate **II-R1- $\pi$ -INT**. The transition state corresponds to the interaction of the  $\pi$ -electron cloud of the acetylene group with one of the  $sp^2$  Si atoms ( $Si_{(1)}$ ) and the activation barrier is 14.82 kcal/mol. **II-R1- $\pi$ -INT** transforms into the  $\pi$ -

addition product through a second transition state **II-R1- $\pi$ -TS2**, possessing a barrier height 1.81 kcal/mol. Low barrier heights and the overall exoergic value 35.03 kcal/mol suggest that the  $\pi$ -addition reaction is feasible under normal conditions. Interestingly, the product **II-R1- $\pi$ -PDT** has a bicyclic housane structure, consistent with the experimental reports (H. Zhao et al. 2018), which implies the significant role of the nature substituents on the reactivity of cyclotrisilene

#### 5.4.1.2 $\sigma$ -insertion

The intermediates and transitions states located for  $\sigma$ -insertion reaction between **II** and **R1** is represented in Figure 5.3

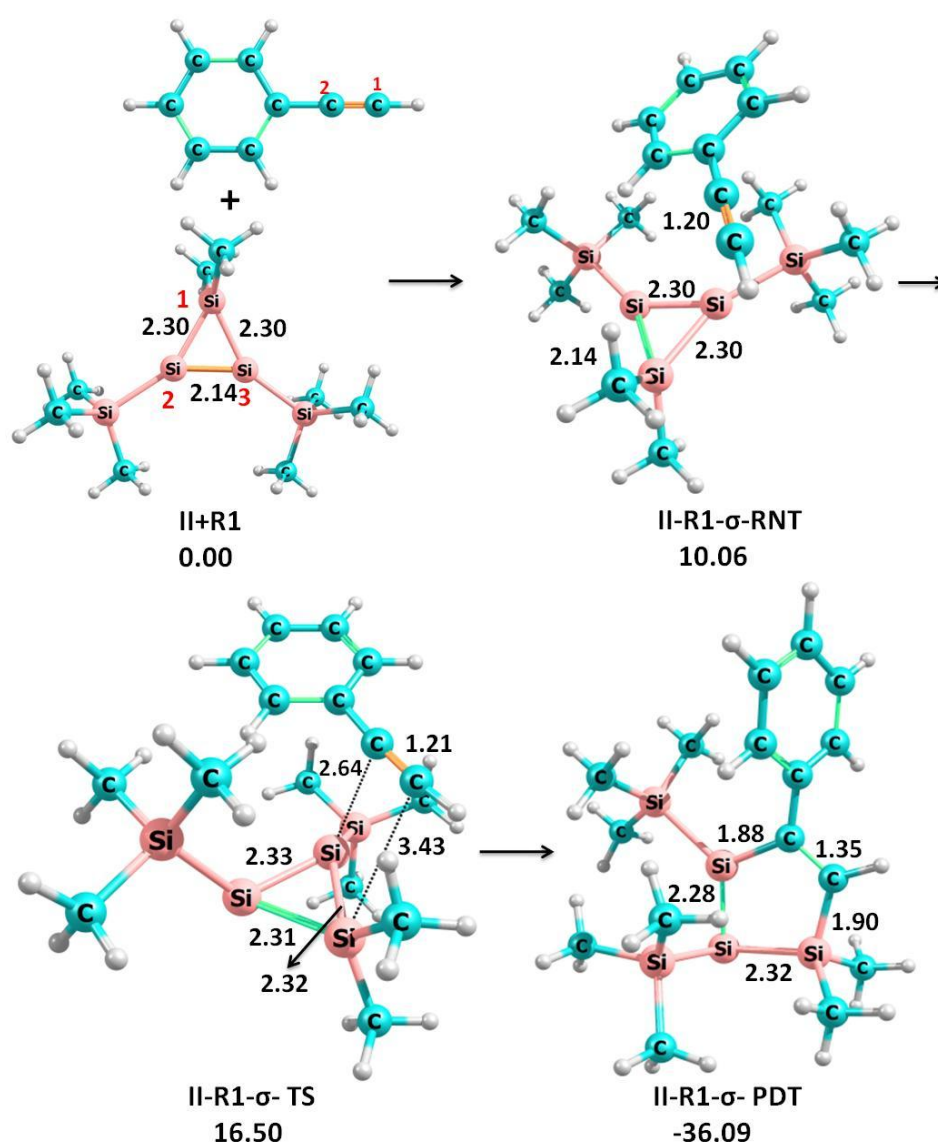


**Figure 5.3** Intermediates and transitions states involved in the  $\sigma$ -insertion pathway of **II** and **R1**. Relative free energies are given in kcal/mol and bond lengths in Å

The  $\sigma$ -insertion reaction of acetylenic group of **R1** into the Si<sub>(1)</sub>-Si<sub>(3)</sub> bond of **II** is observed to be a direct single step process. This insertion is found to be initiated by the formation of the reactant dispersion complex, **II-R1- $\sigma$ -RNT** possessing a relative energy 10.06 kcal/mol. The reactant complex **II-R1- $\sigma$ -RNT** proceeds to a transition state, **II-R1- $\sigma$ -TS** in which the  $\pi$ -electron cloud of the acetylenic group establish strong interactions with one of the sp<sup>2</sup> the silicon atoms (Si<sub>(1)</sub>) and the sp<sup>3</sup> silicon atom (Si<sub>(3)</sub>) of the cyclotrisilene ring. **II-R1- $\sigma$ -TS** is transformed to the final product **II-R1- $\sigma$ -PDT**. The required activation energy is 16.50 kcal/mol, and the overall reaction is exoergic by 36.09 kcal/mol. High exoergicity and low activation barrier indicate that the reaction is feasible under ambient conditions.

#### 5.4.1.3 Ring opening reaction.

The intermediates and transitions states located for the ring opening reaction between **II** and **R1** is represented in Figure 5.4

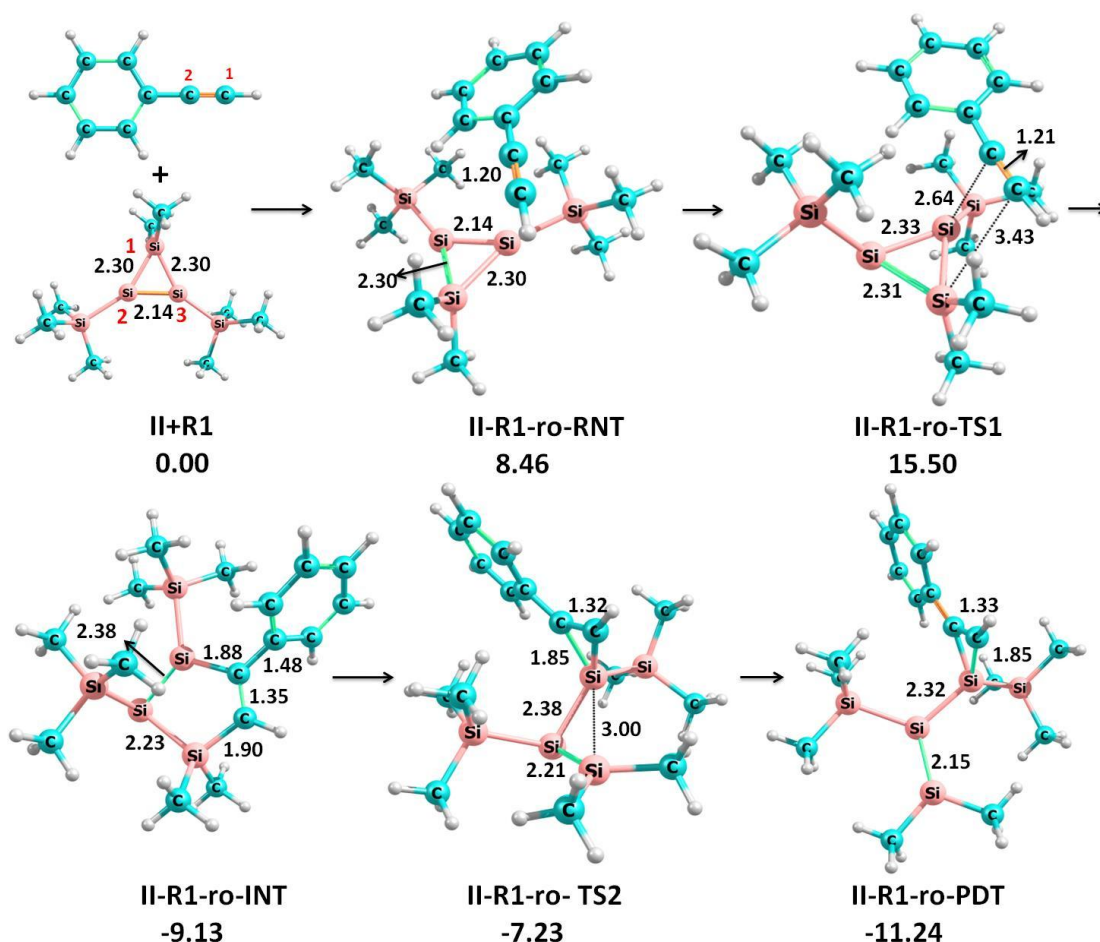


**Figure 5.4** Intermediates and transitions states involved in the ring opening pathway of **II** and **R1**. Relative free energies are given in kcal/mol and bond lengths in Å

The ring opening reaction pathway between **II** and **R1** is very much similar to that of  $\sigma$ -insertion reaction between the two. The initially formed reactant dispersion complex (**II-R1-ro-RNT**) led to the transition state (**II-R1-ro-TS1**) which corresponds to an attack on  $\text{Si}_{(1)}\text{-Si}_{(3)}$  bond of **II** by the  $\pi$  - electron cloud of the acetylene group of **R1**. The reaction is advanced by the transformation of **II-R1-ro-TS1** to an intermediate, **II-R1-ro-INT** is exoergic by 9.13 kcal/mol, and the activation energy is 15.50 kcal/mol.

**II-R1-ro-INT** is progressed to a second transition state, **II-R1-ro-TS2**, during this step, the pentagonal ring structure of the intermediate is ruptured at the  $\text{C-Si}_{(3)}$  bond and a new  $\text{C-Si}_{(1)}$  bond is formed. Meanwhile, a strong interaction is developed between  $\text{Si}_{(1)}$  and  $\text{Si}_{(3)}$  ( $r_{\text{Si}_{(1)}\text{-Si}_{(3)}} = 3.0\text{\AA}$ ). The activated complex **II-R1-ro-TS2** is transformed to the final ring opened product **II-R1-ro-PDT** by the complete rupture of the  $\text{Si}_{(1)}\text{-Si}_{(3)}$  bond. The activation barrier is 1.9 kcal/mol, and the overall reaction is exoergic by 11.24 kcal/mol. The ring-opened product represents a disilene with a silylene moiety stabilized by the coordination of acetylenic group.

#### 5.4.1.4 Exocyclic sigma insertion

The intermediates and transition states located for the exocyclic  $\sigma$ -insertion reaction between **II** and **R1** is represented in Figure 5.5



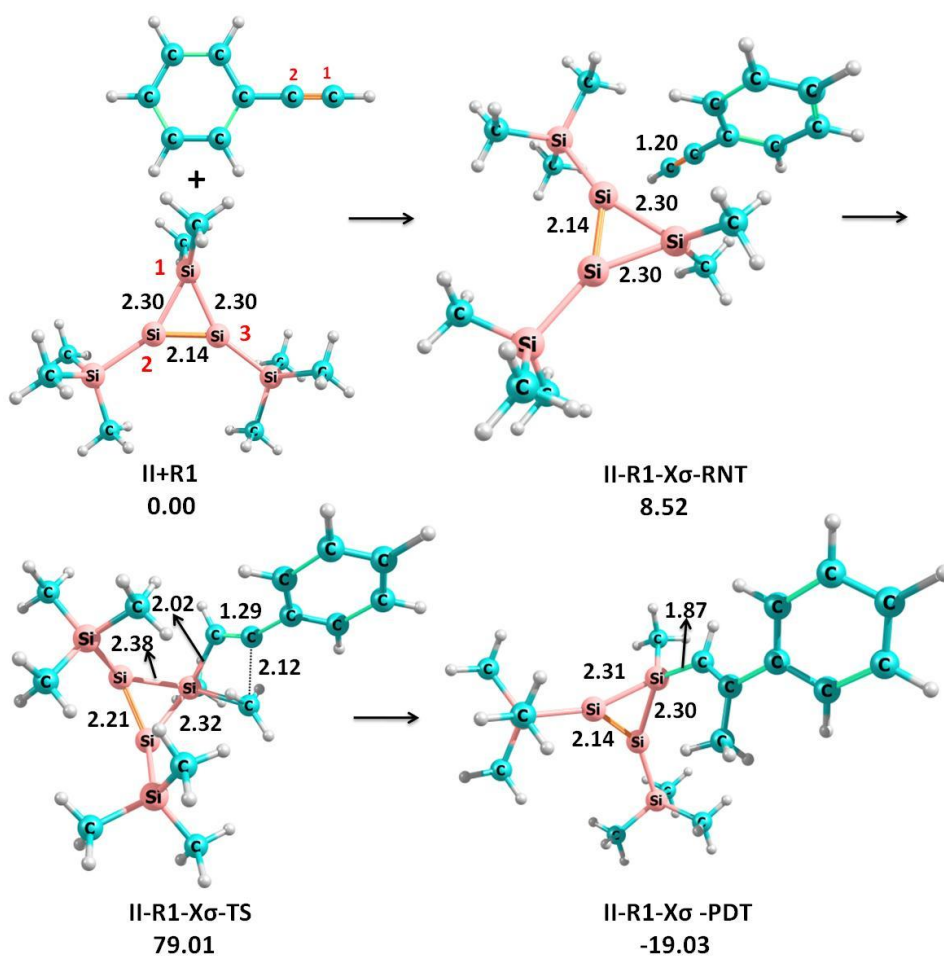


**Figure 5.5** Intermediates and transition states involved in the exocyclic  $\sigma$ -insertion pathway of 1,2-bis(trimethylsilyl)-3,3-dimethyl cyclotrisilene (**II**) and Phenyl acetylene (**R1**). Relative free energies are given in kcal/mol and bond lengths in Å

In the exocyclic  $\sigma$ -insertion, the acetylene group of **R1** inserts into the bond between  $sp^3$  Si atom of the cyclotrisilene ring and a substituent ( $Si_{(3)}-CH_3$ ) of **II**. The initially formed reactant dispersion complex **II-R1-x $\sigma$ -RNT** has a relative energy 8.52 kcal/mol. The reactant complex is advanced to an activated complex **II-R1-x $\sigma$ -TS1** which can directly transformed to the product, **II-R1-x $\sigma$ -PDT**. Despite the overall reaction being exoergic by 19.03 kcal/mol, the reaction is kinetically impossible at ambient conditions due to a high activation barrier of 79.01 kcal/mol.

Free energy profile diagrams of the four reaction pathways between **II** and **R1** are given in Figure 5.6



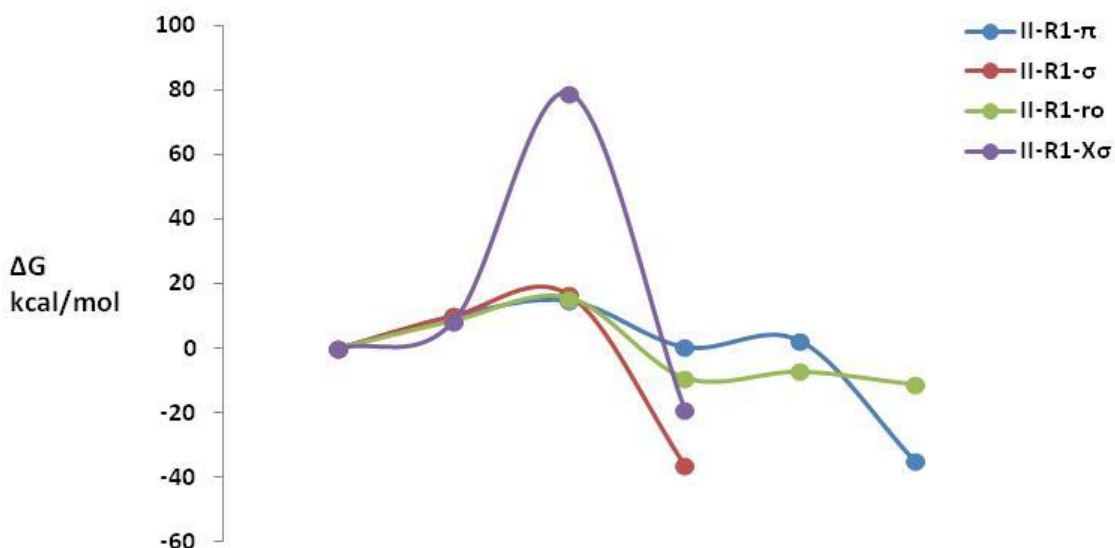


**Figure 5.6** Comparative free energy profile diagram for the different reaction pathways between **II** and **R1**.

Out of the four reaction pathways between **II** and **R1** demonstrated above, the  $\sigma$ -insertion reaction and the exocyclic  $\sigma$ -insertion reactions are direct conversion of the reactants to products. The other two; the  $\pi$ -addition reaction and the ring opening reaction, are calculated to be two-step processes. The  $\pi$ -addition reaction generated a housane shaped product with the bridging bond connecting two Si atoms, whereas the  $\sigma$ -insertion yielded a pentagonal product carrying a Si-Si double bond. The reaction pathway is found to be more stabilized in the  $\pi$ -addition reaction. Even though less exothermic, the ring opening reaction pathway is also commendably stabilized.

Energetics of the four possible reaction pathways between **II** and **R1** suggest that the  $\pi$ -addition,  $\sigma$ -insertion, and ring opening reactions are feasible under normal conditions, whereas the exocyclic  $\sigma$ -insertion is kinetically not feasible.

## 5.4.2 Reaction pathways of $c\text{-Si}_3\text{Me}_2(\text{SiMe}_3)_2$ (**II**) and $\text{CH}_3\text{-C}\equiv\text{CH}$ (**R2**)

### 5.4.2.1 $\pi$ -addition

As observed with **II** and **R1**, a direct  $2\pi + 2\pi$  addition pathway, generating a four membered ring addition product could not be located in this case also. Instead, a two-step reaction pathway has been identified for the reaction between the acetylenic group of **R2** and the silenyl part of **II**. The intermediates and transition states located are presented in Figure 5.7

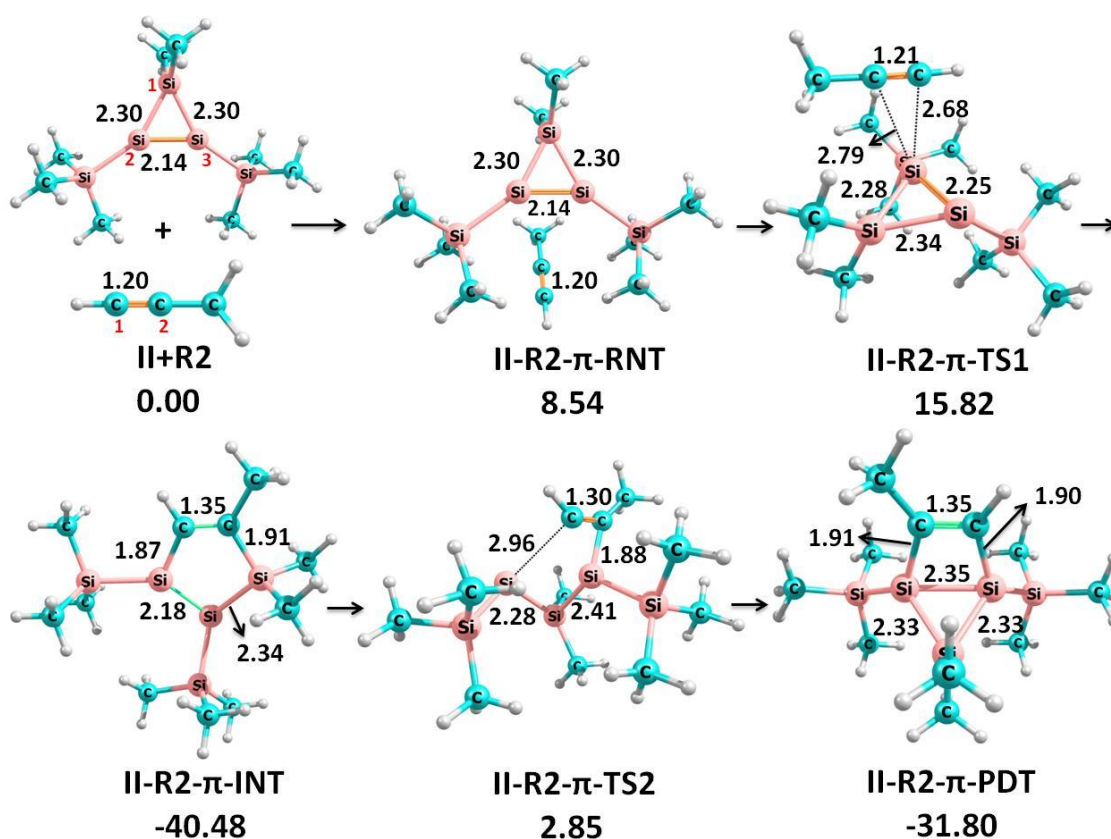


**Figure 5.7** Intermediates and transitions states involved in the  $\pi$ -addition pathway of **II** and **R2**. Relative free energies are given in kcal/mol and bond lengths in Å.

The  $\pi$ -addition reaction between **II** and **R2** commenced by the formation of a reactant complex **II-R2- $\pi$ -RNT** bearing a relative energy 8.54kcal/mol. The reactant complex advanced to an activated complex **II-R2- $\pi$ -TS1**, the  $\pi$ -electron cloud of the acetylenic part of **R2** established a strong interaction with the tricoordinate Si<sub>(1)</sub> of **II**, which primarily affected the Si<sub>(1)</sub>-Si<sub>(2)</sub> double bond ( $r_{\text{Si}(1)\text{-Si}(2)} = 2.25\text{Å}$ ). The activation energy required for the formation of **II-R2- $\pi$ -INT** is 15.82 kcal/mol. Formation of **II-R2- $\pi$ -INT** is highly exoergic as revealed by its very low relative energy, -40.48 kcal/mol. The pentagonal ring shaped intermediate bears a double bond between Si<sub>(1)</sub> and Si<sub>(2)</sub> which is in conjugation with C=C and in fact, it is same in structure as the  $\sigma$ -insertion product between **II** and **R2**.

The reaction is advanced further by the transfiguration of **II-R2- $\pi$ -INT** to a new activated complex **II-R2- $\pi$ -TS2**. The highly endoergic character of this step indicates the stability of the intermediate. The transition state **II-R2- $\pi$ -TS2** is rearranged to the housane-shaped **II-R2- $\pi$ -PDT**. Even though the overall reaction is exoergic by 31.80 kcal/mol, the high second activation barrier of 37.63 kcal/mol suggests the thermodynamic and kinetic non-feasibility of the reaction.

### 5.4.2.2 $\sigma$ -insertion

The intermediate and the transition state located for the  $\sigma$ -insertion reaction between **II** and **R2** is represented in Figure 5.8

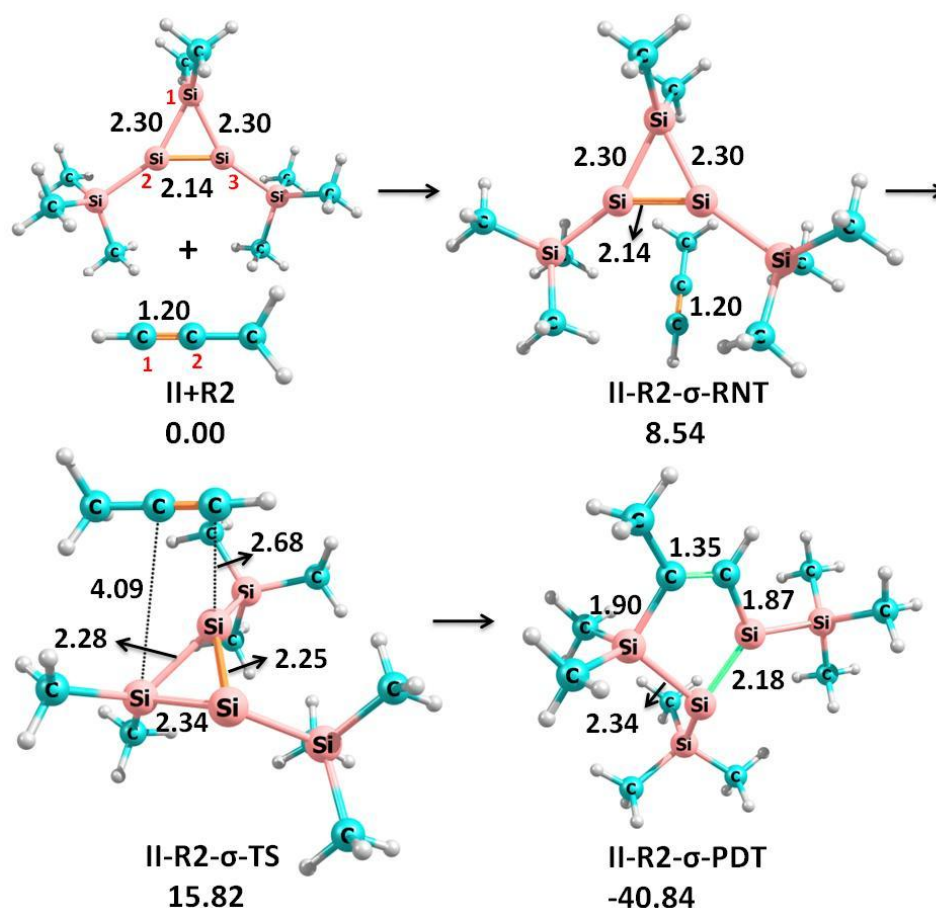


**Figure 5.8** Intermediates and transition states involved in the  $\sigma$ -insertion pathway **II** and **R2**. Relative free energies are given in kcal/mol and bond lengths in Å.

During the  $\sigma$ -insertion reaction between **II** and **R2**, the initially formed reaction complex **II-R2- $\sigma$ -RNT**, with relative energy 8.54 kcal/mol transformed to an activated complex **II-R2- $\sigma$ -TS**. The activated complex is characterized by the a weakened  $\text{Si}_{(1)}\text{-Si}_{(2)}$  double bond ( $r_{\text{Si}_{(1)}\text{-Si}_{(2)}} = 2.25$  Å) and a strong interaction-buildup across the  $\text{Si}_{(1)}\text{-Si}_{(3)}$   $\sigma$ -bond of **II** and the acetylenic  $\pi$ -bond of **R2**. The new interaction-buildup is principally at the expense of the weakening of the  $\text{Si}=\text{Si}$  double bond; as obvious from the changes induced on the other bonds, which are quite minor ( $r_{\text{Si}_{(1)}\text{-Si}_{(3)}} = 2.34$  Å,  $r_{\text{Si}_{(2)}\text{-Si}_{(3)}} = 2.28$  Å). The activated complex **II-R2- $\sigma$ -TS** is directly transformed to the product **II-R2- $\sigma$ -PDT**, by the completion of the  $\text{Si}_{(1)}\text{-C}_{(1)}$  and  $\text{Si}_{(3)}\text{-C}_{(2)}$  interactions to proper  $\sigma$ -bonds and the cleavage of the  $\text{Si}_{(1)}\text{-Si}_{(3)}$  bond. The product is a pentagonal shaped one with  $\text{Si}_{(1)}\text{-C}_{(1)}$  and  $\text{Si}_{(3)}\text{-C}_{(2)}$  bond distances 1.87 Å and 1.90 Å respectively. The  $\text{Si}_{(1)}\text{-Si}_{(2)}$  bond maintain its double bond status in the final

product also, with a bond length 2.18Å. The activation barrier for the  $\sigma$ -insertion is 15.82 kcal/mol, and the formation of the pentagonal product **I-R1- $\sigma$ -PDT** is exoergic by 40.48 kcal/mol. The high exoergicity and low activation energy of the  $\sigma$ -insertion reaction between **II** and **R2** confirms its practicability under normal laboratory conditions.

### 5.4.2.3 Ring opening

The intermediates and transitions states located for the ring opening reaction between **II** and **R2** is represented in Figure 5.9

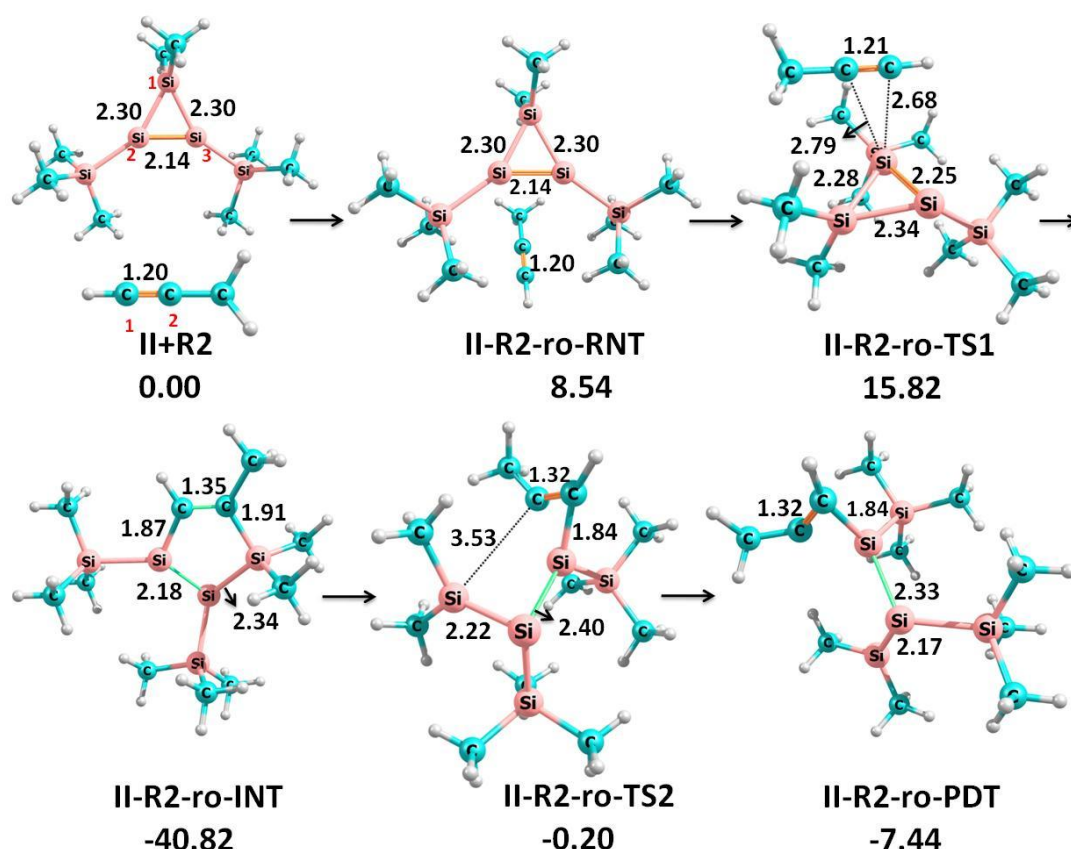


**Figure 5.9** Intermediates and transitions states involved in the ring opening pathway of **II** and **R2**. Relative free energies are given in kcal/mol and bond lengths in Å.

The ring opening reaction between with **II** and **R2** commenced by the formation of a reactant dispersion complex, **II-R2-ro-RNT** which has a relative energy 8.54 kcal/mol. The reactant complex is advanced to an activated complex **II-R2-ro-TS1**. At this point of the reaction, a strong interaction is developed between the  $\pi$ -electron cloud of the acetylenic group of **R2** and Si<sub>(1)</sub> of **II**. The activated **II-R2-ro-TS1** is advanced to an intermediate **II-R2-ro-INT**, is exoergic by 40.82 kcal/mol, and the activation energy is 15.82 kcal/mol. The highly exoergic nature of this step confirms the extensively stabilized structure of the intermediate. It worth noticing that the intermediate formed in the ring opening reaction

closely resembles the corresponding intermediate **II-R2- $\pi$ -INT** that formed during the  $\pi$ -addition reaction. Interestingly, both are equivalent to the  $\sigma$ -insertion reaction product **II-R2- $\sigma$ -PDT**.

**II-R2-ro-INT** is advanced to a second transition state, **II-R2-ro-TS2**. The completion of the breaking of the C-Si<sub>(3)</sub> bond resulted in the formation of the ring opened product **II-R2-ro-PDT**. The activation barrier is 37.82 kcal/mol, and the overall reaction is exoergic by 7.44 kcal/mol. Even though, the ring opening reaction between **II** and **R2** is an exoergic process, the high activation energy at the second step indicates the difficulty in achieving it under the ambient conditions.

#### 5.4.2.4 Exocyclic $\sigma$ -insertion

The Intermediates and transitions states located for the exocyclic  $\sigma$ -insertion reaction between **II** and **R2** is represented in Figure 5.10

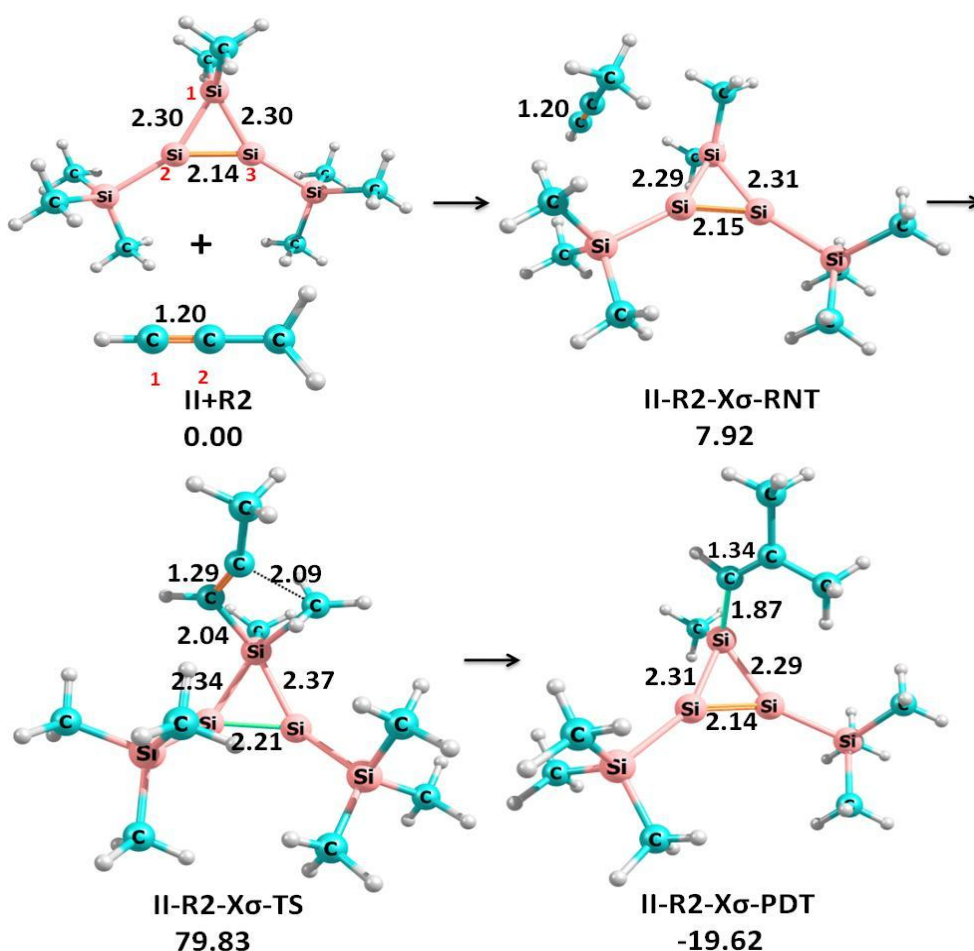


**Figure 5.10** Intermediates and transition states involved in the exocyclic  $\sigma$ -insertion pathway of **II** and **R2**. Relative free energies are given in kcal/mol and bond lengths in Å.



In the exocyclic  $\sigma$ -insertion, the acetylenic part of **R2** inserts into the  $\sigma$ -bond between the  $sp^3$  Si atom of **II** and one of the substituents attached to it ( $Si_{(3)}-CH_3$  bond). The initially formed reactant complex **II-R2-x $\sigma$ -RNT** has a relative energy 7.92 kcal/mol. The reactant complex progressed to an activated complex **II-R2-x $\sigma$ -TS** which can directly transform to the product **II-R2-x $\sigma$ -PDT**. However, the advancement of **II-R2-x $\sigma$ -RNT** to the activated complex involves a formidable energy barrier of 79.83 kcal/mol. Despite the overall reaction being exoergic by 19.62 kcal/mol, the reaction is kinetically unachievable at ambient conditions due to the very high activation barrier.

Free energy profile diagrams of the four reaction pathways between **II** and **R2** are given in Figure 5.11

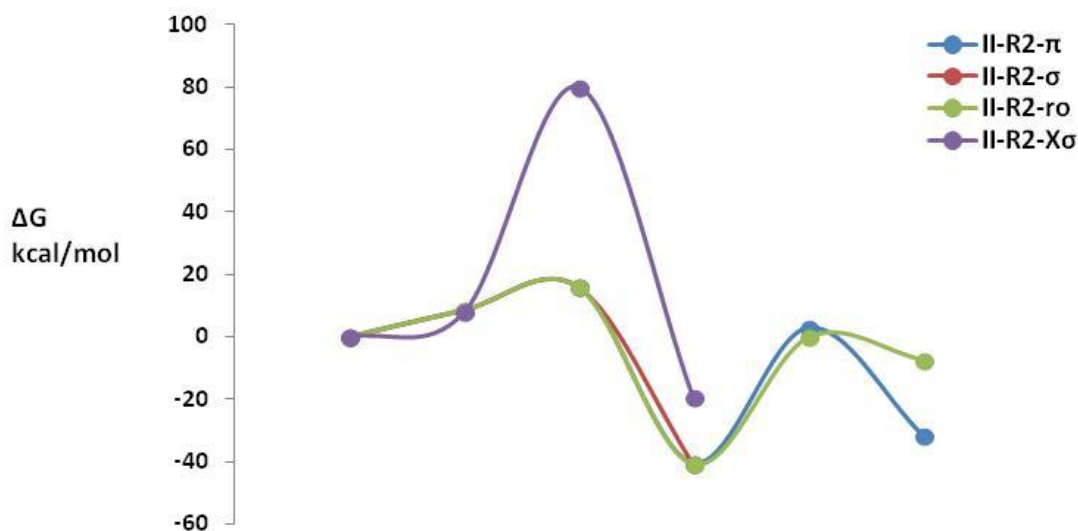


**Figure 5.11** Comparative free energy profile diagram for the different reaction pathways between **II** and **R2**

Out of the four reaction pathways between **II** and **R2** discussed above, the  $\sigma$ -insertion reaction and the exocyclic  $\sigma$ -insertion reactions are direct single-step conversion of the reactants to products. The other two; the  $\pi$ -addition reaction and the ring opening reaction, are calculated to be two-step processes. The  $\pi$ -addition reaction generated a housane shaped product with the bridging bond connecting two Si atoms, where as the  $\sigma$ -insertion yielded a pentagonal product carrying a Si=Si double bond. It is to be noticed that, the ring opening reaction and  $\pi$ -addition pathway are advanced through the  $\sigma$ -insertion product which is formed as an intermediate in both cases. This means that, the  $\pi$ -addition and ring opening reactions are extensions the  $\sigma$ -insertion reaction and the  $\sigma$ -insertion is the spontaneous

reaction between **II** and **R2**. Even though, the  $\sigma$ -insertion,  $\pi$ - addition and ring opening reactions are calculated to be exoergic, the last two involved forbidding activation energy. As usual, the exocyclic  $\sigma$ -insertion is also involved an exorbitant energy barrier. Energetics of the four possible reaction pathways between **II** and **R2** suggest that only  $\sigma$ -insertion reaction is feasible under ambient conditions.

### 5.4.3 Reaction pathways of $c\text{-Si}_3\text{Me}_2(\text{SiMe}_3)_2$ (**II**) with $(\text{CH}_3)_3\text{Si-C}\equiv\text{CH}$ (**R3**)

#### 5.4.3.1 $\pi$ -addition

A two-step reaction pathway has been identified for the  $\pi$ -addition reaction between the acetylenic group of **R3** and the silenyl part of **II**. The intermediates and transitions states located for the reaction are presented in Figure 5.12

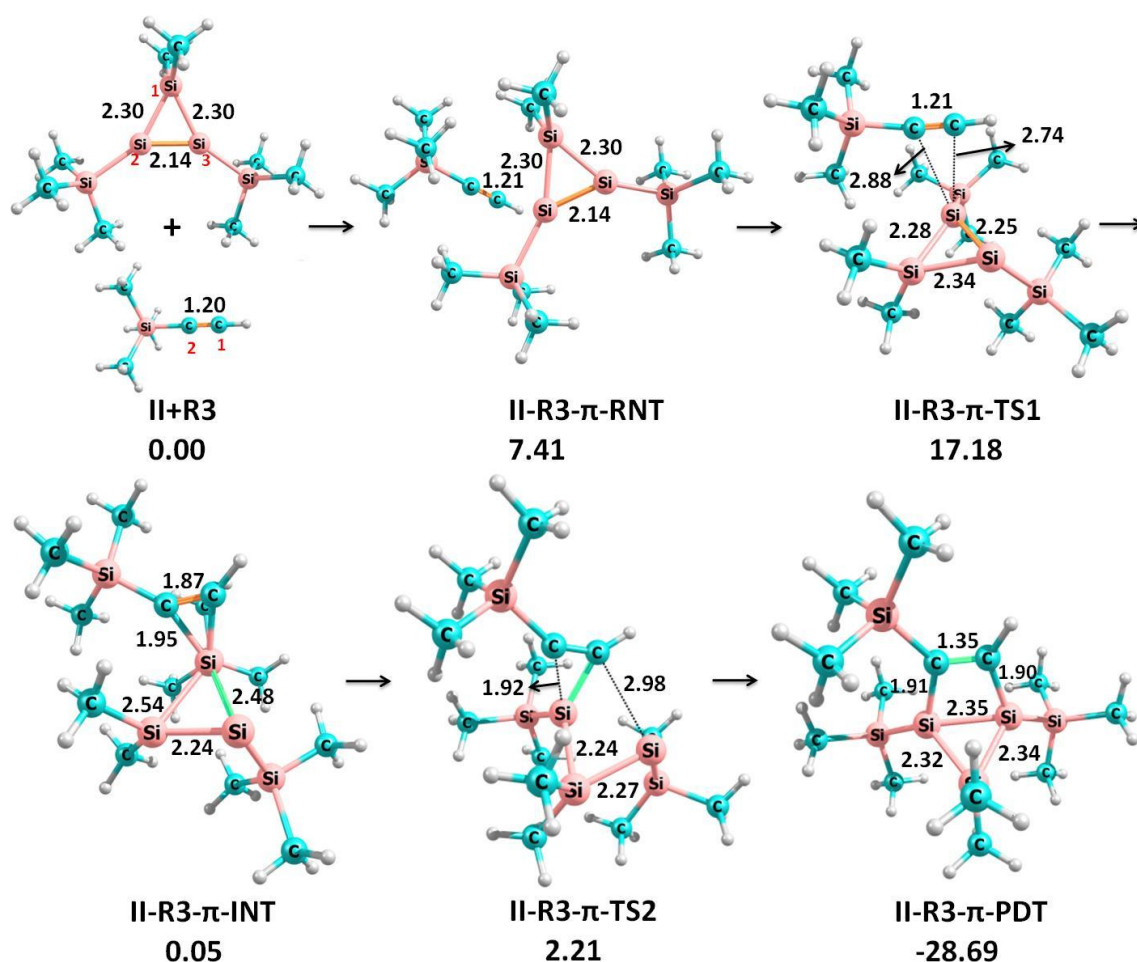


**Figure 5.12** Intermediates and transitions states involved in the  $\pi$ -addition pathway of **II** and **R3**. Relative free energies are given in kcal/mol and bond lengths in Å.

The commencement of the reaction is marked by the formation of a reactant dispersion complex between **II** and **R3**, **II-R3- $\pi$ -RNT** with a relative energy 7.41 kcal/mol.

The dispersion complex is proceeding to a transition state **II-R3- $\pi$ -TS1**, In **II-R3- $\pi$ -TS1**, both the methyl groups of silenyl moiety ( $\text{Si}_{(1)}$  and  $\text{Si}_{(2)}$ ) moves out from the cyclotrisilene plane and the  $\pi$ -electron cloud of the alkyne interacts with one of the unsaturated Si atoms of **II** ( $\text{Si}_{(1)}$ ) leading to a considerable weakening of the  $\text{Si}_{(1)}=\text{Si}_{(2)}$  double bond, as indicated by the extension of the bond distance from 1.14Å to 2.25Å.

**II-R3- $\pi$ -TS1** is advanced to an intermediate **II-R3- $\pi$ -INT**. The activation energy required for the formation of **II-R3- $\pi$ -INT** is 17.18 kcal/mol. Strong bonding interaction of the acetylenic group of **R3** with the ring silicon atom  $\text{Si}_{(1)}$  of **II** in **II-R3- $\pi$ -INT** led to the rupture of the  $\pi$ -bond between  $\text{Si}_{(1)}$  and  $\text{Si}_{(2)}$  ( $r_{\text{Si}_{(1)}=\text{Si}_{(2)}} = 2.48 \text{ \AA}$ ) and an elongation of the  $\text{Si}_{(1)}-\text{Si}_{(3)}$  bond ( $r_{\text{Si}_{(1)}-\text{Si}_{(3)}} = 2.54 \text{ \AA}$ ). **II-R3- $\pi$ -INT** progresses to the second transition state **II-R3- $\pi$ -TS2**. The activated complex **II-R3- $\pi$ -TS2** is transformed to the housane-shaped  $\pi$ -addition product **II-R3- $\pi$ -PDT** with activation barrier is 2.16, the low activation barrier and high exoergic (-28.69 kcal/mol) nature of the reaction support its feasibility under ambient conditions.

#### 5.4.3.2 $\sigma$ -insertion

The intermediates and transitions states calculated for the exocyclic  $\sigma$ -insertion reaction between **II** and **R3** is represented in Figure 5.13



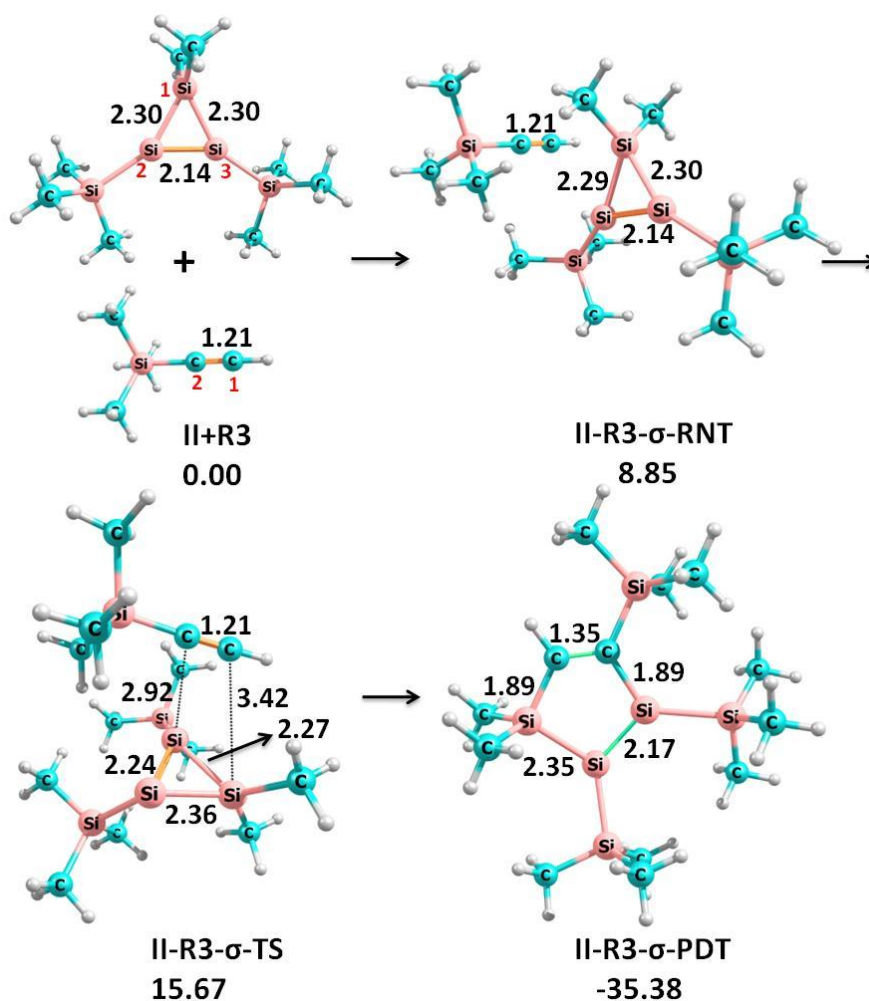


**Figure 5.13** Intermediates and transitions states involved in the  $\sigma$ -insertion pathway of **II** and **R3**. Relative free energies are given in kcal/mol and bond lengths in Å.

The  $\sigma$ -insertion reaction of the acetylenic group of **R3** into the  $\text{Si}_{(1)}\text{-Si}_{(3)}$   $\sigma$ -bond of **II** is a single step process that is initiated by the formation of a reactant dispersion complex **II-R3- $\sigma$ -RNT** possessing a relative energy 8.85 kcal/mol. The dispersion complex proceeded to a transition state, **II-R3- $\sigma$ -TS** in which the acetylenic group is oriented along  $\text{Si}_{(1)}\text{-Si}_{(3)}$  bond. Activation barrier for the  $\sigma$ -insertion reaction is 15.67 kcal/mol. During the formation of the transition state the  $\pi$ -electron cloud of the acetylenic group of **R3** develop strong interactions with the ring silicon atoms  $\text{Si}_{(1)}$  and  $\text{Si}_{(3)}$  of **II**. The activated complex **II-R3- $\sigma$ -TS** is straightly trasformed to the product **II-R3- $\sigma$ -PDT** by the rupture of the  $\text{Si}_{(1)}\text{-Si}_{(3)}$   $\sigma$ -bond and the insertion of the acetylenic group across the two Si atoms. The pentagonal ring structured product has a well defined structure and the valency of each Si atom is perfectly satisfied. The reaction is exoergic by 35.38 kcal/mol. The high exoergicity and a moderate activation barrier can be attributed to the release of ring strain associated with the cyclotrisilene and also to the well-difined structure of the product. The relatively low activation energy and high

exoergicity of the  $\sigma$ -insertion reaction suggests that, it would be the preferred pathway between **II** and **R3** in comparison with the  $\pi$ -addition.

### 5.4.3.3 Ring opening

The intermediates and transition states located for the ring opening reaction between **II** and **R3** is represented in Figure 5.14

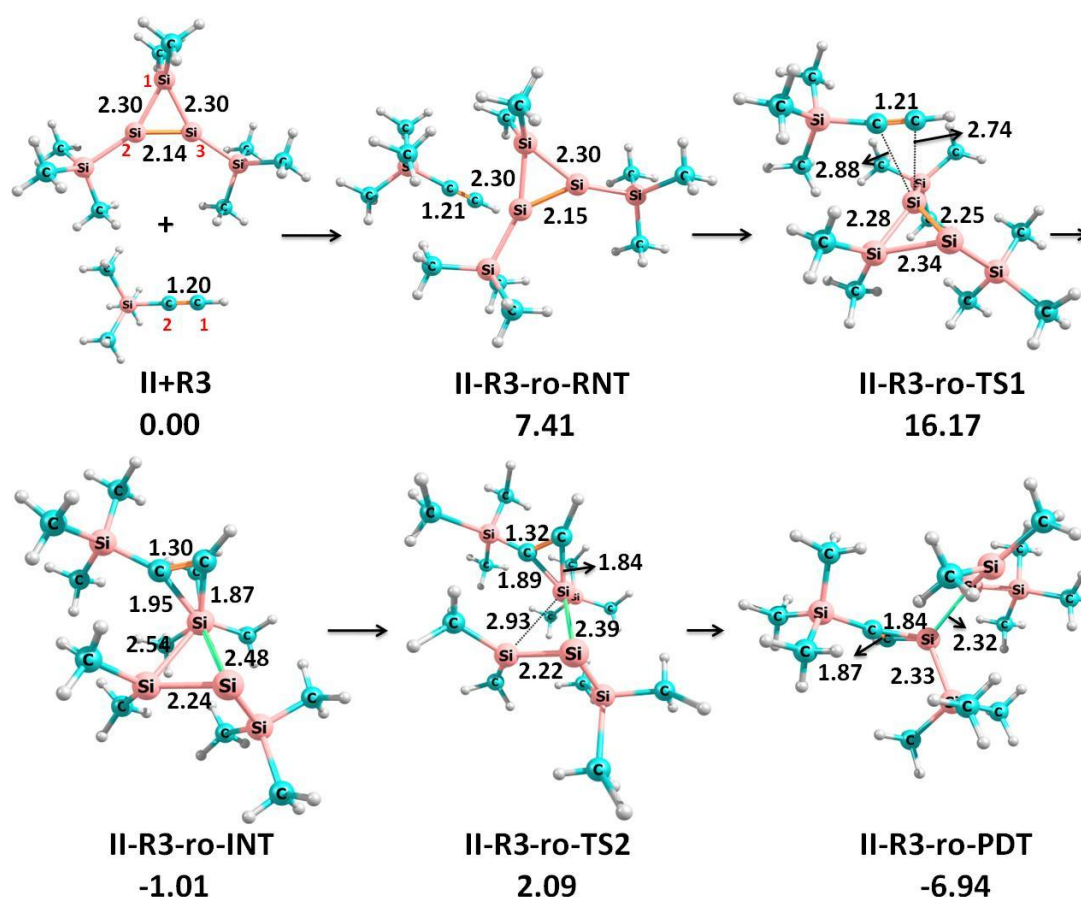


**Figure 5.14** Intermediates and transitions states involved in the ring opening reaction pathway of **II** and **R3**. Relative free energies are given in kcal/mol and bond lengths in Å.

The course of the ring opening reaction between **II** and **R3** is very much similar to that of  $\pi$ -addition reaction between the two. The initially formed reactant dispersion complex (**II-R3-ro-RNT**) possessing a relative energy 7.41 kcal/mol is transformed to a transition state, **II-R3-ro-TS1**. This transition state is formed by the attack on the tricoordinate Si atom ( $\text{Si}_{(1)}$ ) of the trisilene ring by the  $\pi$  - electron cloud of the acetylenic group of **R3**. The transition state is further advanced to an intermediate **II-R3-ro-INT**. The activation energy required for the formation of **I-R3-ro-INT** is 16.17 kcal/mol, in which the acetylenic group strongly bound to the  $\text{Si}_{(1)}$ , which led to the elongation of  $\text{Si}_{(1)}\text{-Si}_{(2)}$  and  $\text{Si}_{(1)}\text{-Si}_{(3)}$  bonds ( $r_{\text{Si}_{(1)}\text{-Si}_{(2)}} = 2.48 \text{ \AA}$ ,  $r_{\text{Si}_{(1)}\text{-Si}_{(3)}} = 2.54 \text{ \AA}$ ). The intermediate **II-R3-ro-INT** is advanced to the

second transition state **II-R3-ro-TS2** by the weakening of the Si<sub>(1)</sub>-Si<sub>(3)</sub> bond ( $r_{\text{Si}(1)\text{-Si}(3)} = 2.93\text{\AA}$ ). The complete cleavage of Si<sub>(1)</sub>-Si<sub>(3)</sub> bond in the transition state **II-R3-ro-TS2** completed the course of the reaction by the formation of the ring opened product, **II-R3-ro-PDT**. The activation barrier is 3.1 kcal/mol, and the overall reaction is exoergic by 6.94 kcal/mol. The ring-opened product represents a disilene with a silylene moiety stabilized by the coordination of acetylenic group.

#### 5.4.3.4 Exocyclic $\sigma$ -insertion

The intermediates and transition states located for the exocyclic  $\sigma$ -insertion reaction between **II** and **R3** is represented in Figure 5.15

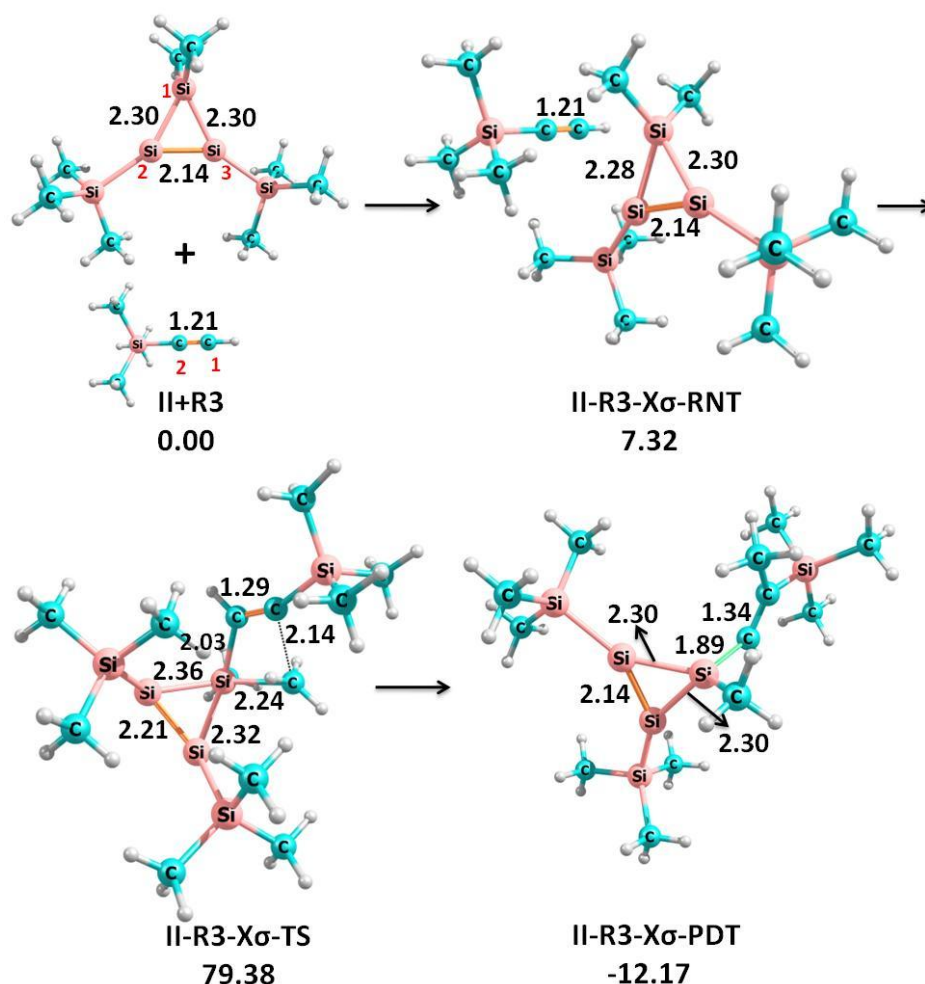


**Figure 5.15** Intermediates and transition states involved in the exocyclic  $\sigma$ -insertion reaction pathway of **II** and **R3**. Relative free energies are given in kcal/mol and bond lengths in  $\text{\AA}$ .

In the exocyclic  $\sigma$ -insertion, the acetylene part of **R3** inserts into the bond between  $\text{sp}^3$  Si atom of **II** and a methyl substituent (Si<sub>(3)</sub>-CH<sub>3</sub>  $\sigma$ -bond). The initially formed reactant dispersion complex **II-R3-x $\sigma$ -RNT** has a relative energy 7.32 kcal/mol. The reactant complex

changed to an activated complex **II-R3- $\chi\sigma$ -TS** which is directly converted to the product **II-R3- $\chi\sigma$ -PDT**. However, the advancement of **II-R3- $\chi\sigma$ -RNT** to the activated complex involves huge energy barrier of 79.38 kcal/mol. The steric environment which invites high steric pressure for the approach of the reacting species towards each other and the difficulty in attacking a stable saturated Si-C bond explains the much elevated activation energy. Despite the overall reaction being exoergic by 12.17 kcal/mol, the reaction is kinetically impossible at ambient laboratory conditions due to the high activation barrier.

Free energy profile diagrams of the four reaction pathways between **II** and **R3** are given in Figure 5.16

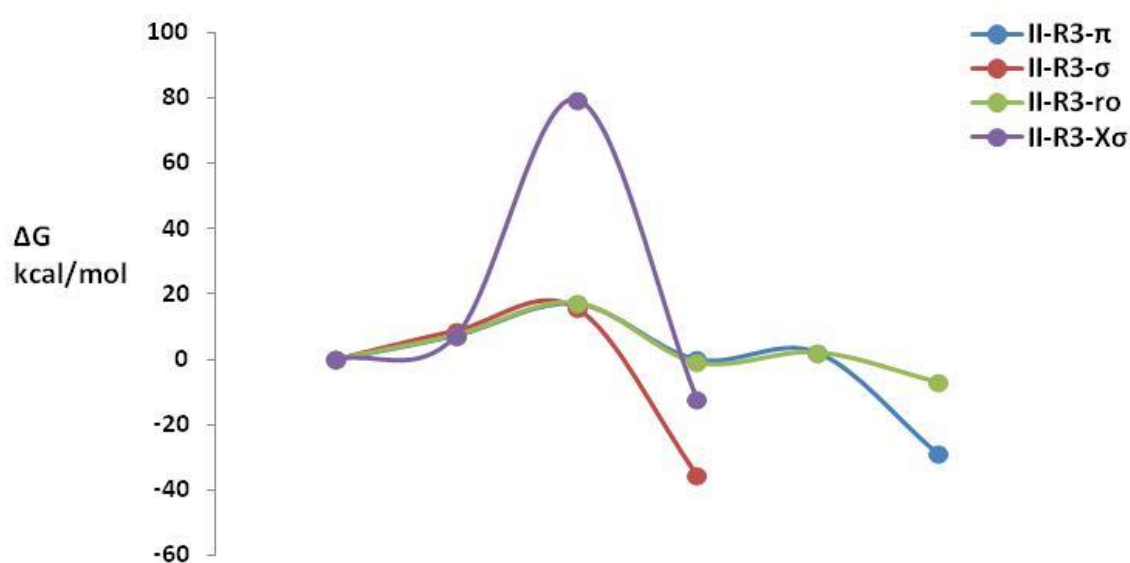


**Figure 5.16** Comparative free energy profile diagram for the different reaction pathways between **II** and **R3**

Out of the four reaction pathways between **II** and **R3** discussed above, the  $\sigma$ -insertion reaction and the exocyclic  $\sigma$ -insertion reactions are direct single-step conversion of the reactants to products. The other two; the  $\pi$ -addition reaction and the ring opening reaction, are found to be two-step processes. The  $\pi$ -addition reaction generated a house-shaped product with the bridging bond connecting two Si atoms, whereas the  $\sigma$ -insertion yielded a pentagonal product carrying a Si-Si double bond. It to be noticed that the ring opening and  $\pi$ -addition pathways are advanced through similar structures till the formation of the second activated complex. The divergence of the pathways emerged with the second transition state as the difference in the selection of in the Si-Si bond subjected to the breaking. Even though, the energetics suggest the feasibility of  $\pi$ -addition,  $\sigma$ -insertion and ring opening reactions between **II** and **R3** under ambient conditions; the spontaneous nature, the lowest activation

energy and the highest exoergicity made the  $\sigma$ -insertion reaction the most preferred pathway with this pair of reactants. The exocyclic  $\sigma$ -insertion is kinetically not feasible due to the exorbitant energy barrier.

Comparing the reactivities of **R1**, **R2**, and **R3** with **II**, the glaring speciality is the inability of **R2** to proceed spontaneously in the  $\pi$ -addition as well as ring opening pathways due to the formidable activation energy associated with the formation of the second transition state. Yet, the  $\sigma$ -insertion reaction of **R2** with **II** is calculated to be highly feasible with low activation energy and high exoergicity. In effect, the intermediates formed in the former two pathways involving **R2** are the  $\sigma$ -insertion product formed by it. However with **R1** and **R3** all the three classes of the reaction paths are feasible under ambient conditions owing to the low activation energy and high exoergicity. The direct formation of the product and highest exoergicity of the  $\sigma$ -insertion reaction confirm its easy attainment compared with the other two pathways. The exocyclic  $\sigma$ -insertion reaction is unattainable with all the three substrates due to the exorbitant activation energy.

#### **5.4.4 Reaction pathways of $\text{c-Si}_3\text{Me}_2(\text{SiMe}_3)_2(\text{II})$ with $\text{C}_6\text{H}_5\text{-CHO}$ (**R'1**)**

##### **5.4.4.1 $\pi$ -addition.**

As observed in the reaction between **II** and **R1**, a two-step reaction pathway has been identified for the reaction between the carbonyl group of **R'1** and the silyl part of **II**. Intermediates and transition states located for the reaction is represented in Figure 5.17

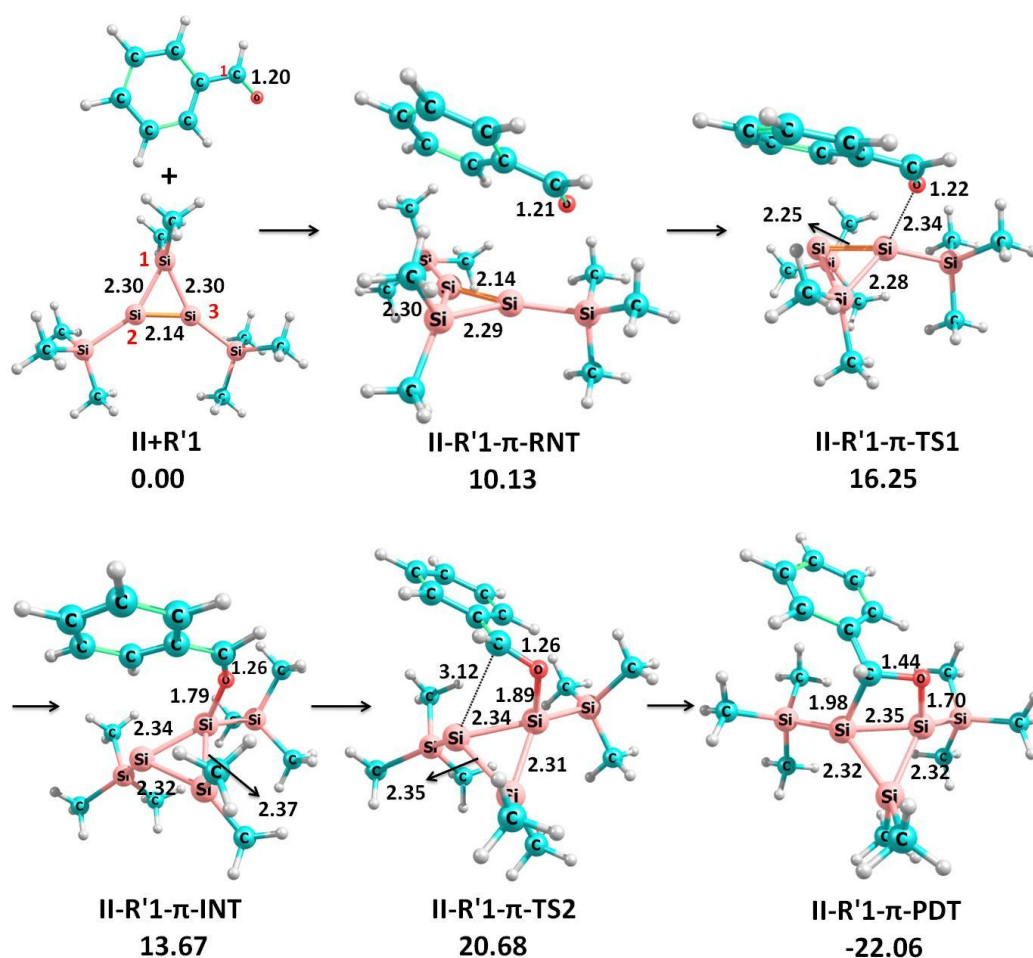


**Figure 5.17** Intermediates and transition states involved in the  $\pi$ -addition pathway of **II** and **R'1**. Relative free energies are given in kcal/mol and bond lengths in Å

The formation of the reactant dispersion complex (**II- R'1- $\pi$ -RNT**), possessing a relative energy of 10.01 kcal/mol marks the commencement of the reaction. The dispersion complex is progressed to a transition state **II- R'1- $\pi$ -TS1**, in which the carbonyl oxygen of **R'1** initiated a bonding interaction with one of the  $sp^2$  silyl silicon atoms of **II** ( $r_{\text{O-Si}_{(1)}} = 2.34 \text{ \AA}$ ). The activated complex advanced to an intermediate **II- R'1- $\pi$ -INT** by the full rupture of the  $\pi$  bond between  $\text{Si}_{(1)}$  and  $\text{Si}_{(2)}$  ( $r_{\text{Si}_{(1)}-\text{Si}_{(2)}} = 2.34 \text{ \AA}$ ). The formation of the intermediate **II- R'1- $\pi$ -INT**, the activation energy required for the formation of **I-R'1- $\pi$ -INT** is 16.25 kcal/mol. Further progress of the  $\pi$ -addition reaction is marked by the formation of another transition state, **II- R'1- $\pi$ -TS2**. During this step a strong interaction between  $\text{Si}_{(2)}$  of **II** and carbonyl carbon of **R'1** is developed ( $r_{\text{C-Si}_{(2)}} = 3.12 \text{ \AA}$ ). The second transition state is transformed to the  $\pi$ -addition product; **II- R'1- $\pi$ -PDT** requires activation energy of 7.01 kcal/mol, and the overall reaction is exoergic by 22.06 kcal/mol. The energetics calculated for the  $\pi$ -addition reaction implies the feasibility of the reaction.



#### 5.4.4.2 $\sigma$ -insertion.

The intermediates and transition states located for  $\sigma$ -insertion reaction between **II** and **R'1** is represented in Figure 5.18

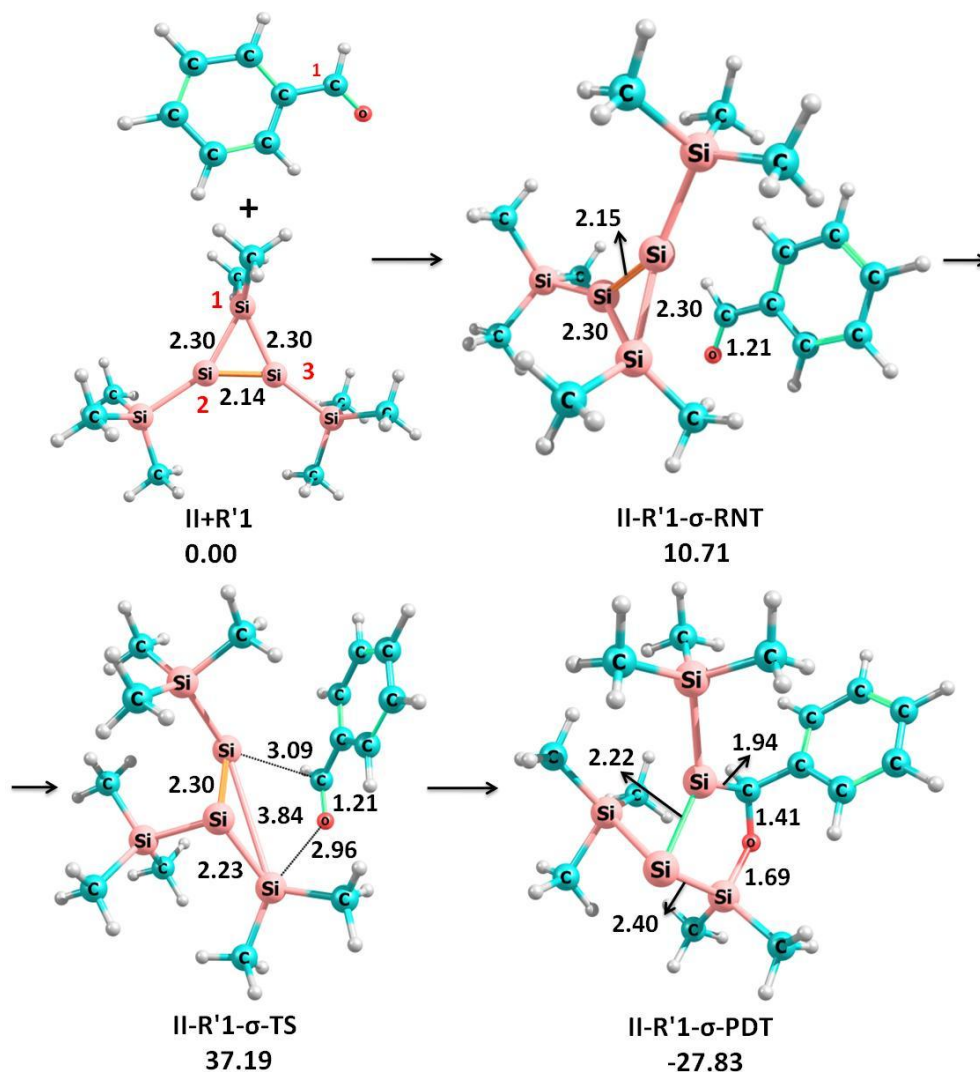


**Figure 5.18** Intermediates and transition states involved in the  $\sigma$ -insertion pathway of **II** and **R'1**. Relative free energies are given in kcal/mol and bond lengths in Å

The  $\sigma$ -insertion reaction between **II** and **R'1** is a direct single-step process. The reaction is initiated by the formation of a reactant dispersion complex **II- R'1- $\sigma$ -RNT**, which has a relative energy, 10.30 kcal/mol. Strong interactions are developed simultaneously between  $\text{Si}_{(1)}$  and  $\text{Si}_{(3)}$  of **II** and carbonyl carbon and carbonyl oxygen of **R'1** respectively. The electron rich  $\text{sp}^2\text{Si}_{(1)}$  extended an interaction to the electropositive end (C atom) of the carbonyl group ( $r\text{C-Si}_{(1)} = 3.09\text{Å}$ ). The activated complex **II- R'1- $\sigma$ -TS** is directly transformed to the  $\sigma$ -insertion product, **II-R'1- $\sigma$ -PDT**. In **II-R'1- $\sigma$ -TS**,  $\text{Si}_{(1)}$ -C and  $\text{Si}_{(3)}$ -O

bond formation takes place, and the barrier height is 37.19 Kcal/mol. Overall, the reaction is exoergic by 27.83 kcal/mol, but a higher activation barrier indicates the non-feasibility of the  $\sigma$ -insertion reaction.

#### 5.4.4.3 Ring opening

The intermediates and transitions states located for ring opening reaction between **II** and **R'1** is represented in Figure 5.19

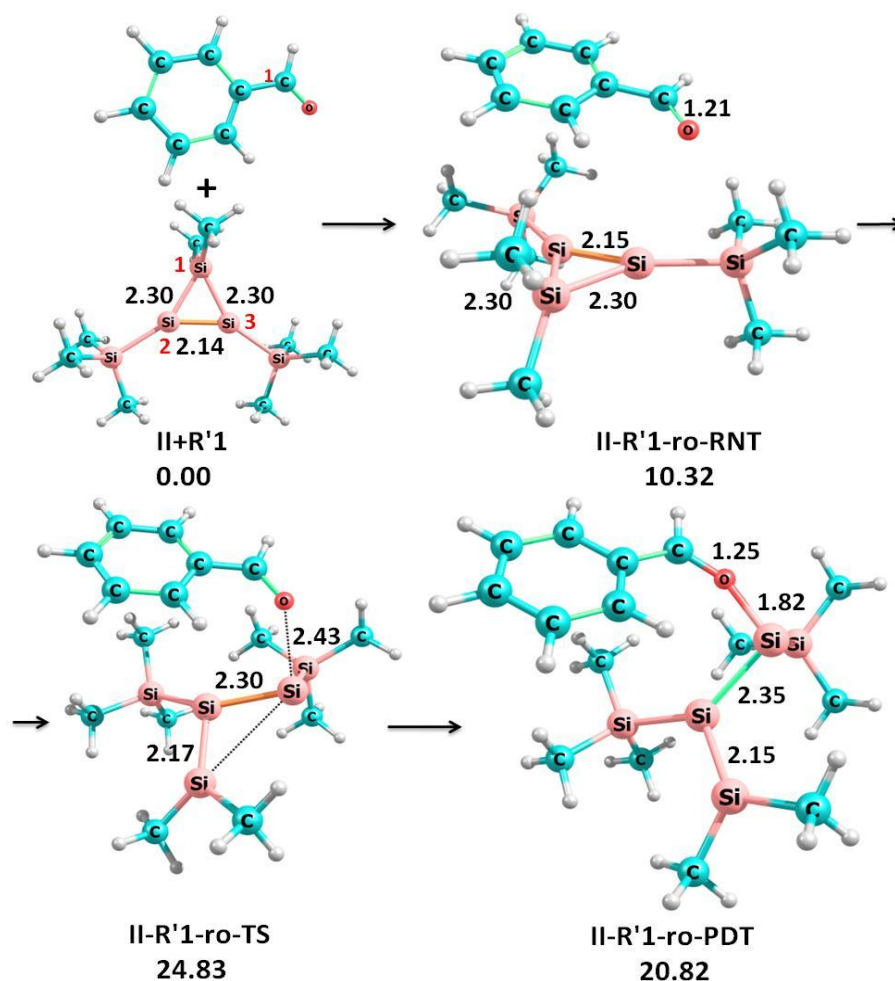


**Figure 5.19** Intermediates and transitions states involved in the ring opening pathway of **II** and **R'1**. Relative free energies are given in kcal/mol and bond lengths in Å

The ring opening reaction between **II** and **R'1** begins with the formation of a reactant dispersion complex, **II-R'1-ro-RNT**, possessing a relative energy 10.30 kcal/mol. The dispersion complex progressed to a transition state **II-R'1-ro-TS**, in which a strong interaction between the disilenyilsilicon atom of **II** and the carbonyl oxygen of **R'1** is established. The evolution of the O-Si<sub>(1)</sub> interaction ( $r_{\text{O-Si}(1)} = 2.43 \text{ \AA}$ ) is associated with the weakening of the Si<sub>(1)</sub>=Si<sub>(2)</sub> double bond ( $r_{\text{Si}(1)=\text{Si}(2)} = 2.30 \text{ \AA}$ ). The Si<sub>(1)</sub>-Si<sub>(3)</sub> bond is advanced



to a cleavage, whereas the Si<sub>(2)</sub>-Si<sub>(3)</sub> bond acquired the characteristics of a double bond ( $r_{\text{Si}(2)=\text{Si}(3)} = 2.17\text{\AA}$ ). The completion of the rupture of the Si<sub>(1)</sub>-Si<sub>(3)</sub> bond resulted in the formation of the ring opened product, **II-R'1-ro-PDT**. The activation barrier is 24.83 kcal/mol, and the overall reaction is endoergic by 20.82 kcal/mol. The product is a disilenylysilylene which carries two functional groups. The absence of the extended stabilisation in the product made the reaction endoergic. The elevated activation energy and endoergic nature of the ring opening reaction forbid its feasibility under ambient conditions.

#### 5.4.4.4 Exocyclic $\sigma$ -insertion reaction

The intermediates and transition states located for the exocyclic  $\sigma$ -insertion reaction between **II** and **R'1** is represented in Figure 5.20

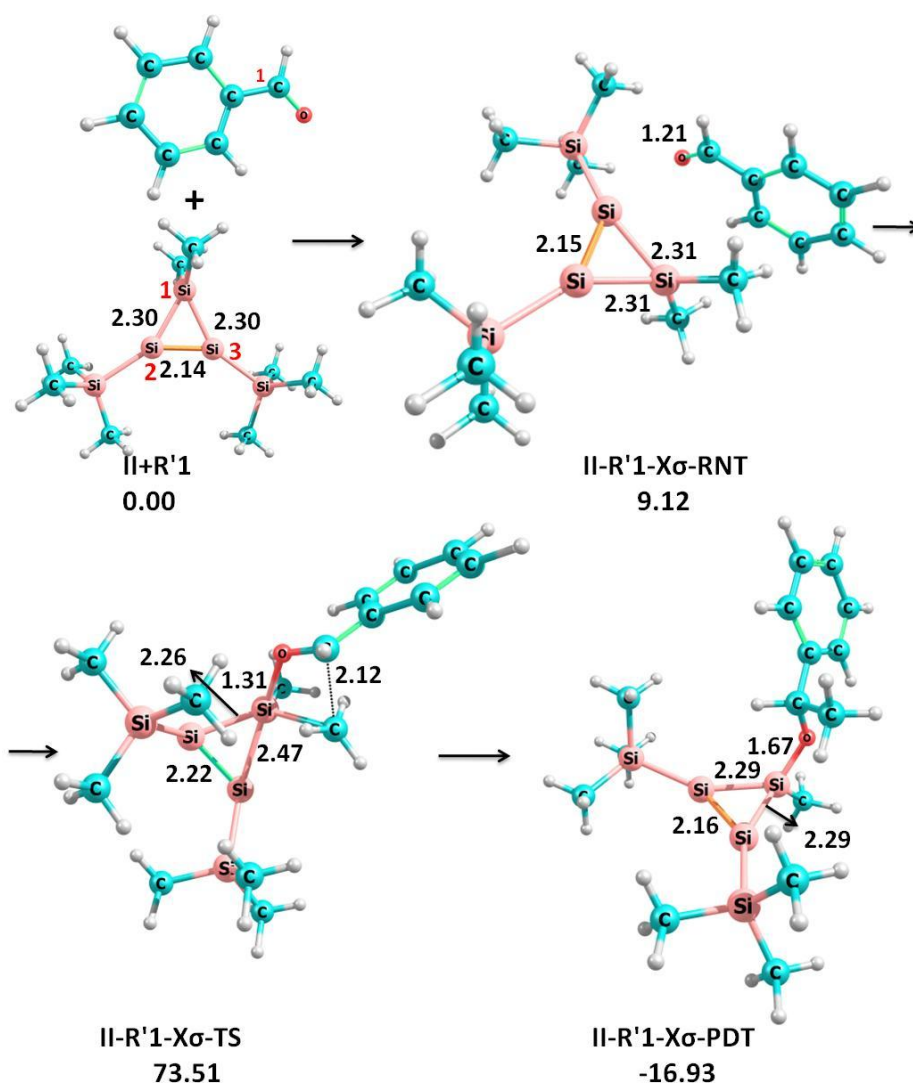


**Figure 5.20** Intermediates and transition states involved in the exocyclic  $\sigma$ -insertion pathway of **II** and **R'1**. Relative free energies are given in kcal/mol and bond lengths in  $\text{\AA}$

During the exocyclic  $\sigma$ -insertion reaction between **II** and **R'1**, the oxygen atom of the carbonyl group of **R'1** displaced one of the  $-\text{CH}_3$  group attached to the tetra-coordinate Si atom of **II**. The expelled  $-\text{CH}_3$  group shifted its position to the carbonyl carbon atom of **R'1**. Even though this reaction is exoergic by 16.90 kcal/mol, it is kinetically not attainable under ambient conditions due the forbidden activation barrier of 73.50 kcal/mol.

Free energy profile diagrams of the four reaction pathways between **II** and **R'1** are given in Figure 5.21

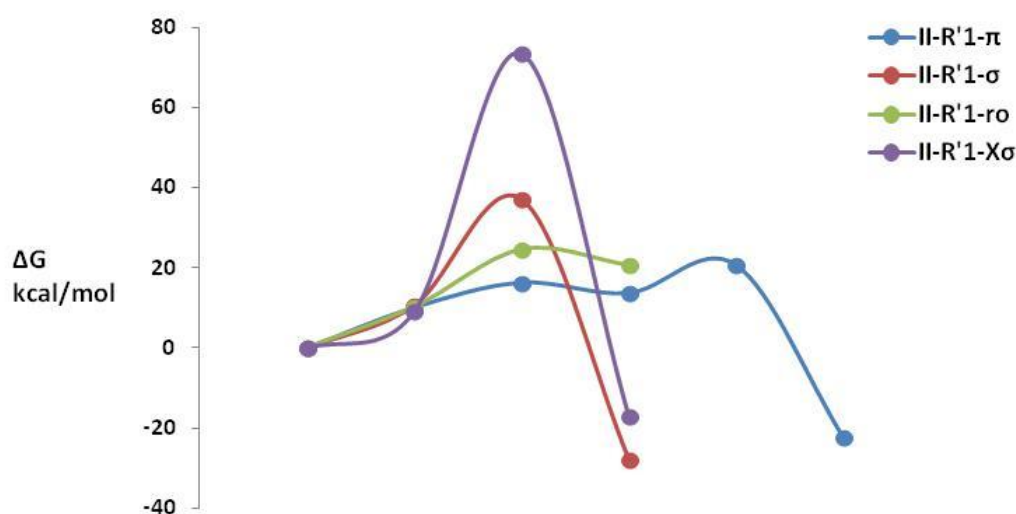


**Figure 5.21** Comparative free energy profile diagram for the different reaction pathways between **II** and **R'1**

Out of the four reaction pathways between **II** and **R'1** explained above; except the  $\pi$ -addition reaction, all are direct single-step conversion of the reactants to the products. The  $\pi$ -addition reaction is calculated to be a two-step process. The  $\pi$ -addition and  $\sigma$ -insertion reactions are exoergic in nature. The  $\pi$ -addition reaction generated house-shaped product with a bridging bond connecting two Si atoms. The  $\sigma$ -insertion reaction yielded a pentagonal product carrying a disilene bond. Curiously, the  $\sigma$ -insertion pathway between **II** and **R'1** involves a formidable activation barrier of 37.2 kcal/mol and is unattainable under normal laboratory conditions. The ring opening pathway between **II** and **R'1** involves a relatively higher activation barrier in addition to its exoergic nature and hence, is also unachievable under ambient conditions. The exocyclic  $\sigma$ -insertion reaction involves huge activation energy and is not practicable under normal conditions.

## 5.4.5 Reaction pathways of $c\text{-Si}_3\text{Me}_2(\text{SiMe}_3)_2(\text{II})$ with $\text{H-CHO}(\text{R}'2)$

### 5.4.5.1 $\pi$ -addition

A direct single-step reaction pathway has been identified for the  $\pi$ -addition reaction between the carbonyl group of  $\text{R}'2$  and the silenyl part of  $\text{II}$ . Intermediates and transition states located for the reaction is represented in Figure 5.22

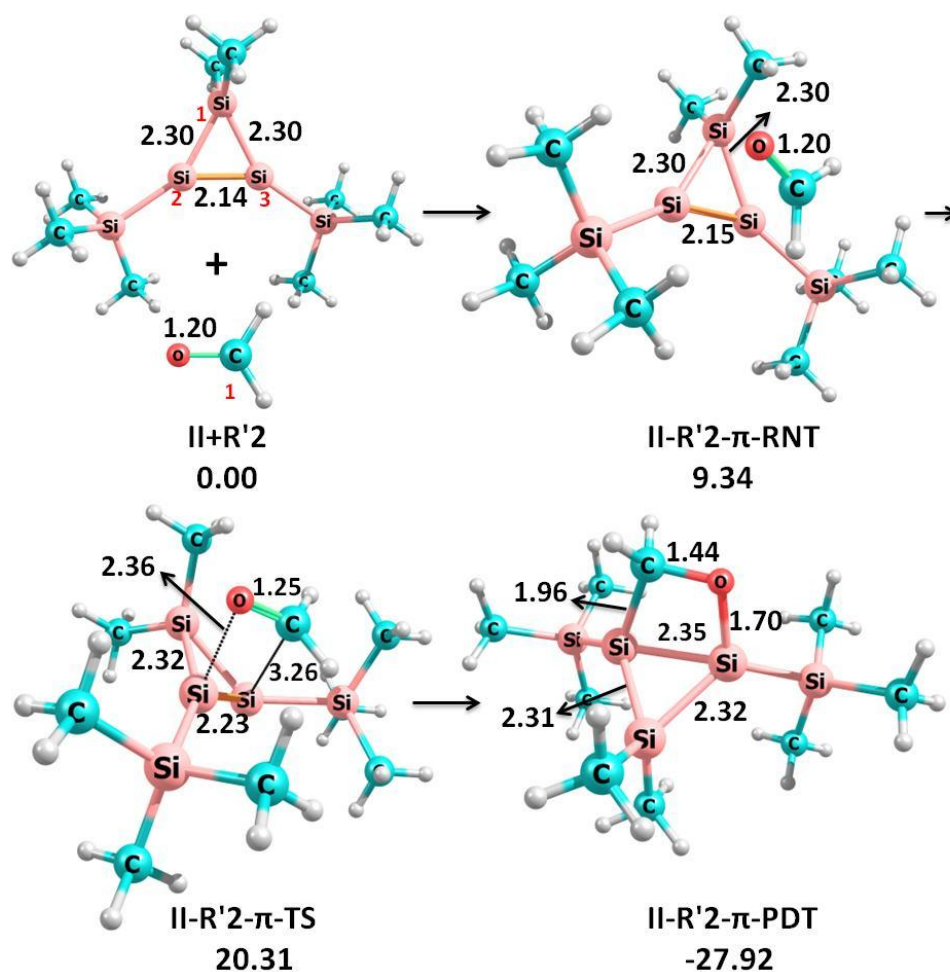


**Figure 5.22** Intermediates and transition states involved in the  $\pi$ -addition reaction pathway of  $\text{II}$  and  $\text{R}'2$ . Relative free energies are given in kcal/mol and bond lengths in Å

The  $\pi$ -addition reaction between  $\text{II}$  and  $\text{R}'2$  is initiated by the formation of reactant dispersion complex between the two namely,  $\text{II-R}'2\text{-}\pi\text{-RNT}$  with relative energy = 9.34 kcal/mol. This dispersion complex is advanced to a transition state  $\text{II-R}'2\text{-}\pi\text{-TS}$ , in which the carbonyl group of  $\text{R}'2$  initiated bonding interactions with one of the  $\text{sp}^2$  silicon atoms of  $\text{II}$ . Progress of this interaction is characterized by the elongation of the  $\text{Si}=\text{Si}$  double bond of  $\text{II}$  and the  $\text{C}=\text{O}$  bond of the carbonyl group of  $\text{R}'2$  ( $r_{\text{Si}(1)\text{-Si}(2)} = 2.23$  Å,  $r_{\text{C=O}} = 1.25$  Å). The activation energy associated with the formation of  $\text{II-R}'2\text{-}\pi\text{-TS}$  is 20.31 kcal/mol. The

progress of **II-R'2- $\pi$ -TS** to the  $\pi$ -addition product, **II-R'2- $\pi$ -PDT**. The required activation energy is 20.31 kcal/mol, and the overall reaction is exoergic by 27.92 kcal/mol, is achieved through the completion of the formation of the Si<sub>(1)</sub>-O and Si<sub>(2)</sub>-C bonds. The product is a bicyclic housane-shaped one. The bridging Si-Si bond of the product confirms the classical  $\pi$ -addition identity of the reaction. The product possesses no multiple bonds. The moderate activation energy and high exoergic value of the  $\pi$ -addition reaction between **II** and **R'2** predicts its practicability under normal laboratory conditions.

#### 5.4.5.2 $\sigma$ -insertion reaction

The intermediates and transitions states located for  $\sigma$ -insertion reaction between **II** and **R'2** is represented in Figure 5.23

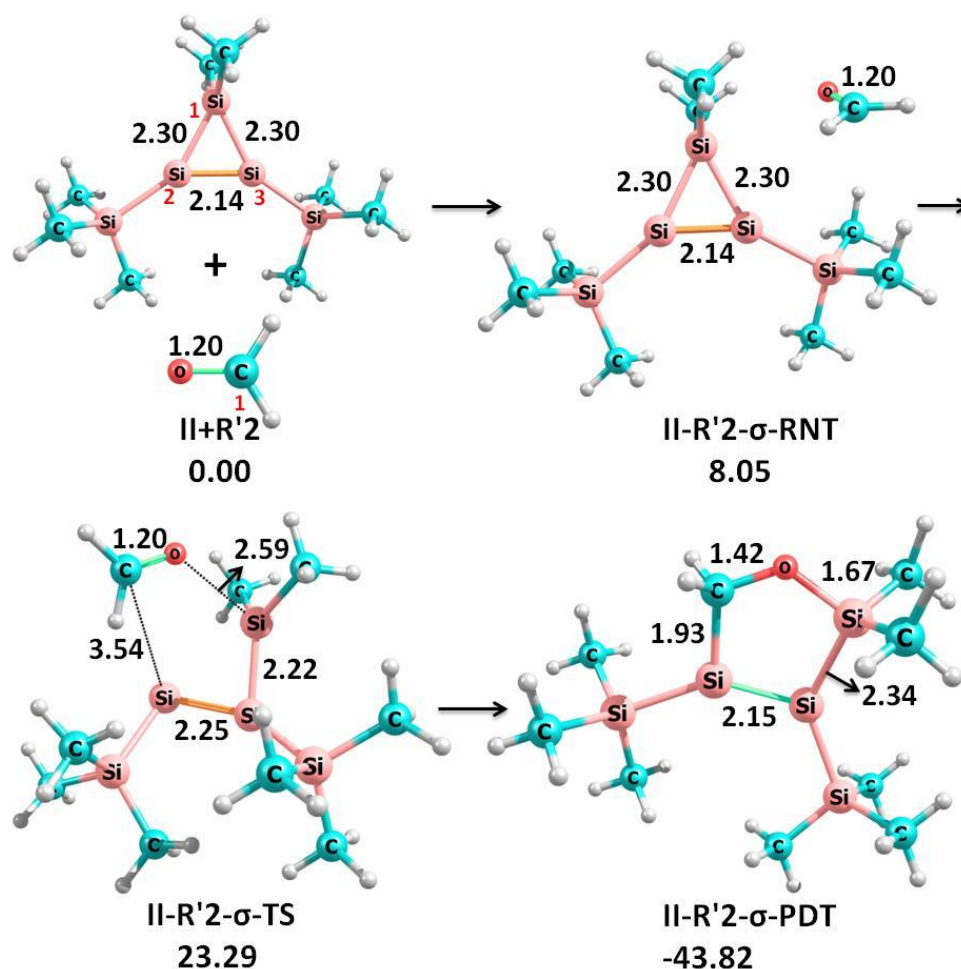


**Figure 5.23** Intermediates and transitions states involved in the  $\sigma$ -insertion reaction pathway of **II** and **R'2**. Relative free energies are given in kcal/mol and bond lengths in Å

Due to the small size of **R'2**, the  $\sigma$ -insertion reaction between it and the cyclotrisilene **II** also is a direct single-step process. The  $\sigma$ -insertion reaction is initiated by the formation of

a reactant dispersion complex **II- R'2- $\sigma$ -RNT**, with a relative energy 8.05 kcal/mol. The dispersion complex is progressed to a activated complex **II- R'2- $\sigma$ -TS**, in which strong C-Si<sub>(1)</sub> and O-Si<sub>(3)</sub> interactions are developed between the carbonyl group of **R'2** and cyclotrisilene moiety of **II** ( $r_{\text{O-Si}_{(3)}} = 2.76\text{\AA}$ ,  $r_{\text{C-Si}_{(1)}} = 3.59\text{\AA}$ ). **II- R'2- $\sigma$ -TS** is progressed to the  $\sigma$ -insertion product, **II-R'2- $\sigma$ -PDT**, the activation barrier for the  $\sigma$ -insertion is 23.29 kcal/mol, and the formation of the pentagonal product **I-R1- $\sigma$ -PDT** is exoergic by 43.82 kcal/mol. In the shaping of the final product from the **II- R'2- $\sigma$ -TS**, the  $r_{\text{C-Si}_{(1)}}$  bond distance is revised to 1.93 $\text{\AA}$  from 3.54 $\text{\AA}$  and the  $r_{\text{O-Si}_{(3)}}$  bond to 1.67 $\text{\AA}$  from 2.59 $\text{\AA}$ . Even though the activation energy of the reaction is marginally elevated, the very high exoergicity of the  $\sigma$ -insertion reaction between **II** and **R'2** support its workability at normal laboratory conditions.

### 5.4.5.3 Ring opening

The intermediates and transitions states located for ring opening reaction between **II** and **R'2** is represented in Figure 5.24

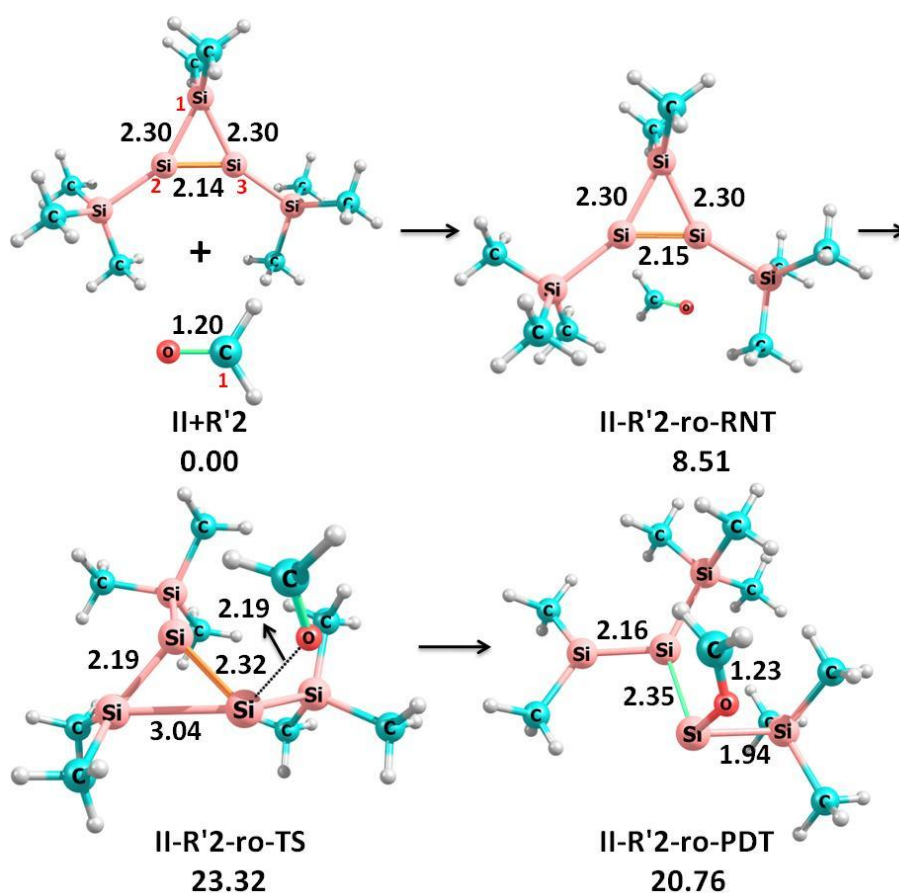


**Figure 5.24** Intermediates and transitions states involved in the ring opening reaction pathway of **II** and **R'2**. Relative free energies are given in kcal/mol and bond lengths in  $\text{\AA}$

The ring opening reaction between **II** and **R'2** begins with the formation of a reactant dispersion complex **II-R'2-ro-RNT**, possessing a relative energy 8.51 kcal/mol. The dispersion complex progressed to a transition state **II-R'2-ro-TS** in which a strong interaction between the disilyl silicon atom of **II** and the carbonyl oxygen of **R'2** is formed. The evolution of the O-Si<sub>(1)</sub> interaction ( $r_{\text{O-Si}_{(1)}} = 2.19 \text{ \AA}$ ) is associated with the weakening of the Si<sub>(1)</sub>=Si<sub>(2)</sub> double bond ( $r_{\text{Si}_{(1)}\text{-Si}_{(2)}} = 2.32 \text{ \AA}$ ). The completion of the rupture of the Si<sub>(1)</sub>-Si<sub>(3)</sub> bond resulted in the formation of the ring opened product, **II-R'2-ro-PDT**. The activation barrier is 23.32 kcal/mol, and the overall reaction is endoergic by 20.76 kcal/mol. The product is a disilylsilylene. Absence of the extended stabilisation in the product made the reaction endoergic. The relatively higher activation energy and endoergic nature forbid the feasibility of the ring opening reaction between **II** and **R'2** under normal laboratory conditions.

#### 5.4.5.4 Exocyclic $\sigma$ -insertion

The intermediates and transitions states located for exocyclic  $\sigma$ -insertion reaction between **II** and **R'2** is represented in Figure 5.25

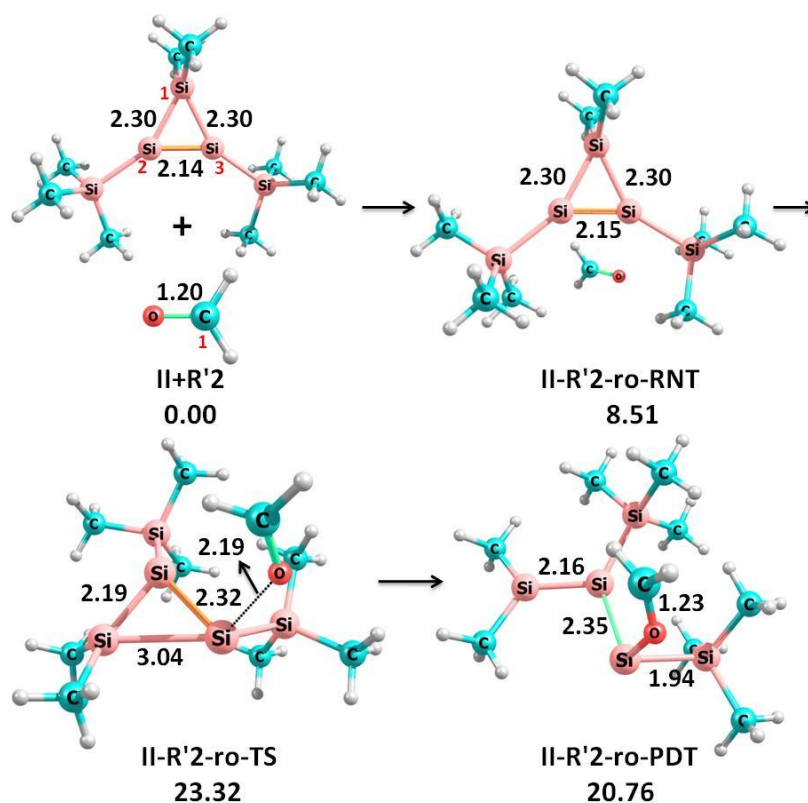


**Figure 5.25** Intermediates and transitions states involved in the exocyclic  $\sigma$ -insertion reaction pathway of **II** and **R'2**. Relative free energies are given in kcal/mol and bond lengths in  $\text{\AA}$



The exocyclic  $\sigma$ -insertion pathway between **II** and **R'2** also is a direct single-step process. The reaction is initiated by the formation of a reactant dispersion complex, **II-R'2-x $\sigma$ -RNT** possessing a relative energy 8.73 kcal/mol. **II-R'2-x $\sigma$ -RNT** progressed to a transition state, **II-R'2-x $\sigma$ -TS** in which the carbonyl oxygen established a strong interaction with the tetra coordinate silicon atom of the cyclotrisilene moiety. Even though the reaction is appearing to be achievable thermodynamically due to the exothermic nature (-23.21 kcal/mol), the exorbitant activation energy (69.74 kcal/mol) denies its kinetic feasibility.

Free energy profile diagrams of the four reaction pathways between **II** and **R'2** are given in Figure 5.26.

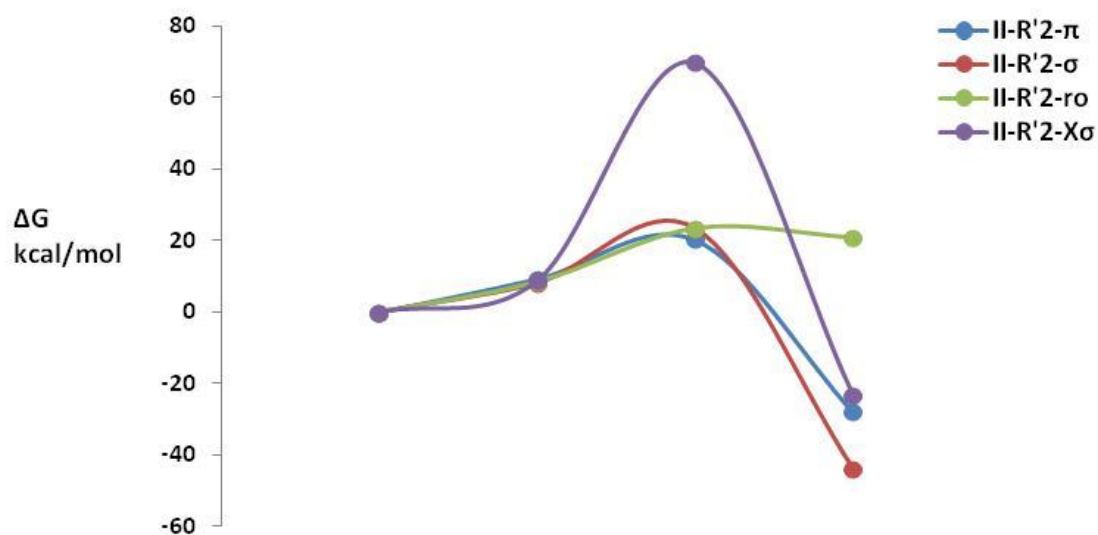


**Figure 5.26** Comparative free energy profile diagram for the different reaction pathways between **II** and **R'2**

All the four reaction pathways between **II** and **R'2** demonstrated above are direct, single-step conversion of the reactants to products. The  $\pi$ -addition reaction generated a housane-shaped product with the bridging bond connecting two Si atoms ( $\text{Si}_{(1)}$  and  $\text{Si}_{(2)}$ ). The activation energies of the  $\pi$ -addition,  $\sigma$ -insertion and the ring opening reactions are in the range of 20-23 kcal/mol. The  $\sigma$ -insertion reaction is highly exoergic followed in magnitude of exoergicity by the  $\pi$ -addition reaction and are seems to be practicable under normal laboratory conditions. The ring opening reaction is calculated to be endoergic and therefore is not workable under ambient conditions. The relatively higher activation energy and exothermic nature forbid the feasibility of the ring opening reaction between **II** and **R'2**. The  $\pi$ -addition product formed between **II** and **R'2** is relatively stabler than that formed between **II** and **R'1**. The  $\sigma$ -insertion reaction yielded a pentagonal product carrying a disilene bond.

The  $\sigma$ -insertion product formed between **II** and **R'2** is much more stable than that formed between **II** and **R'1**. The significantly lower activation energy of the  $\sigma$ -insertion reaction between **II** and **R'2** in comparison with **II** and **R'1** is also worth mentioning. The smaller size of HCHO (**R'2**) in comparison with Ph-CHO (**R'1**) along with the electronic peculiarities of the phenyl substituent account for these differences.

A comparison of the energetics of the four reaction pathways of **II** with alkynes and aldehydes reveals that only the  $\pi$ -addition reaction is uniformly workable with both the class of the substrates. Even though, the  $\pi$ -addition,  $\sigma$ -insertion and the ring opening reactions of **II** with alkyne substrates are exoergic to varying extents, the latter two are not practicable with **R2** due the high activation energy. Regarding the aldehydes, the ring opening reaction involves relatively higher activation energies (>23 kcal/mol) and are endoergic in nature indicating their non-attainability under ambient conditions. Although, the  $\sigma$ -insertion reaction is practicable with **R'2** it is unattainable with **R'1** due the formidable activation barrier. Generally, the activation energy of workable reactions of aldehydes with **II** are higher than that of alkynes with **II** by  $\approx$ 5 kcal/mol. The exoergic of the reactions of **II** with the substrates are also remarkably higher for those with the alkynes. The activation energy of the exocyclic  $\sigma$ -insertion reactions of **II** with substrates are lower for the reaction with aldehydes; but, the barrier height is nowhere near the practicable range with them too.

While comparing the kinetics of the reaction pathways of the cyclotrisilenes **I** and **II** with the five substrates examined, the primary difference comes into the view is the higher relative energy of the initially formed dispersion complex with the latter; in almost all reactions. The increased energy requirement is due to the greater steric hindrance encountered during the approach of the substrates as a result the largersize of substituents attached to the cyclotrisilene ring of **II**. The exocyclic  $\sigma$ -insertion reaction is invariably involved exorbitant activation energy in all cases and need not be discussed. Regarding the other three pathways, though the reactions of **I** with the substrates proceed generally through a better stabilized course than those with **II**, the activation energy is 2-3 kcal/mol less in most of the kinetically feasible reactions of **II**. The exoenergeticity is calculated to be greater in most of the reactions of **I** than that of **II**. A significant peculiarity to be noticed in the reaction between **II** and **R2** is the non-feasibility of  $\pi$ -addition and ring opening reactions under ambient conditions due to the high activation energy encountered. Apparently, in both these cases the intermediate formed is the  $\sigma$ -insertion product between the two; which is highly stable. Even though  $\pi$ -



addition,  $\sigma$ -insertion and ring opening reactions between **I** and **R'1** are proceed with low activation energy, the latter two involves non-practicably high activation energy when the cyclotrisilene involved is **II**. The reactions between **II** and **R'2** also involves relatively greater activation energy than those involving **I**.

## 5.5 Conclusion

We have made a thorough computational exploration of the possible interactions of phenyl acetylene ( $C_6H_5-C\equiv CH$ ; **R1**), propylene ( $CH_3-C\equiv CH$ ; **R2**), trimethylsilylacetylene ( $(CH_3)_3Si-C\equiv CH$ ; **R3**), benzaldehyde ( $C_6H_5-HC=O$ ; **R'1**) and formaldehyde ( $H_2C=O$ ; **R'2**) with 1,2-bis(trimethylsilyl)-3,3-dimethyl cyclotrisilene( $c-Si_3Me_2(SiMe_3)_2$ ; **II**). Four reaction path ways;  $\pi$ -addition,  $\sigma$ -insertion, ring opening and exocyclic  $\sigma$ -insertion were identified and the energetics and mechanisms were studied systematically. The former three substrates (**R1**, **R2** & **R3**) are alkynes carrying different substituents and the latter two (**R'1** & **R'2**) are aldehydes with different substituents.

Among all the five substrates analyzed, the  $\pi$ -addition and  $\sigma$ -insertion reactions are found to be invariably the most favored reaction pathways. Except for **R'2**, the  $\pi$ -addition reaction is a two-step process, whereas the  $\sigma$ -insertion is a single-step process with all the five substrates. In all the cases  $\pi$ -addition reaction generated a housane-shaped product, whereas the  $\sigma$ -insertion reaction culminated in pentagonal ring product. Due to the well-defined nature of the product generated, the  $\sigma$ -insertion reactions are found to be significantly more exothermic than the  $\pi$ -addition reactions. However, the activation energies of both reaction pathways are almost equal. As an exception, the activation barrier of the  $\sigma$ -insertion reaction of **R'1** with **II** is calculated to be far beyond the practicability of the reaction under ambient conditions. Even though, the ring opening reactions of **II** with alkyl substituents are calculated to be spontaneous under ambient conditions due to the low activation energy and exothermic nature, that with the carbonyl compounds are found to be endothermic with elevated activation energies. The exothermicity of the ring opening reactions with the alkyl substrates remarkably lower than that of the  $\pi$ -addition and  $\sigma$ -insertion reactions due to the lower stability of the disilylsilylene product. A singularity to be noticed in the reactions of **II** with **R2** is, its ring opening as well as  $\pi$ -addition reactions proceeds through an intermediate, which is equivalent in all respect to the  $\sigma$ -insertion product between the two. All the reactions of carbonyl compounds with **II** are less exothermic than those with alkynes except for the  $\sigma$ -insertion reaction with **R'2**. Due to the smaller size of **R'2**, all its reactions

with **II** are single-step processes. The  $\sigma$ -insertion pathway can be stated as the most favored reaction of **II** with the substrates. The exocyclic  $\sigma$ -insertion reaction pathway is found to be associated with formidable energy barrier in all the investigated cases. Even though, the magnitude of activation energy is slightly lower with the reaction involving aldehydes, the value is nowhere near in the practicability range of the reaction under ordinary laboratory conditions.

A discussion of the relative reactivity of 1,2,3,3-tetramethyl cyclotrisilene ( $c\text{-Si}_3\text{Me}_4$ ; **I**) and 1,2-bis(trimethylsilyl)-3,3-dimethyl cyclotrisilene ( $c\text{-Si}_3\text{Me}_2(\text{SiMe}_3)_2$ ; **II**) should be centred on the difference in the electronic and steric influence of the substituents; Me ( $-\text{CH}_3$ ) and TMS ( $-\text{Si}(\text{CH}_3)_3$ ) attached to the Si atoms forming the disilene part of the cyclotrisilene ring. TMS has a significantly greater steric bulk. The steric influence is evident in the energy involved in the evolution of the reactant complex itself: in the reactions of **I** it is 3-5 kcal/mol whereas in reactions involving **II**; it is 6-7 kcal/mol. In general, the reaction pathways are better stabilised in the reactions of **I** than the sterically more crowded **II**. Thus, the change of substituents on the cyclotrisilene ring also has an influence on the energetics of the reaction pathways.

## Reference

- Abersfelder, Kai, Deniz Güclü, and David Scheschkewitz. 2006. "An Unsaturated  $\alpha,\Omega$ - Dianionic Oligosilane." *Angewandte Chemie International Edition* 45(10): 1643–45. <https://onlinelibrary.wiley.com/doi/10.1002/anie.200503975>.
- Fukaya, Norihisa, Masaaki Ichinohe, and Akira Sekiguchi. 2000. "New Fused Bicyclic Cyclotrigermenes from Cycloaddition Reactions of Cyclotrigermene." *Angewandte Chemie* 39(21): 3881–84. [https://onlinelibrary.wiley.com/doi/10.1002/1521-3773\(20001103\)39:21%3C3881::AID-ANIE3881%3E3.0.CO;2-3](https://onlinelibrary.wiley.com/doi/10.1002/1521-3773(20001103)39:21%3C3881::AID-ANIE3881%3E3.0.CO;2-3).
- Hajgató, Balázs, Masae Takahashi, Mitsuo Kira, and Tamás Veszprémi. 2002. "The Mechanism of 1,2-Addition of Disilene and Silene: Hydrogen Halide Addition Part 2; for Part 1 See: T. Veszprémi, M. Takahashi, B. Hajgató, M. Kira, *J. Am. Chem. Soc.* 2001, 123, 6629." *Chemistry - A European Journal* 8(9): 2126. [https://onlinelibrary.wiley.com/doi/10.1002/1521-3765\(20020503\)8:9%3C2126::AID-CHEM2126%3E3.0.CO;2-2](https://onlinelibrary.wiley.com/doi/10.1002/1521-3765(20020503)8:9%3C2126::AID-CHEM2126%3E3.0.CO;2-2).
- Ichinohe M, Igarashi M, Sanuki K, and Sekiguchi A. 2005. "Cyclotrisilylium Ion: The Persilaaromatic Compound." *J. Am. Chem. Soc.* 127(28): 9978–79.
- Kinjo, Rei et al. 2007. "Reactivity of a Disilyne  $\text{RSi}\equiv\text{SiR}$  ( $\text{R} = \text{Si}$  i Pr[CH(SiMe<sub>3</sub>)<sub>2</sub>]<sub>2</sub>) toward  $\pi$ -Bonds: Stereospecific Addition and a New Route to an Isolable 1,2-Disilabenzene." *Journal of the American Chemical Society* 129(25): 7766–67. <https://pubs.acs.org/doi/10.1021/ja072759h>.
- Kira, Mitsuo, and Takeaki Iwamoto. 2006. "Progress in the Chemistry of Stable Disilenes." In , 73–148. <https://linkinghub.elsevier.com/retrieve/pii/S0065305505540036>.
- Kira, Mitsuo, Takeaki Iwamoto, and Chizuko Kabuto. 1996. "The First Stable Cyclic Disilene." 7863(c): 10303–4.
- Lee, Vladimir Ya. et al. 2000. "The First Three-Membered Unsaturated Rings Consisting of Different Heavier Group 14 Elements: 1-Disilagermirene with a SiSi Double Bond and Its Isomerization to a 2-Disilagermirene with a SiGe Double Bond." *Journal of the American Chemical Society* 122(37): 9034–35. <https://pubs.acs.org/doi/10.1021/ja001551s>.
- Lee, Vladimir Ya., Shogo Miyazaki, Hiroyuki Yasuda, and Akira Sekiguchi. 2008. "Isomeric Metamorphosis: Si<sub>3</sub>E (E = S, Se, and Te) Bicyclo[1.1.0]Butane and Cyclobutene." *Journal of the American Chemical Society* 130(9): 2758–59. <https://pubs.acs.org/doi/10.1021/ja800111r>.
- Lee, Vladimir Ya., Hiroyuki Yasuda, and Akira Sekiguchi. 2007. "Interplay of E<sub>n</sub>E'<sub>3-n</sub> C Valence Isomers (E, E' = Si, Ge): Bicyclo[1.1.0]Butanes with Very Short Bridging Bonds and Their Isomerization to Alkyl-Substituted Cyclopropenes." *Journal of the American Chemical Society* 129(9): 2436–37. <https://pubs.acs.org/doi/10.1021/ja068229n>.
- Leszczyńska, Kinga et al. 2012. "Reversible Base Coordination to a Disilene." *Angewandte Chemie - International Edition* 51(27): 6785–88.
- Power, Philip P. 1999. " $\pi$ -Bonding and the Lone Pair Effect in Multiple Bonds between Heavier Main Group Elements." *Chemical Reviews* 99(12): 3463–3504.
- Scheschkewitz, David. 2009. "Anionic Reagents with Silicon- Containing Double Bonds." *Chemistry - A European Journal* 15(11): 2476–85. <https://chemistry-europe.onlinelibrary.wiley.com/doi/10.1002/chem.200801968>.
- Sekiguchi, Akira, Rei Kinjo, and Masaaki Ichinohe. 2004. "A Stable Compound Containing a Silicon-Silicon Triple Bond." *Science* 305(5691): 1755–57. <https://www.science.org/doi/10.1126/science.1102209>.
- Sekiguchi, Akira, and Vladimir Ya. Lee. 2003. "Heavy Cyclopropenes of Si, Ge, and SnA New

Challenge in the Chemistry of Group 14 Elements.” *Chemical Reviews* 103(4): 1429–48.  
<https://pubs.acs.org/doi/10.1021/cr0100300>.

Uchiyama, Kei et al. 2007. “Thermal and Photochemical Cleavage of SiSi Double Bond in Tetrasil-1,3-Diene.” *Journal of the American Chemical Society* 129(35): 10638–39.  
<https://pubs.acs.org/doi/10.1021/ja0741473>.

Wiberg, Nils, Wolfgang Niedermayer, Heinrich Nöth, and Markus Warchhold. 2001. “Auf Dem Wege Zu Einem Disilin -Si≡Si-: Bildung von RHSi=SiHR Und Hinweise Auf Die Intermediäre Bildung von RSi≡SiR (R = SiH(SitBu<sub>3</sub>)<sub>2</sub>).” *Zeitschrift für anorganische und allgemeine Chemie* 627(8): 1717–22.  
[https://onlinelibrary.wiley.com/doi/10.1002/1521-3749\(200108\)627:8%3C1717::AID-ZAAC1717%3E3.0.CO;2-E](https://onlinelibrary.wiley.com/doi/10.1002/1521-3749(200108)627:8%3C1717::AID-ZAAC1717%3E3.0.CO;2-E).

## Chapter 6: Recommendations

---

The current research, titled “*Quantum Mechanical Assessment of Substituent Effect of Doubly Bonded Silicon Compounds*,” delves into the computational analysis of reactions involving substituted silenes (compounds with C=Si) and cyclotrisilene (compounds with Si=Si), with a particular emphasis on substituent effects. This novel area of double bond chemistry in silicon compounds presents significant opportunities for exploration, especially considering that our understanding of silenes and disilenes remains nascent.

In the second chapter, we investigate the polar nature of the C=Si bond and the resulting regioselectivity of its addition reactions. Our findings indicate that substituents have a profound impact on both the polarity of the silene bond and the electrophilicity of the silicon center. Although our studies have focused on a limited range of substituents, there remains considerable potential for further exploration. For example, the strategic selection of substituents may facilitate head-to-head dimerization, contrasting with the head-to-tail dimerization observed in our current investigations. This underscores the need for additional research into the potential for altering the dimerization mechanism through appropriate substitutions.

The third chapter focuses on small molecule activation by substituted silenes and the influence of substituents on silene-silylene rearrangements. Given that small molecule activation is predominantly addressed by costly catalytic elements such as platinum, the introduction of multivalent silicon compounds provides promising alternatives, particularly in critical applications like hydrogen generation. Our initial findings, derived from a limited set of substituents on simple silenes, suggest significant results; however, further exploration of a broader variety of substituents with diverse electronic and steric properties could yield valuable insights. Additionally, varying the principal silene could enhance small molecule activation outcomes.

We have observed that the generation of silylene from silene, which is effective in activating stable bonds, is significantly influenced by the substituents attached to the silene. This rearrangement presents an opportunity for further investigation with a wider range of substituents that can modify the electronic framework of the C=Si bond.

Chapters four and five examine the reactions of alkynes and aldehydes with substituted cyclotrisilenes, although our studies are currently limited to only two substituted

cyclotrisilene molecules. Our investigations involved reactions with three alkynes and two aldehydes, yet the promising results indicate numerous potential multivalent compounds capable of reacting with Si=Si bonds, opening vast avenues for future research.

The study of organosilicon reactive intermediates has experienced rapid growth, signaling a rich landscape for further exploration and innovative applications in synthetic chemistry. Our investigations into the inductive effects employed to modify the polarity of the C=Si bond demonstrate that substituting both carbon and silicon with groups exhibiting contrasting mesomeric effects can effectively reverse polarization, potentially enabling new synthetic routes, including head-to-head dimerization.

Understanding the effects of stronger electron donors and acceptors on silenes remains a valuable area for future investigation. Such insights could lead to more efficient activation strategies for small molecules, enhancing their industrial viability. Moreover, our findings suggest that the regioselectivity of small molecule activation appears largely independent of the substituents used, highlighting the necessity of testing this observation with more potent electron donors and acceptors.

Finally, disilenes, due to their inherently weak  $\pi$ -bonding, are anticipated to serve as effective synthetic equivalents of silylenes. The unique electronic characteristics of cyclotrisilene enable [2+2] cycloaddition reactions with unsaturated molecules, presenting opportunities for the development of organic-inorganic hybrid polymers. Future studies should encompass a broader range of unsaturated systems to fully exploit these potentials.

In précis, the small molecule activation capabilities of cyclotrisilene and other silicon compounds hold considerable promise for industrial applications. Silylenes are already recognized for their ability to activate stable molecules such as H<sub>2</sub>, CO, CO<sub>2</sub>, N<sub>2</sub>O, O<sub>2</sub>, H<sub>2</sub>O, C<sub>2</sub>H<sub>4</sub>, and NH<sub>3</sub>. The advancement of these compounds into practical catalysts, particularly for hydrogen generation from water, could catalyze a new industrial revolution.

Addressing research gaps in organosilicon chemistry, particularly regarding silenes and cyclotrisilenes, is crucial for advancing knowledge and applications in this field. First, comprehensive studies on a wider variety of substituents, encompassing different electronic and steric properties, are essential to understand their influence on reaction mechanisms and outcomes. Additionally, there is a need for detailed investigations into the mechanisms of dimerization reactions to clarify factors influencing head-to-head versus head-to-tail pathways, particularly the role of reverse polarity. The stability and reactivity of silylenes and

disilenes require further exploration, especially for synthesizing stable variants and studying their interactions with diverse substrates. Moreover, understanding the mechanisms behind the activation of small molecules by these compounds is vital for enhancing their catalytic potential, particularly in processes like hydrogen generation and CO activation. Research should also focus on regioselectivity in reactions, investigating the effects of substituents with more potent electron donors and acceptors. The reactivity of cyclotrisilene with unsaturated compounds should be expanded to identify new synthetic pathways and applications in organic-inorganic hybrid materials. Furthermore, theoretical and computational studies are needed to model organosilicon intermediates, aiding in predicting reactivity patterns and stability. Bridging laboratory findings with industrial applications through collaborations will help assess scalability and economic viability, while understanding the long-term stability and environmental impact of these compounds is essential for developing safe, sustainable applications. By addressing these gaps, future research can significantly enhance the field of organosilicon chemistry, leading to innovative solutions across various domains, including catalysis, materials science, and sustainable energy.

## LIST OF PUNBLICATIONS

1. Electronic effects of substituents on the reactivity of silenes: a computational analysis. Amrutha Kizhuvethath, Jose John Mallikasseri, and Jomon Mathew. *Structural Chemistry* 35.1 (2024): 119-133.
2. Unraveling the reaction pathways of cyclotrisilenes: a computational analysis. Amrutha Kizhuvethath, Jose John Mallikasseri, and Jomon Mathew. *Theoretical Chemistry Accounts* 143.3 (2024): 23.

## LIST OF CONFERENCE PRESENTATIONS

1. Substituted Cyclotrisilene Generates Stable Silene- The Divalent Silicon Compound: The Latest in Silicon Chemistry, *Emerging Frontiers in Chemical Science EFCS-2022*, Farook College, Kozhikode, Kerala, January 2023.
2. The effect of Substituents on the Dimerization and Trimerization Reactions of Silene- Computational Analysis. *Emerging Frontiers in Chemical Science EFCS-2018*, Farook College, Kozhikode, Kerala, November 2018.

## LIST OF TRAINING PROGRAMMES ATTENDED

1. "Gaussian16: Theory and Practice Workshop" Radisson Blu, Dwarka, Delhi, January 2018.